Investigating fouling and cleaning during the filtration of Gum Arabic to save water and reduce energy

Hayward, Emily

Award date:
2016

Awarding institution:
University of Bath

Investigating fouling and cleaning during the filtration of Gum Arabic to save water and reduce energy

Emily Ruth Hayward

A thesis submitted for the degree Doctor of Philosophy

University of Bath

Department of Chemical Engineering

September 2015

UNIVERSITY OF BATH

Centre for Sustainable Chemical Technologies

I. Declaration of Authorship

This is all my own work except where I have indicated via references or other forms of acknowledgement.

Signature:

Date:

II. Acknowledgements

There are many people I would like to thank for helping me through this PhD. I would like to thank my supervisor Dr. Mike Bird who has provided the tools and resources to complete this work, contributed ideas and insight, and helped with the development of the flat sheet ceramic membrane rig. I would also like to thank my co-supervisors Dr. Darrell Patterson and Professor Chick Wilson for their feedback, comments and insight into my findings.

I would also like to thank Dr. Arto Pihlajamaki from Lappeenranta University of Technology, Finland for allowing me to carry out zeta potential measurements and for all of the help with setting up the equipment and insight provided about the results.

I would like to thank Dr. Chris Wright from Swansea University for allowing me access to AFM for adhesion measurements, and to Yuan He for the help and insight provided while making measurements and analysing the data.

I would like to thank David Carr at *Kerry Ingredients* for providing spray dried Gum Arabic powder, and for bringing invaluable commercial relevance to this project. Gratitude is also given to David Carr and Andy Rice for running GPC samples for me at *Kerry Ingredients.*

I would like to thank Paul Frith for his help in designing and producing the flat sheet membrane rig. Without this, the experiments I could carry out would have been very limited.

I would also like to thank my fellow students and the technical team at the University of Bath who have allowed collaboration, insight and have helped to keep me sane throughout the project, and of course fix things when they went wrong.

I would like to thank the DTC in sustainable chemical technologies and EPSRC for funding, for enabling me to develop new skills throughout this project, and the opportunities I have had to travel to Lappeenranta and attend conferences. Additionally thanks to my cohort from the DTC for all the fun we've had as well as insightful conversations related to the PhD and developing ideas.

Finally I would like to thank my Husband Tim, and the rest of my family, for their support and care while I have carried out this project. Without your constant encouragement I would not have managed it.

III. Abstract

Gum Arabic is an exudate from *Acacia* trees and grows mainly in the sub Saharan region with Sudan being one of the world's largest producers. Gum is imported as kibbled amber aggregates which undergo dissolution, filtration and pasteurisation to remove any contaminants before being spray dried to produce a fine white powder suitable for use. Gum Arabic is widely used industrially, particularly in the food industry as it is a very effective emulsification agent. During the industrial processing of Gum Arabic, large quantities of both water and energy are used. Water and energy consumption are particularly high during the dissolution and spray drying processes. Approximately 14000 tons of wastewater are produced each year from *Kerry Ingredients* processing plant in Cam, UK containing ca. 2.0 wt. % Gum Arabic.[1] This requires expensive disposal methods.

The application of membrane technology can reduce the volume of water required during processing allowing the potential for recycling rather than requiring fresh water supplies. In addition, the method of microfiltration can separate Gum Arabic from the waste stream. This reduces the waste created during processing, resulting in a more sustainable process. The filtration of complex food products inevitably leads to fouling – the build-up of unwanted deposits on the membrane surface and in the membrane pores. This project investigates the chemistry and engineering of the Gum adhesion and removal process. This work is a study of what is occurring during fouling, methods to reduce it, and cleaning strategies to help restore the membrane following fouling. A proof of principle has been established, highlighting the potential for separating Gum Arabic from waste streams.

Presented here are the findings from the filtration of Gum Arabic through commercially available Membralox™ alumina microfiltration tubular ceramic membranes. In addition, the use of flat sheet alumina ceramic membranes has been studied to gain an insight into the mechanisms of fouling and removal.

During microfiltration, the use of high crossflow velocities (2.3 m s^{-1}), low transmembrane pressure (1.5 bar), and operation under dynamic conditions was found to minimise fouling. Fouling is predominantly in the form of a cake or gel layer on the membrane surface. Applying an increased crossflow velocity therefore helps to sweep foulants from the membrane surface and reduce the thickness of the foulant layer. The application of a low transmembrane pressure is expected to lead to a less compact foulant layer leading to a reduced resistance to permeate flow. Membranes with pores in the range of 0.2 – 2.0 µm were investigated, with little change in the

steady state filtration flux. This suggests that the system is not limited by the pore size but rather the foulant limits mass transfer.

Analysis carried out on the foulant layer, using a variety of analytical techniques, confirmed that most of the fouling was on the surface and was caused by a mixture of organic components and calcium.

This work also investigated cleaning of the membranes following fouling. Use of sodium hydroxide, citric acid and Ultrasil 11 gave different flux recoveries and properties following cleaning. The surfaces of the membranes have been studied to gain an insight into the mechanisms of removal during cleaning. The most effective cleaning method during the first cycle is to clean with 0.5 wt. % sodium hydroxide followed by 0.1 wt. % citric acid. This lead to a flux recovery of 86 ± 5 %. It has been hypothesised in this study that the sodium hydroxide leads to swelling of the foulant layer leading to a more open structure which increases the effectiveness of cleaning with citric acid. Citric acid allows chelation of calcium present in the foulant as well, as sodium remaining on the surface following cleaning with sodium hydroxide. The addition of sodium hypochlorite to the sodium hydroxide solution aids in improving the flux recovery with an increase ca. 5 wt. % observed. The use of Ultrasil 11 contains sodium hydroxide, surfactants and EDTA. This was therefore investigated as a one-step cleaning agent, allowing swelling and chelation to occur simultaneously. The flux recovery of 50 ± 6 % was lower than that for the two stage cleaning process. This suggests that dissolution of Gum in citric acid as well as chelation improves removal.

Multiple fouling and cleaning studies were carried out to investigate the long term impact of cleaning with sodium hydroxide/sodium hypochlorite alone and a two stage clean with sodium hydroxide/sodium hypochlorite followed by citric acid. The two stage clean outperformed that of the alkali clean alone in terms of selectivity and permeate flux. While the flux recovery was greater for the two stage clean after cycle 1, little difference was observed after multiple cycles.

Pre-treating membranes allows a method to control the surface properties with the hydrophobicity, zeta potential and adhesion strength showing marked changes following simple pre-treatments with sodium hydroxide or citric acid. The effect of pre-treatment on the selectivity and throughput has been reported in this study. While pre-treatment was not shown to reduce the fouling propensity, pre-treatment with citric acid resulted in an increase in rejection of Gum Arabic from 60 % to 85 % for the first cycle using a 0.5 μm flat sheet membrane.

IV. Contents

I. Declaration of Authorship i

II. Acknowledgements ii

III. Abstract iii

V. List of Figures xii

VI. List of Tables xvii

VII. Nomenclature xix

VIII. Abbreviations xxii

1. Introduction 1

1.1 Gum Arabic 1

1.2 Food process engineering and membranes 1

1.3 Thesis outline 4

1.4 Aims and objectives 5

1.5 Outputs and awards 6

2. Literature review 8

2.1 What is Gum Arabic? 8

2.1.1 Introduction 8

2.1.2 Composition 11

2.1.3 Nutrition 14

2.1.4 Rheology 15

2.1.5 Charge 16

2.1.6 Other 16

2.1.7 Production process 17

2.1.8 Issues with Gum Arabic waste 17

2.2 Membranes 20

2.2.1 Membrane separation 20

2.2.2 Membrane classification 20
2.2.3 Membrane performance 22
2.2.4 Membrane material 23
2.2.5 Filtration modes 25
2.2.6 Membrane configuration 26
2.2.7 Membrane flux 28
2.3 Fouling 29
2.3.1 Fouling mechanisms 30
2.3.2 Types of foulant 33
2.3.3 Flux decline due to fouling 35
2.3.4 Factors influencing fouling 36
2.3.5 Methods to reduce fouling 37
2.3.6 Rejection of solutes 40
2.4 Cleaning 40
2.4.1 Physical cleaning 41
2.4.2 Chemical cleaning 42
2.5 Membrane characterisation 44
2.5.1 Contact angle 45
2.5.2 Zeta potential 46
2.5.3 Porosimetry 49
2.5.4 FTIR 50
2.5.5 SEM 50
2.5.6 AFM 51
2.5.7 FDG 53
2.5.8 Summary 53
2.6 Membranes and wastewater 53
3. Materials and Methods 56

3.1 Introduction 56

3.2 Materials and reagents 56

3.2.1 Foulant: Gum Arabic 56

3.2.2 Water 56

3.2.3 Cleaning agents 57

3.2.4 Membranes 58

3.3 Equipment 58

3.3.1 Filtration equipment 58

3.3.2 Modifications 61

3.4 Experimental procedures 62

3.4.1 Pure water flux measurement 62

3.4.2 Fouling experiments using Gum Arabic 63

3.4.3 Rinsing conditions 63

3.4.4 Cleaning experiments 64

3.4.5 Sample collection 64

3.4.6 Pre-filtration of Gum 64

3.4.7 Static fouling 65

3.5 Gum measurements 65

3.5.1 Solids concentration 65

3.5.2 Concentration 65

3.5.3 Viscosity measurement 66

3.5.4 pH and conductivity 66

3.5.5 Chemical oxygen demand 66

3.5.6 Particle sizing 66

3.5.7 Gel permeation chromatography (GPC) 67

3.6 Membrane analysis 67

3.6.1 Effective contact angle measurement 67

3.6.2 Zeta potential 68
3.6.3 Scanning electron microscopy 69
3.6.4 FTIR 69
3.6.5 Raman 69
3.6.6 Fluid dynamic gauging 70
3.6.7 Colorimetric analysis of membranes 71
3.6.8 Atomic force microscopy 72
3.6.9 Mercury porosimetry 72
3.6.8 Modelling 73
4. Proof of concept 75
4.1 Physical properties of reconstituted Gum 75
4.1.1 Viscosity 75
4.1.2 Particle size 78
4.1.3 Chemical oxygen demand 80
4.1.4 pH 81
4.2 Membrane characterisation 81
4.2.1 Pure water flux characterisation 82
4.2.2 Use of flat sheet ceramics 83
4.3 Separation 92
4.3.1 Removal of Gum Arabic from model waste suspension 92
4.3.2 Feed and bleed filtration 93
4.4 Flux decline 95
4.4.1 Resistance in series model allowing fouling analysis 96
4.5 Discussion 98
4.6 Summary 99
5. Optimum filtration conditions 100
5.1 Filtration conditions 101

5.2 Process parameters 102
5.2.1 Static and dynamic fouling 102
5.2.2 Concentration of Gum 104
5.2.3 Crossflow velocity 106
5.2.4 Transmembrane pressure 109
5.2.5 Temperature 113
5.3 Membrane material properties 114
5.3.1 Pore size 114
5.3.2 Porosimeter data 119
5.3.3 Surface modification 120
5.3.4 Roughness 123
5.4 Solution/suspension properties 125
5.4.1 Pre-filtration 126
5.5 Characterisation 127
5.5.1 Mechanistic picture of fouling 127
5.5.2 More detailed analysis of the foulants 131
5.6 Discussion 139
5.7 Summary 141
6. Cleaning of membranes fouled with Gum Arabic 143
6.1 Cleaning conditions 144
6.2 Rinsing with water 144
6.3 Chemical cleaning 146
6.3.1 Sodium hydroxide 147
6.3.2 Sodium hypochlorite 149
6.3.3 Citric acid 151
6.3.4 Ultrasil 152
6.4 Mechanical cleaning 153

6.4.1 Backwashing 153
6.4.2 Sonication 155
6.4.3 Shear stress (FDG) 156
6.5 Cleaning temperature 160
6.6 Chemical analysis of cleaned membranes 161
6.6.1 Effective contact angle 161
6.6.2 FTIR 162
6.6.3 SEM 164
6.6.4 SEM-EDX 165
6.6.5 Zeta potential 167
6.6.6 AFM 170
6.6.7 Adhesion 171
6.7 Discussion 177
6.8 Summary 179
7. Multiple cycles – the importance of the cleaning protocol 180
7.1 Introduction 180
7.2 Flux recovery 181
7.3 Filtration flux 184
7.4 Resistance-in-series analysis 185
7.5 Removal of Gum Arabic 188
7.6 Summary and main findings of Chapter 7 189
8. Influence of pre-treatment on the fouling of Gum Arabic 191
8.1 Pre-treatment with citric acid 191
8.1.1 Rejection of Gum Arabic 193
8.1.2 Effective contact angle 194
8.1.3 Flux and Membrane resistance 195
8.1.4 FTIR and Raman spectroscopy 198

8.1.5 Zeta potential measurements 201
8.1.6 SEM-EDX 204
8.1.7 AFM 204
8.1.8 Discussion of pre-treatment with citric acid 210
8.2 Pre-treatment with sodium hydroxide 211
8.2.1 Rejection of Gum Arabic 211
8.2.2 Effective contact angle 211
8.2.3 Flux and membrane resistance 212
8.2.4 FTIR and Raman spectroscopy 214
8.2.5 Zeta potential measurements 216
8.2.6 SEM-EDX 218
8.2.7 AFM 219
8.2.8 Discussion of NaOH pretreatment 223
8.3 Summary 223
9. Conclusions, recommendations and future work 225
9.1 Conclusions 225
9.2 Recommendations 227
9.3 Future work 227
9.3.1 Hybrid system 228
9.3.2 Gum pre-treatment 228
9.3.3 Alternative membrane systems 229
9.3.4 Cleaning agents 230
10. Bibliography 231
Appendix A 246
Appendix B 249
Appendix C 264

V. List of Figures

Figure 1.1	Scrubber system currently and proposed changes	4
Figure 2.1	Wattle blossom structure of Gum Arabic	12
Figure 2.2	Proposed structure of Gum Arabic	12
Figure 2.3	Process classification of membranes	21
Figure 2.4	Principle of crossflow filtration	26
Figure 2.5	Representation of concentration polarisation	30
Figure 2.6	Schematic of pore blocking mechanisms	32
Figure 2.7	Schematic illustration of the filtration procedure	36
Figure 2.8	Model of the electrical double layer in aqueous solution	47
Figure 2.9	Schematic illustration of AFM characterisation	52
Figure 3.1	Photograph of filtration system	59
Figure 3.2	Schematic diagram of filtration apparatus	60
Figure 3.3	Photograph of membrane and housing	60
Figure 3.4	Photograph of flat sheet (plate and frame) module	61
Figure 3.5	Schematic diagram of flat sheet crossflow module	62
Figure 3.6	Fluid dynamic gauging equipment	70
Figure 4.1	Kinematic viscosity of Gum Arabic suspensions	76
Figure 4.2	Variation in viscosity with concentration and temperature	76
Figure 4.3	Reynolds numbers for Gum Arabic suspensions	78
Figure 4.4	Size distribution of Gum Arabic particles	79
Figure 4.5	Size distribution of Gum Arabic particles after 24 hours	80
Figure 4.6	COD as a function of Gum concentration	81
Figure 4.7	PWF through 0.8 µm virgin Membralox membrane at pressures 0.5 – 3 bar.	82
Figure 4.8	SEM image of 0.8 µm flat sheet membrane	84
Figure 4.9	Pore size distribution for 0.8 µm membrane	85
Figure 4.10	FTIR of virgin membrane	86
Figure 4.11	Raman spectra of virgin membrane excited at 785 nm	87
Figure 4.12	Apparent zeta potential of virgin membrane	88
Figure 4.13	AFM image of virgin membrane	90
Figure 4.14	Typical adhesion curve for virgin membrane	91
Figure 4.15	Adhesion strength across 8 x 8 µm area on virgin membrane	92

Figure 4.16	Photograph of feed, permeate and retentate samples following filtration	93
Figure 4.17	Concentration of Gum Arabic in feed and permeate throughout 100 litre feed and bleed experiment	94
Figure 4.18	Flux decline curve throughout feed and bleed experiment	95
Figure 4.19	Hydraulic resistance for 1 filtration cycle of 0.8 µm tubular ceramic membrane	97
Figure 5.1	Hydraulic resistance following static and dynamic fouling	103
Figure 5.2	Hydraulic resistance of 0.8 µm membrane during the filtration of Gum of concentrations 1.0 to 4.0 wt. %	104
Figure 5.3	Flux decline curve over 5 minutes for the filtration of 1.0 – 4.0 wt. % Gum	105
Figure 5.4	Permeate flux profile at varying crossflow velocities	107
Figure 5.5	Normalised permeate flux at crossflow velocities 1.5 – 2.3 m s^{-1}	108
Figure 5.6	Permeate flux ramping from 1.0 to 4.5 bar	110
Figure 5.7	Transient membrane flux at TMP 1.0 – 3.0 bar	111
Figure 5.8	Normalised membrane flux at TMP 1.0 – 3.0 bar	112
Figure 5.9	Influence of temperature on membrane resistance	113
Figure 5.10	Normalised flux decline (flat sheet 0.2 – 2.0 µm)	118
Figure 5.11	Normalised flux decline (tubular ceramic 0.2 – 0.8 µm)	119
Figure 5.12	Apparent zeta potential of virgin and fouled membranes	122
Figure 5.13	AFM micrographs of virgin and fouled membranes	125
Figure 5.14	Influence of pre-filtration on filtration flux	126
Figure 5.15	FTIR spectra of Gum Arabic	131
Figure 5.16	FTIR spectra of membrane fouled with Gum Arabic	132
Figure 5.17	SEM images of virgin and fouled membranes (flat sheet)	133
Figure 5.18	SEM images of virgin and fouled membranes (tubular ceramic)	134
Figure 5.19	Raman spectra of membrane and Gum	135
Figure 5.20	Typical force curve of adhesion	136
Figure 5.21	Adhesion curve for retraction of silica probe from membrane surface	137
Figure 5.22	Adhesion curve for the approach of silica probe to the membrane.	138
Figure 6.1	FTIR trace for virgin fouled and rinsed membranes	146
Figure 6.2	Membrane resistance for tubular ceramic membrane during fouling and cleaning	148

Figure 6.3	Flux recovery for tubular ceramic membrane during fouling and cleaning	148
Figure 6.4	Influence of addition of sodium hypochlorite to sodium hydroxide during cleaning	150
Figure 6.5	Influence of the concentration of NaOCl on cleaning efficiency	151
Figure 6.6	Permeate flux following cleaning in forward and backwards direction	154
Figure 6.7	Flux recovery following cleaning in forward and backwards direction	154
Figure 6.8	Lightness measurements of membrane fouled with Gum Arabic under shear stress 0 – 300 Pa	157
Figure 6.9	Redness measurements of membrane fouled with Gum Arabic under shear stress 0 – 300 Pa	158
Figure 6.10	Yellowness measurements of membrane fouled with Gum Arabic under shear stress 0 – 300 Pa	158
Figure 6.11	Photographs of Gum in cleaning solution	159
Figure 6.12	Influence of cleaning temperature on membrane performance	160
Figure 6.13	FTIR spectra of fouled and cleaned membranes	163
Figure 6.14	FTIR spectra following mechanical cleaning	164
Figure 6.15	SEM images of alkali, and alkali and acid cleaned membranes	165
Figure 6.16	SEM images of fouled membranes highlighting calcium aggregates	167
Figure 6.17	Zeta potential measurements for cleaned membranes	168
Figure 6.18	AFM images of fouled and cleaned membranes	171
Figure 6.19	Adhesion curve for the retraction of silica probe from fouled and cleaned membranes	172
Figure 6.20	Force mapping of Ultrasil cleaned membrane	174
Figure 6.21	Adhesion curve for the approach of silica probe to fouled and cleaned membranes	176
Figure 7.1	Flux recovery over 10 cycles following two cleaning protocols	182
Figure 7.2	Flux recovery compared to virgin membrane over 10 cycles following two cleaning protocols	183
Figure 7.3	Filtration flux for 4 cycles following cleaning with 2 cleaning protocols	185
Figure 7.4	Resistance in series analysis of alkali cleaned membrane over 10 cycles	186
Figure 7.5	Resistance in series analysis of two stage cleaned membrane over 10 cycles	187
Figure 7.6	Rejection coefficient over 10 cycles with 2 cleaning protocols.	189

Figure 8.1	Surface layers of alumina showing coordination of surface oxygen atoms with a carboxylic acid and citric acid.	192
Figure 8.2	Influence of pre-treatment with citric acid on the rejection of Gum Arabic throughout a 60 minute filtration	194
Figure 8.3	Influence of pre-treatment with 0.1 % citric acid on the permeate flux during the first 5 minutes of fouling cycle.	196
Figure 8.4	Raman spectra of alumina excited at 785 nm before and after pre-treatment with citric acid	199
Figure 8.5	FTIR traces of Alumina with no pre-treatment, and pre-treated with 0.1 % citric acid	200
Figure 8.6	FTIR traces of Gum Arabic, alumina fouled with Gum Arabic and citric acid pre-treated alumina fouled with Gum Arabic.	201
Figure 8.7	Comparison of zeta potential for untreated membrane and membrane treated with 0.1 % citric acid.	203
Figure 8.8	Comparison of zeta potential for fouled membranes with and without 0.1 % citric acid pre-treatment.	203
Figure 8.9	Typical approach curves for silica colloidal probe with a virgin and acid pre-treated membrane highlighting forces between the membrane and probe.	206
Figure 8.10	Adhesion distance and strength for retraction of silica probe from alumina membranes pre-treated with water and citric acid	207
Figure 8.11	Adhesion as colloidal probe approaches surface of virgin membrane and citric acid pre-treated membrane following fouling with 2.0 wt. % Gum Arabic.	208
Figure 8.12	Adhesion as colloidal probe is retracted from the surface of virgin membrane and citric acid pre-treated membrane following fouling with 2.0 wt. % Gum Arabic.	208
Figure 8.13	Influence of pre-treatment with 0.5 wt. % sodium hydroxide on the permeate flux during the first 5 minutes of a fouling cycle.	213
Figure 8.14	FTIR of membrane pre-treated with citric acid (top) and pre-treated with NaOH (bottom).	215
Figure 8.15	Membranes fouled with Gum Arabic following no pre-treatment and alkali pre-treatment	215
Figure 8.16	Comparison of zeta potential for untreated membrane and membrane	217

	pre-treated with 0.5 wt. % sodium hydroxide.	
Figure 8.17	Comparison of zeta potential for fouled membranes with and without 0.5 wt. % sodium hydroxide pre-treatment.	218
Figure 8.18	Adhesion curve for the approach of silica probe to a) membrane pre-treated with water (virgin membrane) and b) membrane pre-treated with 0.5 wt. % sodium hydroxide.	220
Figure 8.19	Adhesion curve for the retraction of a silica probe to a) membrane pre-treated with water (virgin membrane) and b) membrane pre-treated with 0.5 wt. % sodium hydroxide.	220
Figure 8.20	Adhesion strength on the approach of silica probe to membranes fouled with Gum Arabic following pre-treatment with a) water and b) sodium hydroxide.	222
Figure 8.21	Adhesion strength on the retraction of silica probe to membranes fouled with Gum Arabic following pre-treatment with a) water and b) sodium hydroxide.	222

VI. List of Tables

Table 2.1	Uses for Gum Arabic	10
Table 2.2	Estimated costs of polymeric vs. ceramic membranes	55
Table 3.1	Chemical composition of P3-Ultrasil 11	57
Table 3.2	Parameters used to model fouling mechanism	73
Table 4.1	Membrane resistance of virgin membranes	83
Table 4.2	Fouling resistances calculated using resistance in series model	97
Table 5.1	Effect of CFV on flux and solids retention of an aged membrane	108
Table 5.2	Influence of pore size of Membralox tubular ceramic membranes	117
Table 5.3	Influence of pore size on flat sheet ceramic membranes	117
Table 5.4	Mercury intrusion porosimeter data for virgin and fouled membranes	119
Table 5.5	Contact angle of virgin and fouled membranes	120
Table 5.6	S_a (mean roughness) for virgin and fouled membranes	124
Table 5.7	Experimental fit to fouling mechanisms by Hermia and Field	130
Table 5.8	Elemental composition obtained using SEM EDX	134
Table 5.9	Adhesion distance and strength measured for virgin/fouled membranes with colloidal probe	136
Table 6.1	Measured contact angle for membranes following cleaning	161
Table 6.2	Elemental analysis of fouled and cleaned membranes using SEM EDX	166
Table 6.3	Mean roughness of cleaned membranes	170
Table 6.4	Adhesion distance and strength following cleaning	172
Table 8.1	Contact angle of water on membrane surface for virgin and acid pre-treated and fouled measured by sessile drop	195
Table 8.2	Membrane resistance for 0.5 µm alumina membranes during fouling following no pre-treatment and pre-treatment with citric acid	197
Table 8.3	Normalised membrane resistance for 0.5 µm alumina membranes during fouling following no pre-treatment and pre-treatment with citric acid where the membrane resistance is set to 1.0	197
Table 8.4	Fouling mechanisms for acid pre-treated membrane	198
Table 8.5	SEM-EDX analysis of membrane surface for virgin membrane, acid pre-treated membrane and fouled membranes.	204
Table 8.6	Adhesion distance and strength between pre-treated membranes and colloidal probe.	205

Table 8.7	Adhesion distance and strength between acid pre-treated membranes which have been fouled with Gum Arabic and a colloidal probe.	207
Table 8.8	Contact angle of water on membrane surface for virgin and NaOH pre-treated and fouled, measured by sessile drop	212
Table 8.9	Membrane resistance for 0.5 µm alumina membranes during fouling following a) no pre-treatment and b) pre-treatment with 0.5 wt. % sodium hydroxide.	213
Table 8.10	Normalised membrane resistance for 0.5 µm alumina membranes during and following a) no pre-treatment and b) pre-treatment with 0.5 wt. % sodium hydroxide. The membrane resistance is set to 1.0.	213
Table 8.11	Fouling mechanism for membranes pre-treated with alkali	214
Table 8.12	SEM-EDX analysis of membrane surface for virgin membrane, sodium hydroxide pre-treated membrane and fouled membranes.	219
Table 8.13	Adhesion distance and strength between virgin and NaOH pre-treated membrane and colloidal probe.	219
Table 8.14	Adhesion distance and strength between virgin and alkali pre-treated membranes which have been fouled with Gum Arabic and a colloidal probe.	221

VII. Nomenclature

A	area	m^2
C	concentration	wt. %, gL^{-1}, ppm
C_b	bulk concentration	wt. %, gL^{-1}, ppm
C_F	feed concentration	wt. %, gL^{-1}, ppm
C_p	concentration in permeate	wt. %, gL^{-1}, ppm
E	current	mV
F	force	N
J	flux	$L\ m^2\ h^{-1}$
J_C	pure water flux following cleaning	$L\ m^{-2}\ h^{-1}$
J_W	pure water flux	$L\ m^{-2}\ h^{-1}$
J_0	pure water flux	$L\ m^{-2}\ h^{-1}$
K	fluid consistency index	$Kg\ s\ m^2$
k	spring constant (AFM)	$N\ m^{-1}$
k	conductivity (Zeta potential)	$\mu S\ cm^{-1}$
k_x	constant (blocking models) where x denotes the blocking mechanism e.g., c = cake	-
L	length (of channel or membrane thickness)	m
L*, a*, b*	CIE Lab 1976 colour space coordinates	m
m	mass ratio of wet to dry cake	-
N	number of channels	-
P	pressure	Pa, bar
Q	flow rate	$m^3\ s^{-1}$
R	resistance	m^{-1}
r	retention	-
R_a	rejection coefficient	-
R_c	cake resistance	m^{-1}
R_{C1}	resistance following first clean	m^{-1}
R_{C2}	resistance following second clean	m^{-1}
R_{CC}	resistance removed by chemical cleaning	m^{-1}
R_{cp}	concentration polarisation resistance	m^{-1}
R_f	fouling resistance	m^{-1}
R_I	irreversible resistance	m^{-1}

Nomenclature

R_L	resistance of loosely bound foulants	m^{-1}
R_m	intrinsic membrane resistance	m^{-1}
R_r	risible resistance	m^{-1}
R_T	total resistance	m^{-1}
Re	Reynolds number	-
s	mass fraction of solids in feed	-
S_a	mean surface roughness	nm
t	time	s, min
T	temperature	^oC
%T	percentage of transmission	%
u	velocity	$m\ s^{-1}$
V	volume	m^3
α	separation factor	-
α’	cake specific resistance	$m\ kg^{-1}$
γ	filtrate density (blocking laws)	$kg\ m^{-3}$
γ	interfacial energy (contact angle)	N
ΔE	difference in current	mV
ΔP	pressure difference	Pa, bar
Δt	time difference	s, minutes
ΔV	difference in volume	L
ε_0	permittivity if a vacuum	$F\ m^{-1}$
ε_r	dielectric constant of water	$F\ m^{-1}$
μ	kinematic viscosity	$m^2\ s^{-1}$
μ_p	viscosity of permeate	$m^2\ s^{-1}$
π	osmotic pressure	Pa
σ	blocked area per unit volume	m^{-1}
ζ	zeta potential	mV

Prefixes

c	centi
G	Giga
M	Mega
m	mili
n	nano
p	pico
µ	micro

VIII. Abbreviations

AFM	Atomic force microscopy
AG	Arabinogalactan
AGP	Arabinogalactan-protein complex
ATR	Attenuated total reflection
BOD	Biological oxygen demand
BSA	Bovine serum albumin
CA	Citric acid
CFV	Crossflow velocity
CIP	Clean in place
CML	Carboxylate modified latex
COD	Chemical oxygen demand
COP	Cleaning out of place
CP	Concentration polarisation
CSCT	Centre for Sustainable Chemical Technologies
DRIFTS	Diffuse reflectance infrared transform spectroscopy
EDTA	Ethylenediaminetetraacetic acid
EDX	Energy dispersive X-ray spectroscopy
EPS	Extracellular polymeric substances
EPSRC	Engineering and Physical Sciences Research Council
EU	European Union
FAO	Food and Agricultural Organisation of the United Nations
FDG	Fluid dynamic gauge
Fn	Fouled n times $n \geq 1$
FnCx	Fouled n times and cleaned x times n, $x \geq 1$
FTIR	Fourier transform infra-red spectroscopy
FR	Flux recovery
GA	Gum Arabic
GCMS	Gas chromatography mass spectrometer
GP	Glycoprotein
GPC	Gel permeation chromatography
HPSEC	Hydrophobic interaction chromatography
IEP	Isoelectric point

IET	Institution of Engineering and Technology
LUT	Lappeenranta University of Technology
MF	Microfiltration
MW	Molecular weight
MWCO	Molecular weight cut off
NaOCl	Sodium hypochlorite
NaOH	Sodium hydroxide
NF	Nanofiltration
NMR	Nuclear magnetic resonance
NOM	Natural organic matter
PT	Pre-treat
PWF	Pure water flux
RFD	Relative flux decline
RIS	Resistance in series
RO	Reverse osmosis
RSC	Royal Society of Chemistry
S_a	Mean surface roughness
SANS	Small angle neutron scattering
SDS	Sodium dodecyl sulphate
SEM	Scanning electron microscopy
TDS	Total dissolved solids
TEM	Transmission electron microscopy
TMP	Transmembrane pressure
TSS	Total suspended solids
UF	Ultrafiltration
UK	United Kingdom
USA	United States of America
UV	Ultraviolet
ZP	Zeta potential

1. Introduction

1.1 Gum Arabic

Gum Arabic is widely used industrially, particularly in the food industry, and is often known as E414.[2] It has excellent emulsification properties leading to its use in the production of soft drinks for the encapsulation and dispersion of flavour oils. Gum Arabic originates as an exudate from *Acacia* trees found mainly in sub Saharan Africa.[3, 4] Gum is obtained through a tapping process whereby the trees exude Gum Arabic as a defence mechanism. More than 90 % of commercial Gum Arabic is obtained from wild trees.[5] Worldwide the industry was valued at $578.7 million in 2014, and this is expected to increase to $800.3 million by 2019.[6]

Gum is tapped from the trees and golden aggregates are collected by hand. These aggregates are then sorted and selected based on quality and sent to market.[3] Companies such as *Kerry Ingredients* take the Gum, and process it into a spray dried powder suitable for industrial applications.[7] During this processing the Gum is dissolved in large quantities of water before going through coarse filters allowing the removal of bark, sand and other contaminants. The Gum is also heated to allow pasteurisation.[8] Finally, the Gum is spray dried before being packaged. During the spray drying process water is removed from the system. This water contains ca. 2.0 wt. % Gum Arabic. The disposal of this water is an expensive process with land injection required due to the high BOD and COD associated with Gum waste.

Gum Arabic is composed mainly of high molecular weight polysaccharides and their calcium, magnesium and potassium salts.[9] The main sugars in Gum Arabic are arabinose, galactose, rhamnose and glucuronic acid. The discoveries of both galactose and arabinose were made from Gum Arabic, this leads to their naming after Gum Arabic.[10] The functional component of Gum Arabic is an arabinogalactan-protein complex which leads to its excellent emulsification properties.

1.2 Food process engineering and membranes

There is currently the need and drive to make processes in all industries more sustainable. The provision of food, water and energy in a sustainable and affordable manner are some of the key issues facing 21st Century society. Food process engineering plays an important part in each of these areas.[11] In 2013 the IChemE produced a roadmap detailing key resources which should be focused on, and reduced, with both water and energy being considered as key resources which

need to be protected.[12] Water use has been growing at twice the rate as the population within the last century, and while there is not yet a global water scarcity issue as such, this is likely to happen over the next few decades.[13] It is therefore important to consider the ways in which water can be recycled with a low energy penalty. One promising solution which allows for the recovery of both water and products is membrane filtration.

As with most industries, the food industry requires continual update, refinement and process optimisation. With this there is the requirement for innovation. In terms of production, biotechnology and advanced farming techniques allow crop intensification. Food scientists and engineers generally have responsibility for processes, combining ingredients, ensuring hygienic production and food safety. While these are of great importance, scientists and engineers should also be responsible for making controlled physiochemical and biochemical changes to food products. Yanniotis *et al.* reported that there are four cornerstones which could help promote innovation and improvements to the food process engineering sector, in which research should be carried out:[11]

i) Process efficiency improvement – saving water and energy while minimising pollution and waste. This allows a reduction in the cost and environmental impact without reducing quality
ii) Development of adjusted food processes and products – this allows a better understanding of the microstructure and chemical interactions leading to improved products
iii) Food safety assurance – hygienic design of equipment and packaging allowing improved food safety
iv) Product quality improvement by intelligent design – this allows automation and improvement in process control. This can result in improved management of production lines creating better flexibility.

This project aims to consider the first of these cornerstones by conducting research into improving the efficiency during the production of Gum Arabic, allowing a reduction in waste and saving water.

One industry where much research has previously been carried out in the area of filtration is the dairy industry. This demonstrates advancements in processing. Milk is received and must be cooled, stored and tested. Following this pasteurisation, homogenisation and standardisation are carried out, and only after this can the milk be bottled and sent to market, or for further processing

to make products such as yoghurt and cheese. Each operation involves individual pieces of equipment which require continual development, refinement and require energy for use and cleaning. An innovation occurred in this industry through the development of the simultaneous emulsification and mixing nozzle allowing a reduction in energy consumption by up to 90 %.[14] The requirement for capital expenditure was also reduced as the homogenisation and mixing processes can be combined.

The dairy industry also provides a good case study for the use of membrane technologies. Many advancements in microfiltration and ultrafiltration for the food industry have arisen from dairy applications.[15] Membrane technologies have been used to reduce the water use for cheese making, allow cold pasteurisation, and they can also be used to separate streams for added value.[16-19] Membranes can be operated under ambient conditions, allowing a low energy requirement, and they can be easily scaled up.

The application of membranes to the processing of Gum Arabic has previously been studied by Decloux *et al.*[20] and Bechervaise and Bird,[21] with the earliest studies carried out in 1996. This highlights the novelty of this project. No previous work has currently been carried out on water recovery, or the reuse of Gum Arabic from waste streams. This forms the basis of this project. The use of membranes offer a low energy method of separation compared to other methods such as distillation, for this reason they have been chosen for use in the project.

There are limitations to the application of membrane processes to the food industry, with membrane fouling being the most severe. Fouling is the deposition of unwanted materials limiting the flow rate and reducing throughput. Membrane fouling is complex and crosses a wide range of scientific disciplines leading to interplaying phenomena. Fouling is described in more detail in Section 2.3. Understanding why fouling occurs and how it limits the membrane performance allows chemical engineers to make rational decisions in improving the process. This thesis focuses on membrane fouling and subsequent cleaning to gain an insight as to how microfiltration can be effectively applied to improve the process efficiency of Gum Arabic. Figure 1.1 illustrates the current process, indicating the plant which should remain (in black) and the plant which should be removed to reduce the waste production (in red). It is proposed that replacing the red plant with the microfiltration system (in green) will allow recycling of the water and recovery of Gum Arabic.

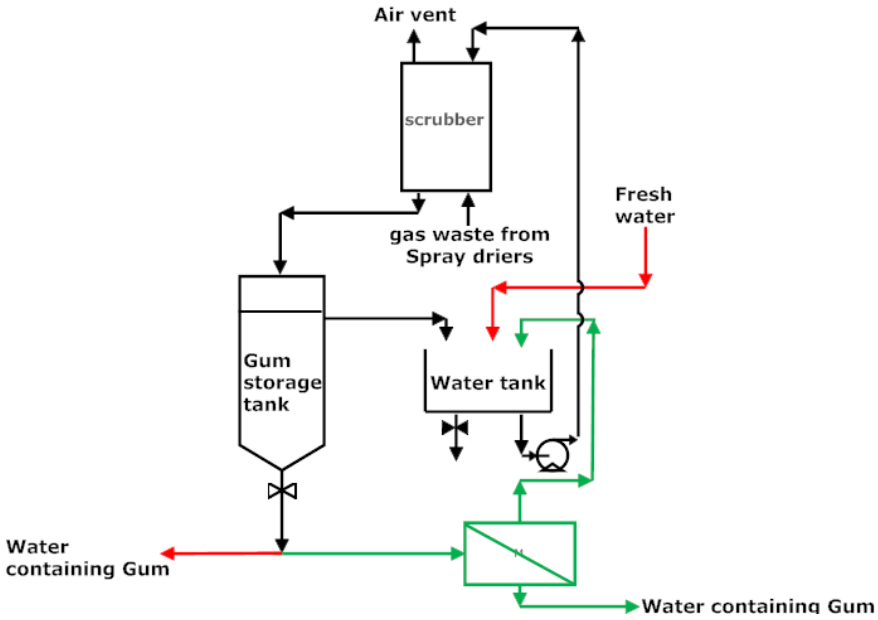

Figure 1.1: Scrubber system current (black/red) and proposed (black/green).

1.3 Thesis outline

This thesis has been divided into nine chapters, five of which are the results and discussion of experimental work carried out to meet the aims and objectives set out in Section 1.4. Each results chapter contributes towards the general scope of the thesis. The overall aim was to gain an understanding into the fouling and cleaning during the microfiltration of Gum Arabic. This aim was in part to lead to an improvement in the process efficiency for the industrial processing of Gum Arabic.

Chapter 2 presents a review of current literature and scientific theory around the areas of membrane filtration and Gum Arabic. This allows the research to be contextualised.

Chapter 3 details the materials used, and the methods by which experimental work was carried out.

Chapter 4 reports and analyses the properties of Gum Arabic and membranes as well as showing that microfiltration offers a promising solution in waste management.

Chapter 5 investigates and reports the optimum conditions required to minimise fouling, while also gaining an understanding of why fouling is occurring.

Chapter 6 discusses the requirement for cleaning following membrane fouling. It details the effectiveness of different cleaning agents leading to an insight about the mechanisms of removal of the foulant layer.

Chapter 7 demonstrates the impact of the aging process on membranes over multiple foul and clean cycles. This offers a perspective on the synergy between fouling and cleaning.

Chapter 8 describes the influence of pre-treatment of the membranes with two cleaning agents, and discusses the impact this has on separation as well as the fouling propensity.

Chapter 9 concludes the results presented in Chapters four to eight. It also presents ideas for further study surrounding the area of membrane filtration of Gum Arabic.

1.4 Aims and objectives

This thesis focuses on membrane fouling and subsequent cleaning to gain an insight as to how microfiltration can be effectively applied to improve the process efficiency of Gum Arabic processing. In order to achieve this aim, the research objectives were:

- Evaluate the feasibility of microfiltration technology to remove Gum Arabic from model waste streams
- Investigate the properties of alumina membranes and a model waste solution
- Study factors influencing the selectivity and permeate flux including process parameters, membrane material properties and solution properties
- Characterise changes made relating to the surface science of the membrane and foulant
- Develop an effective cleaning strategy allowing the membranes to be reused following fouling, and to gain an understanding of the interactions between the membrane, foulant, and cleaning agent
- Consider the aging of membranes and how this is influenced over multiple cycles with different cleaning agents
- Explore the application of pre-treatment on membrane selectivity and fouling propensity

1.5 Outputs and awards

Oral presentations at national and international conferences

'Product and water recovery from Gum Arabic waste streams' presented at 7th IWA Specialised Conference and Exhibition on Membrane Technology in Water and Wastewater Treatment, Toronto, Canada. 25th – 29th August 2013

'Product and water recovery from Gum Arabic waste streams using membranes' presented at CSCT summer showcase, Bath, UK. 16th – 18th September 2013

'Understanding Fouling and Cleaning of ceramic membranes during the separation of Gum Arabic from water during processing' presented at Fouling and Cleaning in Food Processing, Cambridge, UK. 31st March – 2nd April 2014

'Surface interactions occurring during the microfiltration of Gum Arabic feeds using ceramic membranes' presented on my behalf by Dr. Darrell Patterson at International Congress on Membrane and Membrane Processes, Suzhou, China. 20th – 25th July 2015

Poster presentations at national and international conferences

'Investigating fouling and cleaning during the filtration of Gum Arabic' presented at Gums and Stabilisers for the Food Industry, Wrexham, UK. 5th – 9th May 2013

'Fouling and cleaning phenomena during the recovery of Gum Arabic from aqueous streams by filtration' presented at CSCT summer showcase, Bath, UK. 7th – 9th July 2014

'Developing an understanding of the fouling and cleaning phenomena during the recovery of Gum Arabic from aqueous streams using microfiltration' presented at CSCT summer showcase, Bath, UK. 6th – 8th July 2015

Awards

Royal society of Chemistry (RSC) travel grant

Institution of Engineering and Technology (IET) travel award

Energy YES winner 2014

Runner up for University of Bath 2nd year Chemical Engineering departmental presentation

Publications

Conference paper: ‘Fouling and cleaning of ceramic membranes during the dewatering of Gum Arabic waste streams’ in Fouling and cleaning in food processing: Green cleaning 2014, P 257-264. University of Cambridge, 2014.

2. Literature review

This chapter gives an overview of research which has been carried out on Gum Arabic as well as the classical theory of membrane technology. It aims to include an overview of up to date literature surrounding membrane technologies for the food industry, and how this can be applied to improve the efficiency and sustainability of Gum Arabic processing.

2.1 What is Gum Arabic?

2.1.1 Introduction

Gum Arabic is an exudate from the branches and stems of the acacia tree.[2] It is the oldest and most widely used of all tree exudates and is produced as part a natural defence mechanism.[3, 22] It has been used as an article of commerce for over 5000 years, having started out as an adhesive in mineral pigments and for the flaxen wrappings used in embalming mummies.[3] Despite there being over 1000 different species of the acacia tree, *Acacia senegal* (hashab) and *Acacia seyal* (talha) are most widely used commercially due to the superior properties they possess.

2.1.1.1 Background and origin

Gum Arabic is named after its place of origin / port of export. It can be grown in the semi-arid areas of Australia, India and America, but is mainly found in the wide belt of semi-arid land stretching across sub-Saharan Africa known as the 'Gum belt'.[3, 4, 23] The Gum belt extends over Benin, Burkina Faso, Chad, Eritrea, Ethiopia, Mali, Mauritania, Kenya, Niger, Nigeria, Senegal, Somalia, Sudan and Uganda.[4] Sudan is the world's largest producer and exporter of Gum Arabic, with 80 – 90 % of the world market.[4, 6] The best quality Gum is also traditionally associated with Sudan.[3] The biggest importer is Europe, with France and the U.K. having the largest markets for Gum Arabic. The highest quality Gum is found in the Sudanese Kordofan region, and this is used as the benchmark when determining the quality obtained from other areas.[4]

Gum Arabic formation (gummosis) is promoted when the tree is subject to stress conditions such as drought, heat, and attack by insects or systematic wounding (tapping).[3, 23] Virtually all Gum harvested comes from the tapping of trees. At the beginning of the dry season (end of October/ beginning of November) incisions are made in the branches and bands of bark are stripped off.

After 5 weeks the Gum has hardened and can be picked off and collected for cleaning and grading. This process may be repeated for 5 or 6 collections depending on the weather conditions and health of the tree.[4]

The FAO and EU have defined Gum Arabic as "a dried exudation obtained from the stems and branches of *Accacia Senegal* or closely related species of Acacia. It consists mainly of high molecular mass polysaccharides and their calcium, magnesium and potassium salts, which on hydrolysis yield arabinose, rhamnose and glucuronic acid." The EU specification also adds that the molecular mass should be ~350000 g mol^{-1}. However there is little scientific justification for this.[3]

2.1.1.2 Uses

Gum has a wide range of uses across many industries. It is one of the most widely used biopolymers on an industrial scale.[24] Gum has a large number of food applications (E-number 414)[2] due to the wide range of properties it possesses. Gum is completely soluble in water and shows excellent emulsification properties, attributed to the arabinogalactan-protein fraction.[25, 26] It has a hydrophobic polypeptide backbone and hydrophilic carbohydrate units which stabilise the emulsion at the oil-water interface. Jayme *et al.* reported that the steric contribution is dominant in stabilising emulsions with Gum Arabic, however the electrostatic contribution is also important.[24] Table 2.1 illustrates some of the wide range of industries and uses of Gum Arabic.

Table 2.1: Uses for Gum Arabic[2, 4]

Industry	**Function**
Confectionary	Provides clarity (e.g. wine gums) Prevents sucrose crystallisation Provides a controlled flavour release Texture modification (provides fibrous fruit like texture) Coating agent (e.g. chewing gum) Pigment stabiliser
Aerated confectionary (e.g. marshmallows and meringues)	Whipping agent Stabilising agent[9]
Soft drinks	Emulsifier[9, 27, 28]
Beer	Foaming agent
Pharmaceuticals	Suspending agent Emulsifier Adhesive Binder for tablets[27]
Cosmetics	Stabiliser (in creams and lotions) Viscosity increaser (lotions) Adhesive agent (blusher) Foam stabiliser (liquid soap)
Lithography	Preparation of etching and plating solutions
Paints	Dispersant[27]
Textiles	Thickening agent for printing pastes
Ink and pigments	Dispersant
Ceramics	Dispersant
Polishes	Dispersant
Other	Stabilisation of metal nanoparticles and nanotubes[25]

Over the years, there have been investigations to find alternatives to Gum Arabic which are more cost effective and offer security of supply. However the alternatives have proved to be poor substitutes particularly for emulsification applications. Gum Arabic has the ability to form stable emulsions over a wide pH range and in the presence of electrolytes. Finding an alternative which is stable over such a broad range is a huge challenge.[24] Gum Arabic possesses a unique combination of functionalities which have not been found in any alternative product therefore complete substitution is impossible.

2.1.2 Composition

2.1.2.1 Structure

Gum Arabic is complex and much work has been carried out to try and identify its structure. Gum can exist in a number of forms[4] making the understanding of its structure more of a challenge. Research on Gum Arabic has been on-going for around 70 years,[29] yet the structure is still not completely agreed on. Gum is a branched chain complex polysaccharide,[2] which may be neutral or slightly acidic. It can be split into three main fractions; arabinogalactan, arabinogalactan-protein complex and glycoprotein. These components can be separated through fractionation.[30, 31] Due to the presence of protein and polysaccharide, Gum Arabic possesses amphiphilic character. The exact composition and molar mass of Gum depends on its source, and is affected by factors such as the age of the tree, climatic conditions and soil environment.[3] Gum formed by Acacia Senegal has a molar mass ca. 380,000 g mol^{-1} and a typical composition of:[9]

- 39 - 44 % galactose
- 24 - 27 % arabinose
- 12 – 16 % rhamnose
- 14 – 16 % glucuronic acid
- 1.5 – 2.6 % protein
- 0.22 – 0.39 % nitrogen
- 12.5 – 16.0 % moisture

Gum typically exists as a mixed magnesium, calcium and potassium salt, with the composition dependent on where the Gum is grown, and the minerals present in the soil.[4]

Around 93 % of the structure of Gum Arabic is associated with the core carbohydrate – arabinogalactan (AG).[32] Two main hypotheses have been formed about the structure of Gum. Qi *et al.*[29] suggested a 'twisted hairy rope' structure, whereas many others have suggested a wattle blossom structure. [2, 23, 24, 33-38] The wattle blossom structure is more commonly accepted as the proposed structure and is illustrated in Figure 2.1. There are a limited number of high resolution techniques which can be used to effectively identify the structure of Gum Arabic due to its complex nature and ability to change both chemically and structurally.[27] A number of processes have been investigated recently which provide further evidence for the wattle blossom structure. Al-Assaf *et al.* looked at enzyme digestion along with gel permeation chromatography (GPC). They showed a high molecular weight peak (AGP) can be broken down into a single peak with a similar

molecular weight to the AG fraction.[9] This provides further evidence for the wattle blossom structure as it suggests AG units are attached to a polypeptide chain via hydroproline.

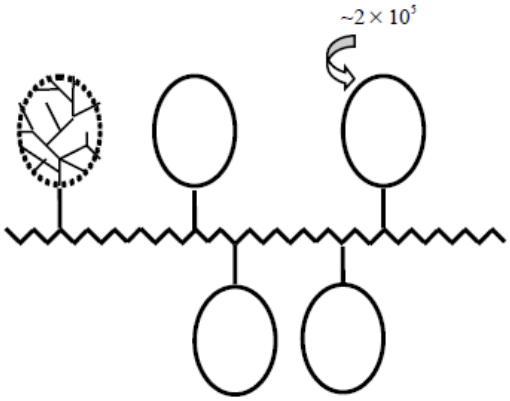

Figure 2.1: Wattle blossom structure model of Gum Arabic, reproduced from Jayme *et al.,* arabinogalactan blocks are shown linked to a polypeptide chain.[24]

Recently Nie *et al.* used GC-MS and NMR to determine more about the structure of Gum Arabic.[32] Their results are in agreement with the highly branched wattle blossom model, confirming the structure is a highly branched polysaccharide with a backbone composed of 1,3-linked galactopyransyl residues substituted at O-2, O-4 or O-6 positions. The proposed structure is shown in Figure 2.2 below.

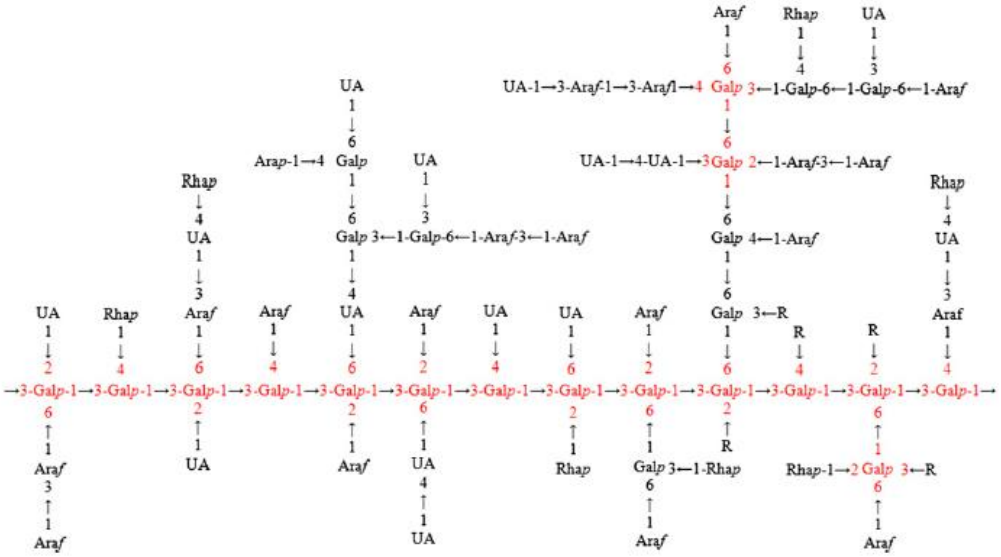

Figure 2.2: Proposed structure of Gum Arabic, reproduced from Nie *et al.* R is one of the following residues: T-Rha*p*1, T-$_L$-Ara*f*1, T-$_L$-Ara*p* 1, T-UA1, T-$_L$-Ara*f*1, 3-$_L$-Ara*f*1, T-UA1, 4-UA1. All of the galactose and uronic acid are in β-$_D$ form, and all of the arabinose and rhamnose are in the α-$_L$ form.[32]

2.1.2.2 Arabinogalactan

Arabinogalactan (AG) is the main component, and accounts for ca. 90 % of the Gum.[39] It has a molecular weight of 2.8 x 10^5 g mol^{-1} (observed from dynamic light scattering) and contains only about 0.35 % protein.[9, 39] Much research has been carried out to find out the structure of the AG component, with Sanchez *et al.* proposing that it has a thin disc (elliptical) morphology with a thickness below 2 nm. This has since been confirmed by a number of other research groups including Nie *et al.* who studied the structure in great detail using a combination of GC-MS and NMR.[22, 23, 32, 40]

The core carbohydrate structure of the AG component is composed mainly of arabinose (35.5 %), galactose (27.3 %) and galacturonic acid (13.7 %) with small amounts of rhamnose (1.8 %) and glucoronic acid (0.6 %).[41] The backbone of the AG component is made up of 1,3-linked galactopyranosyl residues which are substituted in the O-2, O-4 and O-6 positions. The AG fraction of Gum Arabic is very stable, and is not effected by enzyme hydrolysis.[22] This suggests that the peptide backbone is inaccessible to the enzymes, and this occurs in both acidic and alkaline conditions.[32]

2.1.2.3 Arabinogalactan-protein complex

The arabinogalactan-protein complex (AGP) is responsible for the emulsification and adhesion properties of Gum.[9] It makes up ca. 10 % of the total Gum and has a much larger molecular mass than the AG fraction, ca. 1 – 2 x 10^6 g mol^{-1}.[23, 39] Around 10 % of the AGP component is protein, accounting for approximately 50 % of the total protein in the Gum. AGP consists of a polypeptide chain, possibly containing 250 amino acids, with short arabinose side chains, and much larger blocks of carbohydrate with a molar mass of 4.0 - 4.5 x 10^4 g mol^{-1}.[23, 32] The carbohydrate has a highly branched structure, and this is consistent with the wattle blossom structure (Figure 2.1). The polysaccharide moieties (carbohydrate) are linked through amino acid residues, primarily *O*-serine and *O*-hydroxyproline, to the protein backbone.[42] The AGP complex adopts a compact conformation of ca. 36 nm.[23, 40] The AGP component of Gum Arabic can adopt one of two distinct conformations depending on the molecular weight.[22] The use of SANS measurements has shown the conformation exists as a tri-axial ellipsoid or an elliptical cylinder.[22]

The AGP fraction of Gum Arabic can be broken down into smaller units which are very similar in size to the AG fraction. A number of different authors have investigated the hydrolysis of AGP as

they try to fully understand the Gum structure. It has been reported that hydrolysis of the AGP unit leads to very similar units to the AG fraction of Gum, this can be done either enzymatically (e.g. using prolytic enzyme)[22] or chemically (e.g. sodium borohydride/ sodium hydroxide).[23] Al-Assaf *et al.* reported that filtration using small pore sizes could be an alternative method to dissociate the AGP fraction.[9] Filtration leads to the dissociation of AGP into smaller AG and GP units with the breaking of some covalent bonds. The different methods of degradation of the AGP unit lead to the formation of different units. Renard *et al.* investigated the use of proteases to determine the method of assembly of the AGP units, and concluded that covalent linkages seems a more likely hypothesis than hydrophobic interactions or hydrogen bonding due to the action of the proteases.[22]

2.1.2.4 Glycoprotein

The final and smallest component of Gum is glycoprotein (GP). This is only ca. 1 % of the total Gum and has a molecular mass ca. 2 x 10^5 g mol^{-1}.[23] The glycoprotein has the largest amount of protein of any of the Gum components.[8, 39, 43] The GP fraction contains different amino acid compositions from both the AG and AGP fractions, and is rich in hydroxyl, proline and serine.[9] It has also been observed that this fraction contains significantly less sugar than either the AG or AGP fractions. Motlagh *et al.* reported that the protein contains a number of disulphide linkages.[27] The GP structure seems to be the most stable. Mahendran *et al.* reported that this component is not degraded by the prolytic enzyme.[23] As there are no glycoprotein standards it can be a great challenge to quantify the GP fraction of any particular Gum sample.[27]

Both of the AGP and GP components have polyproline II, β-sheet and random coil secondary structures, but no secondary structures have been reported for the AG component.[23]

2.1.3 Nutrition

Gum Arabic has been studied for its benefits to health, due to the wide use in the food industry. Ali *et al.* carried out a review of many studies to determine the biological effect of Gum Arabic.[2] It was found that Gum Arabic is completely safe for ingestion, with no change observed to rats when Gum Arabic was added as a dietary component. Gum Arabic has very little calorific value in humans.[5]

There is some dispute about the antioxidant properties of Gum Arabic. Al-Majed *et al.* suggested that when Gum Arabic was administered to rats an antioxidant mechanism occurred leading to a cardio-palliative effect,[44, 45] however Ali found that there was no change in the level or free radicals, ascorbic acid or lipid peroxidation after 8 days.[46] Based on the studies carried out and information available it cannot be claimed that Gum Arabic has antioxidant effects.

The influence of Gum Arabic on intestinal adsorption has been widely studied. It has been shown in rats that the addition of Gum Arabic to the diet increases the adsorption and can reverse diarrhoea.[47-49]

2.1.4 Rheology

The rheology of Gum Arabic has been studied by a number of research groups.[50-53] There is some discrepancy between the characteristics. Gum Arabic is generally considered to behave as a Newtonian fluid due to the highly branched structure of the arabinogalactan component.[54] Some authors have reported Gum to be shear thinning at low shear rates (<10 s^{-1}). Newtonian behaviour is agreed on for high shear rates (>100 s^{-1}).[51] Recently Li *et al.* looked at the molecular associations in Gum and have suggested that the shear thinning behaviour observed at low shear rates is due to the elastic contribution to the stress.[50] The apparent stress is elastic like and this leads to a larger number of molecular associations in the Gum leading to a deviation from Newtonian behaviour. At large shear stresses, only the viscous contribution is dominant and complete breakdown of molecular association occurs. Under these conditions the Gum Arabic solution shows Newtonian behaviour. The low viscosity has been attributed to the highly branched structure introducing a relatively compact shape.[25, 51]

Other reports suggest that the concentration of Gum Arabic is the major factor in the rheology. Panda *et al.* reported that at concentrations below 40 wt. % the Gum exhibits Newtonian behaviour and above 40 wt. % the Gum shows pseudo plastic characteristics. Gum has also been shown to swell leading to the formation of a non-sticky gel.[5] At the concentrations and conditions used in this study Gum Arabic exhibits Newtonian behaviour.

2.1.5 Charge

Gum Arabic is a charged molecule, largely due to the amino acid groups and uronic acid. In solution/suspension Gum Arabic has a pH of approximately 4.5, however this varies from sample to sample due to natural variation in the Gum.

Dror *et al.* suggested that the zeta potential of Gum Arabic has a relatively low value (-20 mV) and an isoelectric point of pH 1.8. Based on these relatively low values they suggested charged electrostatic repulsion does not play a dominant role in the stabilisation of emulsions, but rather the stabilisation mechanism is controlled by steric repulsion.[25]

2.1.6 Other

The structure and properties of Gum Arabic are not only influenced by the origin of the Gum, they can also be affected by changes in pressure, temperature or pH. When Gum Arabic is exposed to high temperatures the protein structure has been shown to be denatured resulting in a larger droplet size in an oil and water emulsion.[55] As well as heat treatment, high pressures can also result in denaturation of the protein leading to changes in the functional properties of biopolymers. High pressures (100 MPa to 1GPa) can influence the hydrogen bonding and electrostatic interactions in proteins, however the primary structure of Gum Arabic seems not to be affected. A high hydrostatic pressure can denature and aggregate proteins, and also cause protein gelation due to an effect on the disulphide bonds. Gel forming properties of Gum Arabic have been shown to be affected by high pressures (800 MPa).[26] As well as structure, Ma *et al.* showed that applying a high pressure could influence the emulsification properties. It was suggested this is as a result of reducing the hydrodynamic volume through interlinking of the sugar chains. [26] Gum Arabic can by hydrolysed with a strong base.[27]

The main component of Gum is polysaccharide based. Therefore, it is important to consider some properties and tendencies of polysaccharides when considering Gum Arabic. Polysaccharides have a tendency to associate in aqueous solutions, which influences the molecular associations and can have a profound effect in the performance of a given application (e.g. emulsification) due to influences in the molecular weight, size and shape.[9] Hydrogen bonding, hydrophobic association, ion mediated association, electrostatic interactions, concentration dependence and presence of proteins can all effect the behaviour of Gum Arabic.[9]

2.1.7 Production process

In order for Gum Arabic to be used as a food additive it needs to undergo processing to remove any bark, bacteria and contaminants. Due to the nature and collecting method of the Gum, there may be a lot of impurities which need to be removed and there are a number of different processing steps required. Firstly the raw Gum undergoes mechanical grinding, in a process called kibbling, which breaks down the Gum into particles of specific sizes.[3] The Gum is then dissolved in large quantities of water to allow filtration to remove impurities. In the aqueous state, Gum is pasteurised to kill any bacteria and then can undergo spray drying or roller drying.[3] Spray drying is a technique commonly used with polysaccharides and involves the elimination of water from solutions through spraying the solution in a current of hot air.[9]

During the processing the Gum is subject to a number of temperatures; the Gum may be heated to 70 – 80 °C during the pasteurisation step. This and the mechanical grinding can lead to a change in the composition of Gum Arabic.[3] During the spray drying process aggregation of the Gum can occur through hydrophobic associations leading to changes in the surface properties of the peptide moieties, as the protein begins to unfold, making them more hydrophilic.[9] It has been noticed that a strong aggregate peak is formed in spray dried samples when compared to raw Gum due to these harsh processing conditions.[9]

The spray drying process involves the elimination of water from the Gum, however this process is only around 90 % efficient meaning that ca. 10 % of Gum Arabic is lost into the water stream which comes off the spray driers. This results in very large quantities of water containing a concentration of ca. 2.0 wt. % Gum Arabic which is a challenge to dispose of and can be a pollutant due to the high biological and chemical oxygen demand of this stream.[1]

2.1.8 Issues with Gum Arabic waste

The behaviour of Gum Arabic in solution has been investigated but it is still not very well understood. As it is a polysaccharide it has the tendency to associate in aqueous solutions.[9] Molecular associations can profoundly affect the performance for of a given application due to influences in molecular weight, shape and size.

During processing large quantities of water are required for the dissolution of Gum. Following spray drying ca. 10 % of the product may be lost in the waste stream. This has negative effects both on production efficiency and water reuse. Currently water has to be tankered away due to

the high chemical and biological oxygen demand associated with waste Gum Arabic solutions.[7] This is wasteful, therefore determining a method of separation to allow reuse of both water and Gum Arabic is required to improve the sustainability and efficiency of the process.

2.1.8.1 Temperature at which structure change occurs

Heating Gum Arabic at 110 °C leads to a maturing process which changes the properties. These changes can occur from 50 °C depending on the conditions. During the maturing process the molecular weight and viscosity of the Gum initially decrease. This is due to the dissociation of the protein component, and possibly also due to the elimination of intermolecular hydrogen bonds. After heating for around 2 hours the molecular weight increases and the GP fraction completely disappears.[9] Filtration of Gum Arabic has been shown to reverse this process with around 100 % recovery being reported by Al-Assaf *et al.* following filtration.[9] This indicates the role of hydrophobic interactions.

2.1.8.2 Potential use of size exclusion as a separation process

The particle size of Gum Arabic has been well studied in identifying the structure. Of the three components the AGP is the largest and most functional component; therefore ensuring it can be recovered is of great value. Renard *et al.* studied the shape and size of the isolated AGP component from Gum Arabic using small-angle neutron scattering (SANS), transmission electron microscopy (TEM) and hydrophobic interaction chromatography (HPSEC-MALLS).[56] The molecular weight was observed to be 1.86 x 10^6 g mol^{-1} which is in good agreement with that measured by Mahendran *et al.* previously.[23] The SANS results were fitted using a model based on the thin elliptical cylinder and oblate ellipsoid shapes previously determined by Sanchez.[40] Based on these results the length of the AGP particles are 58 nm for the elliptical cylinder and 75.4 nm for the oblate ellipsoid models. The use of TEM agreed with these size measurements with the presence of two general particle sizes and shapes. There was an elongated shape with a length 80 – 100 nm and width 20 – 30 nm, and an anisotropic spherical shape with a diameter between 50 and 70 nm. It was also noticed that larger aggregates were present, however it was unknown if these were due to the sample preparation or the nature of the Gum. The presence of aggregates has also been reported by Dror *et al.* in low concentration aqueous Gum solutions suggesting that it is likely to be due to the nature of the Gum.[25] Recently Lopez-Torez *et al.* carried out work into

the structure of Gum Arabic in solution, and found that Gum macromolecules adopt an ellipsoid structure which has an average radius of 30 nm.[57]

The size of Gum Arabic particles is much larger than the size of water molecules, this means that size exclusion can be used as a possible method to separate Gum from aqueous solutions.

2.1.8.3 Use of membrane separation

One method to separate out components through size exclusion is membrane technologies. One great advantage of the application of membranes as a separation process is that they can be operated at ambient temperatures. This allows a reduction in both costs and the environmental impact.[58] The use of membranes does not require additives and low temperature operation means there is less energy consumption compared with other separation processes.[59] They may however be required to operate at higher temperatures to minimise microbial growth, lower viscosity or the retentate (thus lowering pumping cost) and to improve the mass transfer and flux.[60]

The unique properties of membranes allow up scaling and downscaling, and they can easily be integrated into other processes.[58] This suggests they are a suitable process to investigate for improving the efficiency and sustainability of Gum Arabic processing to allow recycling of water and Gum Arabic.

2.2 Membranes

2.2.1 Membrane separation

Filtration is traditionally the separation of particulate material from a fluid mixture by passing the fluid through a porous material (the filter) which retains the solids on or within itself. A membrane is an interface which divides two bulk phases. Separation processes using membranes effectively began over 50 years ago with simple organic molecules. For example cellulose was used for the desalination of water.[61] Over the last three decades membranes have attracted the attention of chemists, chemical engineers and bioprocess engineers due to their unique separation principle – efficient separation and selective transport when compared to other unit operations.[58]

Membrane filtration as a mechanism for separation, is defined by 'the pressure driven separation of components of a fluid mixture by selective permeation through the membrane separating the concentrate (or retentate) stream from the permeate stream'.[62] The phase flowing into the membrane is classified as the feed stream, and the phase which is transmitted through the membrane is classified as the permeate stream. In crossflow filtration there is a third stream present, the proportion of the feed which is not transmitted. This stream is transported away from the membrane and is often referred to as the concentrate, or retentate.

A membrane has the ability to transport one or more components more readily than the others due to differences in the chemical and/or physical properties between the membrane and permeating components. A driving force is applied to the feed to allow separation; this may be in the form of a pressure, concentration, electrical potential or temperature difference.[62] In this thesis pressure difference is used as the driving force as it is most appropriate for the feed concerned and is commonly used in industrial processes.

2.2.2 Membrane classification

Membranes are classified by their pore size or molecular weight cut off (MWCO), and can be separated into four distinct categories. The largest of these is microfiltration (MF) which is generally considered to have pore sizes between 0.1 and 5 μm. The next classification is ultrafiltration (UF). For ultrafiltration the pore sizes are usually in the range of 10 – 100 nm, however they are generally classified by the molecular weight cut off of 2000 – 200 000 Da. The MWCO is the size of molecule where 90 % will be rejected; however this varies for different

manufacturers.[63] The next smallest technology is nanofiltration, with pore sizes generally around 1000 Da (1 nm). The last category generally considered along with MF, UF and NF is reverse osmosis (RO). In reverse osmosis the principle of filtration is fundamentally different. MF, UF and NF are pressure driven filtration processes, where the separation mechanism is size exclusion, whereas in RO the driving force is chemical with the principle of osmosis being used. Figure 2.3 illustrates the pore sizes and pressures associated with MF, UN, NF and RO.

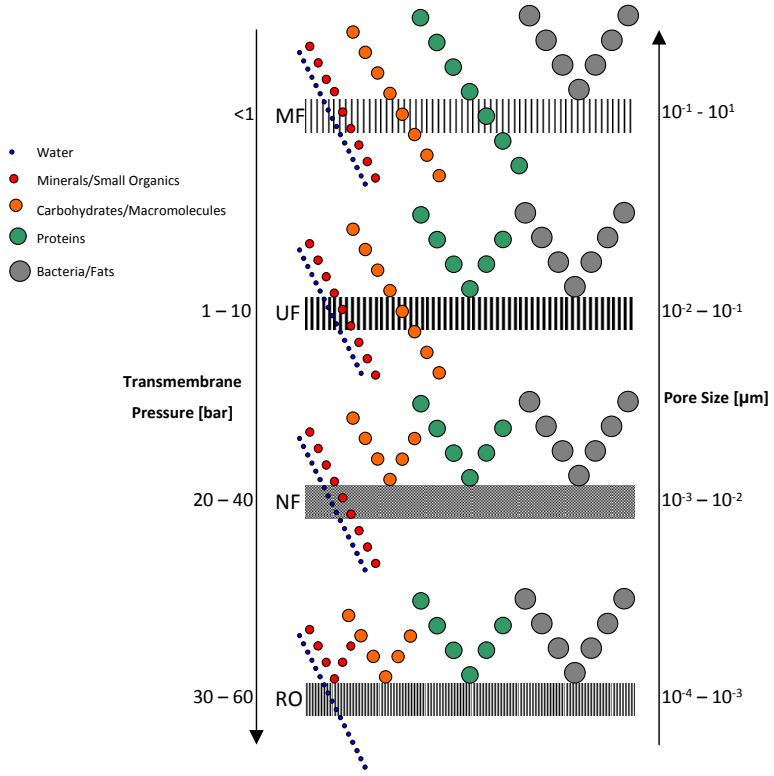

Figure 2.3: Comparison of process classification, membrane pore size, transmembrane pressure range and examples of the species typically separated in each process. Diagram used with permission from Iain Argyle and adapted from Mulder.[64, 65]

The uses of membrane separation is very varied, ranging from MF for the removal of bacteria and solids from food streams, or product clarification, to UF for solvent separations and dewatering, to desalination of seawater by RO to provide drinking water. Membranes provide an absolute barrier to particles which are larger than their pore size.[66]

Information presented in this section is, for the most part, representative of MF and UF processes as these sizes are most appropriate for the removal of Gum Arabic from a model wastewater feed.

2.2.2.1 Microfiltration

In microfiltration, permeable membranes are used to separate particles in the micrometer size range. MF membranes were first commercialised in the 1920s and were commonly used for analysing bacteria in water. In the 1960s the number of successful MF applications grew rapidly and now they are currently used in fields such as the food, biotechnological, automobile and electronics industries.[67, 68] MF is commonly used for the separation of colloid suspensions, bacteria, fat droplets and yeast cells.[60] It is usually operated at relatively low transmembrane pressures (0.1 – 3.0 bar) and with high permeate fluxes (up to 100 000 L m^{-2} hr^{-1} bar^{-1} for un-fouled membranes).[69] Often MF membranes suffer from intra-pore fouling.

2.2.2.2 Ultrafiltration

Due to the smaller pore sizes of ultrafiltration compared with microfiltration, a higher pressure is generally required for separation. The solutes retained by UF are generally those with molecular weights greater than 1000 atomic units, however this is dependent on the nature of the membrane selected for use. This means salts, sugars, organic acids and smaller peptides are transmitted while polysaccharides, proteins and fats are rejected. UF membranes are often anisotropic, meaning they have a finely porous surface layer supported on a much more open microporous substrate. The microporous substrate allows the membrane to have mechanical strength while the finely porous layer performs the separation.[68] Over the past couple of decades the use of UF for clarification and decolourisation has increased, particularly in the food industry due to the simple operation and low power consumption.[70]

2.2.3 Membrane performance

The performance or efficiency of a membrane can be determined by the selectivity or the flow through the membrane. The flow through the membrane is defined as the flux, and is a measurement of the volume of permeate per unit area over a defined time and is commonly expressed as litres per meter squared per hour (L m^{-2} h^{-1} or LMH). The separation can be measured by the retention (r) or the separation factor (α). r can be determined using Equation 2.1 where C_f is the concentration of solute in the feed and C_p is the concentration of solute in the permeate. When r = 1, complete retention has been achieved, and when r = 0 the solute and solvent are allowed to pass freely through the membrane.[65]

$$r = \frac{C_f - C_p}{C_f} = 1 - \frac{C_p}{C_f}$$ Equation 2.1

The separation factor is measured using Equation 2.2, where Y_A and Y_A are the concentration of A and B in the permeate respectively, and X_A and X_B are the concentration of components in the feed solution.[65]

$$\alpha_{A/B} = \frac{{}^{Y_A}/_{Y_B}}{{}^{X_A}/_{X_B}}$$ Equation 2.2

The separation factor is usually used in gaseous systems therefore this thesis reports separation in terms of retention.

2.2.4 Membrane material

There are a large number of materials which can be used for membrane production depending on the required properties of the membrane. They can be classified into three groups; synthetic polymers, modified natural products and miscellaneous. Synthetic polymers may include polyamides, polysulphones and silicone rubbers. Modified natural products are often cellulose based, such as cellulose acetate, and miscellaneous includes ceramics, inorganics, metals and liquid membranes.

Polymeric membranes are much cheaper to produce than ceramic membranes, however generally ceramic membranes have higher chemical, mechanical and thermal stability.[71, 72] The choice of membrane depends on the operating conditions, with ceramics being used where aggressive cleaning, and longer lifetimes are required. There are a wide variety of techniques used in the production of membranes, and these include sintering, stretching, track etching, phase separation, sol-gel processing, vapour deposition and solution coating.[73] The preparation method has a large influence on the membrane properties such as surface roughness and pore size.

A comparison between polymeric and ceramic membranes has been carried out by a number of authors in order to compare their filtration performance, with ceramic membranes generally outperforming polymeric ones. Hofs *et al.* reported that the removal of organic matter was higher when using ceramic membranes compared to polymeric ones, with the ceramic membranes generally showing a reduction in irreversible fouling.[74] Lee and Cho showed that ceramic membranes showed improved permeability when compared to equivalent polymeric membranes for the removal of natural organic matter. Ceramic membranes were also more effective in the

removal of disinfection by-product precursors.[75] Lee and Kim showed that physical and chemical cleaning are 45 % more effective with ceramic membranes than polymeric ones following fouling with natural organic matter;[76] and Majewska-Nowak showed excellent long term stability and performance with ceramic membranes compared to polymeric ones for the filtration of dye particles.[77]

Ceramic membranes have been chosen for use in this study as they have a high mechanical resistance allowing the use of high crossflow velocities. They have a wide range of pH and temperature tolerances being able to withstand pH values between 0.5 and 13.5, and temperatures over 100 ^{o}C. Ceramic membranes also allow aggressive cleaning regimes with the use of NaOH up to 3 wt. %, nitric acid up to 2 wt. %, and sodium hypochlorite can be used as an oxidising/sanitation agent.[78] Ceramic membranes are also known to have a longer lifespan, which has improved further over the past decade.[79]

Membranes are often categorised by their wettability: how hydrophilic or hydrophobic they are. The wettability influences the separation in a number of ways. The interactions between the feed and the membrane are dependent on how hydrophobic the membrane is and how easily water is transported through the membrane. In addition, different foulants are known to adsorb better to different membranes depending on the surface interactions, for example hydrophobic membranes adsorb more proteins than hydrophilic membranes.[80] This leads to the choice of a hydrophilic membrane when using a feed containing protein as the fouling is reduced. Generally hydrophilic membranes have superior properties with regards to fouling, however for some applications hydrophobic membranes perform better.

Another structural factor to consider when working with membranes is whether the membrane is symmetric or asymmetric. Symmetric membranes have a uniform pore size distribution throughout the whole membrane, whereas asymmetric membranes have a very dense top layer (< 0.5 μm) which is known as the 'active layer'. The active layer is supported on a much thicker porous sub-layer. The active layer allows separation, with the sub-layer acting only as a support for the active layer. The development of asymmetric membranes led to a breakthrough in industrial applications as the permeation rate is inversely proportional to the thickness of the active layer.[65] Ideally membranes have a high porosity to allow high fluxes and a narrow pore size distribution to ensure uniform selectivity.

The surface charge of the membrane is important in determining the fouling properties. If both the membrane surface and foulant have the same charge, adhesion of material to the membrane

is reduced. This helps to prevent membrane fouling. If the charge of the membrane and foulant are opposing then the fouling is increased. Gum Arabic is known to have a slight negative charge due to the acidic groups. This means reduced fouling would be expected for a negatively charged membrane.

A wide variety of these membranes are available commercially. In the food and beverage industry the most commonly used MF and UF membranes are organic polymers or ceramics.

2.2.5 Filtration modes

There are two operational modes which are commonly used in membrane separation processes, dead end filtration and crossflow filtration.

2.2.5.1 Dead end filtration

Dead end filtration is the traditional and simplest operational mode for membrane separation processes. The feed flows perpendicular to the membrane leading to a pressure gradient across the membrane. Some material is transmitted through the membrane, and the retained particles accumulate at the surface in the form of a cake layer. The build-up of a cake layer over time leads to a reduction in the flux, and a reduction in the flux quality through the increase in concentration of rejected components in the feed. This method is analogous to a simple sieve and is not commonly used in industry due to the instantaneous flux decline. The use of dead end filtration is generally only used when the feed stream has a very low solids content, for example pharmaceutical sterilisation cartridges and in small scale laboratory or pilot studies.[60, 81] When low total suspended solid feeds are used with dead end filtration it may be required to operate with cycles of backwash, where some of the permeate is forced back through the membrane to produce a flow in the opposite direction. This opposing flow allows the removal of some of the cake layer which may build up on the surface.[66]

Dead end filtration is often used with a stirrer, this produces a pseudo crossflow and can be useful for laboratory applications. With stirred dead end filtration cells the filtration is usually small, for this reason they are unsuitable for industrial food production.

2.2.5.2 Crossflow filtration

Crossflow filtration is more commonly used in industry as it possesses a number of advantages over dead end filtration. It was initially developed to reduce the impact of membrane fouling, however it has become very popular due to a lower energy requirement.[61] The flow of feed is swept across the membrane tangentially rather than perpendicularly as illustrated in Figure 2.4. This leads to a shear force over the membrane surface.[65] Crossflow filtration has the advantage that any material deposited on the membrane surface in the form or a cake layer, or which has been concentrated, can be disrupted and carried away in the feed flow. This reduces the flux decline. As the feed flows through the module, the composition changes as a function of distance as it is separated into a retentate and permeate stream. The retentate recirculates through the system allowing concentration of the retentate.[65] For efficient separation, high mass transfer is required from the feed to the permeate. The mass transfer is dependent on the shear rate, and can be achieved by creating high tangential velocities or turbulence as close to the membrane surface as possible.[60] The turbulence can be quantified by calculating the Reynolds number for the feed passing over the membrane. Crossflow filtration is used in virtually all commercial large scale pressure driven membrane processes.[69] For this reason crossflow filtration has been studied in this thesis.

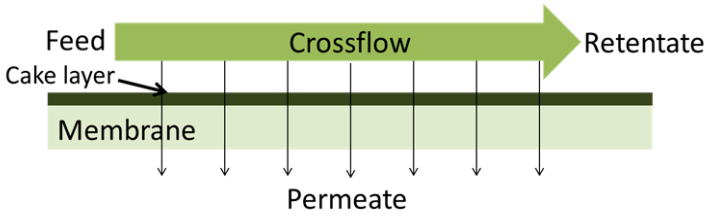

Figure 2.4: Principle of crossflow filtration

2.2.6 Membrane configuration

Membranes are housed in a module which offers physical separation of the retentate and permeate streams, mechanical support for the membrane (if required), high membrane packing densities, easy access for cleaning and replacement, and good mass transfer characteristics. Over the past few decades a lot of research has been carried out to develop new membrane modules and meet the requirements for efficient separation.[58] There are four common types of modules which are used in crossflow filtration, namely flat sheet, spiral wound, hollow fibre and tubular.[65, 73] Each has its own advantages and disadvantages.

2.2.6.1 Plate and frame module

The simplest module configuration is the plate and frame (flat sheet) module. This consists of flat sheets of membrane separated using spacers to allow permeate to flow out. The membranes are sandwiched in a rig with the feed flowing one side of the membrane and the permeate the other side. The disadvantages of the plate and frame module is the high capital cost along with average running costs and difficulties in cleaning, although the membranes can be easily replaced.

2.2.6.2 Spiral wound module

Spiral wound modules have several flat sheet membranes separated by mesh spacers and rolled around almost like a 'Swiss roll'. The feed flows into the module through a feed spacer, and the permeate can be collected in the middle of the module through the permeate spacer (commonly a perforated central tube). Spiral wound modules usually have a diameter around 0.1 m and a length of 0.9 m. Spiral wound modules have a number of advantages – they are the cheapest to operate and install, and they are very compact. This leads to them commonly being used in industry. The main disadvantage of this configuration is that it is prone to fouling due to low retentate flows, and the design makes mechanical cleaning almost impossible.[65] Spiral wound membranes can be cleaned using chemical cleaning agents, however as polymeric membranes are often used, this limits the temperature and concentration of cleaning agents which can be used.

2.2.6.3 Hollow fibre module

Hollow fibre modules have bundles of fine fibres (0.1 – 2.0 mm diameter) of filter materials bundled together inside a tubular housing unit. They were pioneered by DuPont for the desalination of seawater. Hollow fibre systems can handle high throughputs of feed, however they are unsuitable when a high solid content is present. This system requires the largest capital investment and the membranes are difficult to clean. However the fouling tendency and therefore requirement to clean is low (although they can be backflushed to allow cleaning). In addition the packing density of this module is very high allowing a large surface area.

2.2.6.4 Tubular membrane module

Tubular membranes are usually ceramic. With the tubular module the membrane is cast inside a porous support tube providing a large surface area. The membrane is housed inside a perforated stainless steel pipe with feed flowing through the central channels, and permeate flowing to the outside of the tube. Tubular membranes are commonly used where a turbulent flow is required, such as the presence of a high solids concentration in the feed. The tubular module requires high plant investment and high running costs, however it is easily scalable and membranes are easily replaced. The membranes used are very brittle and often expensive, however they are highly resistant to both chemical cleaning and heat treatment, and can even be autoclaved to remove bacteria. This often results in a much greater lifetime than flat sheet membranes.

Much research is ongoing to develop new membrane modules with improved mass transfer characteristics for both MF and UF operations.[58] Recent developments include rotating disk filters,[82, 83] conically shaped rotors,[84] cylindrical Taylor vortex devices[85] and helical coiled Dean vortex systems.[86, 87]

In this study both tubular ceramics and the plate and frame module have been investigated. This is detailed further in Chapter 3.

2.2.7 Membrane flux

Membrane flux (*J*) is the term used to measure the flow rate of permeate through a membrane. It can be defined as the volume per unit area per unit time. The flux is used as the basis for calculating the membrane performance and allows a quantitative comparison between membranes. Equation 2.3 allows the flux to be calculated where *J* is the membrane flux, ΔV is the volume change over time Δt, and A_m is the membrane area.

$$J = \frac{\Delta V}{A_m \Delta t} \qquad \text{Equation 2.3}$$

When pure water is transported through a membrane the flux remains constant (if all other parameters remain constant). This can be defined as the 'pure water flux' (PWF) and is used as a benchmark for all other filtrations with that membrane. When other solutions or materials flow through the membrane there may be a decrease in the permeate flux. The flow through a membrane is defined by Darcy's law which states that the flux is proportional to the driving force, and inversely proportional to the membrane resistance (Equation 2.4).

$$Flux = \frac{Driving\ force}{Resistance}$$ Equation 2.4

For a solution where the solvent is freely transferable the convective flux through the membrane can be described using Equation 2.5 where ΔP is the hydrostatic or transmembrane pressure, $\Delta\pi$ is the osmotic pressure, μ is the viscosity of the feed solution, R_T is the total hydraulic resistance (composed of the membrane resistance, R_m and any additional resistances caused by the interaction of the feed with the membrane). The osmotic pressure is affected by the temperature and concentration, and is generally considered negligible when working with MF and UF.

$$J = \frac{\Delta P - \Delta\pi}{\mu(R_T)}$$ Equation 2.5

A reduction in the permeate flux is caused by an increase in resistance; this is usually caused by a phenomenon called fouling. Over time the resistance will increase towards a maximum.[66]

2.3 Fouling

Membrane fouling is anything which leads to a reduction in flux which cannot be reversed through a change in operating conditions.[88] It is often characterised as a reduction in permeate flux through a membrane as a result of increased resistance due to concentration polarisation, pore blocking and cake formation.[89] This is due to the formation of unwanted deposits (or growth) of dissolved, suspended or chemically generated species from the feed onto the membrane. The immediate effect of fouling is to cause a reduction in permeate flux. The long term effect may be irreversible fouling which can lead to a reduction in the membrane lifetime. Fouling leads to a reduction in the membrane performance,[90] and can impair the separation properties of the membrane.[67, 91-95] Fouling is the main problem in the widespread use of membrane technologies.[96] It leads to an increase in production cost. This increase in production cost is associated with an increased energy requirement, chemical cleaning, reduction in membrane life expectancy, downtime of processing to allow for cleaning, and additional labour associated with maintenance.[71, 97]

Membrane fouling is an inevitable phenomena and is one of the greatest hurdles which needs to be overcome to treat wastewater.[71, 72] Fouling is an extremely complex process and has not been precisely defined.[97] However, generally it occurs when rejected particles are not transported from the surface of the membrane back into the bulk stream.

2.3.1 Fouling mechanisms

A number of different forms of fouling are known, each leading to an increase in the total resistance of the membrane. The main types are concentration polarisation, complete pore blocking, standard blocking, intermediate blocking, and cake formation. Other forms such as gel layer formation[98] and biofouling[89] may also be present. During the filtration of complex feeds, such as Gum Arabic, multiple fouling mechanisms can occur either simultaneously or independently.[99]

2.3.1.1 Concentration polarisation (CP)

Concentration polarisation is fouling caused by the convection of solutes being larger than their diffusion. For separation to occur the concentration in the feed must be higher than the concentration in the permeate. As separation occurs the concentration of solute on the feed side of the membrane will increase, and will form a concentration gradient in the feed solution. There is a convective force taking the feed to the membrane surface, and the concentrated solute will have a diffusive force due to the mass transfer over the concentration gradient as it diffuses back into the feed/ retentate (Fick's first law). Under steady state conditions the convective and diffusive forces will be in equilibrium. CP occurs as the diffusive backflow leads to a reduction in the permeate flux, and it can also lead to a build-up of high solute concentration on the membrane surface.[65] This is illustrated in Figure 2.5.

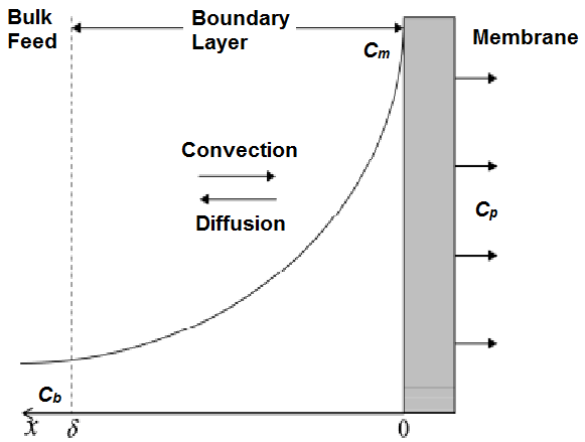

Figure 2.5: Representation of concentration polarisation, showing the convective and diffusive solute mass transfer over the concentration polarisation boundary layer. δ is the boundary layer thickness, χ is the distance from the membrane surface, C_b is the bulk concentration, C_m is the concentration at the membrane surface and C_p is the concentration of solute in the permeate. Adapted from Mulder.[65]

The concentration polarisation reduces the concentration difference of the permeating components across the membrane, thus reducing both flux and membrane selectivity.[68] Generally high flux membranes suffer from higher concentration polarisation than lower flux membranes.

2.3.1.2 Complete pore blocking

Complete pore blocking (also called pore plugging) occurs when a particle completely blocks a pore and prevents anything else being able to permeate through that pore. This occurs when a particle has a larger diameter than the pore diameter as illustrated in Figure 2.6.

2.3.1.3 Standard blocking

Standard blocking (also called pore constriction) occurs when particles are deposited on the membrane surface, and in the membrane pores. The build-up occurs with particles which are smaller than the pores, causing constriction of them and eventually leads to complete blocking of the pores. This is illustrated in Figure 2.6.

2.3.1.4 Intermediate blocking

Intermediate blocking occurs when a particle is deposited on an existing particle on the membrane surface, or blocks the membrane surface. This again is illustrated in Figure 2.6, and represents a build-up of particles.

2.3.1.5 Cake formation

The final and possibly most common form of fouling is cake formation. This occurs when particles deposit onto particles which are already on the membrane surface and leads to the building of a new layer on top of the active layer of the membrane. If the channels between the adsorbed particles on the membrane surface are narrower than the membrane pore diameter, the cake layer will act as the active layer on the membrane. This prevents transportation of smaller particles through to the permeate.[61] The formation of a cake layer is represented in Figure 2.6.

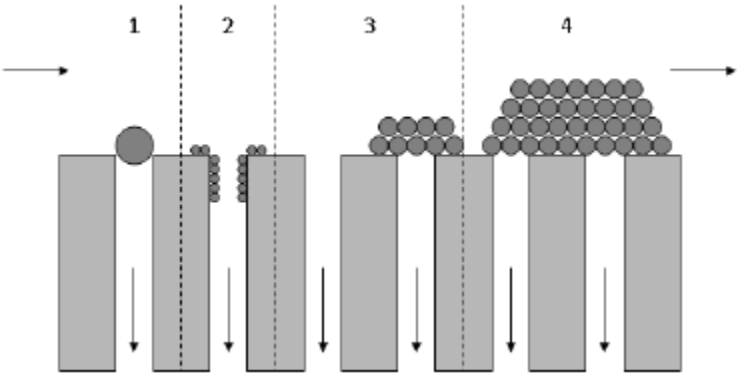

Figure 2.6: Schematic of pore blocking mechanisms from Bowen *et al*.[100] where (1) complete pore blocking, (2) standard blocking, (3) intermediate blocking and (4) cake filtration.

Modelling what will happen in membrane separation is difficult as filtration is a very complex process. There are a large number of factors which need to be considered to allow an effective model to be used.[63] However in 1982 Hermia[101] developed a set of pore blocking laws which allow the determination of the fouling mechanism for non-Newtonian fluids in dead-end filtration. If the permeate flux vs. permeate volume is linear, complete pore blocking occurs. If the natural log of filtration time vs. permeate volume is linear, intermediate pore blocking is dominant. If time/volume vs. time is linear standard pore blocking is prevalent and if time/volume vs. permeate volume is linear, a cake layer is being formed on the membrane surface.[91, 102, 103]

These models were originally developed for polymeric membranes, however Lee *et al.* reported that the same laws can be applied to ceramic membranes.[72] More recently Field *et al.*[93] extended these laws to describe crossflow filtration by the inclusion of a back diffusion term shown in Equation 2.6.

$$-\frac{dJ}{dt} = K(J - J^*)\,J^{(2-n)} \qquad \text{Equation 2.6}$$

Where *t*, *K* and *n* are constants depending on the blocking mechanism involved. *K* is a system specific decay constant, and n is a mechanism specific index. *J* denotes the flux, whereas J^* denotes the flux at steady state. Fitting of an experimental curve to Equation 2.6 allows an indication of the fouling mechanism which is occurring.

The mechanisms of fouling are all related and may all occur at the same time during filtration. However it is likely that one mechanism will dominate, which may change throughout the filtration. In microfiltration the process is generally membrane limited at the start (due to inherent membrane resistance). Usually, initial fouling is mostly due to complete pore blocking, but as the

filtration progresses cake formation becomes the dominant fouling mechanism and shows greatest resistance.[72, 89, 97]

There are also two distinct types of fouling phenomena, 1) macro-solute or particle adhesion, this is the result of intermolecular interactions which occur between the particles and the membrane even in the absence of filtration, and 2) filtration induced deposition, which is over and above that observed in the static system.[96]

2.3.2 Types of foulant

In addition to the possible fouling mechanisms, the type of foulant also plays an important role in understanding what is happening on the membrane surface. The type of foulant is particularly important when it comes to considering cleaning to restore the PWF. Different cleaning agents work better for the removal of the various forms of foulant. The types of foulant can be separated into chemical and/or structural similarity and are usually grouped as inorganic, organic, microbial and particulate.[91] The combination of foulants present will depend on the nature and composition of the feed solution.[67]

2.3.2.1 Inorganic fouling

Inorganic fouling is scale formation resulting from an increase in the concentration of one or more species beyond their solubility limit.[97] This leads to their precipitation on the membrane surface. Inorganic fouling is usually due to minerals and other inorganic materials. The fundamental mechanisms and processes involved in inorganic fouling are not fully understood, as they are dependent on many factors including the membrane characteristics, module geometry, feed solution characteristics and operating conditions.[71] Al-Amiudi and Lovitt suggested the high concentration of rejection ions on the membrane surface could lead to the aggregation of dissolved matter into colloidal sized particles.[97] This results in an increase in fouling as these particles cause pore blocking. Inorganic fouling is known to shorten the membrane lifetime.[71]

One example of an inorganic foulant is calcium. This has been shown to increase fouling in dairy streams through the formation of a salt bridge between the membrane and protein.[60] A similar phenomenon was reported by Li and Elimelech when considering fouling with humic acid.[104] During the study of adhesion forces through AFM, much greater adhesion was observed in the

presence of calcium. This increased adhesion has been attributed to the ability of Ca^{2+} ions to complex between carboxylate groups on the humic acid. This resulted in a denser fouling layer and therefore an increased hydraulic resistance. Calcium can also have a neutralising effect on negatively charged foulants, this reduces the repulsive electrostatic forces and results in increased fouling. Recently Mahlangu *et al.* studied the influence of the calcium concentration on the formation of foulant layers.[105] They reported that at low concentrations calcium leads to an increase in flux decline for the reasons detailed above, however at high concentrations foulant flocs can form, this results in a decrease in the cake resistance.

Gum Arabic is a salt containing calcium, magnesium and potassium[4] therefore inorganic fouling is likely to occur during the membrane filtration of wastewater streams containing Gum.

2.3.2.2 Organic fouling

Organic fouling is caused by the deposition of organic constituents on the membrane surface. A wide range of organic molecules have a strong affinity to stick to the membrane surface through an adsorptive mechanism.[91] Organic fouling is an issue for many industrial processes, and especially for wastewater treatment which contains natural organic matter (NOM). Organic fouling may be reversible or irreversible.[97] As Gum Arabic is composed mainly of polysaccharides, it would be expected that organic fouling would be dominant. It has been reported previously by Ye *et al.* that polysaccharides can form sticky deposits and hydrogels on a membrane surface.[106] Fouling behaviour can be different for different feeds, and can be dependent on the polysaccharide present.[102] Fouling with Gum Arabic may be severe due to the presence of both proteins and polysaccharides in the feed. Susanto *et al.* reported that crosslinking occurs when both polysaccharides and proteins are present in the feed.[107] This leads to an increase in the hydraulic resistance of cake fouling compared to feeds which contain either protein or polysaccharide alone.

A wide range of factors can affect organic fouling; these include the surface structure and chemical properties of the membrane, ionic strength and pH of the feed solution, concentration of monovalent and divalent ions, and operating conditions. The surface structure and chemical properties of the membrane are of particular importance as molecules such as proteins have a higher affinity for hydrophobic than hydrophilic membranes.

2.3.2.3 Microbial

Microbial fouling, also called biofouling, can occur when microorganisms such as bacteria or yeast are present in the feed solution, or have contaminated it. Often a few bacteria become embedded in the membrane surface, or in the pores, and begin to multiply.[89] This leads to the formation of a biofilm on the membrane surface reducing the permeate flux. Often organic matter is formed as a by-product of the biofilm formation and can form a hydrated gel known as extracellular polymeric substances (EPS).[108] The EPS can act as a protective barrier for the bacteria and means that cleaning by hydraulic and some chemical mechanisms has no effect.[65] Biofouling is known to destroy the structural integrity of the membrane, and can lead to system failure.[89]

2.3.2.4 Particulate

Particulate fouling is caused by particles which are of a similar size to the pores, or larger. This results in the pores getting blocked. It is usually caused by biologically inert or inorganic particles and is not associated with adsorptive mechanisms like the other fouling types. Hydraulic cleaning is sufficient to remove these foulants as they have no interaction with the membrane.[109, 110]

2.3.3 Flux decline due to fouling

During MF and UF the flux decline due to fouling can be very severe, this can lead to a change in membrane properties. As detailed above there are a wide range of foulants, and fouling mechanisms, each of these has an impact on the flux decline. Some fouling is reversible, some irreversible and some permanent. The use of the pure water flux allows a measurement of the membrane behaviour under constant conditions. Figure 2.7 illustrates an example filtration graph detailing what happens to the flux during a typical fouling and cleaning experiment.

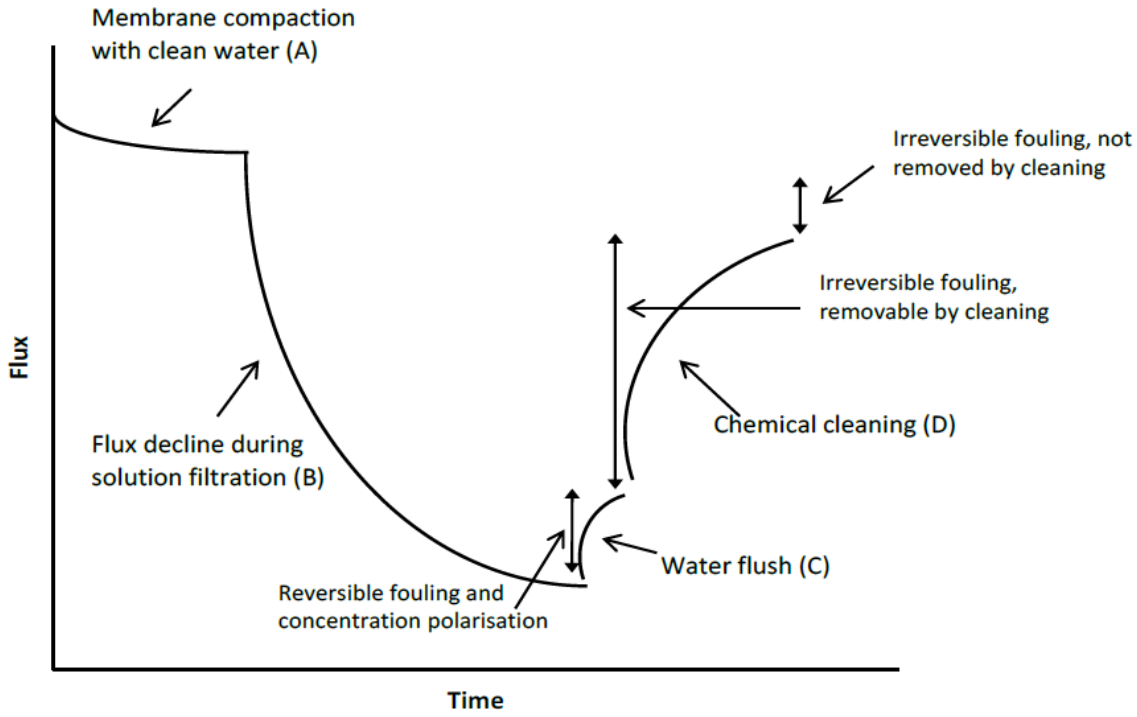

Figure 2.7: Schematic illustration of the filtration procedure after Jones.[111]

The flux decline observed due to fouling can be caused by any of the fouling mechanisms detailed in Section 2.3.1. Chemical cleaning is often used to restore the PWF and is discussed in Section 2.4.2.

2.3.4 Factors influencing fouling

In order to minimise fouling of membranes a great deal of research has been carried out. Research has tried to identify factors which influence fouling, and develop mitigation strategies.[72] Some of the key factors which affect membrane fouling include membrane type, properties of the membrane materials, process configuration, operating conditions, water quality parameters (e.g. dissolved oxygen concentration)[90] and cleaning strategies.[72, 97] The particle size is also known to influence the fouling rate, in general smaller particles create more fouling, with a greater cleaning resistance than larger particles.[89] The mechanism for the growth of fouling from small particles has been hypothesised by a number of research groups. Gilron and Hasson suggested that flux decline is due to blockage formed by lateral growth of deposits on the membrane,[112] whereas Pervov reported that it is crystal formation on the bulk followed by deposition on the membrane surface.[113] In reality it is likely to be a combination of these two extremes.[97]

2.3.5 Methods to reduce fouling

A number of methods have been investigated to reduce fouling. Some of those shown to be effective include:[110]

- Addition of coagulants to cause molecules to form larger particles which can easily be swept off the membrane surface
- Use of a dispersed phase to disrupt concentration polarisation
- Introduction of flow instability by low frequency axial pressure and velocity pulsing or injecting air into the feed stream
- Cross flushing by periodically stopping the permeate flow
- Backwashing using either fluid or gas
- Forward and backward pressure pulsing to remove the cake layer
- Pulsed electric field to remove particulate foulants when both the particles and membrane are charged
- Use of curved channels to create vortices
- Rapid back pulsing
- Altering the surface of the membrane

These methods have all been shown to reduce fouling, but their relative effectiveness depends on the particular system, due to the complex nature of fouling. Some more detailed examples of factors affecting fouling are given below.

2.3.5.1 Temperature

Temperature has an effect on the viscosity and the mass transfer coefficient of the solution. As the temperature is increased so is the permeate flux, due to a decrease in the viscosity and an increase in the diffusivity of the feed.[114] However, the maximum usable temperature may be limited by the membrane configuration, and other components in the system. When working with proteinacious feeds the temperature needs to be carefully considered to prevent denaturing of the proteins which will have a dramatic effect on the filtration and fouling properties. In addition, the energy consumption in pre-heating feed solutions needs to be considered when deciding what the optimum temperature conditions are.

2.3.5.2 Crossflow velocity

In crossflow filtration the crossflow velocity can be altered to affect the type of flow – laminar or turbulent. Industrially, turbulent conditions are normally used, this allows the removal of accumulated substances at the membrane surface.[115] The use of a high crossflow velocity, and thus shear rate can reduce concentration polarisation by increasing the mass transfer away from the membrane surface.[69, 116, 117] Increasing the crossflow velocity increases the energy consumption and may require several pumps to achieve turbulent flow – this needs to be considered when looking at the process efficiency.

2.3.5.3 Transmembrane pressure

The transmembrane pressure (TMP) has a large influence on both separation efficiency and permeate flow. Field *et al.* proposed the critical flux theory where "on start up there exists a flux below which a decline in flux with time does not occur; above it fouling is observed. This flux is the critical flux and its value depends on the hydrodynamics and other variables".[93] If the critical flux is exceeded then reducing the TMP does not restore the original membrane flux, resulting in hysteresis of the flux.

The TMP plays a large part in the operating conditions and can control whether the flux is below the critical flux. Below the critical flux fouling is not observed. The TMP can also be used to control filtration either in the pressure dependent region or pressure independent region. In the pressure dependent region as the TMP increases so does the permeate flux, and in the pressure independent region the flux becomes constant, and no longer increases with increasing TMP. In the pressure dependent region the TMP and flux have a linear relationship. A number of researchers have found that as the TMP increases so does the retention of solids using both MF and UF.[79, 99]

The pressure independent region is often referred to as the limiting flux and is mass-transfer controlled. This occurs when the concentration of foulants on the membrane surface is such that they form a gel layer. In this region the flux may decline with increasing TMP due to the compaction of the cake or gel layer on the membrane surface.[118-120] Previous work carried out by Decloux *et al.* showed that during the filtration of high concentrations of Gum Arabic the filtration was governed by mass transfer.[20] This was concluded as the limiting flux region was obtained for TMP as low as 0.3 bar.

2.3.5.4 Backpulsing/ backwashing

Backpulsing and backwashing have been shown to be effective in reducing the fouling by a number of authors including Head and Bird,[121] and Ma *et al.*[110] However, Ma *et al.*[96] also reported that the flux recovery after a long period of use was less when the membrane had been treated with backpulsing and Bechervaise[21] showed that backwashing was ineffective for a membrane fouled with 15 – 20 wt. % Gum Arabic.

2.3.5.5 Membrane surface characteristics

Many studies have been carried out to try to determine the influence of the membrane surface on fouling.[63, 67, 92, 96, 110] The membrane properties can influence the structure of the initial fouling layer, and membrane chemistry can affect the adsorption rate of the first few layers of deposited material.[122] Surface characteristics such as the membrane material, zeta potential, surface charge density and hydrophobicity can all play a role. The feed solution is important when considering changing the membrane surface to reduce fouling. Ma *et al.* showed that for carboxylate modified latex (CML) particles, the surface chemistry had little impact on fouling,[96] but several other researchers have reported a reduction in the irreversible fouling of a protein (BSA) by surface modification of the membrane.[110] If the foulants are charged they will interact more with a membrane of opposite charge and be repelled by a membrane of like charge. This is exploited with many thin film composite membranes when the feed solution is charged.[63]

Charging the membrane can be achieved in a number of ways, photografting techniques[110], electron radiation, UV radiation, plasma treatment. A coating can be used or chemical modification can be achieved. A number of chemicals which are commonly used as cleaning agents are known to modify the membrane surface, and this may influence the fouling of the membrane following cleaning cycles. Cleaning with sodium hydroxide (caustic soda) or acid can result in a noticeable change in the hydrophobicity of a membrane due to interactions between the cleaning agent and membrane surface.[92] Both sulphonic and sulphuric acid groups can interact with the membrane surface. These surface groups are deprotonated at a neutral pH.[63] SDS is a weaker cleaning agent, however prolonged exposure of a membrane surface to SDS results in a slight negative charge on the membrane.[92] In this study α-alumina membranes are used; the surface of these is easily charged using cleaning agents due to the presence of hydroxyl groups on the membrane surface.

It is likely that when the foulant is present in low concentrations in the feed, membrane properties are important, however when the foulant is present in high concentrations the physical deposition of the foulant will dominate.[110] The physical deposition of foulant results in foulant – foulant interactions between those on the membrane surface and those in solution.

In certain membrane systems selective absorbance of key foulants onto the membrane surface leads to the generation of a beneficial fouling layer. A beneficial fouling layer can lead to improvements in the permeability or selectivity of the system.[115, 123]

2.3.6 Rejection of solutes

Another important factor in membrane applications is the ability of the membrane to reject solutes from passing through the membrane to the permeate. The most important properties are the membrane material and pore size, however other factors also influence the solute transmission.[91] For the membrane the porosity (number of pores in the upper layer), MWCO, pore size, surface charge, hydrophobicity and surface morphology all have an impact on the ability to reject solutes.[63] Kosutic and Kunst reported that a membrane with the smallest pore size does not always have the highest solute rejection.[124] This is especially true when working with low MW, non-charged organic molecules.[63]

The composition of the feed should also be considered with the molecular weight, molecular size (width and length), acid dissociation constant (p*K*a), hydrophobicity and diffusion coefficient all having an influence on solute transmission.[63] All of the factors which need to be considered make modelling and gaining a full understanding of the process a huge challenge which has not yet been achieved.

2.4 Cleaning

Due to the reduction in permeate flux associated with fouling, it is important both scientifically and economically to have a method to remove the foulants, and an understanding of how they are effectively removed.[91] Cleaning is one of the most important steps in maintaining membrane performance.[80] Cleaning is also a very important stage in the food industry where cleaning is generally carried out at least once a day. In order for a membrane process to be cost effective the foulants must be removed quickly and efficiently. Process conditions should be optimised to

reduce the fouling process, but eventually cleaning will be inevitable. The length of time for a cleaning cycle should be minimised as this is effectively downtime for the process. In addition the cleaning, and impact it has on the membrane, must be considered as the cleaning should not impact negatively on the membrane lifetime, and should not cause any damage to the membrane surface, particularly the active layer.

Cleaning can either be done *in-situ* or *ex-situ*.[89] There are usually four types of cleaning which can be implemented; physical, chemical, biological and enzymatic. Cleaning methods are often developed through trial and error,[91] however optimisation is required. It is possible that a higher flux than the initial PWF is obtained following cleaning, this may be due to damage to the membrane.[91, 97] This should be avoided otherwise the selectivity may be impaired and the membrane lifetime reduced.

2.4.1 Physical cleaning

There are a number of physical methods used to remove a foulant from the membrane surface. Generally these are most effective when the foulant is non-adhesive.[110] Physical cleaning methods may be hydraulic, mechanical or electrical. Hydraulic cleaning methods are most common and include backwashing (flow reversal), backpulsing (backpressure applied in rapid pulses), cross flushing (flowing with no permeation), and sonication.[66, 89, 96, 110] It has been found that backwashing is effective for non-adhesive fouling and there are many reports of it being used in the literature. It can be an energy intensive process but avoids the need to drain the system which is a requirement for chemical cleaning methods. Sonication has also been shown to be effective, however it has been shown to remove cake formation far more effectively than pore blocking.[89] Hydraulic cleaning techniques are rarely found to restore the maximum membrane flux.[125]

Mechanical cleaning is rarely done, and involves scouring fouled surfaces with an abrasive material. It has great limitations due to the mechanical strength and accessibility of the membrane surface, therefore its use is limited to tubular systems. In these systems oversized sponge balls can be used at high velocity.[65]

Electric cleaning is being investigated more recently with the development of ‘smart membranes’ where the material properties can be controlled using an electric field. This allows the charge on the membrane to be altered by the electric field. This results in a change in the membrane

properties. This change may result in reduced adhesion between the foulant and membrane resulting in removal of the foulant.[126-128]

2.4.2 Chemical cleaning

Chemical cleaning is the most common cleaning technique industrially. It is often used to remove adhesive foulants from the membrane. Cleaning agents can affect the foulant in a number of different ways; the morphology may be changed through swelling or compaction, the surface chemistry may be changed, or the cohesive forces between the foulant and the membrane can be weakened.[91] To ensure effective cleaning without damaging the membrane, and minimise material costs, the optimal use of chemicals needs to be defined. Conditions such as the concentration, exposure time, temperature, pH, flow rate and pressure must all be investigated.[63, 92] Chemical cleaning can be performed in a number of different ways:[65]

1) Cleaning in place (CIP): this is defined as "the cleaning of complete items of plant or pipeline circuits without dismantling or opening of the equipment and with little or no manual involvement on the part of the operator".[129] This is the easiest method and most common industrially.
2) Cleaning out of place (COP): the membrane is removed from its module and placed in a separate tank, usually with a higher concentration of chemical cleaning agents.
3) Chemical wash: chemicals are added directly to the feed stream.
4) Chemical enhanced backwash: chemical cleaning combined with physical cleaning.[130]

Common cleaning agents include acids (hydrochloric, sulphuric, nitric and citric), bases (NaOH), metal chelating agents (EDTA), surfactants (SDS), oxidising agents (sodium hypochlorite), enzymes and a combination of these.[91, 97] When selecting a cleaning agent the chemical reaction between the cleaning agent and the foulant, and the mass transfer of the cleaning agent should be considered. Reactions between the cleaning agent and foulant include hydrolysis, peptization, saponication, solubilisation, dispersion and chelation.[91] Cleaning agents should also prevent further fouling from occurring, have good chemical stability and low cost.

Acids are used as a cleaning agent when minerals or metal films are to be dissolved. The acid allows the minerals which have precipitated on the membrane surface to be dissolved and removed from the membrane surface.[131] In general hydrochloric acid is more effective than nitric acid or sulphuric acid at removing minerals.[91] In these studies of Gum Arabic, any acids used had

to be compliant with food industry standards and therefore citric acid was used. Citric acid can chelate metal cations. Additionally Gum Arabic is soluble in citric acid.[5]

Alkali cleaning is used to solubilise carbonates, bind ion salts, regulate pH, emulsify fat and peptise proteins. Cleaning with sodium hydroxide (caustic) has been shown to be very effective for the removal or organic and proteinacious foulants.[131] The presence of hydroxyl ions in the caustic solution disrupts the foulant layer by increasing the ionic strength, increasing the solubility of the organic foulants and increasing the pH.[91]

Oxidising agents such as sodium hypochlorite have a number of uses in cleaning. Firstly they allow foulants to be oxidised which can assist with their removal from the membrane surface.[131] Secondly they act as a disinfectant.[21] Oxidising agents are particularly useful where biofouling is present as they can break down the protective film formed during bacteria growth.[89]

Surfactants are both hydrophobic and hydrophilic, and can be used to reduce the surface tension of adjacent molecules which can lead to the removal of foulants.[89] For surfactants to be effective their concentration must be above the critical micelle concentration. Surfactants can improve the wettability and rinsability of membrane surfaces allowing better contact with cleaning agents. Membrane manufacturers generally specify the maximum limits for the use of chlorine, acid and caustic, but do not specify the use of surfactants and chelating agents despite their widespread use commercially.

Chelating agents such as EDTA allow the removal of metal cations through complexation. EDTA works best at high pHs as all four carboxylate groups are deprotonated, as opposed to only two at neutral or low pH. Li and Elimelech showed that EDTA was useful at breaking down a cross-linked gel layer of organic deposits which had been stabilised by Ca^{2+} ions.[104]

Often combination cleaning is used as it allows multiple foulants with different properties to be removed.[63, 91, 92, 131, 132] Cleaning can also lead to surface modification of the membrane and can change the isoelectric point.[67, 132]

2.4.2.1 Cleaning efficiency

The cleaning efficiency can be a function of a number of parameters including the hydrodynamic conditions, temperature and concentration of the cleaning solution.[133] The cleaning efficiency at each stage of the cleaning cycle can be evaluated by the ratio of the PWF after cleaning (J_c) to the

PWF measured before fouling (J_w). The percentage flux recovery ($\%J_r$) can be calculated using Equation 2.7.

$$\%J_r = \left(\frac{J_c}{J_w}\right) \times 100 \qquad \text{Equation 2.7}$$

2.4.2.2 Fouling and cleaning synergy

While the flux recovery is widely used as an indicator to establish the effectiveness of cleaning agents at restoring the PWF, it gives little information about changes to the surface chemistry and behaviour. It is therefore important to investigate multiple fouling and cleaning cycles as the membrane is rarely restored to its pristine state. Blanpain-Avet *et al.* suggest that achieving a stable steady state where no further flux decline is observed is more important than recovering the membrane to its pristine condition.[134] It is generally accepted that the performance of a system should be judged on membrane performance after fouling and cleaning, e.g. how quickly re-fouling occurs rather than comparing to the pristine membrane.[81, 116, 125, 135] The use of membrane characterisation detailed in Section 2.5 can be used to identify changes in the membrane surface following fouling and cleaning.

2.5 Membrane characterisation

There are a wide range of techniques available for the characterisation of membranes. The technique used depends on the information which is required. While determining the flux recovery, as detailed in Section 2.4.2.1, gives some information about the effectiveness of cleaning agents, it does not provide a full understanding about changes which may be occurring to the membrane surface. Often a membrane autopsy is useful to gain conclusive information and a better understanding of the types and extent of membrane fouling. It can also be used to determine the effectiveness of cleaning agents and identify any damage caused to the membrane. This section details a number of methods commonly used by membrane scientists to gain information about the surface condition.

2.5.1 Contact angle

The wettability or hydrophobicity of a membrane is a measure of how readily a liquid contacts a solid surface. The hydrophobicity of a membrane is widely associated as a gauge for the fouling potential. It is generally accepted that more hydrophobic surfaces show a greater affinity to adsorb materials, and thus have a greater fouling tendency.[63, 99, 136-138] While not fully understood it is assumed that the increased fouling potential is due to hydrophobic interactions.[139] Hydrophobic attraction occurs from van der Waals forces between molecules. These hydrophobic interactions occur as there is a natural tendency for the attraction between solutes and membranes of similar chemical structures. Additionally feed streams often contain hydrophobic organic matter, this has a greater affinity for hydrophobic surfaces and can result in increased fouling with hydrophobic membranes in aqueous systems.[60]

The contact angle can be used as a measure to determine the hydrophobicity of a membrane. Changes in the hydrophobicity help allude to the characteristics of the foulant species, and can be used to identify the surface condition following cleaning and surface treatments.[140] If a membrane is hydrophilic the contact angle will be less than 90°, and for hydrophobic membranes the contact angle will be greater than 90°.

The principle behind contact angle measurements can be considered in terms of thermodynamics through the Young's equation (Equation 2.8). This analysis allows the interfacial free energies between a solid, liquid and vapour phase to be determined.

$$\gamma_{LV} \cos\theta = \gamma_{SV} - \gamma_{SL} \qquad \text{Equation 2.9}$$

Where γ is the interfacial energy between the phases, and subscripts *s, v* and *L* stand for solid, vapour and liquid respectively. θ is the contact angle for the system.

The contact angle can be affected by many factors including the material manufacturing process, the roughness of the surface and the purity of water used to measure the contact angle. Additionally for membranes as the surface is rough and porous there are additional factors which need to be considered when measuring the contact angle. For rough or porous surfaces the water droplet can bridge over air pockets leading to alterations in the contact angle. Additionally the pores can be wetted leading to alterations in the measured contact angle. For this reason in membrane science the contact angle is often measured as the effective contact angle, which can be used as a comparison between samples rather than as an absolute measurement.

There are a number of methods which allow the contact angle to be determined, these include the sessile drop, captive bubble and Whilhelmy plate methods. The sessile drop method involves measuring the contact angle of a drop of water on the surface. The captive bubble method allows the profile of an air bubble to be measured which is in contact with a membrane immersed in liquid. The Whilhelmy plate method involves the immersion and withdrawal of a sample in and out of a liquid while measuring the advancing and receding contact angles. The captive bubble method has the advantage that the membrane can remain immersed in solution preventing any changes to the membrane which may occur on drying.

2.5.2 Zeta potential

The surface charge on a membrane can have a significant influence on its fouling tendencies. The interaction between molecules in solution and the surface of a membrane results in adsorption. This can be minimised when the surface and solute have the same charge. If a surface and molecules in the solution have a high charge density they usually repel each other resulting in a reduction in fouling and often an increase in selectivity. Zeta potential (ZP) is useful to identify any particle-particle and surface-particle interactions. Often this is influenced by the pH, and gives a good indication of how foulants change with pH.[67] The surface charge on a membrane is related to the zeta potential. For macroscopic surfaces, such as MF membranes, the ZP can be measured through streaming potential measurements.

When a membrane surface is brought into contact with an aqueous electrolyte solution they acquire an electric surface charge. This may occur through several mechanisms and is referred to as the electrical double layer. The surface groups can become ionised, or adsorption of ions or macromolecules may occur. When ions are present in a system which contains an interface, there will be variation in the ion density near the surface. This variation in ion density can be represented in a profile such as that in Figure 2.8.

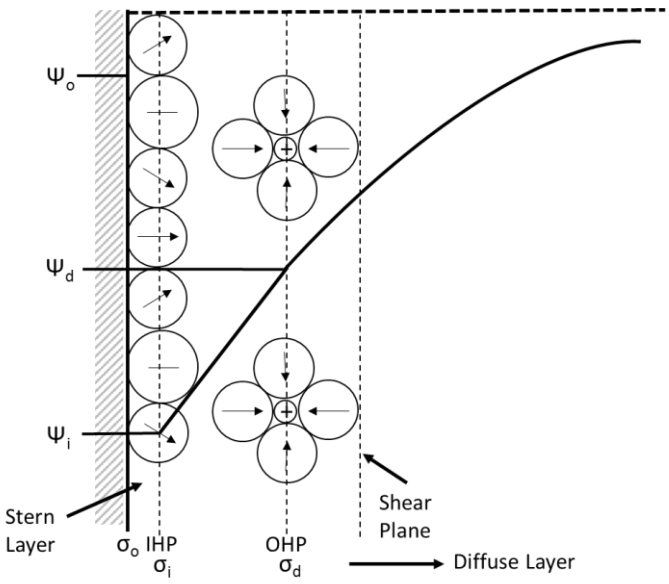

Figure 2.8: A model of the electrical double layer in aqueous solution after Hunter.[141] IHP is the inner Helmholtz plane, and OHP is the outer Helmholtz plane. Ψ_0 is the potential at the surface of the membrane, Ψ_d is the potential at the surface of the diffuse layer, Ψ_i is the potential at the IHP. σ_0, σ_i and σ_d are the change densities at the membrane surface, IHP and at the surface of the diffuse layer respectively. χ is the distance from the solid surface inside the double layer.

In solution the presence of a surface charge results in the attraction of counter ions to the surface. This results in a charge density in the surface plane, with the concentration decreasing as distance from the surface increases. The counter ions on the surface balance the membrane charge resulting in neutrality being maintained, and results in variation in the electrical potential between the solid surface and the bulk solution/ material in suspension.[141] The counter ions adsorbed to the membrane surface is the stern layer, and the rest of the counter ions are dispersed in the diffuse layer. The variation of potential with distance from the surface is illustrated in Figure 2.8. The potential of the surface with respect to the bulk sirface is represented by Ψ_0 and is called the surface potential. This can become zero at a certain concentration of ions in solution, and is called the point of zero charge. The pH at which this occurs is often referred to as the isoelectric point (IEP).

The diffuse double layer theory assumes that there exists a stationary plane inside the double layer. The solvent molecules near to the surface remain stationary due to the electric field of the surface, whereas the rest of the diffuse double layer moves along with the flow.[142] This plane is referred to as the surface of shear, with the potential at the plane being the zeta potential. The zeta potential can be measured either by streaming potential or electro-osmosis.

Nystrom *et al.* reported that the streaming potential is the best way to characterise the zeta potential of different membranes.[143] The use of streaming potential allows variability in the charge density of the membrane to be detected. When an electrolyte solution is forced through a membrane, through hydraulic pressure, a streaming potential is generated. The liquid flowing through the membrane pores carried a net charge and the flow gives rise to a streaming current. The streaming current and potential can be measured by electrodes at either side of the membrane. Using the streaming potential measurements the zeta potential can be calculated using the Helmholtz-Smoluchowski equation (Equation 2.10).

$$\zeta = \frac{\Delta E}{\Delta P}\frac{\mu\kappa}{\varepsilon_0\varepsilon_r} \qquad \text{Equation 2.10}$$

Where ζ is the zeta potential, ΔE is the streaming potential, ΔP is the transmembrane pressure drop, μ is the viscosity of solution, κ is the conductivity of electrolyte in the pores (approximated as bulk conductivity), ε_0 is permittivity of a vacuum, and ε_r is the relative dielectric constant of the electrolyte.

Chan and Chen reported that most streaming potential systems measure the sign (+/-) and change in a system rather than the absolute value.[144] This means the quantity should be used for a comparison between samples rather than as an absolute numerical value.

Zeta potential has been widely used for the analysis of membrane fouling. Measurement of a virgin membrane allows an indication as to the species which are likely to attract to the membrane surface. Comparing the zeta potential of a virgin membrane, and following cleaning of a fouled membrane allows the charge regeneration to be determined. Nabe *et al*. reported that for membranes with only a charge difference at selected pHs, protein adsorption varied.[145] Fouling was greatest when the membrane and protein were oppositely charged. Weis *et al.* reported that following fouling with spent sulphite liquor, surfactant based cleaning agents were ineffective at restoring the initial membrane charge, with the surfactant molecule attaching to the membrane or foulant layer following cleaning.[146] They also showed that sodium hydroxide was more effective at restoring the membrane charge. This sort of information in invaluable in understanding the long term performance of a membrane system.

Klein *et al.* studied the zeta potential of Gum Arabic when investigating the interactions between Gum Arabic and whey protein. They found the Gum had a negative zeta potential ranging from -7 to -30 mV.[147] The presence of uronic acid (sugar acid) groups within the Gum Arabic structure are responsible for the negative charge above the IEP.

2.5.3 Porosimetry

The porosity, mean pore size and pore size distribution of a membrane will significantly affect the membrane properties in terms of selectivity and flux. Highly porous membranes tend to have a greater throughput than membranes with a few pores. Additionally the porosity can be used to give a comparison between virgin and fouled membranes giving an indication of the type and extend of fouling which has occurred.

Manufacturers typically quote a nominal pore size of a membrane, however this gives little information about the pore size distribution or porosity of a membrane. It is therefore important to characterise the membranes to establish these properties. There are a wide range of techniques available which give different information about the pore size and distribution. Broadly these can be separated into visual, gel or liquid permeation, and solute permeate methods.

Visual techniques include scanning electron microscopy (SEM) and atomic force microscopy (AFM). These can be used to image the membrane and allow physical measurement. This allows direct observation, however it gives little detail about the porosity and can be prone to artefacts which can alter the results. Additionally following conditioning, fouling or cleaning, care must be taken when drying the membranes to ensure the pores do not collapse. Cross-sectioning may also be difficult without damaging the membrane structure.[148]

Solute permeation is used for membranes in the UF range or below, and allows classification in terms of molecular weight cut off (MWCO). The MWCO is usually defined as the maximum molecular weight for which 90 % of that particle is rejected by the membrane. Generally polyethylene glycols are used for these measurements.[63]

Permeation of gas or a liquid through the membrane is the most common method to measure the porosity and pore size distribution. Methods such as bubble point, gas adsorption, thermoporometry and mercury porosimetry are commonly used.[63] This thesis uses mercury porosimetry to measure the pore size and porosity. This is an accurate method for porous solids and measures the porosity through the penetration of mercury into a known mass of sample. The penetration of mercury at a known pressure allows the pore size and volume to be determined.

2.5.4 FTIR

Fourier transform infrared spectroscopy (FTIR) is a useful technique to understand the nature of deposits adhered to a membrane surface. It is often used within membrane science to confirm the nature of chemical species or functional groups adsorbed onto the membrane surface. IR radiation, typically in the range of 400 to 4000 cm^{-1} is aimed at the surface and the reflection detected. Depending on the chemical bond present, absorption of the radiation will occur leading to a peak in the FTIR trace. Bonds with ionic character have strong absorption in the IR range leading to strong FTIR signals.

FTIR can be operated in two modes. The most common is attenuated total reflection (ATR) mode. In this method the sample is pressed against a diamond tip. Light passes through the ATR crystal in such a way that it is reflected several times, traveling through the crystal as a standing wave. Some of the light is adsorbed at certain frequencies and the intensity of the spectrum is proportional to the number of reflections detected by a detector.[144, 149]

The second mode of operation, which has been used in this thesis is diffuse reflectance infrared transform spectroscopy (DRIFTS). This is ideal where the membrane has a high absorbance e.g. alumina. DRIFTS detects only the functional groups on the surface. In DRIFTS mode the radiation is scattered on the surface and radiation collected in a curved mirror and focused on a detector.

FTIR can be used to detect foulants, as well as determine the effectiveness of cleaning.[99, 140] FTIR is a non-destrictive technique, however analysing the data can be difficult as some bonds and functional groups absorb at the same frequency. Nystrom *et al.* reported difficulties at identifying the foulants when filtering lactoferrin and BSA through regenerated cellulose.[143] The issues arrose from the OH groups in the membrane overlapping with the protein foulants.

2.5.5 SEM

Scanning electron microscopy (SEM) is commonly used within membrane science to image the surface or cross section of a membrane. Images allow the membrane surface to be analysed and give a clear indication of fouling and cleaning.[89, 91] This allows a good comparison of the surface of a fouled/ cleaned membrane with a virgin membrane. SEM works by scanning the surface with a focused beam of electrons under high vacuum. The atoms are excited by the electron beam and secondary electrons are produced based on the angle at which the beam meets, these are detected on a detector and an image produced.

An SEM can be fitted with an energy dispersive X-ray (SEM-EDX) which allows elemental analysis of the surface. SEM-EDX uses X-rays to excite electrons, for which each element has a unique atomic structure and therefore excitation energy. The number and energy of X-rays emitted from the sample can be measured using an energy dispersive spectrometer and the element determined based on the energy difference between atomic shells in the atom structure.

2.5.6 AFM

Atomic force microscopy (AFM) is useful in determining the topography of the membrane. A three dimentional image of the surface can be created as well as the roughness determined. It has been well reported that rougher surfaces have a greater fouling tendancy as foulants can get trapped in troughs on the surface.[60, 150] Additionally Riedl *et al*. reported that a rougher surface can result in a more open fouling layer.[151] AFM can be operated with the sample either in air or in liquid. This means the topography and roughness of membranes can be measured without changes to the structure.[152]

An AFM works through a probe with a nanoscopic tip which is attached to a cantilever and it allows sub micron features to be determined. A laser bead is focused on the back of the cantilever, and deflected to a dual element photodiode. As the tip moves up and down with the surface the topography can be determined through plotting the laser reflection against the tip height.[153] A schematic of AFM is shown in Figure 2.9. The mean roughness (S_a) can be determined from average deviation in the Z plane with reference to the x-y plane.

AFM can be operated in contact tapping or non-contact mode. In non-contact mode the intermolecular interactions can be determined between the sample and probe. This is useful when working with soft or elastic materials. In contact mode the tip is in direct contact with the surface as the cantilever moves across the surface. This allows high resolution images to be obtained rapidly, however it is not ideal for sticky or rough surfaces. Tapping mode is similar to non-contact mode in that the cantilever osscilates at a set frequency, however in tapping mode the probe contacts the surface with a specified force allowing deveations in the height to be determined. Tapping mode is the standard mode of operation used as it gives high lateral resolution and lower contact forces which leads to less indentation on soft surfaces.[154] AFM has the great advantage that it can be carried out in an aqueous medium meaning that membranes don't need to be dried out before measurements are made, preventing any changes to the topography.[155]

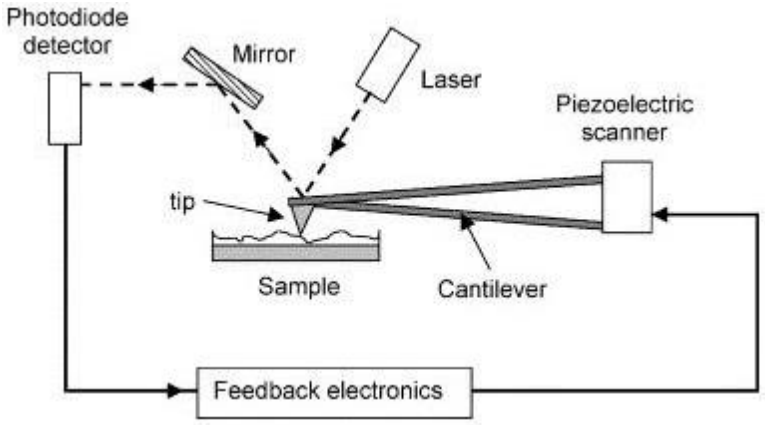

Figure 2.9: Schematic illustrating AFM characterisation after Chan and Chen. [144]

AFM has been used by a large number of authors to study membranes, and particularly the changes following fouling.[156-160]

As well as being a useful tool to determine the topography of a surface, AFM can be used to measure the intermolecular interactions between a probe and the surface. This technique was developed by Ducker *et al.* who used a silica sphere (colloidal probe) to measure the interactions between the sphere and a flat mica (silica) surface.[161] The results obtained agreed with double layer theory with slight discrepencies very close to the surface which were attributed to hydration forces.

The colloidal probe method works by bringing a colloidal probe (typically silica) to the surface at a controlled rate, and then retracting again at a controlled rate. Any alterations in the force either attraction or adhesive can be measured. Measurements are possible in the piconewton range making this a very sensitive technique.[144, 155]

This technique has previously been used within the membrane science field as it allows characterisation of the interactions between the probe and virgin, fouled and cleaned surfaces. These interactions can be quantified and help to build up a picture of the surface interactions occuring during the fouling or cleaning processes. Previous work carried out by both Bowen *et al.* and Chan and Chen showed weaker interactions between a BSA doped probe and a membrane fouled with BSA compared to the doped probe and a virgin membrane.[144, 162] This highlights for BSA the interaction is greater with a virgin membrane, silica or PES, than with the foulant layer.

2.5.7 FDG

Fluid dynamic gauging (FDG) is a relatively new technique which is normally used to measure the thickness and deformation behaviour of soft fouling deposits. Tuladhar *et al.* developed the system[163] with the inspiration coming from pneumatic gauging.[164] Fluid dynamic gauging overcomes some of the issues with pneumatic gauging as it can be used with soft deposits and in a liquid environment.[163]

Fluid dynamic gauging measurements can be made in real time and *in situ.* The gauge features a nozzle which is held at a height 'h' from the surface, liquid from the surrounding reservoir can be drawn into the nozzle with suction caused by a syringe pump. There is a pressure difference between the liquid near the surface and the discharge end of the gauge resulting in fluid flow into the nozzle. The suction pressure, mass flow rate and height of the nozzle are all related allowing the height to be calculated from the flow rate at a fixed suction pressure. Generally FDG is used to measure the deposit thickness. The use of FDG to measure the thickness of a foulant layer on a porous surface has previously been carried out by Chew and coworkers.[165-169]

In addition to using the FDG system to measure the deposit thickness it can also be used to apply a suction pressure by fixing the height and flow rate of the gauge. This allows the shear stress applied to the foulant layer to be controlled.[169]

2.5.8 Summary

While each of the techniques above give valuable information about the surface condition of the membrane, a single method does not always give sufficient information to develop a complete description of what is occurring during fouling and cleaning. It has been reported by a number of authors that combining a number of techniques can be used to obtain a clear representation of the mechanisms occuring during filtration and cleaning.[99, 140, 170]

2.6 Membranes and wastewater

Membranes are becoming increasingly attractive in their use for water treatment.[63, 96] They have the ability to remove hardness, colour, biogenetics, disinfection by-products, and can recover valuable products for other applications.[71] They are particularly useful where a high quality

product is important[63] as they continuously produce a high quality effluent independent of the feed water quality.[66] The use of membranes for separation does not require the use of additives meaning that product recovery can be achieved without altering the structure and properties of the substance being recovered. This has advantages in the separation of Gum Arabic from the waste stream formed during Gum processing. Gum can be recovered without changing its properties leading to a greater process efficiency.

If recovery is not required, membrane technologies result in only small amounts of solids for disposal.[59] Other advantages of membrane technologies for wastewater treatment are the small footprint as there is not the requirement for chemical usage (other than for cleaning), and they do not involve a phase change.[66, 91, 171] Membranes also have the ability to comply with the most stringent regulations for public health, environmental protection and separation processes at room temperature.[91]

Traditionally the use of membranes in wastewater treatment has been limited due to their high cost. Recently it has been found that their cost is decreasing and they are now seen as a new, viable and cost effective option for water treatment.[61, 66, 72, 172] Membrane separation processes are also known to be compact, have simple automation and control and therefore don't have very high operating and maintenance requirements, these help make them a cost efficient process.[59]

Despite their potential uses, membrane fouling remains an issue due to the complex nature of wastewater.[71, 89] It has been reported that membrane replacement due to fouling is the single largest operating cost when they are used in wastewater treatment.[110]

A case study comparing polymeric and ceramic membranes on a pilot plant has been recently carried out by *Nanostone water* (Minnesota, USA).[173] Table 2.2 details the costs of setting up the system, membrane replacement cost and other costs such as cleaning, energy and water recovery. The study was carried out over 1 year and assumes that ceramic membranes have a lifetime over ten years, and polymeric membranes have a four year lifetime. For the systems investigated the capital cost was the same, but with the ceramic membranes outperforming the polymerics in terms of separation, without requiring membrane replacement. This led to an estimated saving of $ 1 million in operating costs, as well as a saving of over 30 % more water.[173]

Table 2.2: Estimated coasts of polymeric vs. ceramic membranes for industrial waste water reuse plant based on pilot study by *Nanostone water*.[173]

	Polymeric UF system	*Nanostone* Ceramic UF system
Plant capacity	3.17 M gallon/day	3.17 M gallon/day
Index Capex	1.0 – 1.2 M USD Total system (0.35 – 0.4 M USD Membrane included)	1.0 – 1.2 M USD Total system (0.35 – 0.4 M USD Membrane included)
10 year membrane replacement cost	0.8 M USD (2 replacements)	0.0 M USD (0 replacements)
10 year operating labour cost	0.8 M USD	0.6 M USD
10 year chemical cost	0.45 M USD	0.45M USD
10 year power cost ($0.09/kwh)	0.14 M USD	0.17 M USD
Water recovery	5 M gallon per month discharge (95 % recovery)	3 M gallon per month discharge (97 % recovery)
Total 10 year Opex cost	2.2 M USD	1.2 M USD
Cost of water (Capex + 10 year Opex)	0.29 USD per 1000 gallon	0.20 USD 0per 1000 gallon

The waste stream produced during the processing of Gum Arabic contains ca. 2.0 wt. % Gum Arabic.[7] As detailed in Section 2.1, Gum is a complex polysaccharide. This thesis aims to show it is possible to apply membrane technologies to the recovery of Gum Arabic and water, while obtaining an insight into the fouling mechanisms. This allows for optimum filtration conditions. Understanding fouling allows an effective cleaning procedure to be developed allowing removal of the foulants from the membrane surface and optimising flux recovery.

3. Materials and Methods

3.1 Introduction

This chapter presents the experimental equipment and conditions which were used for the microfiltration, fouling and cleaning of Gum Arabic. It covers the experimental equipment used in (i) crossflow microfiltration with tubular ceramics (ii) crossflow microfiltration with flat sheet ceramics and (iii) analysis techniques.

3.2 Materials and reagents

3.2.1 Foulant: Gum Arabic

Spray dried Gum Arabic was supplied by *Kerry Ingredients* (Cam, UK). A model wastewater suspension was produced by slowly adding spray dried Gum (typically 600 g) to 10 L of water which had been treated by reverse osmosis filtration (RO) and heated to 40 °C. This was created based on information from *Kerry Ingredients* due to their waste stream following spray drying containing ca. 2.0 wt. % Gum Arabic. Small amounts were added over a period of 15 minutes to aid resolubilisation. The Gum suspension was stirred using an overhead stirrer to allow aggregation and ensure full dissolution of the Gum. After addition of the Gum the suspension was left to stir for 60 minutes. The Gum suspension was then diluted to the required concentration (typically 2.0 wt. %) with RO water at 40 °C in the feed tank to a volume of 30 litres prior to filtration. All Gum suspensions were prepared freshly before use to prevent any contamination or evaporation of the feed.

3.2.2 Water

All water used for all experimentation (including Gum reconstitution, membrane rinsing and cleaning solutions, pure water flux measurement, and general laboratory usage) was filtered using an Intercept Ro-S osmosis system (*ELGA Ltd*, Marlow, UK). The water had a conductance of ca. 15 $\mu S\ cm^{-1}$ and a consistent hardness of below 5 ^{o}e (≈ 70 mg L^{-1} $CaCO_3$).

3.2.3 Cleaning agents

Sodium hydroxide (NaOH) of technical grade (*Fisher Scientific*, Loughborough, UK) was used to clean the rig after long periods of inactivity, before any filtration experiments, and to clean membranes fouled with Gum Arabic. NaOH was chosen due to its ability to hydrolyse peptide bonds that link amino acids together in polypeptide chains forming proteins. In addition NaOH has a relatively low cost, is common in industrial use and is compatible with the food industry. Following work carried out by Bird and Bartlett,[174] a concentration of 0.5 wt. % was used as this was shown to be optimum for the removal of protein fouling in a whey protein concentrate foulant. Sodium hypochlorite (NaOCl), of technical grade (*Fisher Scientific*, Loughborough, UK) was used in addition to NaOH as a cleaning agent due to its oxidising and sanitation properties.

Citric acid ($C_6H_8O_7$) (purity 99.5 %) (*Fisher Scientific*, Loughborough, UK) was used to clean fouled membranes after they had been subject to alkali cleaning in order to remove any mineral deposits which had built up on the membrane due to their presence in Gum Arabic.

P3-Ultrasil 11 (*Ecolab*, Minnesota, USA) was also investigated as a cleaning agent. P3-Ultrasil 11 is a commercially available cleaning agent specifically designed for membrane cleaning. It is sodium hydroxide based but also contain a number of surfactants to aid cleaning as well as ethylenediamineteteaacetic acid (EDTA). P3-Ultrasil 11 has been designed specifically to remove foulants commonly found in the food industry such as proteins, fats and other similar foulants. The formulation of P3-Ultrasil 11 is shown in Table 3.1. The presence of EDTA can be significant as it acts as a complexing agent with ions, limiting their presence in the cleaning solution and preventing the redeposition of the removed foulant.

Table 3.1: Chemical composition of P3-Ultrasil 11 (reproduced from *Ecolab* data sheet).

Ingredient	Percentage (wt. %)
Sodium Hydroxide	43.6
EDTA	>30
Anionic surfactants	<5
Non-ionic surfactants	<5

All cleaning solutions were prepared by slowly dissolving the cleaning agent in RO water which had been heated to the required temperature. The volume of cleaning solution was typically 25 litres.

3.2.4 Membranes

Tubular ceramic membranes were supplied by *Pall* (Portsmouth, UK) and belong to the Membralox^{TM} P19-40 range. These membranes are commercially available tubular ceramic membranes. Membralox membranes with pore sizes of 0.2, 0.5 and 0.8 μm were studied. These membranes contain nineteen 1.02 m long channels, each with an internal diameter of 4×10^{-3} m. The effective filtration area of the module was 0.244 m^2. The membrane is an α-alumina ceramic membrane which is comprised of a double layer.

Flat sheet ceramic membranes were supplied by *Kerafol* (Eschenbach, Germany). These membranes were custom made using α-alumina with a size of 220 x 110 mm with a thickness of 2 mm. Pore sizes of 0.2, 0.5, 0.8 and 2.0 μm were studied. The flat sheet membrane was inserted into a custom made rig containing inserts with eleven channels 0.22 m long and 4×10^{-3} m wide. The channel diameter was selected to mimic the flow in the channels of Membralox membranes. This allows identification and analysis of the membranes and alludes to the mechanisms of fouling and cleaning.

The choice of membranes was made due to the high chemical and thermal stability of α-alumina. The use of flat sheet membranes allowed analysis to develop a mechanistic understanding which could not be obtained using the tubular ceramic membranes. The tubular ceramic membranes were investigated to allow a comparison to the flat sheet membranes since these are available commercially, and are industrially relevant.

3.3 Equipment

3.3.1 Filtration equipment

A semi-industrial microfiltration unit with a tubular ceramic membrane was used for crossflow filtration. The rig was designed by Bechervaise,[21] Head and Bird;[18] and can be seen in Figure 3.1 (photograph) and Figure 3.2 (schematic). The apparatus contains two circulation loops: a feed

pump (*LAWARA* centrifugal pump SKM70/33 SP) circulates the feed from the tank. The tank contains a heating coil attached to a heat exchanger (*Conair Churchill* 18 200) to allow temperature control. Pumping allows the feed to be fed into the retentate circulation loop. In the retentate circulation loop a triplex plunger positive displacement pump (CAT 1051, capable of generating up to 2.3 m^3 h^{-1}) circulates the feed. Valves are present to allow the transmembrane pressure and crossflow velocity to be controlled independently of each other. Pressure transducers (*Cole Palmer* 68075, range 0 – 250 PSIG), a thermocouple, an electromagnetic flow meter (*Magflo* MAG 2560) and a balance (*Ohaus*, Scout Pro, SPR4001) are fitted to allow the operating conditions and permeate flux to be automatically logged to a computer. A cooling system was fitted to the system and the heat exchanger connected to the mains water to allow temperature control, to within one degree Celsius, with two pumps adding heat to the system. The pressure transducers were fitted at the feed inlet (P_1), retentate outlet (P_2) and permeate outlet (P_3) to allow the transmembrane pressure to be calculated using Equation 3.1.

$$TMP = \frac{(P_1+P_3)}{2} - P_2 \qquad \text{Equation 3.1}$$

Lab view software was used to collect the filtration data such as run time, feed, retentate and permeate pressures, mass of permeate and temperature. Data was analysed using Microsoft Excel software and plotted using Sigmaplot. An example flux calculation is shown in Appendix C.

Figure 3.1: Photograph of filtration system set up for tubular ceramic membranes.

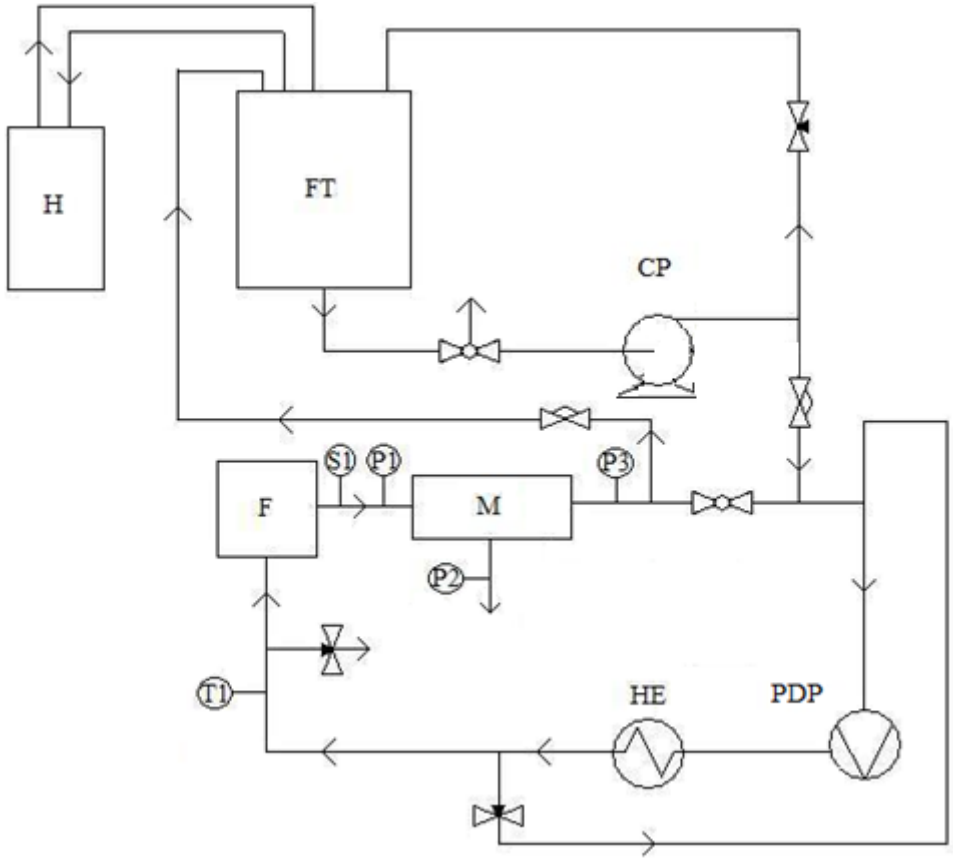

Figure 3.2: Schematic diagram of filtration apparatus. Where FT- feed tank, H- oil circulation pump and heater, M- membrane module, F- flow meter, HE- heat exchanger, CP- centrifugal pump, PDP- positive displacement pump, T- thermocouple, S- sampling point and P- pressure transducer. Diagram adapted with permission from Head & Bird (2013).

The membrane was housed in a stainless steel tubular housing supplied by *Pall* (Portsmouth, UK). In order to secure the membrane inside the housing rubber gaskets were fitted to the ends of each membrane. Pictures of the tubular ceramic membrane and housing unit are shown in Figure 3.3.

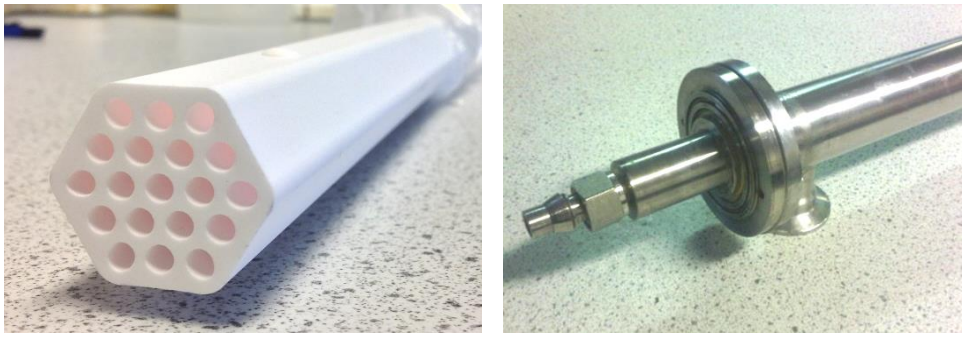

Figure 3.3: Pictures showing cross section of membrane (left) and housing (right)

3.3.2 Modifications

Modifications were made to the above rig to allow the filtration using flat sheet ceramic membranes. A plate and frame module was designed and built by Paul Frith at the University of Bath. In the module, the membrane was sandwiched between two plastic inserts containing 11 square channels with a diameter of 4 x 10^{-3} m square, and a length of 0.22 m. This design was chosen to simulate the flow through the tubular ceramic membranes allowing a comparison under consistent operating conditions.

The module was built using polyethylene to allow it to be compatible with sodium hypochlorite. This was encased in a piece of 0.01 m thick 316 grade stainless steel to give it strength and resistance to high pressures. O-rings were used to form a seal with the membrane. The plate and frame module can be seen in Figure 3.4 (photo) and Figure 3.5 (schematic).

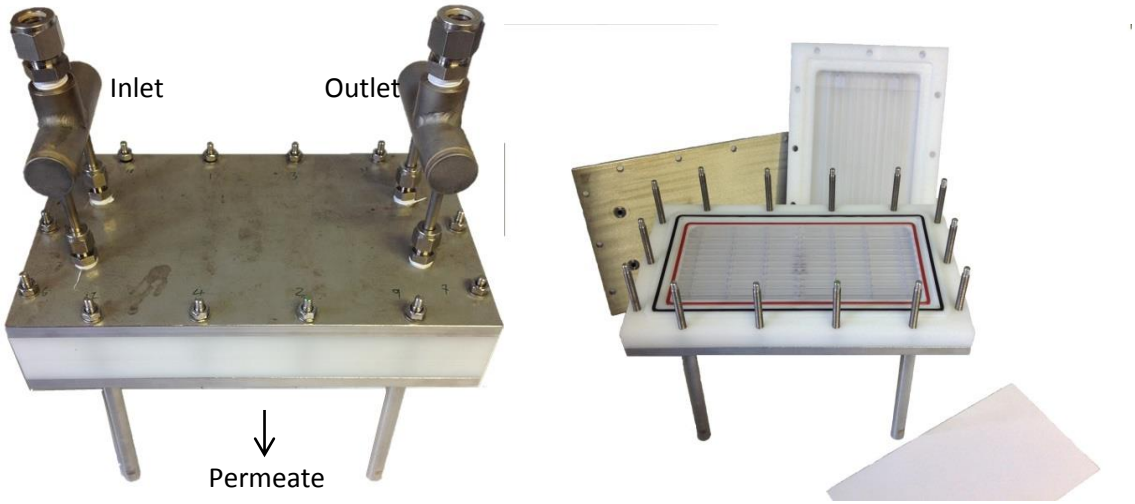

Figure 3.4: Photograph of plate and frame module for flat sheet membranes. This can be attached to the rig described in Figure 3.1 via the inlet, outlet and permeate fittings illustrated.

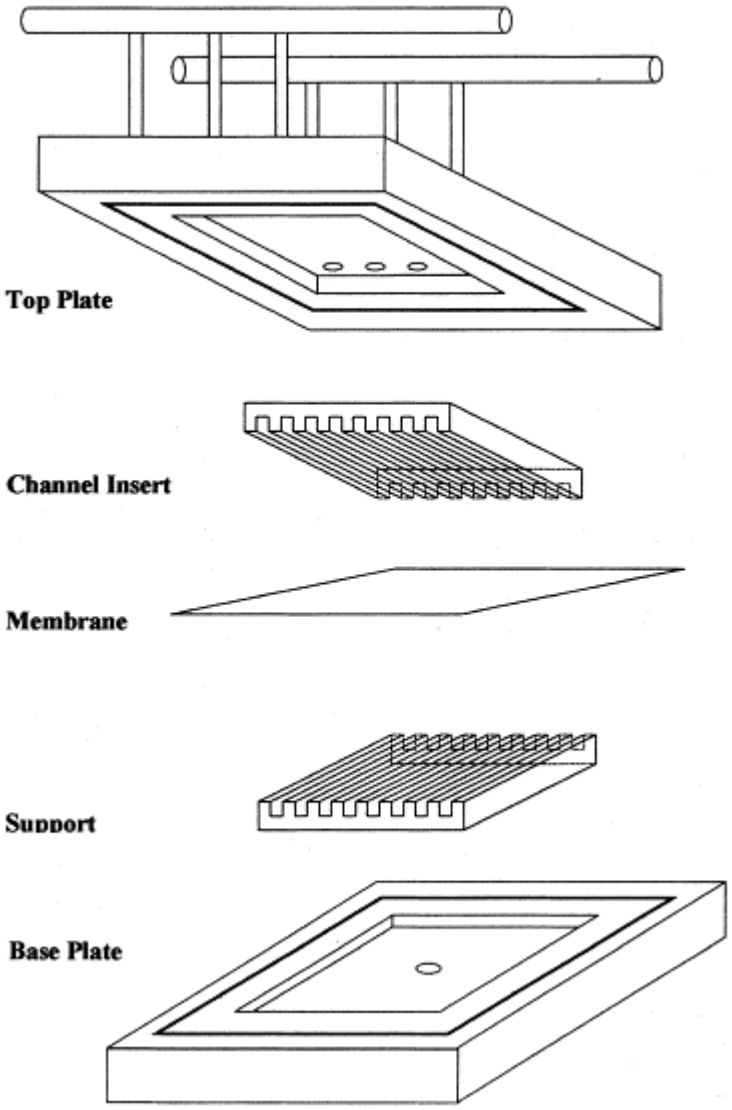

Figure 3.5: Schematic diagram of flat sheet crossflow module adapted from Bird.[175]

3.4 Experimental procedures

3.4.1 Pure water flux measurement

Prior to fouling, a pure water flux (PWF) measurement was taken to allow quantification of the initial membrane flux. After each fouling and cleaning cycle, the PWF was again measured. Quantifying any changes in PWF observed between fouling and cleaning cycles allow the fouling/ cleaning to be quantified. This allows the flux recovery following cleaning to be identified.

The PWF was measured over a twenty minute period by filtration of 30 L pure water at 40 °C with a crossflow velocity of 2.3 m s^{-1} (Re = 13982) and with the TMP ranging from 1.0 to 3.0 bar (typically

1.5 bar). The conditions used for PWF measurements were kept constant to allow the membrane performance to be evaluated at each stage of the experiment. Calculating the PWF also allows calculation of the membrane resistance using Darcy's law.

3.4.2 Fouling experiments using Gum Arabic

Model waste suspensions were created as detailed in Section 3.2.1 by reconstituting spray dried Gum Arabic in water. The operating conditions were altered by a single parameter which could include temperature, crossflow velocity, or transmembrane pressure to observe the impact this had on permeation, flux and membrane resistance. Both the retentate and permeate were recycled to the feed tank, with the exception of small samples taken for analysis (with the exception of the feed and bleed experiments where only the retentate was recycled). This allowed a constant feed concentration minimising any concentration effects during filtration. All fluxes were recorded at five second intervals and samples were taken at various points during the filtration. Pseudo steady state can be approximated by the use of Equation 3.2 which represents a point where flux decline (J) over time (Δt) is at a rate of less than 5 % variation,[100] i.e. the flux difference between J_f at time t and Δt e.g. 30 seconds is less than 5 % of $J_f(t)$. This was observed for each of the experiments and is discussed in the results section.

$$\frac{J_F(t-\Delta t)- J_F(t)}{J_F(t)} < 0.05 \qquad \text{Equation 3.2}$$

The standard filtration conditions used in this thesis are filtration of 2.0 wt. % for 60 minutes at 40 ^{o}C with TMP 1.5 bar and CFV 2.3 m s^{-1}.

3.4.3 Rinsing conditions

The role of rinsing in preparing the membrane for cleaning is extremely important. Removing as much of the deposited layer as possible allows the efficiency of the cleaning cycle to be maximised, both in terms of time and cleaning agent requirements.[176] Water alone was shown to be ineffective at removing Gum Arabic from fouled membranes therefore rinsing was done at ambient temperatures to prevent additional energy usage. The rinsing time used was 15 minutes as this is the standard used industrially.[149]

3.4.4 Cleaning experiments

Cleaning solutions were prepared by dissolving the cleaning agent in water and heating to the required temperature. Temperature was optimised as discussed in Section 6.5. Cleaning solutions were run through the membrane for a 20 minute period, monitoring any changes in flux over this time. It was found that cleaning for longer times did not result in any improvements in the flux recovery. Cleaning was evaluated in terms of the observed flux recovery. The cleaning efficiency could be calculated by the ratio of the PWF after cleaning (J_C) to that before fouling (J_W), and percentage flux recovery ($\%\ J_r$) identified using Equation 3.3.

$$\%\ J_r = \left(\frac{J_c}{J_w}\right) \times 100 \qquad \text{Equation 3.3}$$

Standard cleaning conditions were used of cleaning at 60 ^{o}C with TMP 1.0 and CFV 2.3 m s^{-1} unless otherwise specified.

3.4.5 Sample collection

Samples were obtained simultaneously from the feed/ retentate and permeate streams at regular time intervals during filtration. The samples were collected in glass sample tubes and used to measure and compare the concentration of Gum in the different process streams over time. In addition to the concentration; factors such as the pH, conductivity, COD and solids could be measured.

3.4.6 Pre-filtration of Gum

Pre-filtration was carried out through a 25 µm stainless steel cartridge filter (*PCI-Memtech*, Swansea, UK). The stainless steel filter module was connected to an Amicon 5 L pressurised feed vessel (*Merk Milipore*, Billerica, USA) which was pressurised using a nitrogen cylinder (*BOC*, Guildford, UK). The feed tank and filter were connected with stainless steel piping and *Swagelok* fittings.

3.4.7 Static fouling

In order to measure the adhesion of Gum Arabic or Arabinogalactan to alumina without the presence of convective forces the PWF of a membrane was measured, and then the membrane was soaked in a foulant suspension at 40 ^{o}C for 20 minutes.

3.5 Gum measurements

The quality of the feed and permeate were determined to identify separation. Each parameter was measured in triplicate and is reported as the average with the standard deviation.

3.5.1 Solids concentration

Dry weight analysis was carried out by measuring the mass of a clean, dry test tube and adding a known amount of Gum suspension to the test tube. The test tube and Gum suspension were weighed and the mass recorded. The samples were put in an oven at 50 °C for 48 hours to allow the water to evaporate, leaving the dried Gum remaining. A temperature of 50 °C was used to prevent any denaturing of the protein which can happen at higher temperatures. The final mass of Gum was recorded and used to calculate the concentration of Gum present in the sample.

The total dissolved solids (TDS) and total suspended solids (TSS) were measured following the Standard Method 2540-Solids.[177]

All measurements were carried out using a balance accurate to four decimal places.

3.5.2 Concentration

The different streams were measured using a Brix r^2 mini handheld refractometer (*Reichert technologies*, Depew, NY, USA). The refractometer was calibrated for Gum suspensions and used to calculate the concentration, and this was compared with the dry weight samples. This allowed quick analysis to gain an insight into Gum rejection before the dry weight could be analysed. Brix readings were calibrated to be accurate to 1 dp, meaning that while they offered quick analysis during the filtration, dry weight measurements were used for the reported data as this can be accurate to 4dp.

3.5.3 Viscosity measurement

Viscosity measurements were made using a Cannon-Fenske routine viscometer size 200 (*Cannon instrument,* State college, PA, USA). A Gum suspension was inserted into the viscometer and placed in a constant temperature bath and the temperature allowed to stabilise for 15 minutes. The efflux time was measured for the sample to travel between two points on the viscometer. Five repeats were measured for each sample, at each temperature, allowing the average and standard deviation to be calculated.

3.5.4 pH and conductivity

The pH and conductivity were measured using a pH 5+ and CON11 meters (*Oakton instruments*, Vernon Hills, IL, USA) respectively. Samples were cooled to room temperature before the pH and conductivity were measured to minimise error in the analysis. Samples were measured in triplicate and are accurate to 1 decimal place.

3.5.5 Chemical oxygen demand

The chemical oxygen demand (COD) is an important parameter in determining water quality. COD was measured colourmetrically using LCK cuvettes (*Hach Lange*, Salford, UK) containing sulphuric acid and potassium dichromate. 2 mL of sample was added to each cuvette, heated for 2 hours at 148 °C and cooled before inserting into a DR2800 eco machine (*Hach Lange*, Salford, UK) for the COD value to be determined.

3.5.6 Particle sizing

To determine the particle size of reconstituted Gum Arabic suspensions, a 10.0 wt. % Gum Arabic suspension was measured using a light scattering Malvern Mastersizer X (*Malvern Instruments Ltd*, Malvern, Worcestershire, UK). The sample was inserted into a Malvern small volume sample dispersion unit (*Malvern Instruments Ltd*, Malvern, Worcestershire, UK) with a stirring speed of 3000 rpm. Two different lenses were used to obtain measurements (45 mm and 300 mm from the 6358 series) to allow measurements of particles in the range of 0.1 – 600 µm diameter. A concentration of 10.0 wt. % was required as concentrations lower than this did not give

reproducible results. This was due to the low concentration of particles in suspension, high polydispersity, and irregular shape of Gum particles.

3.5.7 Gel permeation chromatography (GPC)

GPC analysis allows the components of Gum in a sample to be separated and therefore allows any differences in the composition to be analysed. The Gum can be fractionated which allows there to be more of one component present in the sample e.g. reduced levels of AGP.

The samples were sent to *Kerry Ingredients* (Cam, UK) where GPC analysis was carried out. The samples were filtered through a 0.2 µm syringe filter before being injected to a Malvern GPC-Max instrument (*Malvern Instruments*, Malvern, UK) fitted with a GE Superose-6 10/300 GL gel column and triple detection system (*GE*, Uppsala, Sweden). The triple detection system uses right angle and low angle light scattering, refractive index and ultraviolet. The samples pass through the column at 0.5 mL min^{-1}. The molecular weight and percentage of AGP is determined using OmniSec software.

3.6 Membrane analysis

3.6.1 Effective contact angle measurement

Effective contact angle is a useful way to measure the wettability of a membrane which gives information about the hydrophobicity of the membrane. Hydrophobic membranes have a contact angle greater than 90 º and hydrophilic membranes have a contact angle less than 90 º (tending towards 0 º for very hydrophilic membranes). The sessile drop method was used to measure the contact angle using a *DataPhysics* QCA 20 contact angle goniometer (*Dataphysics*, Filderstadt, Germany) with SCA 20 software. A 1 µL drop of ultrapure water was placed on the membrane surface using a syringe and instantaneously the contact angle between the droplet and membrane was calculated on both sides (using Young-Laplace model built into the SCA software). Due to the highly porous nature of the membranes the procedure was repeated at 10 different points on the membrane with measurements taken from both sides of the membrane. This produced a total of 20 measurements which were then averaged. The measurements were taken as quickly as possible to reduce volume changes due to permeation or evaporation. Due to the high

permeation through the membranes, and therefore large margin of error, the contact angles should be used relative to each other than taken as absolute values.

3.6.2 Zeta potential

The surface charge of membranes can have a significant effect on the fouling and separation properties of a membrane. The surface charge density is related to the zeta (ζ) potential of the membrane. Streaming potential measurements can be used to determine the ζ-potential of a membrane. The streaming potential is induced when an electrolyte solution flows across a stationary surface, or through the pores of a stationary membrane.

Zeta potential measurements were carried out at Lappeenranta University of Technology, using a small disk of membrane with a surface area of 18.1 cm^2. The membrane was supported in a polycarbonate module fitted with two sets of Ag/AgCl electrodes allowing measurement of the streaming potential across the membrane (through the pores). A 0.001 $molL^{-1}$ KCl solution was prepared and heated to 25 ^oC using a double jacketed glass vessel. An *Ismatec* BVPZ magnetic pump was used to pump the KCl solution through the membrane and could be adjusted to change the TMP. The solution was pumped through the membrane and allowed to stabilise for 10 minutes prior to measurements. The pressure was measured using a pressure sensor (*Honeywell* 242PC100G 0 – 7 bar). At each pH examined, five different TMPs were measured and the flow kept constant. This allowed the zeta potential to be determined using the Helmholtz – Smoluchowski equation without corrections, as shown in Equation 2.10. Equation 2.10 only holds if the Debye length of the solution is small compared to the radius of the pores, which is fulfilled for the membranes and ionic strength used in this study.

The temperature was measured at four different points using PLM-1 temperature sensors. In the feed vessel the pH was monitored using a *Schott Gerate GmbH* Herate CG822 pH meter. The ζ-potential was measured over a pH range of 3 – 8. Out with these conditions the electrodes can become damaged leading to unreliable measurements. All of the measurements were collected using acquisition software programmed with Microsoft QuickBasic version 4.5 and using ADDA 14 interface card. The results were then analysed using Microsoft Excel and plotted using Sigmaplot.

3.6.3 Scanning electron microscopy

The morphology of the membranes and identification of the nature of the fouling layer was determined using a JEOL JSM-6480LV field emission scanning electron microscope (*JEOL*, Tokyo, Japan). The samples were prepared for SEM by being attached to double sided carbon tape and placed in a desiccator under high vacuum for 24 hours. The samples were then coated with gold to improve the image quality using an Edwards Sputtercoater 8150B with a coating time of 4 minutes under argon.

INCA software was used with an INCA X-Act SDD x-ray detector for EDX analysis (*Oxford Instruments*, Cowfold, UK) to allow determination of the elemental composition of the surface layers of the membrane. Uncoated samples were used for this, and the analysis was carried out in low vacuum mode (15 Pa).

3.6.4 FTIR

The presence of fouling deposits and effect of cleaning and pre-treatment on the membranes was analysed using Fourier transform infra-red spectroscopy (FTIR). This is useful for obtaining information about chemical bonds present and gives a good indication as to the condition of the membrane surface, and any organic foulants present. An FTIR Frontier spectrometer (*Perkin-Elmer*, Waltham, USA) was used to measure over wavenumbers of a range of 600 – 4000 cm^{-1}. Initially the samples were measured in ATR mode (attenuated total reflection), however due to the strong absorbance of alumina masking any other peaks, DRIFTs mode (diffuse reflectance infrared Fourier transform spectroscopy) was used as this is more sensitive to the surface layer. 15 scans were taken and averaged for each sample, with a resolution of 0.5 cm^{-1}. Bio-Rad laboratories 'Know it all' software was used to analyse the spectrum and determine the peaks present.

3.6.5 Raman

Raman spectroscopy was used to determine if there were any changes to the alumina structure following pre-treatment, fouling or cleaning. Spectra were obtained using a *Thorlabs* IK series Raman spectrometer (New Jersey, USA) fitted with a HE-Cd laser allowing light of wavelengths 532

and 785 nm. The Sample was enclosed in a *Renishaw* RE 04 Raman microscope enclosure (Wotton-under-Edge, UK) for analysis.

3.6.6 Fluid dynamic gauging

Fluid dynamic gauging is a relatively new and sensitive way to measure the thickness of soft deposits on a surface. In addition, fluid dynamic gauging can be used to apply a quantified shear stress to a surface allowing quantification of the stress required for foulant removal. The apparatus used was based on that reported by Chew *et al.*[165] with a few modifications, such as the inclusion of a syringe pump. An illustration of the apparatus is shown in Figure 3.6.

The apparatus consisted of a Perspex tank of 450 x 450 x 250 mm and a nozzle of diameter 3/8 inch (d_t). The nozzle was connected at one end to a straight section of siphon tube of diameter d_1 (A – B, true length of straight tube 0.42 m), and at the other end to a curved section with a diameter d_2 (B – C, true length ~1.30 m). The nozzle was fully submerged in the tank, is held normal to the gauging surface at height h (clearance height), which can be altered using a micrometer. Fluid was sucked from the quasi-stagnant surroundings into the nozzle and then through siphon tube sections 1 and 2 to a syringe pump (*Cole-Palmer* 110, Veron Hills, IL, USA). The suction pressure Δp_{14} was kept constant by fixing the hydrostatic head, H.

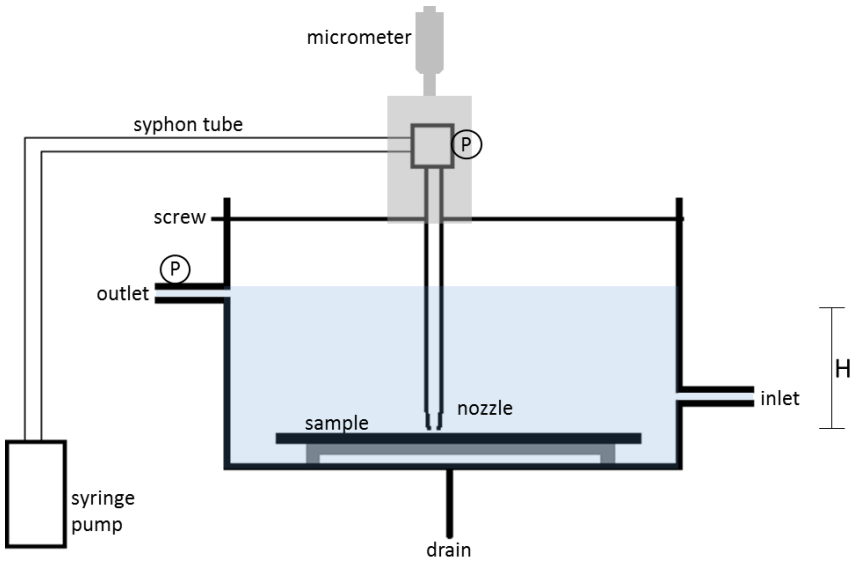

Figure 3.6: Diagram of fluid dynamic gauging rig

The spindle of micrometer *M1* (*Mitutoyo*, Kanagawa, Japan) was used to control the vertical movements of the gauge relative to the gauge surface. This allowed the clearance height to be set to a known distance.

The difference in pressure between the tank and the gauge (Δp_{14}) was monitored using an Omega PX26-001DV (*Omega Engineering*, Cheltenham, UK). Due to the hydrostatic head being fixed, differences in pressure are created by changing flow rate and the distance the gauge is from the surface.

The temperature was maintained at a constant temperature (± 0.5 °C) via a heating coil circulating from a Technie water bath (*Bibby scientific*, Staffordshire, UK) fitted with a Grant GD120 heater (*Grant Instruments*, Cambridgeshire, UK).

3.6.7 Colorimetric analysis of membranes

To determine the removal of Gum Arabic under varied shear stresses, a Periodic acid Schiff (PAS) staining protocol was used to stain the polysaccharide pink allowing colorimetric analysis to be used to determine the relative colour change (and hence Gum removal) compared to a control.

The membranes were fouled and subjected to shear stresses through fluid dynamic gauging. The samples were then soaked in a 0.5 % periodic acid (*Fisher Scientific*, Loughborough, UK) solution for five minutes allowing any polysaccharides to be oxidised. The membrane was then rinsed using distilled water. The sample was then placed in Schiff reagent (*Fisher Scientific*, Loughborough, UK) for 15 minutes and then washed in lukewarm tap water for 5 minutes (as per PAS protocol). During this step the polysaccharides, which had been oxidised to aldehydes, react with the Schiff reagent to produce a dark pink colour.

The colour was analysed using a Nixon AZ100 microscope (*Nixon Instruments*, Amsterdam, Netherlands) fitted with a Photonic PL3000 light (*Photonic*, Seeböckgass, Austria). Data was collected using Matlab and analysed using ImageJ to allow the RGB values of the sample to be determined.

3.6.8 Atomic force microscopy

Atomic force microscopy (AFM) is useful in analysing roughness and topography of the surface, but can also be used to determine surface interactions through the use of a colloidal probe. AFM measures the force as a function of displacement which can be varied using a piezoelectric crystal. A laser beam is aligned with the cantilever and small movements/deflections of the cantilever can be detected through a photodiode. A *Nanosurf* easyscan 2 (Lanhen, Germany) was used to image and calculate the roughness of the membranes. Imaging was carried out in tapping mode with a scan rate of 0.4 Hz and a resolution of 256 lines over a 10 x 10 µm area. The images were obtained using a *BudgetSensors* TAP 190 Al-G probe (Sofia, Bulgaria) with a resonance frequency of 190 kHz and a force constant of 48 Nm^{-1}. The cantilever spring constant was verified through the thermal tuning software of the AFM. For the roughness measurements a 20 x 20 µm area was studied under the same conditions. *Nanosurf* easyscan software was used to calculate the average roughness in terms of S_a based on the average height at each of the points measured on the membrane. Three areas were measured for the roughness, and the average and standard deviation are reported.

In order to measure the adhesion forces of the membranes, a colloidal probe was used. Measurements were carried out on a Nanowizard 2 (*JPK*, Berlin, Germany). The colloidal probe was a silica (glass) bead of diameter 10 µm. The silica bead was attached to the end of a DWP-10 cantilever using glue. The DWP-10 cantilever was manufactured by *Veevo Probes* (Plainview, NY, USA). The cantilever spring constant was 0.12 Nm^{-1}. The force measurements were obtained in a solution of deionised water to allow the interactions in solution to be identified. Measurements were carried out at 25 ^{o}C.

To measure the adhesion force, the colloid probe was first brought into momentary contact with the surface using a specified force constant. The loading force was kept constant to allow comparative measurements. The colloid probe was then retracted from the surface. 10 repeats were carried out on different parts of the membrane surface and the average has been reported with the standard deviation representing the error.

3.6.9 Mercury porosimetry

The pore size distribution and pore volume of membranes was measured using a *Micrometrics* Autopore III Mercury Intrusion Porosimeter (*Micrometrics Instruments*, Norcross, USA). Wet

membrane samples were oven dried at 60 °C for 24 hours, and then cut into small pieces of approx. 0.2 x 1 cm^2. Approximately 10 g of membrane pieces were packed into a 3 cm^3 penetrometer (*micrometrics* ref 16-0734, constant 22.065 µL pF^{-1}). The porosimetry was characterised by applying a range of pressures (30 – 30,000 psi) to the sample immersed in mercury. The pressure required to intrude mercury into the pores, and the volume of mercury intruding was used to determine the pore size distribution, and pore volume of the membrane samples.

3.6.8 Modelling

Modelling of the dominant fouling mechanism was carried out using the fouling mechanisms described by Hermia[101] and extended for crossflow by Field.[93] Table 3.2 shows the filtration laws and parameters as determined by Field with the right hand column denoting the linearised form detailed by Nataraj *et al.*, Madaeni and Samieirad, and Tracey and Davis.[91, 102, 103] Experimental data was measured every 5 seconds over a 60 minute period. The experimental data was plotted in the linear form of the equations, this allowed an r^2 value to be determined as per Nataraj *et al*.[102] In order for the model to fit the r^2 should be ≥ 0.99. Data was broken down into 0 – 5 minutes, and 5 – 60 minutes throughout the filtration and fitted to the model as this was deemed most appropriate for observing any changes to the fit over time.

Table 3.2: Parameters used in modelling the fouling mechanism

Law	K	N	equation	Linearised form
Cake filtration	$K_c = \frac{\alpha' \gamma s}{AR_0Q_0(1-ms)}$	0	$\frac{d^2t}{dV^2} = K_c$	$\frac{t}{V} = k_C V + \frac{1}{J_0}$
Intermediate pore blocking	$K_I = \frac{\sigma}{A_0}$	1	$\frac{d^2t}{dV^2} = K_I \frac{dt}{dV}$	$\ln t = k_I V + \frac{1}{J_0}$
Standard pore blocking (pore constriction)	$K_s = \frac{2C}{LA_0} {Q_0}^{1/2}$	1.5	$\frac{d^2t}{dV^2} = K_S \left(\frac{dt}{dV}\right)^{3/2}$	$\frac{t}{V} = k_s t + \frac{1}{J_0}$
Complete blocking	$K_b = u_0 \sigma$	2	$\frac{d^2t}{dV^2} = K_b \left(\frac{dt}{dV}\right)^2$	$J = J_0 - k_b V$

Where:

A = filter membrane surface area (m^2)

C = volume of solid particles retained per unit filtrate volume (-)

J = permeate flux ($Lm^{-2}h^{-1}$)

J_0 = pure water flux ($Lm^{-2}h^{-1}$)

K = fluid consistency index (non-Newtonian fluids) (kg s m^2)

k_x = constant relating to blocking model where x represents the blocking mechanism e.g. c is cake (-)

L = membrane thickness (m)

m = mass ratio of wet to dry cake

Q = flow rate (m^3s^{-1})

R = filter resistance (m^{-1})

s = mass fraction of solids in feed

t = filtration time

u = filtrate linear velocity (ms^{-1})

V = filtrate volume (cumulative) (m^3)

α' = cake specific resistance (mkg^{-1})

γ = filtrate density (kgm^{-3})

σ = blocked area per unit volume (m^{-1})

4. Proof of concept

This chapter details the physical properties of Gum Arabic, and the α-alumina membranes used in this study. Understanding the physical properties of the raw materials helps aid in an understanding of the fouling phenomena. Additionally, this chapter shows that it is possible to remove Gum Arabic from a model waste suspension containing 2.0 wt. % spray dried Gum Arabic using microfiltration membranes.

4.1 Physical properties of reconstituted Gum

4.1.1 Viscosity

An important consideration in membrane separations is the viscosity of the feed. Viscosity can affect the mass transfer to the membrane surface as well as the nature of the flow across the surface during crossflow filtration. The viscosity of reconstituted spray dried Gum Arabic was measured, to identify variations in the temperature and concentration of Gum, using the method described in Section 3.5.3.

Figure 4.1 shows the influence of temperature on the viscosity of Gum Arabic suspensions over a range of 1.0 – 5.0 wt. %, and 20 – 50 ^{o}C. It can be seen that as the temperature is increased, the viscosity decreases, and an increase in the viscosity occurs with the suspension concentration. Figure 4.2 shows the increase in viscosity is linear with the increase in concentration with r^2 = 0.996. The viscosity increase with concentration is greatest at low temperatures. At 20 ^{o}C the viscosity increased from 1.7 mm^2s^{-1} at 1.0 wt. % to 3.9 mm^2s^{-1} at 5.0 wt. %, an increase of 2.2 mm^2s^{-1}. Comparing the change in viscosity at 50 ^{o}C the viscosity increased from 1.0 mm^2s^{-1} at 1.0 wt. % to 2.0 mm^2s^{-1} at 5.0 wt. %, an increase of 1.0 mm^2s^{-1}. These results show that, as expected, reducing the concentration of Gum in suspension, and increasing the temperature reduces the viscosity of a Gum Arabic suspension.

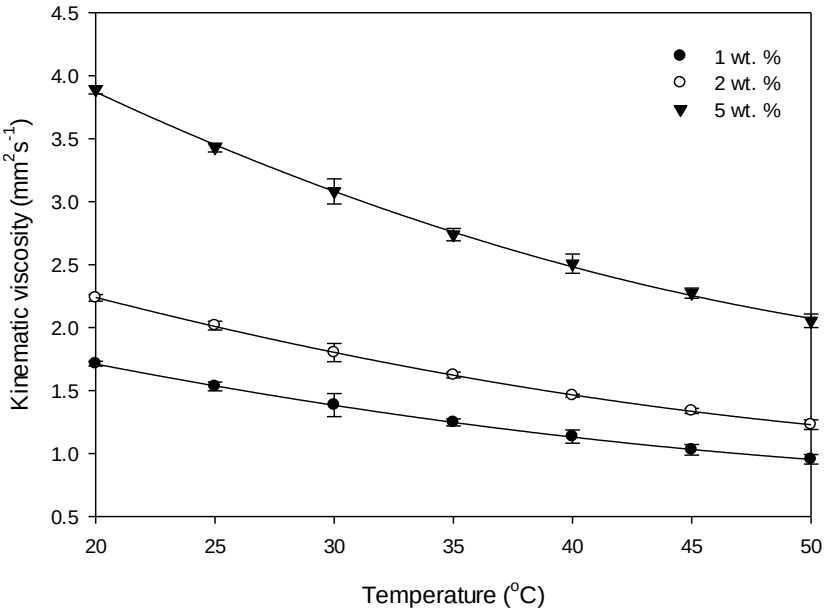

Figure 4.1: Kinematic viscosity of Gum Arabic suspensions in water over a temperature range of 20 – 50 ^{o}C at ambient pressure.

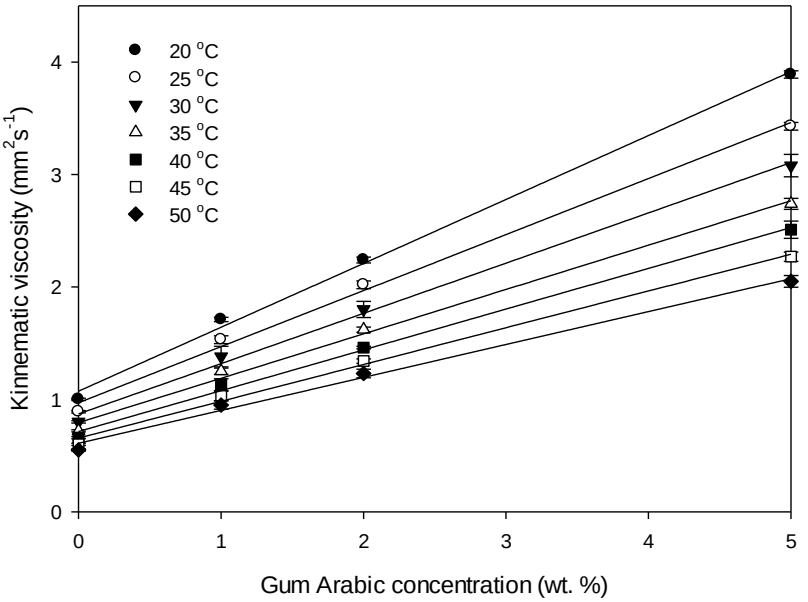

Figure 4.2: Variation of viscosity with concentration and temperature over a range of Gum concentration 0 – 5 wt. % and temperature range 20 – 50 ^{o}C.

Comparing the viscosity of the Gum Arabic suspensions with that of water, it can be seen that Gum Arabic suspensions of 1.0 wt. % have almost double the viscosity of water. This agrees well with the results obtained by Glicksman and Sand who reported that the viscosity of Gum Arabic is much lower than other gums which usually show a high viscosity at 1.0 – 5.0 wt. %.[178] They

reported that Gum Arabic does not show high viscosity until a concentration of 40 – 50 wt. %. The viscosity of permeate containing 0.1 wt. % and 0.2 wt. % were measured and the viscosities at 40 ^{o}C are 0.767 ± 0.120 and 0.889 ± 0.098 mm^{2}s^{-1} respectively. The viscosity of Gum is higher than water, and this has been taken into consideration when calculating the membrane resistance (Section 4.4.1). The viscosity of cleaning solutions was not statistically significantly different from water (P > 0.05) therefore the viscosity of water has been used when calculating the membrane resistance during cleaning.

The nature of the flow across the membrane surface can be established by quantifying the Reynolds number (Re). There are three main flow types, laminar, transient and turbulent, and each of these will influence the mass transfer of the solution to the membrane surface as well as the nature of the flow. For laminar flow Re is less than 2300, transient flow occurs when Re is between 2300 and 4000 and turbulent flow occurs when Re is above 4000. The Reynolds number is calculated using Equation 4.1 where Re is the Reynolds number (dimensionless), u is the velocity (ms^{-1}), L hydraulic radius of the channel (m) and μ is the kinematic viscosity (m^{2}s^{-1}). The Reynolds number is shown for each of the conditions detailed above in Figure 4.3.

$$Re = \frac{uL}{\mu} \qquad \text{Equation 4.1}$$

Under the operating conditions detailed in Section 3.4.2, it can be observed that the flow is turbulent for water, 1.0 wt. % Gum suspensions and 2.0 wt. % Gum suspensions over the temperature range of 20 – 50 ^{o}C. However when the Gum concentration is increased to 5.0 wt. % the flow is turbulent above 45 ^{o}C, and transient between 20 and 45 ^{o}C. With the experimental set up, it is not possible to increase the crossflow velocity above 2.3 m s^{-1} therefore working with a feed concentration below 5 wt. % is desired to ensure turbulent flow.

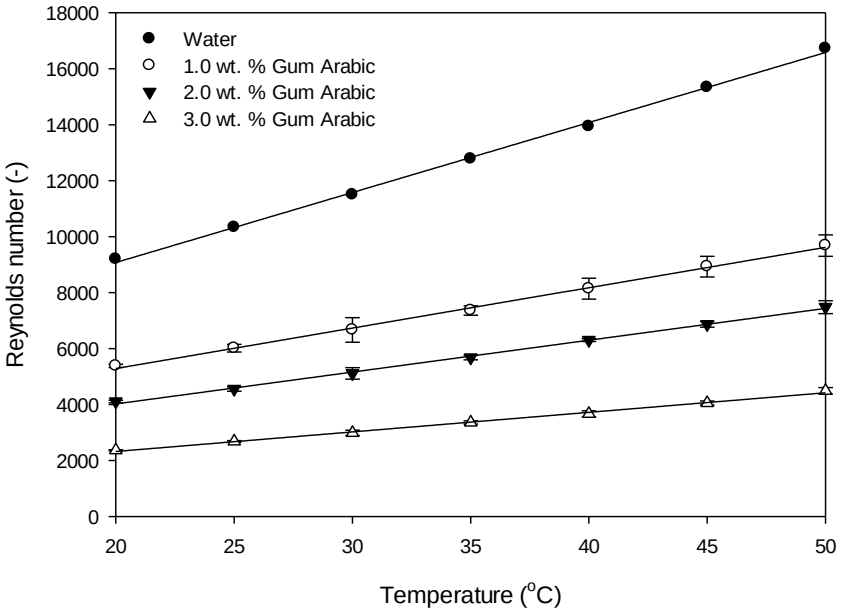

Figure 4.3: Reynolds number for 0.0 – 5.0 wt. % Gum Arabic over temperature range 20 – 50 °C.

4.1.2 Particle size

It is important to consider the particle size one wishes to remove from the feed when selecting a suitable membrane for separation. Generally the pore size should be smaller than the diameter of the particles remaining in the retentate to allow efficient separation via size exclusion. The size distribution of a 10.0 wt. % suspension was measured as described in Section 3.5.6. A 10.0 wt. % suspension was used because suspensions containing 1.0 – 5.0 wt. % Gum Arabic were below the detection limits of the apparatus used. Figure 4.4 shows the size distribution measured for Gum Arabic suspension which had been dissolved in water at 40 °C and stirred for 60 minutes as described in Section 3.2.1, as well as a Gum Arabic suspension pre-filtered through a 25 µm steel filter described in Section 3.4.6.

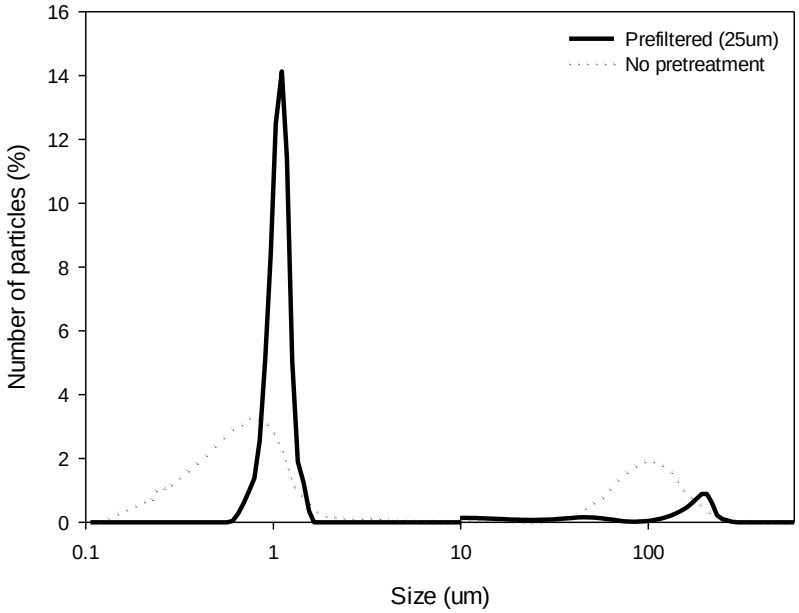

Figure 4.4: Size distribution of particles in Gum Arabic showing the influence of filtering through 25um filter.

It can be observed that there is a broad size distribution of Gum with two distinct peaks, one over the range 0.2 – 3 µm and another 50 – 300 µm. Based on literature data, the size of Gum Arabic molecules range from 20 – 100 nm with some variation due to the Gum structure showing natural variation.[56] Gashua *et al.* reported that agglomeration of Gum Arabic particles can occur over time, and this is particularly pronounced for Gum samples with a high protein content.[179] It has also been noted by Dror that even in low concentrations aggregates are formed leading to larger particles of Gum in suspension.[25] Based on the results obtained, no particles were measured below 0.1 µm suggesting that most of the Gum is present in the form of aggregates. It is likely that the harsh processing conditions such as spray drying the Gum, cause the presence of a large number of aggregates.[9] To decrease the concentration of aggregates and remove the largest particles, the Gum suspension was pre-filtered through a 25 µm filter. It can be observed that pre-filtering the Gum suspension resulted in reducing the number of particles present in the range of 50 – 300 µm and interestingly resulted in a sharp peak around 1 µm. These results confirm the presence of aggregates with pre-filtering through a course filter, as this results in the breaking down of large aggregates into smaller ones. When the Gum suspensions were stored at room temperature for 24 hours, no change was observed for the unfiltered sample, and the presence of larger aggregates returned to the pre-filtered suspension, producing an identical trace to that of the unfiltered sample as shown in Figure 4.5. This shows that the Gum is fully dissolved after stirring for 60 minutes, and also shows the stability of the Gum aggregates in suspension.

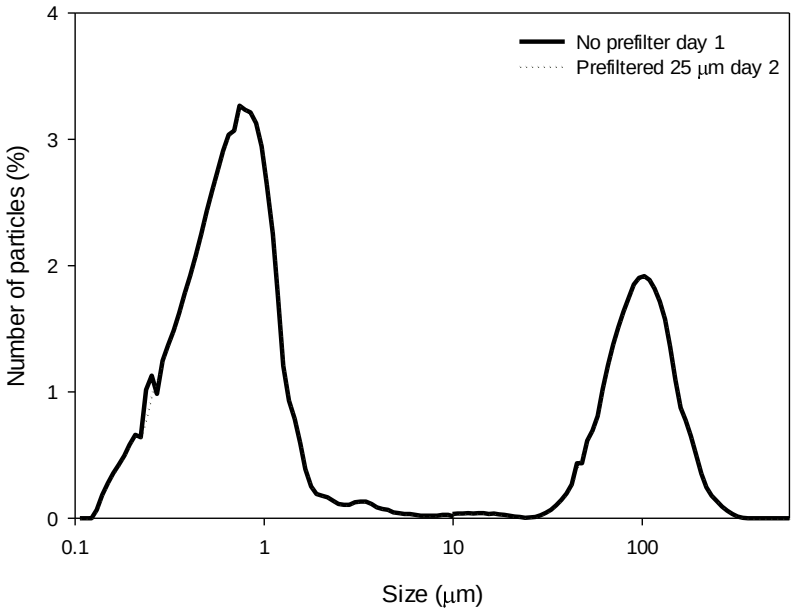

Figure 4.5: Size distribution of Gum Arabic particles, dotted spectra overlaps line spectra showing that the aggregates form at the same level after the pre-filtered sample has been at room temperature for 24 hours.

Results obtained by Lin *et al.* indicate that the particle size has a larger effect on membrane fouling than that of the zeta potential. Fouling is dependent on the total interaction of short range (acid-base) interactions, van der Waals interactions and electrostatic interactions. Zeta potential only affects the electrostatic interactions, whereas particle size effects the interaction energy of all three interaction types.[180]

4.1.3 Chemical oxygen demand

One of the key parameters in the wastewater industry is the chemical oxygen demand, which is a simple way to indirectly measure the level of organic compounds in water. The COD of Gum Arabic suspensions between 0.1 and 2.5 wt. % were measured as described in Section 3.5.5, however Gum suspensions above 1.0 wt. % were above the measurable limits for the available equipment. Figure 4.6 shows that the COD increases linearly with Gum concentration in the range measured, as expected, with Gum primarily being an organic molecule. The COD was measured over time to observe any changes in Gum Arabic suspensions left at room temperature. This allowed an indication of the stability of solutions. It can be seen there was no significant change in the COD after 2 days or 7 days suggesting that the Gum suspensions are stable.

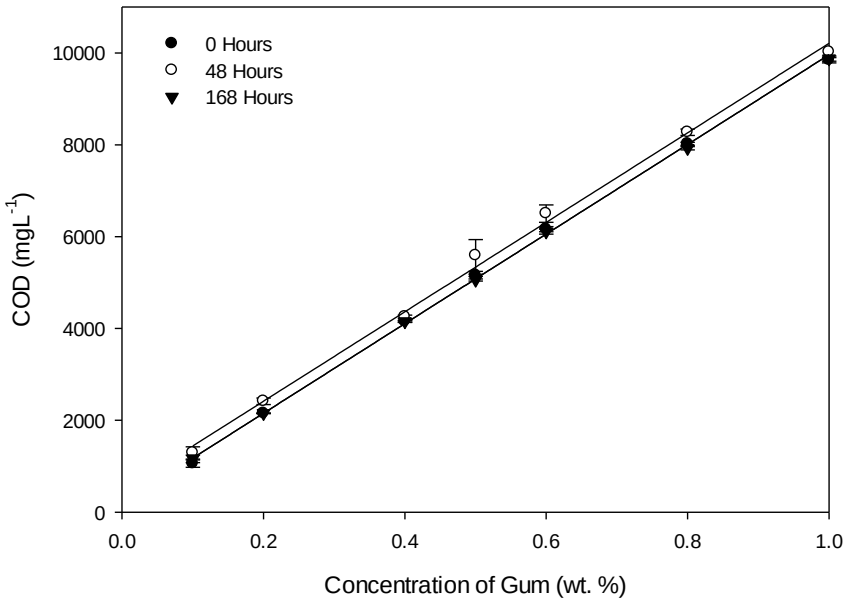

Figure 4.6: COD as a function of Gum concentration.

In order for the wastewater produced at *Kerry Ingredients* to meet requirements for discharge,[181] the COD must be below 6000 mg L^{-1}. This correlates with a Gum concentration of 0.58 wt. %. Based on the current wastewater stream containing 2.0 wt. % Gum removal of minimum 71 % of the Gum is required.

4.1.4 pH

The pH of 2.0 wt. % Gum Arabic was measured to be pH 5.5 ± 0.2. This was measured across different batches with little change observed between batches.

4.2 Membrane characterisation

Prior to initial use, membranes often require conditioning. This removes any preserving solutions present on the membrane and is particularly important when considering polymeric membranes which commonly have a glycerine coating.[182] Conditioning of ceramic membranes is also of importance. It allows the membrane surface to become wet, influencing membrane-surface interactions. Conditioning of membranes used in this study was performed with RO water at 40 ^{o}C, 1.5 bar TMP and 2.3 m s^{-1} CFV for 20 minutes.

4.2.1 Pure water flux characterisation

The pure water flux (PWF) is commonly used by chemical engineers as a benchmark in determining the membrane performance. PWF measurements were performed following conditioning over a range of pressures from 0.6 to 3.0 bar for tubular ceramic membranes as shown in Figure 4.7. As expected the permeate flux forms a linear relationship with the TMP based on Darcy's law shown in Equation 4.2. Using the flux measurements, the membrane resistance (R_m, m^{-1}) can be calculated using Equation 4.2, where *ΔP* is the transmembrane pressure (kg m s^{-2}), *J* is the flux ($Lm^{-2}h^{-1}$), and μ is the dynamic viscosity (kg m^{-1} s^{-1}). R_m = R_T when there is no fouling present. The membrane resistance of each of the membranes used in this study is shown in Table 4.1. It should be noted that the error values are generally high, this reflects membrane variation between individual membranes. Due to the sintering process used during manufacturing of the membranes, there exists a natural variation between individual membranes.

$$R_T = \frac{\Delta P}{J\mu} \qquad \text{Equation 4.2}$$

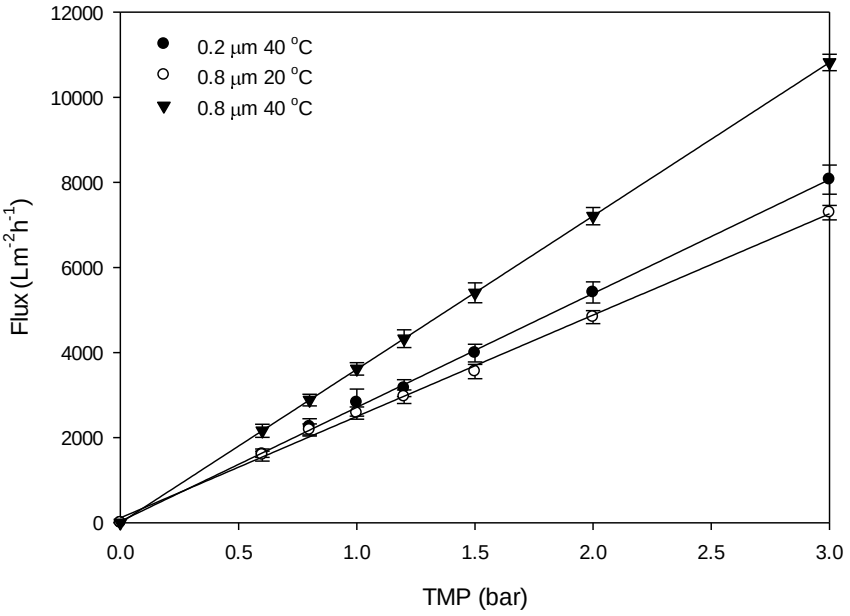

Figure 4.7: PWF through virgin 0.2 and 0.8 µm tubular ceramic membrane at pressures ranging from 0.6 to 3 bar at a CFV 2.3 m s^{-1} and temperatures of 25 °C and 40 °C.

Table 4.1: Membrane resistance of flat sheet and tubular ceramic Al_2O_3 membranes with pore sizes 0.2 – 2.0 µm. Membrane resistance calculated based on average of 2 repeats for tubular ceramic membranes and 3 for flat sheet membranes. Errors represent standard deviation.

Membrane type	Pore size (µm)	Membrane Resistance (x 10^{11} m^{-1})
Tubular	0.8	1.5 ± 0.91
	0.5	1.3 ± 0.83
	0.2	2.0 ± 0.64
Flat sheet	2.0	0.094 ± 0.023
	0.8	0.10 ± 0.8
	0.5	0.23 ± 0.10
	0.2	0.32 ± 0.14

The differences in membrane resistance between the two membranes can be attributed to their porosity. The 0.8 µm Membralox tubular ceramic membrane had a porosity ca. 28 % whereas the porosity for the Kerafol flat sheet membrane of the same pore size was ca. 40 %. The increased porosity leads to a decrease in the membrane resistance as it is easier for fluid to flow through a more porous medium.

4.2.2 Use of flat sheet ceramics

Tubular ceramic membranes are widely available commercially, and are commonly used in industrial applications due to their robustness, compactness and scalability. One drawback of tubular ceramic membranes is their high cost, and the difficulty in analysing the surface due to their shape and structure. Due to the impracticalities of completing analysis on tubular ceramic membranes, a new rig was designed allowing flat sheet ceramic membranes to be investigated as a method to allow membrane characterisation. The rig design and modifications are detailed in Section 3.3.2. For all of the surface analysis detailed below flat sheet ceramic membranes were studied.

4.2.2.1 SEM

SEM imaging was used to investigate the structure and properties of the virgin membrane allowing a comparison to be made following fouling and cleaning. Figure 4.8 shows the structure of a 0.8 µm flat sheet membrane. The membrane is made using a sintering process, and this is clearly evident.

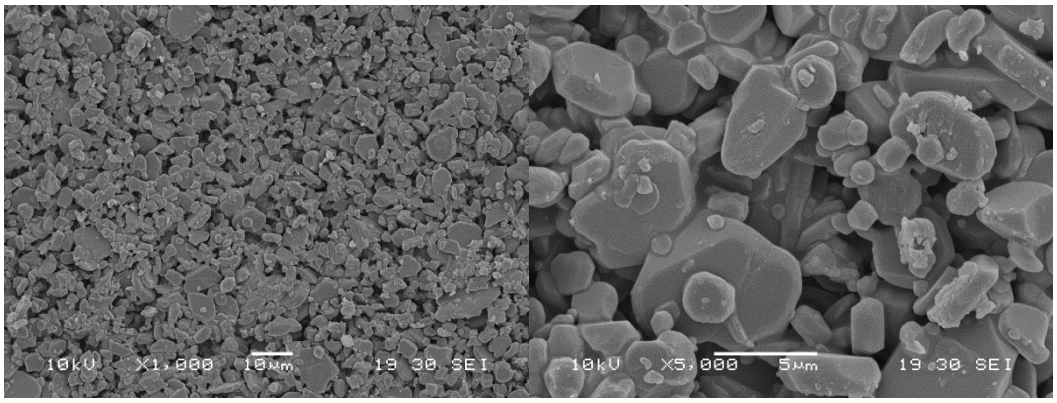

Figure 4.8: SEM image of 0.8 µm flat sheet alumina membrane at two magnifications.

From the left image it can be observed that there is a wide particle size distribution, however this is evenly distributed across the membrane surface. The membrane surface is rough, due to the sintering process. From Figure 4.8 (right) some of the pores can be observed in the membrane. Due to the rough surface fouling, it is hypothesised that fouling will occur both on the membrane surface and in pores.

4.2.2.2 Mercury porosimetry

Following on from the SEM imaging which showed a large distribution in particle sizes forming the membrane, mercury intrusion porosimetry was carried out to determine the pore size and pore size distribution for the membranes. Commonly the pore size is a nominal value with a wide distribution of pores within the membrane matrix. Figure 4.9 shows the pore size distribution calculated from the porosimetry data for membranes with a nominal pore size of 0.8 µm. The porosity was measured to be 39.8 %. It can be seen in Figure 4.9 that most of the pores are ca. 0.8 µm in diameter with a narrow distribution.

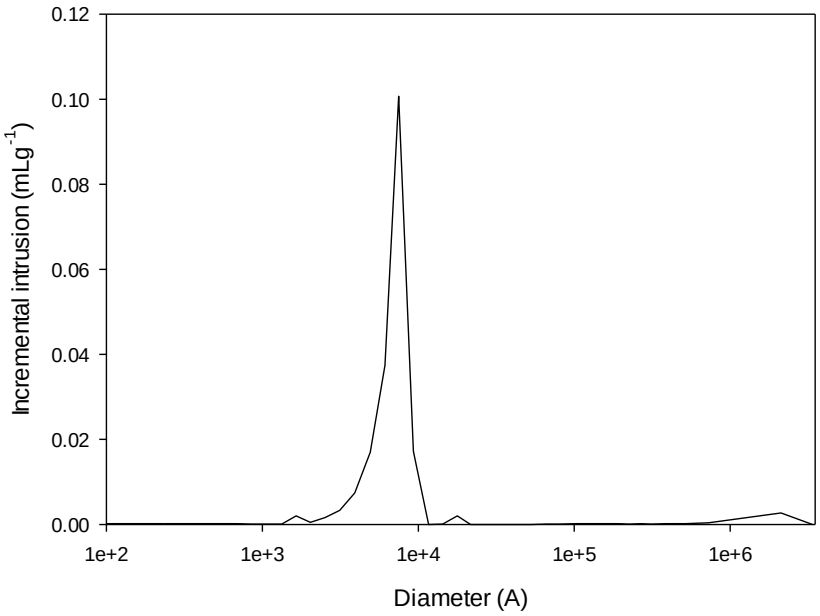

Figure 4.9: Pore size distribution for 0.8 µm membrane.

4.2.2.3 FTIR

FTIR is useful in determining information about molecular vibrations, and thus allows an insight into the bonds present. The intensities of absorption in FTIR depend on the change in dipole moment due to variations in the molecular geometry for the vibrations concerned. Bonds with ionic character tend to give strong IR signals. Figure 4.10 shows the FTIR spectra for a virgin Al_2O_3 membrane, and shows a very strong absorbance between 4000 and 1000 cm^{-1}. This is typical for alumina which has been reported to possess strong absorption due to the ionic character of the Al-O bonds at wavenumbers above 1000 cm^{-1}.[183]

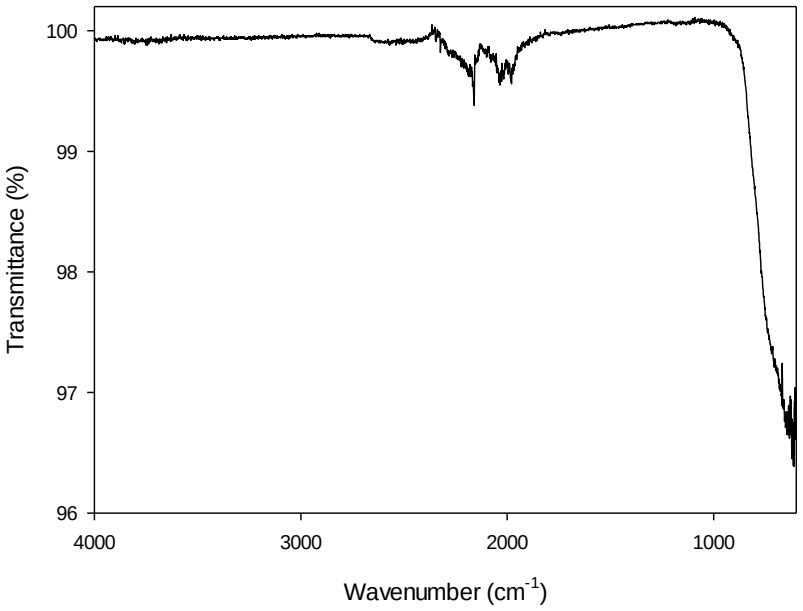

Figure 4.10: FTIR spectra of virgin alumina membrane.

4.2.2.4 Raman spectroscopy

Raman spectroscopy can be applied as a complementary method to IR in the study of molecular vibrations. Raman depends on the change of polarisability associated with the vibration. While FTIR is useful in determining information about bonds with ionic character, Raman is useful in determining information about bonds with covalent character as these tend to give strong Raman signals. Raman spectroscopy is useful in determining the type of alumina as it is able to determine small changes in the chemical structure and composition. The Raman spectra for light of wavelength 785 nm is shown in Figure 4.11. Two peaks can be seen, this is not typical for α-alumina and shows there are some impurities in the sample due to the presence of a small amount of β-alumina.[184] Unfortunately this is a manufacturing defect and was common in all of the flat sheet samples, despite the manufacturer stating that the samples were pure α-alumina. There was no change to the Raman spectra between membranes or following fouling and cleaning indicating that the structure does not change with treatment.

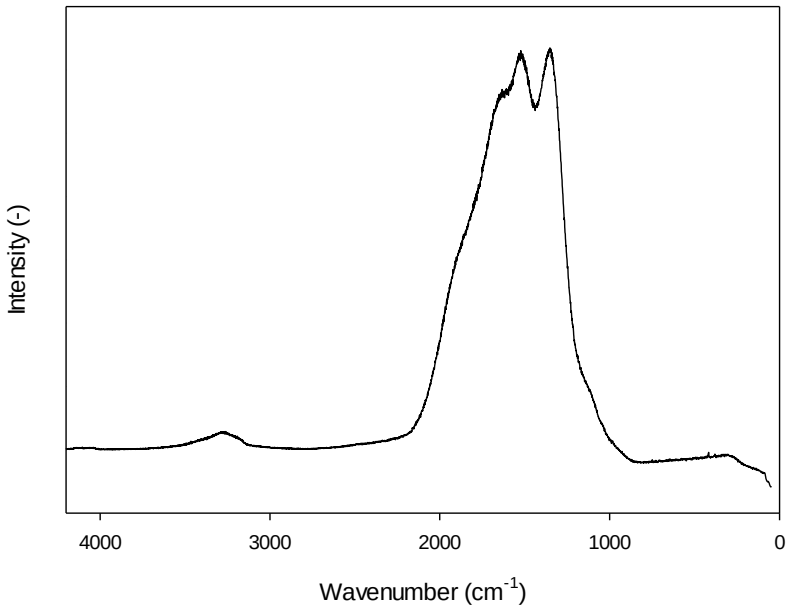

Figure 4.11: Raman spectra of alumina excited with wavelength 785 nm.

4.2.2.5 Zeta potential

The surface charge of a membrane can have a significant effect on the separation and fouling characteristics of a membrane.[185] Surface charge measurements to obtain the apparent zeta potential were carried out as detailed in Section 3.6.2. Figure 4.12 shows the apparent zeta potential over the pH range 3.0 – 8.0. It can be observed that the isoelectric point is below 3.0, and the membrane displays a large zeta potential (-10 to -40 mV) over the range measured.

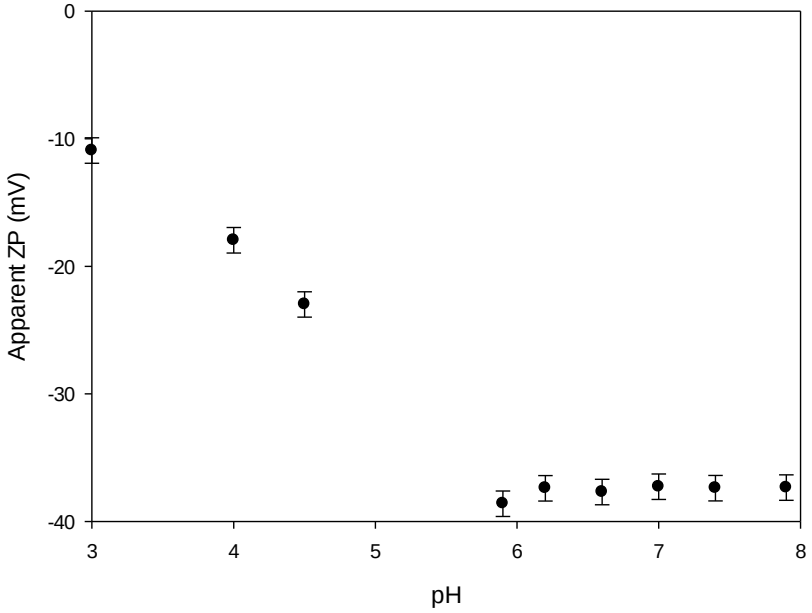

Figure 4.12: Apparent zeta potential of Al_2O_3 membrane over pH range 3.0 – 8.0

The zeta potential shows a strong declining slope as the pH is increased with more negative charge at higher pHs. This indicates that the surface charge is increasing and may be due to the adsorption of negatively charged ions, or more likely due to dissociation of the aluminium oxide on the membrane.[186] When metal oxides are exposed to an aqueous media, the amphoteric surface groups (e.g. AlOH) can dissociate as shown below under acidic or basic conditions:

$$AlOH + H^+ \rightarrow AlOH_2^+ \rightleftharpoons Al^+ + H_2O$$

$$AlOH + OH^- \rightarrow Al(OH)_2^- \rightleftharpoons AlO^- + H_2O$$

At the isoelectric point (IEP), the alumina will either have no charge, or the number of positive and negative charges will be equal, resulting in a net charge of 0. Generally metal oxides are known to have a negative charge at high pH and a positive charge at low pH. Figure 4.12 shows that over the conditions measured, alumina is negatively charged. However, the slope is tending towards zero suggesting that there exists an isoelectric point below pH 3.0. Smit and Stein have previously reported an IEP ca. 3.3 for α-alumina crystals,[187] and Ducker *et al.* reported an IEP of 3.0.[161] It is however, generally accepted that the IEP for crystalline α-alumina is ca. 4[188, 189] and pH 7.0 – 8.1 for alumina particles.[190] These are higher than the value obtained in this study. The differences could be caused by differences in the processing of the membrane, or the polymorph of alumina present.[191, 192] In addition pre-treatment, history, aging and storage of membranes can all lead to different values obtained during streaming potential measurements. Yang *et al.* studied the

surface of alumina particles and crystals in order to try to understand the discrepancies in the IEP. They concluded that the surface hydroxyl groups on alumina, and their coordination have a large role in the surface charge and surface chemistry.[188] The zeta potential is related both to the number of surface hydroxyl groups, and the type of hydroxyl groups. In alumina powders the surface groups are unicoordinated resulting in a high pK_a whereas in alumina crystals the hydroxyl groups are multiply coordinated resulting in a lower pK_a. When the OH is bonded to multiple aluminium atoms it is more acidic. They also reported that heating α-alumina can alter the zeta potential both in magnitude of the charge, and in the IEP.

Chapter 8 discusses the influence of pre-treatment on the membranes. This results in very different IEPs due to changes to the alumina surface.

4.2.2.6 AFM

It has been reported by a number of authors that the surface roughness is one of the most significant properties influencing fouling of membranes. It can have a more significant effect than the physical or chemical operating conditions.[159, 193] The roughness and architecture of alumina membranes has been investigated using AFM. The S_a (mean roughness) was calculated as an average value from each scan line from a 20 x 20 μm image, and was determined to be 361 ± 17 nm for a virgin 0.8 μm membrane. The membranes have a rough surface due to the sintering process used to make them, with alumina particles fused together and pores between the particles. The surface roughness is one parameter which may be very different for the flat sheet and tubular ceramic membranes. It was not possible to carry out AFM on the tubular ceramic membranes due to their high cost and the curvature of the surface inside the channels. The architecture of a virgin flat sheet membrane is shown in Figure 4.13. This again highlights the rough surface observed. The shading intensity shows the vertical profile of the membrane surface with the light regions being peaks and the dark regions representing valleys or depressions in the surface.

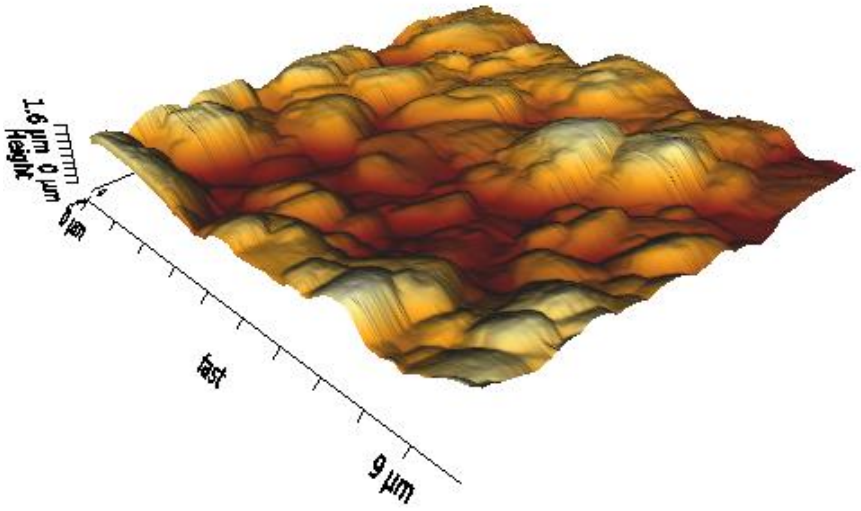

Figure 4.13: 10 x 10 µm AFM image of virgin membrane highlighting the uniform roughness across the membrane surface.

In addition to measuring the roughness of the membrane, the adhesion strength was measured using a colloidal probe as described in Section 3.6.8. The mean adhesion strength was measured as 690 ± 240 pN with an average adhesion distance of 31.8 ± 7.6 nm. A typical force curve was obtained for the virgin membrane and is shown in Figure 4.14. It can be observed that the detachment distance is ca. 30 nm. Bowen and Doneva reported that generally hard inorganic spheres or mineral surfaces have a detachment distance of less than 5 nm.[160] The higher value suggests the formation of long range bonds such as hydrogen bonding, or progressive detachment between the surface and probe.

The adhesion curve shows there are charge or bonding interactions between the virgin membrane and the silica groups on the colloidal probe. It is expected that the OH groups on the membrane surface are responsible for this as the surface of alumina is known to be characterised by OH groups under hydrated conditions. There is a strong adhesion which is released at ca. 31.8 nm, followed by a weak interaction which occurs for a longer distance. This suggests two ifferent types of adhesion and may be due to electrostatic interactions and hydrogen bonding. Interestingly, the force was not even across the whole membrane surface, as shown in Figure 4.15. A similar phenomenon was observed by Yelken and Polat when using AFM with a colloidal probe to determine the electrostatic potential distribution on alumina surfaces.[194] There are a number of factors that may be responsible for this. It could be that the membrane is very rough as illustrated in Figure 4.13. It has been reported previously by Hoek *et al.* that surface roughness can influence the adhesion strength measured using an AFM colloidal probe.[150] They reported

that in valleys the adhesion can be reduced due to wells of low interaction energy. It is also possible that in valleys the probe will be in contact with a larger number of alumina particles. It will therefore receive forces from the sides as well as the bottom of the probe leading to increased adhesion in the valleys compared to the peaks where only the bottom of the silica sphere on the tip is in contact. Alternatively the presence of β-alumina contaminants may result in differences in the material properties at the locations where these impurities exist, leading to differences in the adhesion strength. A combination of these two factors may be occurring simultaneously.

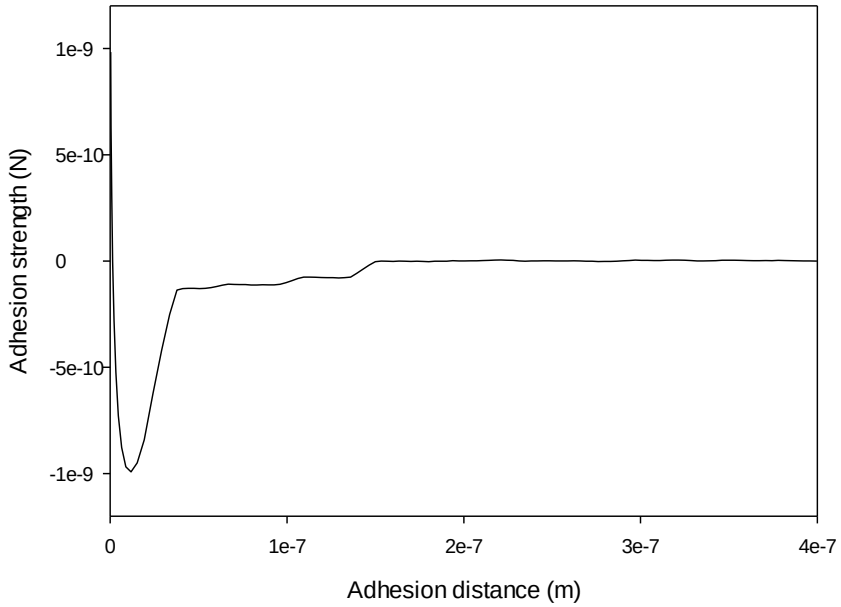

Figure 4.14: Typical adhesion curve for 1 point on the membrane surface. Strong adhesion can be seen over short distances when the colloidal probe is retracted, with a weaker adhesion force over a longer range.

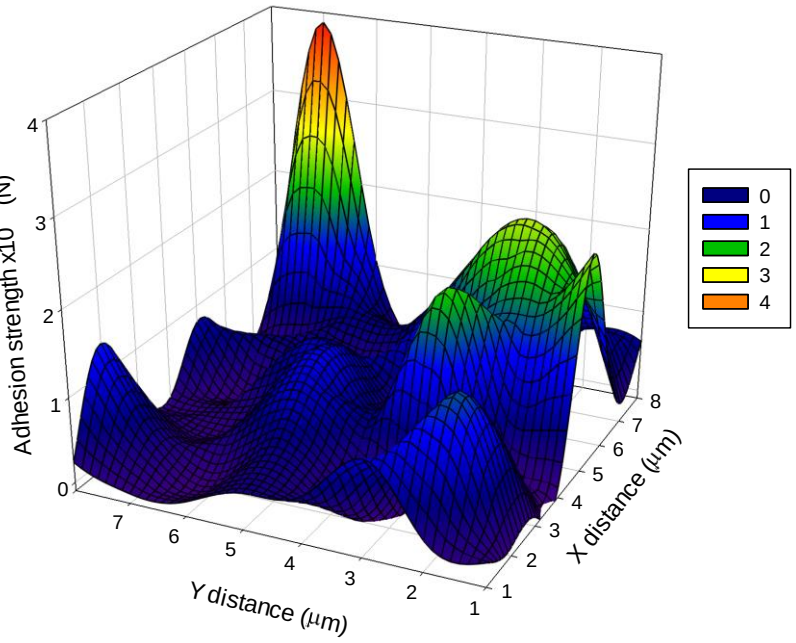

Figure 4.15: Adhesion strength measured using AFM colloidal probe over 8 x 8 µm area showing that adhesion is not constant across the membrane surface.

4.3 Separation

4.3.1 Removal of Gum Arabic from model waste suspension

During the filtration of model wastewater suspension which contain 2.0 wt. % Gum Arabic, the permeate quality was monitored to allow quantification of the transmission of Gum during membrane filtration. This allowed identification of any changes in the permeate quality over time. It was observed that the Gum concentration present in the permeate decreased over the first five minutes, before reaching steady state where the concentration was shown not to change for over 90 minutes (length tested) in recirculation mode. The decrease in concentration is most likely caused by external fouling[195] (e.g. the formation of a cake layer on the membrane surface, which acts as a filter). This is investigated further and discussed in more detail in Chapter 5. Prior to analysis, the permeate appeared lighter and considerably clearer than the feed and retentate samples, this is shown in Figure 4.16. The observed colour difference suggests that there has been removal of Gum Arabic from the permeate stream. This was shown using a handheld refractometer as described in Section 3.5.2. The feed and retentate samples had a concentration of 2.0 wt. % and the permeate had a concentration of 0.2 wt. %. Once a steady state concentration was reached 90 % rejection of Gum was observed through an aged 0.8 µm alumina

tubular ceramic membrane. The importance of membrane aging is detailed further in Chapter 7. Considering the particle size expected for the Gum Arabic, the rejection is higher than anticipated. This high rejection is discussed further in Chapter 5 and is expected to be caused by the formation of a cake layer on the membrane surface.

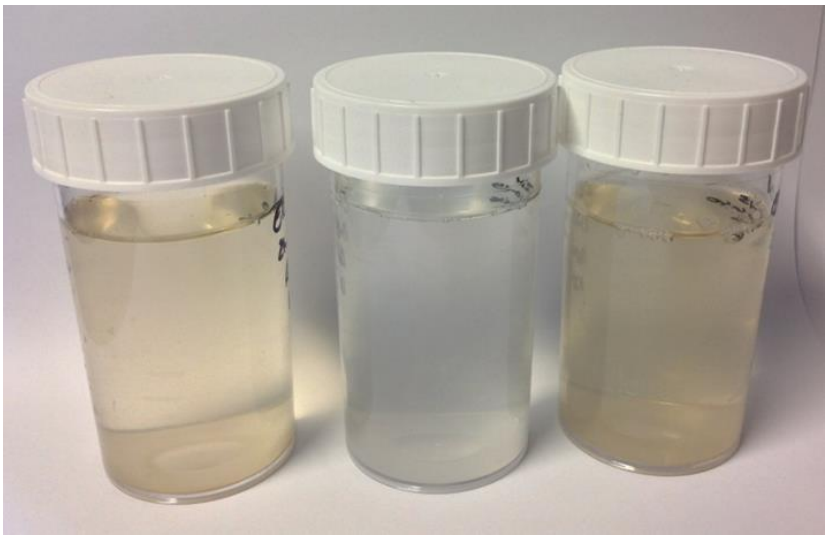

Figure 4.16: Samples of feed (left), permeate (centre) and retentate (right) from the filtration of Gum Arabic through a 0.8 µm tubular ceramic membrane after 90 minutes filtration. Feed and permeate samples 2.0 ^{o}Brix and retentate 0.2 ^{o}Brix.

This is a promising result for the removal of Gum from the wastewater stream. While ideally 100 % rejection of the Gum will be achieved the initial removal of ca. 90 % is a very good starting point, confirming microfiltration may be considered as a process for removing Gum Arabic from wastewater streams. The removal of 90 % Gum allows the concentration of the permeate stream to be below the required COD for discharging the waste stream. The concentration is also at a level low enough that the water can be recycled through the system, allowing water reuse.[7]

4.3.2 Feed and bleed filtration

The results obtained thus far show the potential offered by membrane technologies in separating out Gum Arabic from a wastewater stream. Further processing can occur by separating the streams into the permeate and retentate through a 'feed and bleed' mechanism (concentration mode) where the retentate is recycled to allow a maximum amount of water to be removed from the feed. Work carried out by Bechervaise[21] has shown that up to 20 wt. % Gum Arabic can be filtered through a 0.8 µm Membralox membrane. A feed and bleed experiment was carried out

where the retentate was recycled over a period of 450 minutes sampling the concentration of the feed, permeate and retentate every 5 minutes. During this time the volume of feed was reduced from 100 litres to 15 litres (85 % feed filtered, concentration factor 6.7). Operating under feed and bleed mode could only be carried out over a period of 450 minutes as the feed tank then had insufficient volume to prevent air from entering the system. The concentration could have been continued if the dead volume of the system was smaller. The concentration of Gum present in each sample is shown in Figure 4.17. This is based on two repeats with error bars showing standard deviation. It should be noted that the concentration of Gum in the retentate and feed are virtually identical due to the low flux through the membrane. With the increase in Gum concentration in the feed, an increase in the concentration of Gum in the permeate was observed, with the rejection coefficient decreasing from 0.95 after 5 minutes to 0.88 after 450 minutes. The increase in concentration in the permeate, and reduction in the rejection coefficient, highlights that the filtration is not only occurring through size exclusion, but other factors such as charge are also playing an important role in the separation of Gum Arabic from water. This is discussed further in Chapter 5.

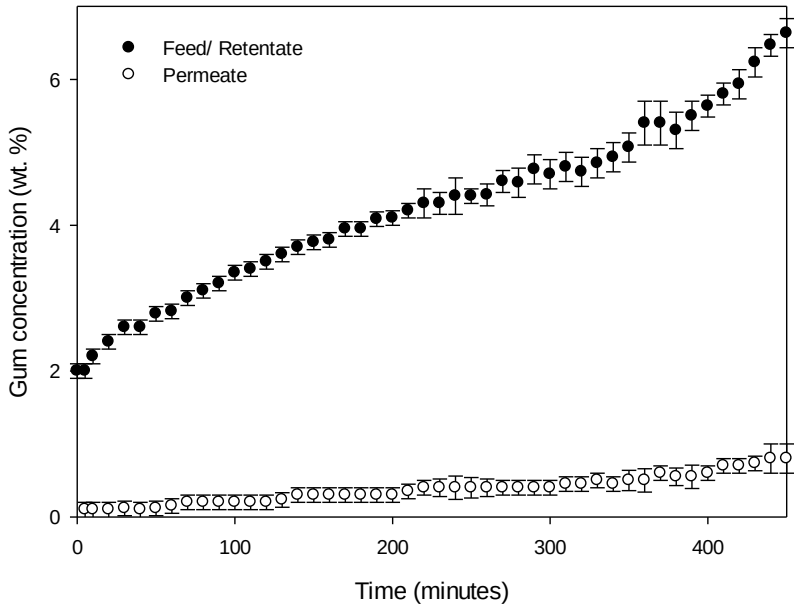

Figure 4.17: Concentration of Gum Arabic in permeate and feed/retentate throughout 100 L feed and bleed experiment though 0.8 µm tubular ceramic membrane at CFV 2.3 m s^{-1} and TMP 1.5 Bar. As the concentration of feed increases an increase in the permeate concentration is observed however good removal of Gum Arabic can be seen.

Increasing the concentration of Gum in the feed/retentate stream allows the Gum to be recycled through the evaporation and spray drying process showing full recovery of the Gum is possible.

In addition the permeate stream can undergo further filtrations through tighter pore sized membranes allowing water containing very little or no Gum to be obtained.

One consideration to make is the change in Reynolds number caused by the increase in Gum concentration as reported in Section 4.1.1. As the Gum Arabic concentration increases throughout the feed and bleed experiment from 2.0 wt. % to 6.5 wt. % at 40 ^{o}C, Re decreases from 6300 to 3000. The transition from turbulent to transient flow will inevitably increase the fouling at the surface of the membrane. The influence of crossflow velocity and Reynolds number is discussed further in Section 5.2.3.

4.4 Flux decline

Throughout fouling, the membrane flux decreases due to an increased resistance caused by the addition of a fouling layer to the membrane. An example of this is shown in Figure 4.18 showing the flux decline over 450 minutes during the feed and bleed experiment discussed in Section 4.3.2. It can be observed there is initially a very steep decline in the flux. However, this levels off somewhat, with the slow reduction in flux correlating with the increase in feed concentration, and decrease in Reynolds number. The flux decline curve is the average flux based on two experiments, with the error bars representing the standard deviation.

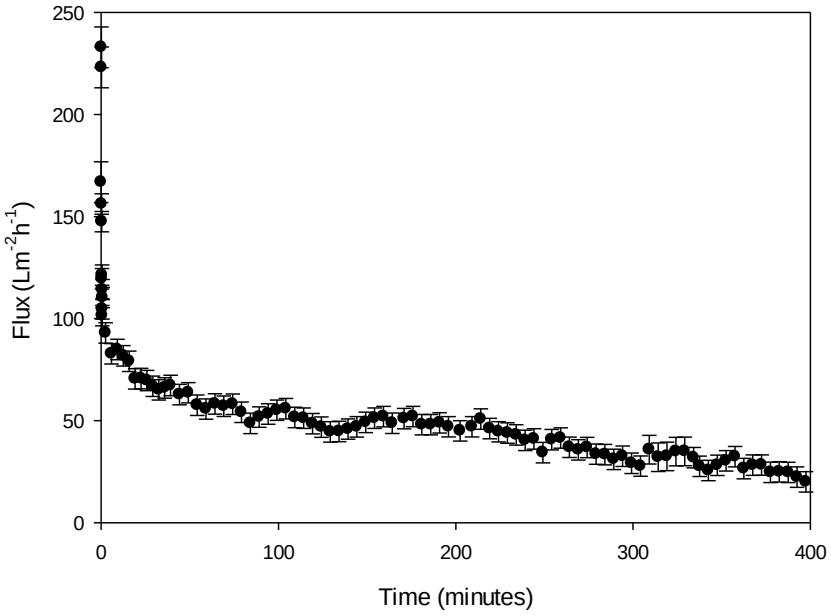

Figure 4.18: Flux decline due to fouling throughout feed and bleed experiment with 100 L 2.0 wt. % Gum Arabic at 40 ^{o}C with 1.5 bar TMP and 2.3 m s^{-1} CFV. (Concentration increases from 2.0 to 6.5 wt. %).

4.4.1 Resistance in series model allowing fouling analysis

The resistance in series model is commonly used to describe the behaviour of fouling during membrane filtration.[196-198] It allows quantification of the change in membrane resistance due to fouling, and the persistence of foulants following cleaning to be identified. Figure 4.19 shows the total resistance measured at different points throughout a cycle of filtration and cleaning, calculated from the general membrane equation (Equation 4.2). Comparing the membrane resistance before and after the filtration of Gum Arabic shows a 50-fold increase in the membrane resistance caused by fouling, highlighting that the filtration of Gum Arabic causes significant fouling. It can be seen that chemical cleaning is required to allow removal of the majority of foulants. This is discussed in more detail in Chapter 6. The resistance in series model can be used to evaluate the role of the different foulant types. These were calculated and their values are shown in Table 4.2. The intrinsic membrane resistance (R_m) was calculated by measuring the flux of RO water through a conditioned membrane. R_T is the total resistance measured at the end of fouling. R_{CP} is the resistance due to concentration polarisation, measured by switching the pumps off for 1 minute and then on again to allow any build-up of concentration due to pressure to be negated. R_r allows the rinsable fouling to be determined, that due to loosely bound foulants. It is defined here as the resistance following rinsing at 1 bar TMP, CFV 2.3 m s^{-1} for 15 minutes. R_{C1} is the resistance following cleaning with 0.5 wt. % NaOH with 200 ppm NaOCl, and R_{C2} is the resistance following cleaning with 0.1 wt. % citric acid. The terms used for resistance are relative and depend on the conditions used. The conditions have been kept constant throughout this work to allow comparison, unless otherwise stated.

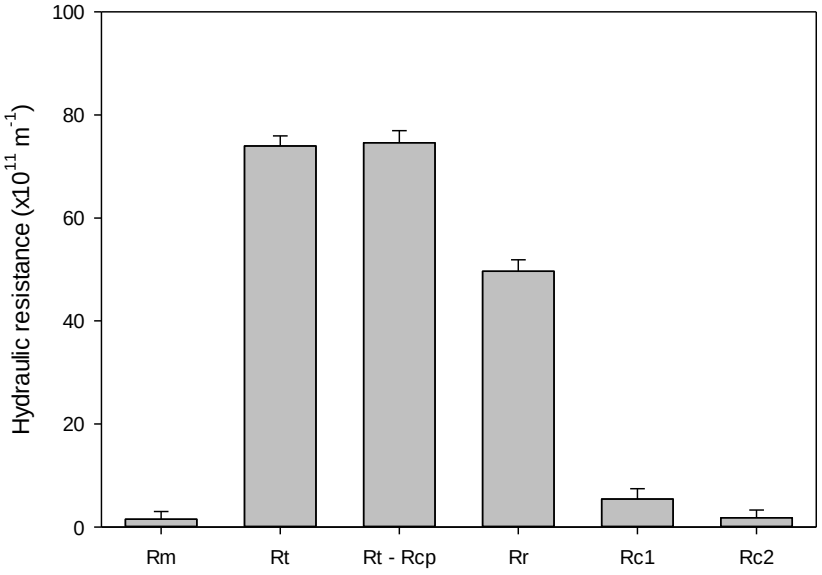

Figure 4.19: Hydraulic resistance calculated from Equation 4.1 for virgin 0.8 µm tubular ceramic membrane where R_m is the membrane resistance, R_T is the total resistance after fouling, $R_T - R_{cp}$ is the total resistance after the elimination of concentration polarisation (concentration polarisation was measured to be 0), R_r is the resistance following rinsing, R_{C1} is the resistance following cleaning with 0.5 wt. % sodium hydroxide/ 200 ppm sodium hypochlorite and R_{C2} is the resistance following cleaning with 0.1 wt. % citric acid. R calculated using water.

Based on the data shown in Figure 4.19 and Table 4.2, it can be observed that fouling results in a large increase in the resistance leading to a decline in permeate flux through the membrane. The fouling is not as a result of concentration polarisation because the Gum contains macromolecules and particles with a low diffusion coefficient.[69] A small amount of the foulant is removed through rinsing with water. However, chemical cleaning is required for effective removal of the Gum. The use of cleaning is discussed further in Chapter 6.

Table 4.2: Fouling resistances determined based on the resistance in series model.

Type of resistance	concentration polarisation	loosely attached foulants	foulants adsorbed onto the membrane surface	Foulants removed by acid cleaning	irreversible fouling
	R_{CP}	R_{RL}	R_{RC1}	R_{RC2}	R_I
R (x10^{11} m^{-1})	0	24.3 ± 4.2	45.1 ± 2.2	3.7 ± 0.1	1.8 ± 0.1

4.5 Discussion

This chapter has shown the main properties of reconstituted Gum Arabic suspensions and alumina membranes, while also showing that microfiltration is a promising technology for the removal of Gum Arabic from a model wastewater stream.

The viscosity of Gum Arabic has been shown to decrease with temperature, thus warranting operation at 40 ^{o}C to allow turbulent flow in the microfiltration rig available.

Particle size analysis showed that there are two distinct peaks for reconstituted Gum, one around 0.2 – 3.0 µm, and the other around 50 – 300 µm. The size of the Gum particles suggest that microfiltration is appropriate to remove these particles from suspension. Pre-filtering the Gum through a 25 µm steel filter breaks down the larger particles to produce a large number of particles with a diameter ca. 1 µm. This suggests that the larger peak is formed by aggregation. Allowing the pre-filtered suspension to sit for 24 hours confirms that aggregation is responsible for the larger particles, as an identical broad peak of particles between 50 and 300 µm returns, mirroring that of the unfiltered sample.

The concentration of Gum in suspension forms a linear relationship with the chemical oxygen demand, and this does not change over time. Based on the limits for discharge of 6000 mg L^{-1}, 71 % removal of Gum from a 2.0 wt. % suspension is required. This has been shown to be possible, and optimisation of this process is discussed further in the next chapter.

It is known that membrane characterisation is important in determining the fouling propensity and separation characteristics of a membrane. Due to the difficulties in conducting surface analysis of tubular ceramic membranes, flat sheet ceramic membranes have been investigated to allow an insight into the properties and characteristics of alumina membranes with Gum Arabic. The membranes investigated have been shown to be operating in the pressure dependent region when operating with RO water. Natural variation in the membrane resistance was observed. Based on this, normalising the results using the membrane resistance allows a clear comparison between different membranes. The use of SEM and mercury porosimetry confirmed that the membranes had pore sizes as stated by the manufacturer. FTIR and Raman spectra were observed showing the alumina behaves as expected and gives a strong signal, however the use of Raman also highlighted that small amounts of β-alumina were present in the flat sheet membranes. Further investigations are required to identify the influence this has. However, as detailed in Chapters 5 and 6, it seems both the tubular ceramic and flat sheet membranes behaved very similarly when investigating the influence of fouling conditions and cleaning agents.

Separation of Gum Arabic has been shown to be possible with over 90 % rejection achieved for an aged 0.8 µm membrane. The use of a feed and bleed (concentration) system has been shown to allow good removal of Gum while concentrating up the retentate. This means the system could be developed to eliminate waste with recycling of both the Gum and the water possible.

The results discussed in this chapter highlight some of the properties of Gum Arabic, and virgin membranes. They also show the possibility of alumina microfiltration membranes to remove Gum Arabic. However, a better understanding of the interactions between the membrane, Gum and cleaning agents is required. This is described in the following chapters.

4.6 Summary

When dissolved in water, Gum Arabic forms a suspension containing aggregated particles. For this reason microfiltration has been deemed appropriate for the removal of Gum Arabic from a model waste solution. The use of microfiltration has been shown to be appropriate with a 0.8 µm Membralox membrane showing ca. 90 % removal of Gum from the feed. This is a very positive result with 71 % removal from a 2.0 wt % suspension required to meet COD requirements for discharge. The additional removal highlights that recycling of the water in the process could be obtained leading to large water savings during processing.

5. Optimum filtration conditions

In Chapter 4 the effectiveness of microfiltration for the removal of Gum Arabic from a model waste stream was demonstrated. In addition to showing that separation is possible, it is important to consider the membrane – foulant interactions to aid in understanding and optimising the process. Fouling of membranes diminishes the process productivity, raises operating costs and shortens the membrane lifetime, therefore it is important to understand the fouling interactions and optimise their reduction. Gum Arabic is a complex polysaccharide with a proteinacious backbone, this means fouling is inevitable as both polysaccharides and proteins have been reported as common foulants.[195, 199]

Fouling is a complex process, of which it can be hard to determine the causes due to the large number of factors which can influence it. The three main factors to consider are:[122, 200]

1) process parameters such as temperature, transmembrane pressure and shear rate near the membrane surface.
2) membrane material properties such as pore size, porosity, hydrophilicity, surface charge and surface topography.
3) solution properties such as pH, salt concentration, amount of protein denaturation and aggregation.

This chapter investigates the process parameters and membrane material properties. Factors such as temperature, transmembrane pressure and crossflow velocity, along with the membrane material properties outlined in Chapter 4 are discussed. The impact of these factors on efficiency of separation and flux is considered. The majority of experiments were carried out using a 0.8 µm membrane. While solution/suspension properties also offer a method to reduce fouling, these were not investigated in this study. The reason these were not investigated was to prevent changes to the structure, composition and properties of the Gum, which may impact the ability to recycle it.

This chapter aims to show that:

- Process parameters can influence fouling during the microfiltration of Gum Arabic.
- Membrane material properties have a significant effect on the fouling and separation of Gum Arabic.
- Cake filtration is the dominant fouling mechanism during the microfiltration of Gum Arabic.

5.1 Filtration conditions

The optimisation of the fouling conditions was carried out and is detailed in Section 5.2. During these experiments one parameter was adjusted, with the other conditions remaining constant. The experiments were carried out at 40 ^{o}C with a TMP 1.5 bar and CFV 2.3 m s^{-1} unless otherwise specified. The suspension used was 2.0 wt. % Gum Arabic in RO water which had not undergone any pre-filtration or changes to the suspension such as pH or ionic strength. Aged membranes were studied to minimise cycle variation as described in Chapter 7. Each study represents three repeats, with the average and standard deviation reported.

Membrane resistances were calculated based on Equation 4.1, using the resistance in series model shown in Equations 5.1 and 5.2.

$$J = \frac{\Delta P}{\mu_p R_T} = \frac{\Delta P}{\mu_p (R_m + R_{cp} + R_F)} \quad \text{Equation 5.1}$$

$$R_F = R_{RL} + R_{CC} + R_I \quad \text{Equation 5.2}$$

Where J is the permeate flux, ΔP the transmembrane pressure, μ_p the viscosity of the permeate, R_T is the total fouling resistance, R_m is the intrinsic membrane resistance, R_{cp} is the resistance due to concentration polarisation, and R_F is the fouling resistance term. The fouling resistance term (R_T) can be broken down into (i) fouling caused by loosely bound foulants which can be removed through rinsing (R_L), (ii) fouling which can be removed through chemical cleaning (R_{CC}) and (iii) irreversible fouling (R_I). The importance of chemical cleaning will be discussed further in Chapter 6.

The efficiency of separation is characterised by the rejection coefficient. This has been used to allow a comparison of the operating conditions. The rejection coefficient (R_a), shown in Equation 5.3, was determined by measuring the concentration of Gum in the permeate (C_p) and the bulk concentration, that of the retentate and feed (C_b).[201] To allow comparison, unless otherwise specified, the concentrations were measured in triplicate when the samples were at steady state (60 minutes from the initial fouling). A rejection coefficient of 1 means that complete separation has occurred, and R_a = 0 means there has been no rejection.

$$R_a = 1 - \left(\frac{C_p}{C_b}\right) \quad \text{Equation 5.3}$$

The identification of these factors is used to create an operating protocol to maximise the throughput of wastewater while minimising the fouling.

5.2 Process parameters

Process parameters such as the TMP and CFV have been shown to significantly affect the separation properties and permeate quality.[79] The process parameters (with the exception of static vs. dynamic fouling) were measured using a tubular ceramic membrane, as this is most representative of industrial practice.

5.2.1 Static and dynamic fouling

It has been well reported that the process conditions influence fouling of a membrane. One process parameter which can influence fouling is the fouling mode – static or dynamic. Under static conditions the interactions between the foulant suspension and the membrane is the only factor which needs to be considered, whereas in dynamic fouling there are a lot of additional forces which can influence the fouling propensity. Under dynamic conditions, factors such as crossflow and transmembrane pressure add additional forces which may lead to increased or reduced fouling, and alterations in the foulant layer. In order to investigate the different modes of filtration, flat sheet ceramic membranes were investigated as described in Section 3.3.2 and 3.4.7. Following fouling the membranes were rinsed and their pure water flux characterised. This is shown in Figure 5.1.

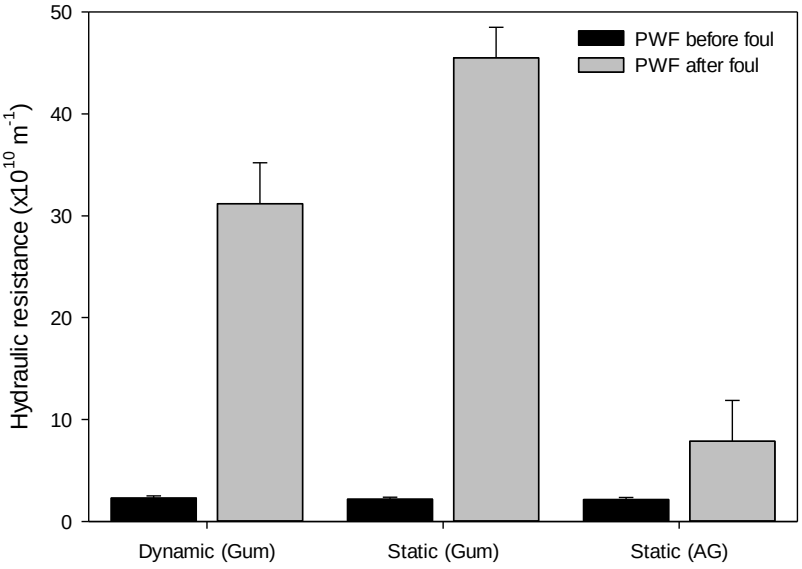

Figure 5.1: Hydraulic resistance following fouling with Gum Arabic (Gum) and Arabinogalactan (AG) under static and dynamic conditions. Membranes fouled with 2.0 wt. % suspensions at 40 ^{o}C. Dynamic studies were carried out with TMP 1.5 bar and CFV 2.3 m s^{-1}.

It can be observed that Gum readily adsorbs onto the surface of alumina. Comparing the Gum and arabinogalactan samples it can be seen that arabinogalactan results in some of the fouling of the membrane, however there is a large proportion which must result from the other components of Gum, e.g. AGP, GP and metal cations. It has been previously reported that proteins are difficult foulants to deal with. They rapidly adsorb onto membrane surfaces and pore walls forming a secondary barrier that decreases permeate flux and changes solute selectivity.[58] These results suggest that while the carbohydrate plays a role in the membrane fouling, the presence of proteins or metal cations may lead to the severe fouling observed.

Fouling is shown to occur under both static and dynamic conditions, with more severe fouling formed under static conditions. This result was unexpected as the role of convective forces towards the membrane surface would be expected to lead to additional fouling. Previously Kanani *et al.* reported that fouling of proteins occurs both under static and dynamic conditions.[200] Generally a monolayer is formed under static conditions and multi-layer fouling occurs under dynamic conditions. Much work has been carried out to try to understand protein fouling but there remains a lack of agreement and understanding about the formation of protein deposits during MF processes.[200] The results obtained in this study suggest that convective forces present in dynamic fouling help to reduce the foulant layer.

5.2.2 Concentration of Gum

This thesis mainly focuses on work carried out using 2.0 wt. % Gum Arabic suspensions for industrial relevance. The waste water at *Kerry Ingredients'* processing plant in Cam, UK contains ca. 2.0 wt. % Gum Arabic.[1] This section however investigates the influence that the concentration of Gum Arabic has on the flux decline, membrane resistance following fouling and the membrane selectivity. An aged 0.8 µm tubular ceramic membrane was used for this study as pristine membranes are known to act differently to aged ones (see Chapter 7).

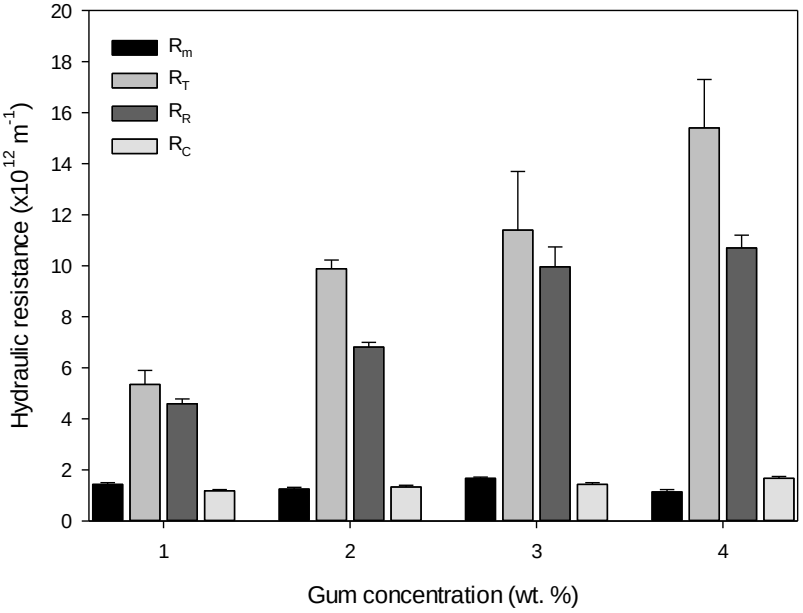

Figure 5.2: Hydraulic resistance for 0.8 µm membrane fouled with 1.0 – 4.0 wt. % Gum Arabic before fouling (R_m), after fouling (R_T), following rinsing (R_R) and following cleaning (R_c).
TMP 1.5 bar, CFV 2.3 m s^{-1} 40 ^oC.

It is important to consider the membrane resistance rather than the flux when comparing the concentration, as this allows viscous effects observed in the flux to be neglected. The permeate flux typically decreases exponentially with concentration due to an increase in viscosity and greater likelihood of attachment of foulants to the surface.[60] Figure 5.2 shows the impact of the concentration of Gum Arabic on the membrane resistance. It can be seen that there is an increase with the membrane resistance as the Gum concentration is increased. Following rinsing with water, there is no significant reduction in resistance, suggesting that loosely bound foulants are not responsible for the increased resistance. Following chemical cleaning, the membrane resistance was restored close to that of the resistance before fouling, showing that the cleanability

was unaffected by the increased fouling resistance. Marshall *et al.* described similar effects when studying the effect of protein fouling on microfiltration membranes.[114]

Figure 5.3 shows flux decline curves for the membranes fouled with Gum Arabic of concentrations 1.0 – 4.0 wt. %. It can be seen that there is no change in the rate of flux decline with concentration, however there is a change in the flux at steady state, with a steady state flux of 35 ± 5 L m^{-2} h^{-1} during fouling with 4.0 wt. % Gum Arabic, compared to 143 ± 6 L m^{-2} h^{-1} during fouling with 1.0 wt. % Gum Arabic. While some of this decline is likely to be as a result of the increased viscosity of the Gum suspension, Figure 5.2 highlights that other factors also influence this. It is possible that the increased concentration of Gum leads to a thicker foulant layer resulting in an increase in the total resistance following fouling. An increase in fouling with increased protein concentration was also reported by Loh *et al.* when investigating protein fouling.[202]

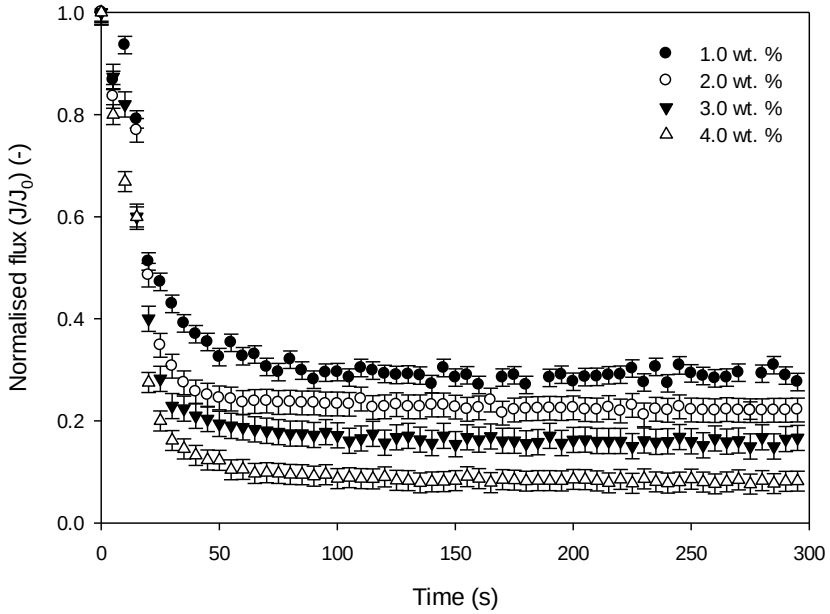

Figure 5.3: Flux decline curves over the first 5 minutes of filtration for an aged 0.8 µm tubular ceramic membrane during the filtration of 1.0 – 4.0 wt. % Gum Arabic at 40 ^{o}C with TMP 1.5 bar, and CFV 2.3 m s^{-1}.

The concentration of the feed had a small influence on the separation properties. The rejection coefficient was 0.91 ± 0.05 and 0.89 ± 0.04 for the membranes fouled with 1.0 and 2.0 wt. % Gum Arabic, however following filtration with higher concentrations of Gum these decreased to 0.86 ± 0.04 and 0.83 ± 0.05 for the 3.0 and 4.0 wt. % feed suspensions respectively. While this increase is small it was shown to be statistically significant ($P < 0.05$). This increase with concentration suggests that as more foulants build up on the membrane surface due to the increased feed concentration, more foulants get transmitted through the membrane. This suggests that while

the presence of a cake or gel layer is expected to be forming on the membrane surface (see Section 5.5) this is not the limiting factor on separation. This contradicts the results obtained by Zuriaga-Agusti *et al.* who reported that for polysaccharide fouling, there was a negligible influence of polysaccharide concentration on membrane fouling. This was explained by the major role on the cake or gel layer on membrane separation once the initial foulant layer has formed.[203]

One interesting observation is that the rejection increases over the first few minutes of filtration before reaching a steady state concentration as the flux reaches steady state. This suggests that the formation of a cake or gel layer on the membrane surface aids in the selectivity of the membrane.

5.2.3 Crossflow velocity

Crossflow velocity (CFV) is a hydrodynamic property which has been shown to influence the rate of fouling for a number of different membrane-based processes.[62, 65] In crossflow filtration the feed flows tangentially along the membrane surface and permeates through the membrane due to the pressure drop across the membrane. The shear force exerted by the feed on the membrane surface allows the formation of a cake layer to be minimised as the presence of a shear force allows deposited particles to be swept towards the retentate side.[65] Increasing the CFV leads to an increase in the shear rate reducing the particle accumulation on the membrane surface.

The rig set up, detailed in Chapter 3, allows CFVs up to 2.3 m s^{-1} to be investigated. Reynolds Number (Re) = 6300 for a 2.0 wt. % Gum Arabic suspension and Re = 13980 for water at 40 °C. This indicates turbulent feed is passing through the membrane channels. The flow across the membrane affects the mass transfer of the feed to the membrane surface. Due to limitations of the rig set up, and in line with industrial practice, each step was carried out under turbulent flow regime.

The effect of the CFV on the permeate flux, and normalised flux of an aged membrane are shown in Figures 5.4 and 5.5. The effect of the CFV on the permeate flux is shown more clearly when the flux is normalised with the CFV of 1.5 m s^{-1} showing a more pronounced flux decline when compared to higher CFVs. The flux decline rate is very similar irrespective of CFV but the steady state flux is reached at different values. The membrane filtration at CFV 1.5 m s^{-1} showed the lowest permeate flux at steady state, 56 L m^{-2} h^{-1}, as well as the largest decline in flux. Increasing the CFV to 2.3 m s^{-1} resulted in an increased flux of 72 L m^{-2} h^{-1} under steady state. It is expected

that the hydrodynamic shear at higher CFVs disturbs the foulants on the membrane surface resulting in a thinner foulant layer and improved filtration efficiency. A number of other researchers have observed a similar phenomenon,[59, 62, 204] and this has been attributed to greater turbulence preventing particle transport to the membrane surface as well as washing away accumulated foulants from the membrane surface. This agrees with the results presented in Section 5.2.1.

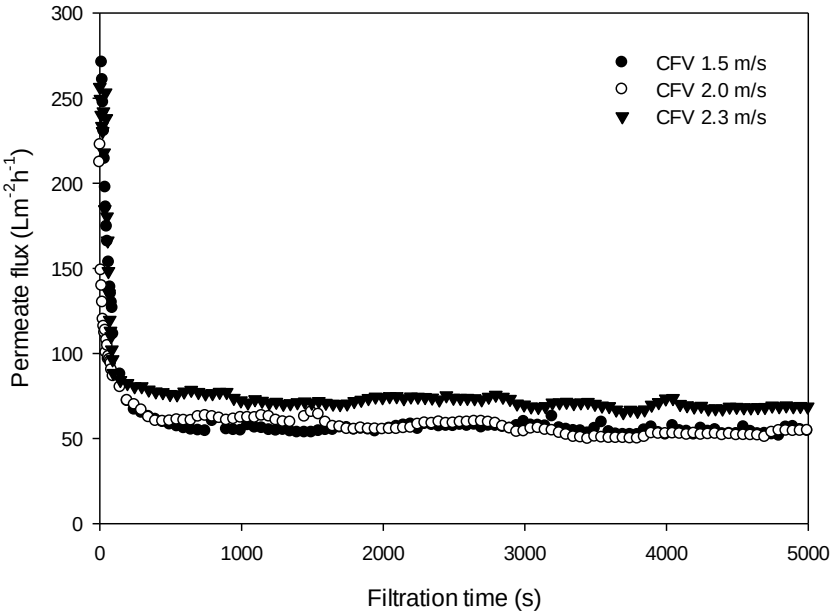

Figure 5.4: Permeate flux profile showing a comparison of flux during fouling with 2.0 wt. % Gum Arabic at CFV of 1.5, 2.0 and 2.3 m s^{-1} of a 0.8 µm tubular ceramic membrane. TMP 1.5 bar, temperature 40 °C.

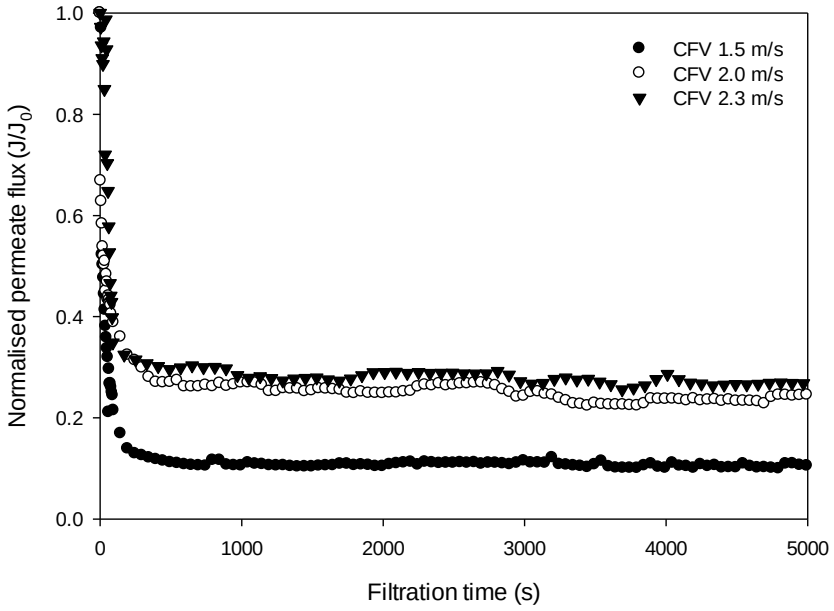

Figure 5.5: Comparison of normalised flux during fouling with 2.0 wt. % Gum Arabic at CFV of 1.5, 2.0 and 2.3 m s^{-1} of a 0.8 µm tubular ceramic membrane. TMP 1.5 bar, temperature 40 °C.

Small changes in the permeate quality were observed with a higher CFV leading to a slight increase in the rejection of Gum. However, other factors such as the number of membrane cycles, have been shown to have a much greater impact on Gum rejection (Chapter 7). It is therefore considered that the influence of the CFV on the permeate quality is negligible.

Table 5.1: Effect of CFV (laminar and turbulent) on a) flux and b) solids retention of an aged 0.8 µm membrane.

Flow	CFV (ms^{-1})	Re(-)	Flux ($Lm^{-2}h^{-1}$)	R_a (-)
Turbulent	1.5	4110	55 ± 2	0.84 ± 0.02
	2.0	5480	58 ± 2	0.86 ± 0.02
	2.3	6300	72 ± 3	0.90 ± 0.02

Lower turbulence at the membrane surface can result in an increased normalised flux decline as the build-up of contaminants may be promoted.[79] The observed results in terms of permeate flux suggest that while increasing the CFV does not completely prevent the formation of a cake layer it is likely that it is reduced, allowing a greater throughput of permeate. This agrees with the

results presented in Section 5.2.1 where the resistance following fouling with Gum Arabic was shown to be reduced under dynamic operating conditions.

5.2.4 Transmembrane pressure

Another hydrodynamic property which is well known to influence the fouling behaviour of a membrane is the transmembrane pressure (TMP). Increasing the TMP leads to an increase in the flux due to an increased pressure drop across the membrane. However it has been widely reported that increasing the TMP can lead to more severe fouling. It is important in understanding the influence of TMP to understand if the system is governed by pressure or by mass transfer. When the system is pressure controlled the TMP increases with increasing pressure, whereas mass transfer controlled systems reach a limiting flux. It was shown in Section 4.2.1 that when operating with water the system is pressure controlled. An aged membrane was subject to pressure ramping during the filtration of Gum Arabic. Initially the Gum was filtered at 1.0 bar and the flux at steady state measured over 30 minutes. Steady state was achieved when Equation 3.2 holds.

Following measurement of the flux at 1.0 bar, the pressure was increased in 0.5 bar increments up to 4.5 bar with each measurement obtained over 30 minutes. Figure 5.6 shows the influence of pressure on the permeate flux at steady state. It can be seen that between 1.0 and 3.5 bar, an increase in the fouling TMP leads to an increase in the fouling flux. When the pressure is increased further (3.5 – 4.5 bar) the flux appears to be in the limiting region with steady state fluxes of 142 ± 5 and 145 ± 10 L m^{-2} h^{-1} for 3.5 and 4.5 bar respectively. Limiting flux usually occurs due to the formation of a cake or gel layer as the solute has reached a maximum concentration.[98] The formation of a cake or gel layer can occur in the pressure dependent region, with increased pressure leading to compaction as a result of the increased driving force.

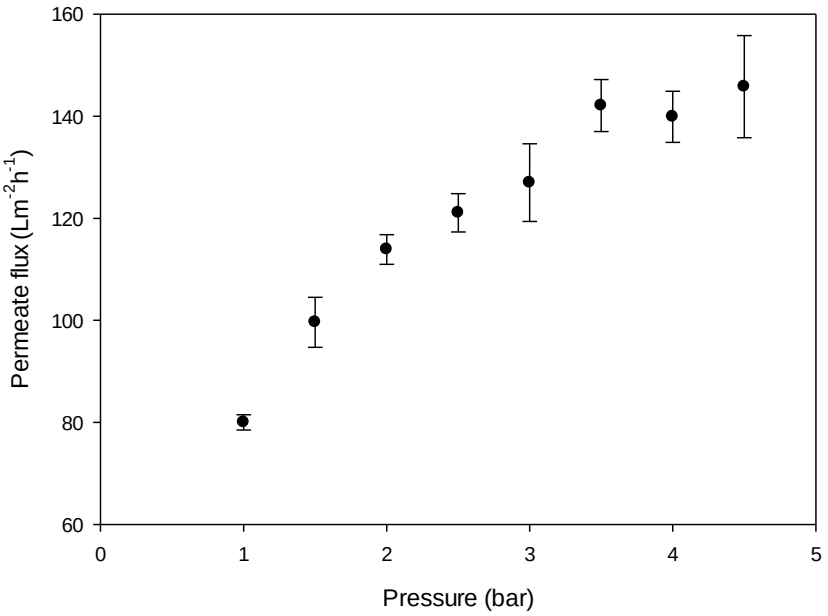

Figure 5.6: Permeate flux during the filtration of 2.0 wt. % Gum Arabic over transmembrane pressures of 1.0 to 4.5 bar through an aged 0.8 µm tubular ceramic membrane at 40 ^{o}C with CFV 2.3 m s^{-1}.

Previous work by Decloux *et al.* reported that when using high concentrations of Gum Arabic in crossflow microfiltration the filtration was governed by mass transfer with the limiting flux region being obtained for transmembrane pressures as low as 0.3 bar.[20] This shows that the concentration of Gum can have a significant effect on the filtration properties. This is also evidence for the formation of a cake or gel layer formation on the membrane, as discussed later in this chapter.

The transient permeate flux (J) and normalised permeate flux (J/J_0) for experiments carried out at 1.0 to 3.0 bar are shown is Figures 5.7 and 5.8. J_0 is the PWF measured before fouling and J is the flux at a time, t. It can be seen that for the filtration of Gum Arabic, an increase in the TMP from 1.5 bar to 3.0 bar led to an increase in the initial permeate flux from 255 L m^{-2} h^{-1} to 594 L m^{-2} h^{-1}. During the filtration, at each of the TMP investigated, an initial rapid decrease in the permeate flux was observed due to membrane fouling. The rate of flux decline was greatest over the first 100 seconds, followed by a stable decrease, before reaching steady state around 500 seconds (Figure 5.7). When the permeate flux was normalised (Figure 5.8) the largest flux decline was observed at 3.0 bar, with the flux decline shown to increase with increasing pressure. After 650 seconds the normalised permeate flux was observed to be 35 % of the PWF at 1.0 bar, and only 17 % of the initial PWF when at 3.0 bar. The increase in permeate flux with increasing TMP can have two effects:

i) There is a greater mass transfer of feed to the membrane surface. This promotes the accumulation and deposition of foulants on the membrane surface and can lead to the formation and growth of a cake layer.

ii) There is a greater force exerted on the feed and foulants, thus pressing them against the membrane. This increased pressure may lead to greater adhesion if the convective forces overcome any electrostatic repulsion. In addition the increased pressure can lead to the formation of a thicker or more dense cake layer (compaction) at the membrane surface.[205]

A number of other research groups have observed a similar trend when using ceramic and polymeric membranes to filter a variety of different solutions/suspensions.[79, 206, 207] It is also well known that polysaccharides contribute to thickening and gelation properties of a solution. This may result in the formation of a gel layer at the membrane surface.[203]

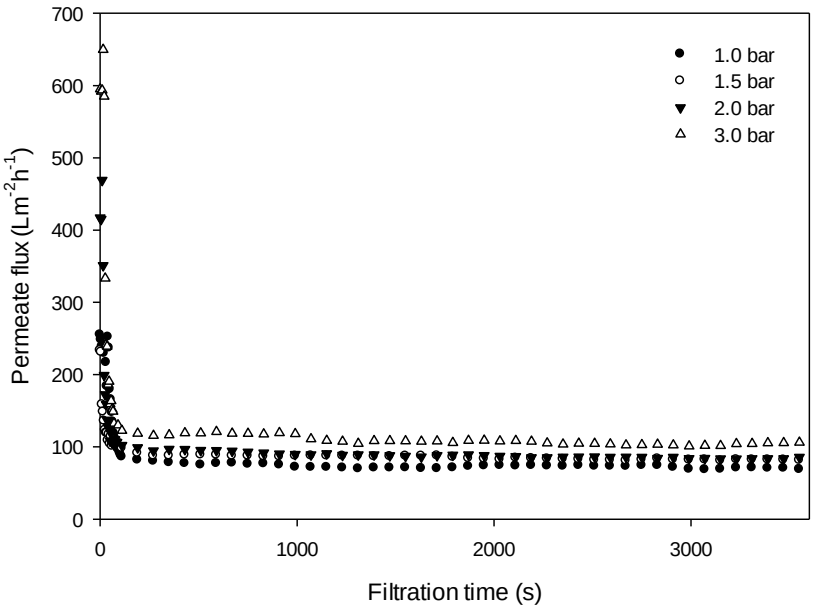

Figure 5.7: Transient permeate flux during the filtration of 2.0 wt. % Gum Arabic at TMP 1.0 – 3.0 bar. CFV 2.3 m s^{-1} at 40 ^{o}C

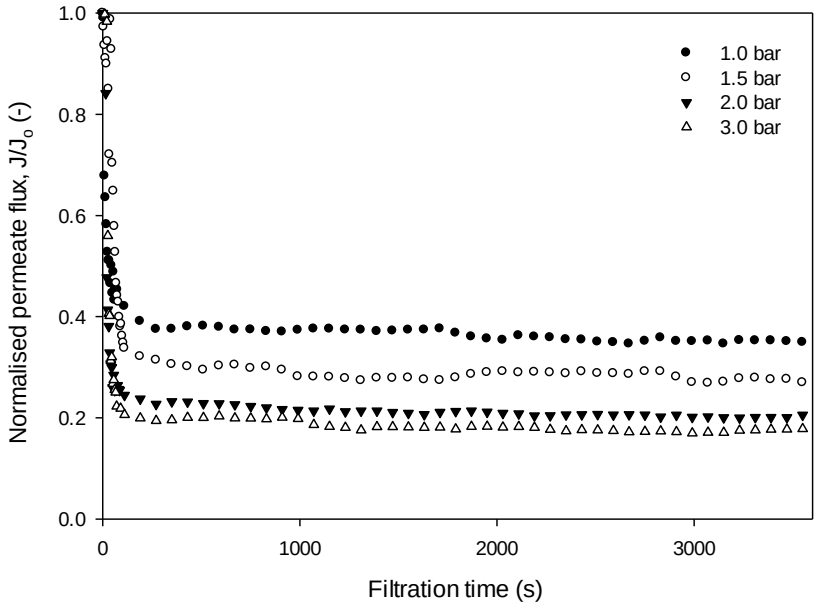

Figure 5.8: Normalised permeate flux during the filtration of 2.0 wt. % Gum Arabic at TMP 1.0 – 3.0 bar. CFV 2.3 m s^{-1} at 40 ^{o}C

Effect of TMP on membrane rejection

The effect of TMP on the permeate quality was investigated, once the system had reached steady state. At 1.0 bar, 90 % rejection was achieved, compared with only 50 % at 4.0 bar. At the beginning of each filtration the concentration of Gum passing through the membrane was highest. However an increased separation efficiency could be achieved after 5 – 15 minutes for each of the TMP investigated. It is expected that most of the Gum Arabic formed a cake or gel layer on the membrane surface, and as this is built up it acts as an extra filtration layer. This could lead to an increase in the separation efficiency of the membrane. This is discussed further in Section 5.5.

Increased rejection is generally found when the TMP is increased, either due to sieving mechanisms or a hindrance to solute transport e.g. establishment of a foulant layer which acts as a dynamic membrane.[122, 134, 208-210] However a reduced retention has also been reported by Alpatova *et al.* during the separation of process water using ceramic membranes[204] and Padanos *et al.* during the filtration of PEGs.[211] The reduction in rejection could be due to an increased level of foulants at the membrane surface at higher TMP or increased pressure forcing the foulants through the membrane.

5.2.5 Temperature

Studies were carried out to investigate the influence of temperature on the resistance following fouling. The resistance measurement allows the change in viscosity due to temperature to be incorporated into the calculation meaning any differences in the resistance are due to other factors. Studies were carried out between 20 and 50 ^{o}C on an aged membrane to prevent degradation of Gum. Figure 5.9 shows the membrane resistance before fouling, after fouling, and following rinsing and cleaning of a membrane fouled with Gum Arabic.

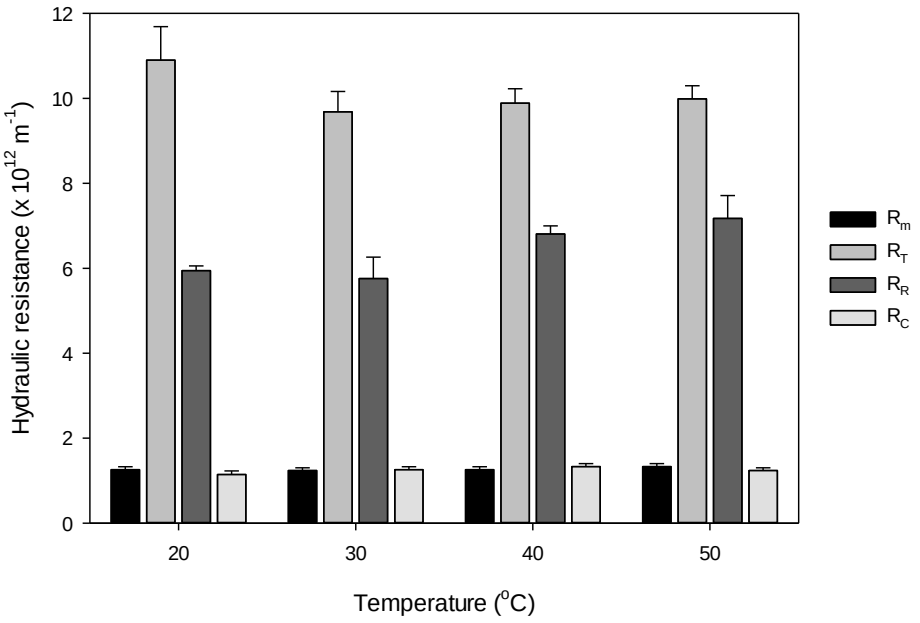

Figure 5.9: Hydraulic resistance during the filtration of 2.0 wt. % Gum Arabic at 20 – 50 ^{o}C. TMP 1.5 bar, CFV 2.3 m s^{-1}. R_m represents the intrinsic membrane resistance, R_T the resistance following fouling, R_R the resistance following rinsing with water and R_C the resistance following chemical cleaning.

Changing the temperature was shown to have no influence on the membrane rejection with ca. 90 % rejection achieved for each temperature studied. Increasing the temperature led to an increase in the permeate flux due to a reduction in the viscosity. However little change is observed in the membrane resistance between 30 and 50 ^{o}C. The solution filtered at 20 ^{o}C led to an increase in membrane resistance. There are a number of factors which may have led to this increase in resistance

i) The formation of aggregates due to decrease in temperature. The suspension was prepared following the standard procedure and then allowed to cool. The formation of aggregates may have occurred during the cooling process.

ii) The formation of a foulant layer may be easier at low temperatures with the suspension being more viscous. It would be expected that a trend would be apparent if this was the case with the membrane resistance decreasing with temperature. However this was not shown from 30 – 50 ^{o}C.

The resistance after rinsing was shown to be lower at 20 and 30 ^{o}C. This implies that the foulant may be more easily removed, suggesting less interaction between the foulant and the membrane surface. A flux recovery of 22 % was observed after rinsing with water following fouling at 20 and 30 ^{o}C compared with a FR of 19 % following fouling at 60 ^{o}C. It is well known that increasing temperature can lead to an increase in reaction rate. Therefore bond formation between the membrane and foulant, or between layers of foulant may be increased at higher temperatures.

As diffusivity and flux increase with temperature, it is generally best to operate at the highest temperature consistent with limits of feed and membrane.[122] This allows a higher throughput, however this needs to be balanced by the flux recovery.

5.3 Membrane material properties

The membrane material properties have been shown to determine the adsorption efficiency of the foulant and influences the first few layers of foulant.[122] It is important to consider the physiochemical interactions of the foulant with the membrane. Due to the difficulty in determining the material properties of tubular ceramic membranes, flat sheet alumina membranes were used for these studies.

5.3.1 Pore size

It is important to consider the size of particles intended to be retained when selecting an appropriate membrane. Macromolecules and proteins are usually much smaller than the pores in MF membranes and should not normally be retained by the membrane.[212, 213] Based on the results shown in Section 4.1.2 membranes in the microfiltration region were selected. While these are larger than the molecular diameter of Gum Arabic, aggregation has been shown to occur. This

leads to the formation of larger particles, predominantly in the size range which corresponds to the pore size in the microfiltration region.[195] While it is understood that tighter membranes generally produce a better permeate quality, higher pressures are required and lower fluxes obtained leading to a reduction in efficiency. In addition several studies have proved that, even with pore sizes much greater than the protein size, fouling under dynamic conditions occurs due to aggregate formation, by hydrophobic and/or electrostatic interactions or by van der Waals forces.[69, 114, 200, 205, 214] Microfiltration has therefore been selected for this study, and as demonstrated in Section 4.3, it has been shown to be applicable to the removal of Gum Arabic from a model waste stream, demonstrating its suitability. The use of ultrafiltration membranes could be used as an additional 'polishing' step to improve retention. However this is outside of the scope of this study.

A number of pore sizes in the microfiltration range were selected; 0.2, 0.5, 0.8 and 2.0 µm. The membranes have been characterised in terms of separation efficiency and permeate quality. The results of this for tubular ceramic and flat sheet membranes are shown in Tables 5.2 and 5.3 for the respective membrane types. Results for both membranes are representative of the first cycle of a virgin membrane. For the flat sheet membranes an interesting trend has been noted: the tighter pore sizes lead to a slight increase in flux at steady state, although this is not statistically significant and is within the error of the experiment. There is a clear difference in the pure water flux for each of the membranes with, as expected, tighter membranes showing an increased resistance. However, following filtration of Gum Arabic for 60 minutes the membrane resistance and flux appear to be the same (within experimental error). This suggests that the pore size is not the limiting factor for eventual flux, and the foulant is limiting mass transfer.

For the tubular ceramic membranes there was little difference in the flux at steady state for the 0.5 and 0.8 µm membranes, however the 0.2 µm membrane showed a reduced flux. For all three membranes the relative flux decline was 98 %. This suggests that the pore size has a greater influence on the eventual flux for tubular ceramic membranes than for flat sheet membranes. The increased rejection was still observed using tighter pore sizes. This could be due to either the pore size or foulant limiting mass transfer.

A number of factors may have contributed to the increase in RFD for the flat sheet membranes with larger pore sizes:

i) The membranes with larger pores have an increased initial permeate flux, therefore more solutes and foulants are convectively driven towards the membrane surface. This enables more solutes to get adsorbed and leads to an increase in pore blockage.[203]
ii) Larger pore size allows a larger number of particles and solutes to be able to go through the pores causing either pore blocking or constriction. Large pore size improves accessibility to the pores increasing the possibility of more solutes being adsorbed either in the pores or on the surface.
iii) Gum aggregates lead to complete pore blocking through being the same size as the pores in the membrane.
iv) The formation of a cake or gel layer on the membrane surface can act as a secondary membrane controlling the process in terms of rejection and selectivity. This leads to increases in the resistance and rejection of the membrane.[114, 215]

Section 4.2.1 shows that the mean aggregate size of unfiltered Gum Arabic is around 0.9 µm. It would be expected that if complete pore blocking was the dominant mechanism the fouling and resistance would be most severe for the 0.8 µm membrane due to the similarity of the particle size and pore size. If the fouling was more severe for the 0.8 µm this would be clear in the resistance and fouling flux. However, as this was not observed for either the flat sheet or tubular ceramic membranes, it is unlikely that complete pore blocking is the main contributor. This is confirmed further in Section 5.5.1.

It is expected that pore blockage, and the formation of a cake or gel layer are likely to be the most dominant mechanisms. This is investigated further in Section 5.5.1. Often, initial fouling is due to pore blockage, whereas over longer filtration times cake formation dominates.[216] The formation of a secondary membrane layer due to the build-up of foulant on the membrane surface is not a new phenomenon, and has been shown by a number of authors.[122, 134, 215, 217] These include Zuriaga-Augusti *et al.,* who reported that despite a larger permeability and pore size, a 150 KDa membrane resulted in a lower flux than a 50 kDa membrane following the filtration of a dye-polysaccharide mixture.[203] Another is Mulder, who stated that rejection can be higher than expected when mixtures of macromolecular solids are present, with the larger solutes forming a secondary dynamic membrane and resulting in higher retention of the low molecular weight solids.[65]

Table 5.2: Influence of pore size of Membralox tubular ceramic membranes. Measurements carried out at 40 ^{o}C with TMP 1.5 bar and CFV 2.3 m s^{-1}. Data for the first cycle of a virgin membrane.

Pore Size (µm)	0.8	0.5	0.2
PWF ($Lm^{-2}h^{-1}$)	5400	6400	4000
R_m (m^{-1})	1.5×10^{11}	1.3×10^{11}	2.0×10^{11}
R_f (m^{-1})	7.4×10^{12}	7.3×10^{12}	1.2×10^{13}
Flux after 60 min ($Lm^{-2}h^{-1}$)	114	116	70.7
R_a (-)	0.3	0.6	0.96
RFD (%)	98	98	98

Table 5.3: Influence of pore size of flat sheet ceramic membranes – data given for the first cycle of a virgin membrane. Measurements carried out at 40 ^{o}C with TMP 1.5 bar and CFV 2.3 m s^{-1}.

Pore Size	2.0	0.8	0.5	0.2
PWF ($Lm^{-2}h^{-1}$)	88000	83000	36000	26000
R_m (m^{-1})	9.4×10^{9}	1.0×10^{10}	2.3×10^{10}	3.2×10^{10}
R_f (m^{-1})	4.0×10^{11}	3.9×10^{11}	3.8×10^{11}	3.5×10^{11}
Flux after 60 min ($Lm^{-2}h^{-1}$)	2000	2100	2200	2400
R_a (-)	0.3	0.3	0.6	0.9
RFD (%)	98	97	94	91
AGP (%)	100	95	91	72

The rejection is the similar for both the tubular ceramic and flat sheet ceramic membranes when the same pore size is investigated. It can be observed that the tighter pore size membranes lead to an improvement in the selectivity. While the flux is very similar for each of the flat sheet membranes, suggesting the formation of a cake or gel layer on the membrane surface, the separation efficiency shows that the pore size of the membrane is still important in determining the selectivity. This becomes less important for multiple cycles. This is discussed further in Chapter 7. There are a large number of particles present in the Gum suspension, in the range of 0.1 – 1.0 µm in diameter, so only the smallest particles can be transported through the 0.2 µm membrane. Meanwhile almost all of the particles can be transported through the 0.8 and 2.0 µm membranes if separation occurs through size exclusion alone. The trend of increased separation with increased pore size suggests that size exclusion is a key factor. However the large increase in separation efficiency between the 0.5 and 0.8 µm membranes, and increased separation following multiple cycles (Chapter 7) suggests that while size exclusion has a role to play in separation, other factors such as charge and surface chemistry also have a role. This is discussed further in Chapters 7 and 8.

The percentage of AGP transmitted through the membranes was measured for the different pore sizes using GPC as detailed in Section 3.5.7. It was observed that as the pore size decreased the transmission of AGP (relative to the total transmission) decreased. This suggests there is

preferential transmission of smaller particles with GP and AG having a smaller size than the AGP fraction of Gum. This leads to the potential use for fractionation and highlights that size exclusion is responsible for at least some of the separation characteristics.

Figures 5.10 and 5.11 show the normalised flux decline curves over the first five minutes of filtration, for the flat sheet and tubular ceramic membranes respectively. It can be observed that for each of the membranes studies there is an initial rapid flux decline followed by a much slower decline. This is common for the filtration of polysaccharides and proteins. Both systems showed that the pore size had little influence on the flux decline between 0.2 and 0.8 µm, however the flux decline was slightly slower for the 2.0 µm membrane. This may be as a result of the pores being larger than the mean pore size of the Gum as shown in Section 4.1.2.

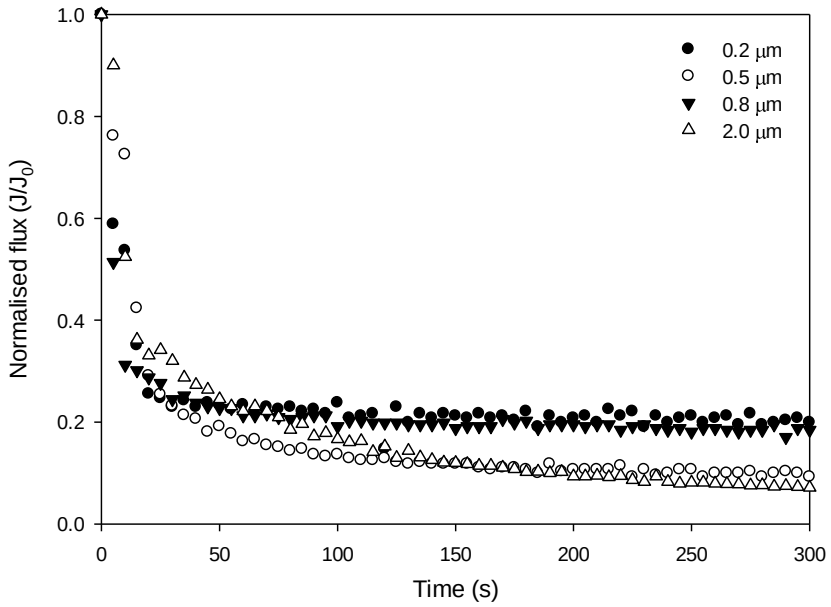

Figure 5.10: Normalised flux decline curve for flat sheet membranes with pore sizes 0.2, 0.5, 0.8 and 2.0 µm over the first 300 seconds of filtration at CFV 2.3 m s^{-1}, TMP 1.5 bar and 40 ^{o}C.

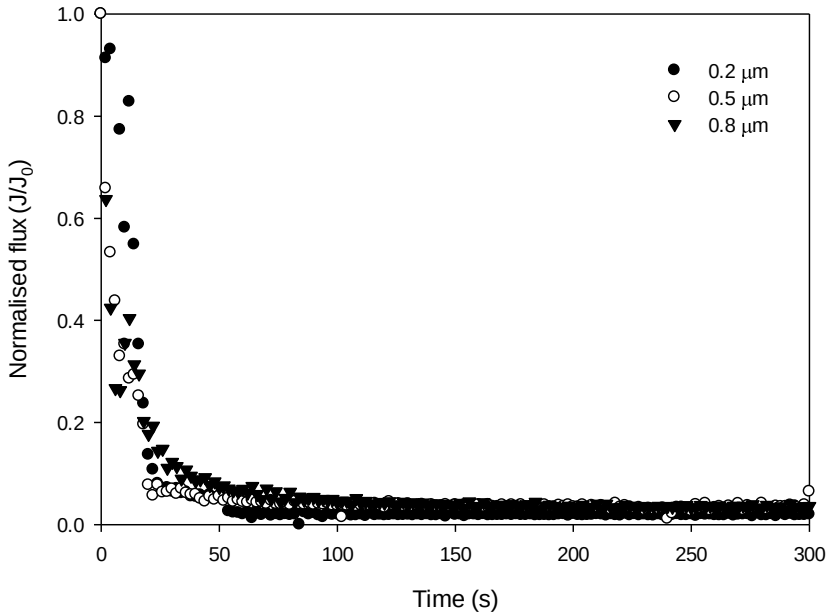

Figure 5.11: Normalised flux decline curve for tubular ceramic membranes with pore sizes 0.2, 0.5, and 0.8 μm over the first 300 seconds of filtration at CFV 2.3 m s^{-1}, TMP 1.5 bar and 40 ^{o}C.

5.3.2 Porosimeter data

Mercury intrusion porosimetry was used to determine the level of internal fouling following filtration. A comparison for a 0.8 μm virgin and fouled membrane was carried out. The bulk porosity and mean pore size are shown in Table 5.4.

Table 5.4: Mercury intrusion porisometry data for virgin and fouled membranes.

Sample	Bulk porosity (%)	Mean pore size (μm)
Virgin	39.77 ± 0.20	0.80 ± 0.02
Fouled	39.82 ± 0.20	0.79 ± 0.03

Little difference was observed in the porosity of the membrane following fouling. This suggests that most of the fouling occurs on the membrane surface rather than in the pores. If the pores contained Gum, a decrease in the porosity would have been observed.

Some pores may not have been measured using this technique. If the pores are not open ended it may be difficult for the mercury to penetrate into the pores. This effect should have been eradicated by vacuum degassing during the sample preparation, however it may lead to small experimental errors.

The mean pore size was very slightly smaller for the fouled sample than that of the virgin membrane. This could be as a result of pore constriction as a result of fouling. However, as the difference is so small and the porosity shows little change, it is more likely that it is as a result of experimental errors and is within the error of the apparatus.

5.3.3 Surface modification

Understanding the surface chemistry of the membranes can help to give an indication of the type of fouling and its mechanism. Membranes have been shown to have a reduced fouling tendency if the surface is hydrophilic, and charged similarly to the key foulants.[218] A number of techniques are available to determine the surface properties. In this study, contact angle and zeta potential have been investigated.

5.3.3.1 Hydrophobicity – effective contact angle

Membrane hydrophobicity is an important factor in determining fouling potential and transmission. The hydrophobicity gives an indication of the surface energy, with more hydrophilic surfaces having a higher surface energy. It has been well reported that hydrophilic membranes are less prone to fouling,[218] with hydrophobicity significantly affecting the level of organic foulants.[199] The virgin membrane is moderately hydrophilic (effective contact angle less than 90 ^{o}). However fouling increases the hydrophobicity as shown in Table 5.5. The results indicate that the membrane is fouled due to the adhesion of a hydrophobic, charged species to the membrane surface.

Table 5.5: Effective contact angle for flat sheet virgin and fouled membranes. Measurements based on average of 10 points on the membrane.

	Virgin membrane	**Fouled – cycle 1 (F1)**	**Fouled - cycle 2 (F2)**	**Fouled – cycle 5 (F5)**
Contact angle (^{o})	37 ± 6	104 ± 7	122 ± 6	116 ± 5

In-pore adsorption is not evidenced by these contact angle measurements, so significant surface fouling by a hydrophobic species is apparent. This agrees with the results discussed in Section 5.3.2. After 2 cycles, the level of hydrophobic foulants increases, but there is no statistically significant change after further cycles. In Gum Arabic, the polysaccharide is hydrophilic with the polypeptide backbone being hydrophobic. These results suggest that a significant proportion of

fouling is resulting from the polypeptide backbone. This in turn suggests proteinacious fouling. Based on the structure of Gum Arabic, it is possible that the carboxylic acids, aldehydes or alcohols in the polysaccharide (AG fraction) form hydrogen bonds with the membrane surface, resulting in the hydrophobic protein backbone protruding. This is one mechanism which could lead to the increase in hydrophobicity. This agrees with the results in Section 5.2.1 where fouling was more severe for Gum Arabic than arabinogalactan alone.

Additionally, the terminal rhamnose groups on the polysaccharide have hydrophobic centres.[219] These may be present on the surface of the foulant layer leading to an increase in contact angle following fouling. At present it is unclear if the hydrophobic backbone or hydrophobic centres in the terminal rhamnose groups are responsible for the increase in hydrophobicity. Both may play a role, or the structure of Gum may be rearranged following adsorption.

5.3.3.2 Zeta potential

Zeta potential is useful in determining the surface charge of a membrane at different pHs. The surface charge influences fouling propensity with similarly charged foulants generally being repelled by the membrane. Solutions with a high charge density keep the molecules away from each other and from the membrane. This usually leads to a reduction in fouling and retention.[143] Transmission of protein can be governed by varying nature of the charge on it (pH), or by the nature and extent of charge on membrane.[220] The measured zeta potential for a virgin and a fouled membrane are shown in Figure 5.12. The virgin membrane showed a charge of -10 to -40 mV with an isoelectric point below pH 3.0. Once fouled, a large reduction in charge was observed, with the fouled membrane showing almost no charge. The fouled membrane shows a zeta potential of 0 to -4 mV and an isoelectric point ca. pH 3.0. The large reduction in charge following fouling is due to changes in the surface chemistry with the attachment of foulants to the surface and/or pore walls. The relatively constant zeta potential over the pH range is typical for complex organic foulants. The use of FTIR in Section 5.5.3.2 confirms that there is adhesion of Gum Arabic to the membrane surface.

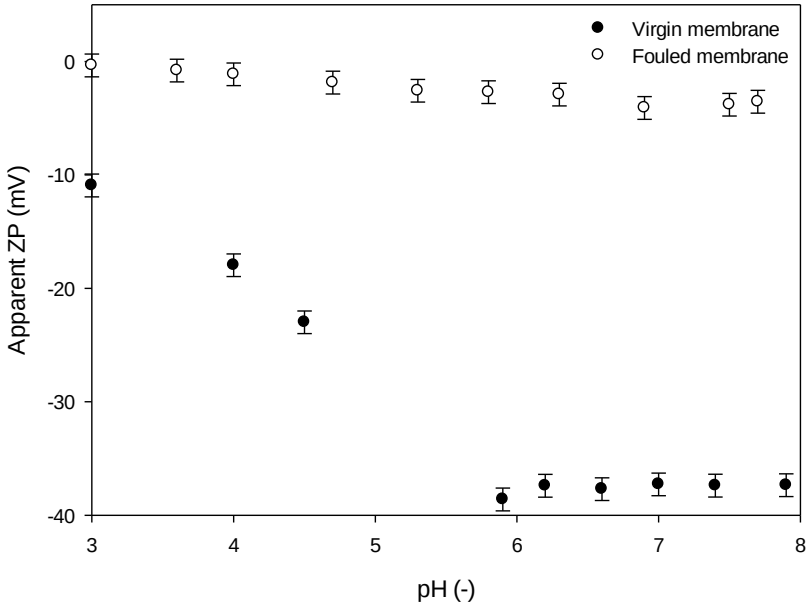

Figure 5.12: Zeta potential of virgin membrane, and membrane fouled with Gum Arabic.

The natural pH of Gum Arabic is ca. pH 5.5 so during filtration the membrane displays a large charge ca. -30 mV. Gum Arabic has also been reported to have a negative zeta potential ranging from -7 to ca. -30 mV, with it showing a low charge around pH 5.5.[147] Gum Arabic and the membrane are both negatively charged at pH 5.5 so it would be expected that some repulsion should occur.

There are several possibilities as to why the fouled membrane shows a large reduction in charge:

i) Many of the amino acids in the Gum structure are known to act as zwitterions and Gum has been shown to have charge buffering effects. This may be responsible for the reduction in zeta potential observed for the fouled membrane, with the positive charged amino acids bonding to the membrane surface and leading to a charge reduction.

ii) Gum Arabic is known to contain small amounts of cations, it typically contains ca. 0.7 % Ca^{2+}.[221] These are likely to be attracted to the negatively charged membrane surface and their attraction could lead to further attraction of anions leading to an increase in fouling. Ca^{2+} can neutralise the negative charges on Gum Arabic molecules or the membrane surface.

iii) During adsorption the conformation of Gum Arabic could change, leading to a redistribution of charges and therefore a more positively charged surface than

expected. While this has not been previously shown for Gum (due to the lack of research in the area) it has been shown to occur for BSA.[222]

The mechanism of attachment of the Gum may be due to one of the methods detailed above, however it is most likely that electrostatic repulsions are not the dominant mechanism resulting in fouling of the alumina membrane. Due to the charge on Gum being low at pH 5.5, the electrostatic forces are expected to be small. Therefore other factors such as van der Waals forces, hydrophobic interactions, hydrogen bonding or convective forces are likely to dominate, resulting in membrane fouling.[143] In water, the alumina surface is known to be hydrated, leading to the formation of OH groups on the membrane surface. These can interact with the polar groups through the formation of hydrogen bonds. There are a large number of polar groups in Gum such as carboxylic acid groups (COOH) found on some of the amino acids, and OH groups present on the sugar molecules which are highly abundant in the arabinogalactan fraction of Gum (arabinose and galactose). It is expected that hydrogen bonding is responsible for membrane fouling, at least in part.

While electrostatic interactions may not be dominant in the adhesion of Gum to the membrane surface, they may have a more dominant role once there is a layer of Gum on the membrane surface. It has been shown previously by Zhang *et al.* that the attachment of Gum Arabic to γ-alumina nanoparticles led to a reduction in their zeta potential.[223] This reduction prevented agglomeration of the particles due to repulsive forces between the particles. This could apply during the fouling of membranes, with the initial foulant layer providing repulsion and preventing further fouling, and potentially increased rejection of Gum.[143]

At a pH above the IEP of the protein most of the side groups in the protein are negatively charged, but some moieties or fragments are still positively charged.[147] The peptide segments are positively charged and can interact with negatively charged hydrocolloid to form a weakly associated complex which does not precipitate.

Because of the potassium, calcium and magnesium salts of weak acid groups found in Gum Arabic, its buffer action is greater in neutralisation of acids than alkalis.[5]

5.3.4 Roughness

The membrane roughness can have a significant influence on fouling, a strong influence on adhesion properties,[160] and rough surfaces can be responsible for the direct entrapment of larger

aggregates. If the roughness is larger than the particle size then direct entrapment of the particles is likely. If the membrane has a low mean roughness, then attachment of the foulant to the membrane is more likely. The roughness and architecture of the top surface of a virgin and fouled flat sheet membrane were measured using AFM in tapping mode. The average surface roughness was determined using the mean deviation from the central plane in the Z direction as described in Section 3.6.8. AFM images of the two surfaces are shown in Figure 5.13 with the roughness values obtained shown in Table 5.6.

Table 5.6: S_a values obtained through AFM measurements for virgin and fouled flat sheet membranes.

	Roughness, S_a (nm)	
Pore Size (µm)	Virgin	Fouled
0.8	361 ± 17	305 ± 75
2.0	368 ± 46	406 ± 88

Little significant variation was observed between the S_a values for the virgin and fouled membranes. For the 0.8 µm membrane, following fouling the roughness was decreased, however the error between samples was much greater suggesting uneven fouling. This agrees with the results obtained by SEM. For the 2.0 µm sample the roughness appeared to increase, however again this was within the experimental error and is not statistically significant ($P>0.05$), therefore no conclusions can be drawn about the surface from the roughness value alone. The use of roughness values can be deceiving as they measure the average deviation from a point. This means that very flat surfaces can have the same roughness value as a surface which has uniform peaks and troughs. It is therefore important to consider visual changes in the AFM micrographs as these can give a better idea of the topography of the membrane surface. Figure 5.13 shows that following fouling the large peaks and valleys present in the virgin membrane are still evident. However, some of the smaller indentations appear to have been smoothed over by the foulant layer. This is again further evidence for the formation of a cake layer on the membrane surface. The changes to the surface may be as a result of direct entrapment of aggregates leading to the formation of a cake or gel layer on the membrane surface, or it may be due to bonding e.g. hydrogen bonding between the foulant and membrane leading to the formation of a cake or gel layer. The surface roughness can influence the foulant layer with rough membranes having been shown to produce a looser foulant layer with lower resistance than the dense layer found on smooth membranes.[151]

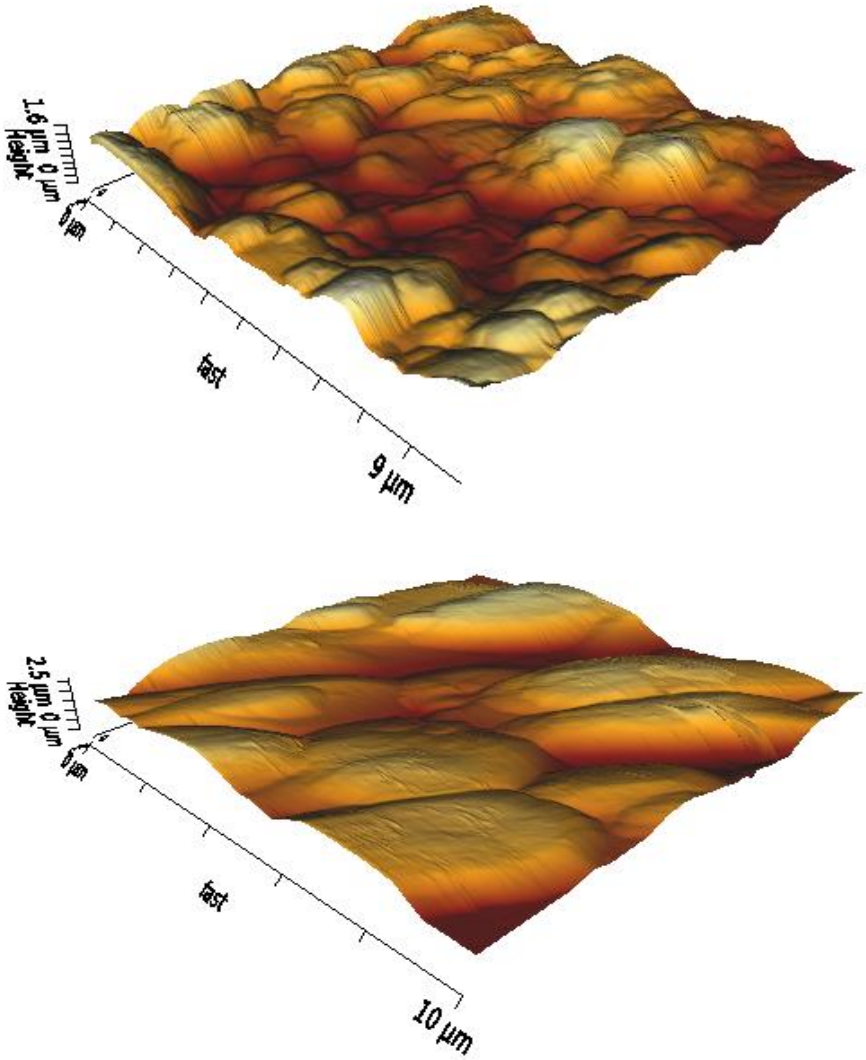

Figure 5.13: AFM micrographs of flat sheet membranes: virgin membrane (top) and fouled membrane (bottom).

5.4 Solution/suspension properties

Solution and suspension properties are another important factor to consider when investigating fouling. As shown in Section 5.3.3.2, the pH has a large influence on the zeta potential, particularly for alumina membranes. Therefore factors such as altering the pH can lead to differences in fouling propensity. In this study little research has been carried out into the effect that solution properties have on fouling, as alterations in the suspension can also influence the quality of Gum Arabic. As the aim of this project is to remove Gum Arabic from waste streams, to allow recycling of both the Gum and water, it was decided that the solution properties would not be altered to prevent any changes to the properties of Gum Arabic. However, one solution property was

investigated: the pre-filtration of Gum, as this should only lead to the removal of large aggregates and not alter the Gum properties. 0.8 µm flat sheet membranes were used to investigate the pre-filtratered and raw suspensions.

5.4.1 Pre-filtration

Gum Arabic was filtered through a 25 µm steel wound membrane as described in Section 3.4.6. This allowed removal of any large aggregates present in the suspension. The presence of aggregates in suspension has previously been reported to govern membrane fouling over the first new minutes of filtration.[122, 200] The permeate fluxes for two suspensions through a 0.8 µm flat sheet membrane are shown in Figure 5.14. One of the suspensions underwent pre-filtration, and one was prepared following the standard protocol. While the flux was improved at the beginning of the cycle for the Gum suspension which had been pre-filtered, after ca. 12 minutes both suspensions resulted in a steady state flux ca. 2100 L m^{-2} h^{-1}. This suggests that while aggregates influence the initial fouling, the removal of aggregates does not prevent or even reduce fouling over time. This suggests that aggregates of Gum Arabic do not play a significant role in membrane fouling during the filtration of Gum.

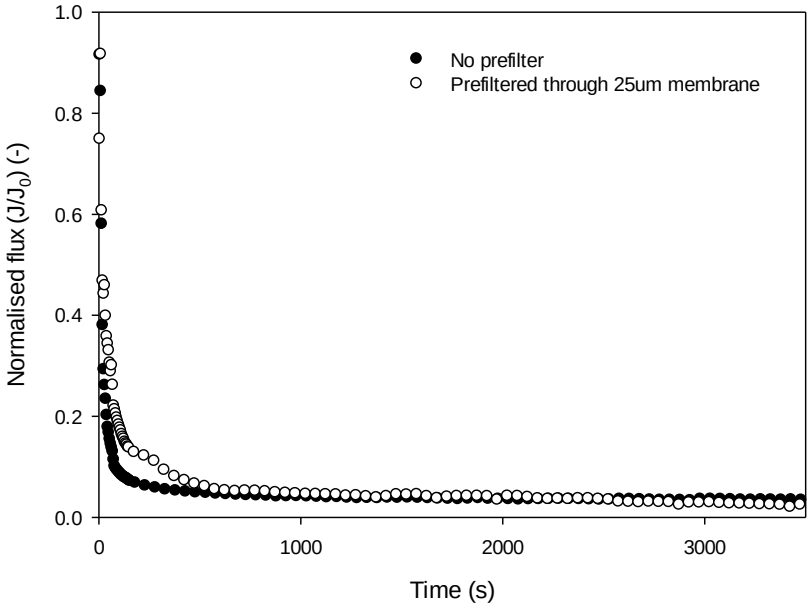

Figure 5.14: Influence of pre-filtering through 25 µm steel membrane on filtration flux of 0.8 µm flat sheet ceramic membrane.

5.5 Characterisation

5.5.1 Mechanistic picture of fouling

The fouling mechanisms have been elucidated based on the four classical models, namely cake filtration, complete, standard and intermediate (pore constriction) pore blocking.[79] [224] The equations used in this study and their corresponding linear forms are shown in Table 3.3. Each of the fouling mechanisms is important in gaining an understanding about how the fouling influences filtration. Understanding the main fouling mechanism allows a method for effective cleaning to be determined. While modelling allows the type of foulant to be determined, it fails to give any information about the severity of the fouling. The standard blocking model assumes that solute adsorbs onto the pore walls whereas the other models assume that fouling occurs on the external surface of the membrane. Complete pore blocking reduces the membrane surface area by reducing the number of pores available for permeate flow, while standard pore blocking (pore constriction) reduces the pore size.[122] All four models assume the resistance to filtrate flow increases with increasing filtrate volume.[103]

Fitting experimental data with the classical models allows the fouling mechanism as well as the evolution over time to be estimated. Generally the curves show similar trends, with an initial concave curve up or down followed by a straight line (see Appendix B). The lack of linearity can be explained by the multiple components contained within the Gum, each which may result in a slightly different fouling mechanism. In addition the blocking mechanisms only account for one type of fouling, whereas it is likely that several fouling mechanisms occur simultaneously. For this reason the fouling mechanism has been broken down into two time regimes: 1-5 minutes, and 5-60 minutes, as the dominant mechanism is shown to change most within this time range. As expected, the dominant fouling mechanisms were found to change over time as shown in Table 5.7. For a fouling mechanism to show a good fit an r^2 value ≥ 0.99 is required.

The sharp flux decline over the first few minutes can be attributed to the adsorption of solutes on the membrane surface, and pore constriction as a result. The specific interactions between the foulants and the membrane surface are dominant here. The subsequent gradual flux decline can be attributed to the formation of a cake layer as a consequence of foulant deposition and accumulation on the membrane surface.[203] The formation of pore constriction or pore blocking followed by cake formation is common during the filtration of polysaccharides.[225]

The concentration polarisation (CP) was measured by switching off the pressure and flow across the membrane, allowing foulants to diffuse from the membrane surface back into the feed. When

the pump is switched back on, instantaneously there was no observed change in resistance due to CP. The presence of any back diffusion would allow an increased flux as soon as the pressure and flow are switched back on. This allowed the resistance due to concentration polarisation (R_{cp}) to be quantified. During the microfiltration of Gum Arabic, no concentration polarisation was observed. This was due to the Gum containing macromolecules and particles with a low diffusion coefficient.[69] The back diffusion of components from the membrane surface into the feed suspension is slow and cannot counterbalance the convective mass transport towards the membrane. This leads to precipitation of the solutes on the membrane surface forming a cake or gel layer. Once the solutes are in a cake/gel layer it is more difficult for back diffusion to occur.

A large number of conditions have been investigated and are displayed in Table 5.7. The curves used to obtain the values displayed in Table 5.7 are shown in Appendix B. It can be seen that while altering the conditions leads to slight changes in the mechanism, generally pore constriction, or a combination of pore constriction and cake filtration dominate over the first five minutes. On the other hand, cake filtration becomes the primary mechanism after five minutes of filtration.

For a 0.8 µm flat sheet membrane both cake filtration and pore constriction show an excellent fit to the respective models, highlighting that both mechanisms occur simultaneously. However pre-filtering the Gum through a 25 µm spiral wound membrane to remove aggregated Gum led to pore constriction being the dominant mechanism with cake filtration showing a poor fit (r^2 = 0.976). This suggests that the aggregates present in the suspension play a role in cake filtration, whereas smaller particles lead to the formation of pore constriction.

Investigating the pore size, it can be seen that for 0.5 – 2.0 µm membranes cake filtration is generally dominant, however for the 0.2 µm membrane none of the models represent a very good fit. It would be expected that cake filtration would dominate with the increased rejection observed for the 0.2 µm membrane, however this is not the case. Standard pore blocking shows the best fit, however this is far from perfect. Further work is required to understand this discrepancy. It may be that less foulants are adhering to the membrane surface with the RFD lower than for the other pore sizes. Alternatively it could be a combination of standard blocking and cake filtration with each preventing the other from attaining a good fit to the model.

These results fit with the results displayed in the previous sections which suggested the formation of a cake or gel layer on the membrane surface. They are also consistent with results obtained by

other authors when investigating the filtration or polysaccharide or protein based feeds, as well as other systems such as process water.[79, 225]

The decrease in Gum concentration, observed in the permeate over the first five minutes of filtration, can be attributed to the formation of a cake layer on the membrane surface. The formation of a cake layer is one of the most common forms of fouling and has been identified by the decrease in permeate flux over the same time period and through modelling. As the cake layer forms, it adds additional hydrodynamic resistance to the membrane flux, and begins to act as the active layer on the membrane surface, allowing less Gum to pass through the membrane. The formation of a cake layer leads to electrochemical and steric interactions between the foulant later and feed suspension leading to increased rejection of the Gum. On reaching steady state the transmission of Gum through the membrane remains constant over extended time periods. A number of runs for 90 minutes were carried out, and no change in concentration of Gum in the permeate stream could be observed.

Table 5.7: fouling mechanism based on blocking laws proposed by Hermia[101] and extended for crossflow by Field *et al.*[93] Values are r^2 values for curve fitting to the linear equation.[91, 102, 103] $r^2 \geq 0.99$ means there is a good fit to the model.

Experiment	Time (min)	Pore blocking	Pore constriction	Cake formation	Intermediate pore blocking	Predominant fouling mechanism
Flat sheet 2.0 µm	5	0.681	0.968	0.991	0.949	Cake
Flat sheet 2.0 µm	60	0.570	0.964	0.985	0.953	-
Flat sheet 0.8 µm	5	0.42	0.998	0.999	0.849	Cake and constriction
Flat sheet 0.8 µm	60	0.5	0.986	0.995	0.931	Cake
Flat sheet 0.5 µm	5	0.473	0.948	0.995	0.919	Cake
Flat sheet 0.5 µm	60	0.499	0.895	0.913	0.933	-
Flat sheet 0.2 µm	5	0.064	0.673	0.689	0.838	-
Flat sheet 0.2 µm	60	0.459	0.603	0.579	0.927	-
Tubular ceramic 0.8 µm c1	5	0.508	0.981	0.996	0.971	Cake
Tubular ceramic 0.8 µm c1	60	0.668	0.918	0.939	0.941	-
Tubular ceramic 0.8 µm c10	5	0.690	0.944	0.996	0.929	Cake
Tubular ceramic 0.8 µm c10	60	0.668	0.918	0.939	0.941	-
Tubular ceramic 0.5 µm c1	5	0.388	0.968	0.974	0.929	-
Tubular ceramic 0.5 µm c1	60	0.102	0.850	0.859	0.924	-
Tubular ceramic 0.5 µm c10	5	0.099	0.766	0.786	0.807	-
Tubular ceramic 0.5 µm c10	60	0.212	0.951	0.960	0.931	-
Pre-filtered	5	0.777	0.995	0.976	0.953	Pore constriction
Pre-filtered	60	0.7605	0.975	0.995	0.965	Cake formation

5.5.2 More detailed analysis of the foulants

The use of a range of further analytical techniques to undertake a more detailed analysis of the foulants allows an insight into the chemical composition and nature of the foulant. It has been shown in Section 5.3.3 that the foulant is hydrophobic in nature. The use of FTIR, SEM, Raman and the adhesion through colloidal probe AFM have all been explored to gain a better understanding of the nature of the foulant.

Dror *et al.* observed that the addition of salt to Gum Arabic dramatically changes the SANS pattern, indicating that the electrostatic interaction determines the distance between aggregates. The addition of salt was found to mask the charged groups on GA.[25]

5.5.2.1 FTIR

FTIR spectra of Gum Arabic, and an alumina membrane fouled with Gum Arabic are shown in Figures 5.15 and 5.16 respectively. A scan of the virgin membrane (shown in Figure 4.10) has been subtracted from the fouled membrane graph so that only the deposited foulant on the membrane surface or within the pores is shown. Limited data has currently been published regarding the FTIR spectra of Gum due to the complex composition of polysaccharides and proteins (polypeptides), creating a complex spectrum.[226, 227]

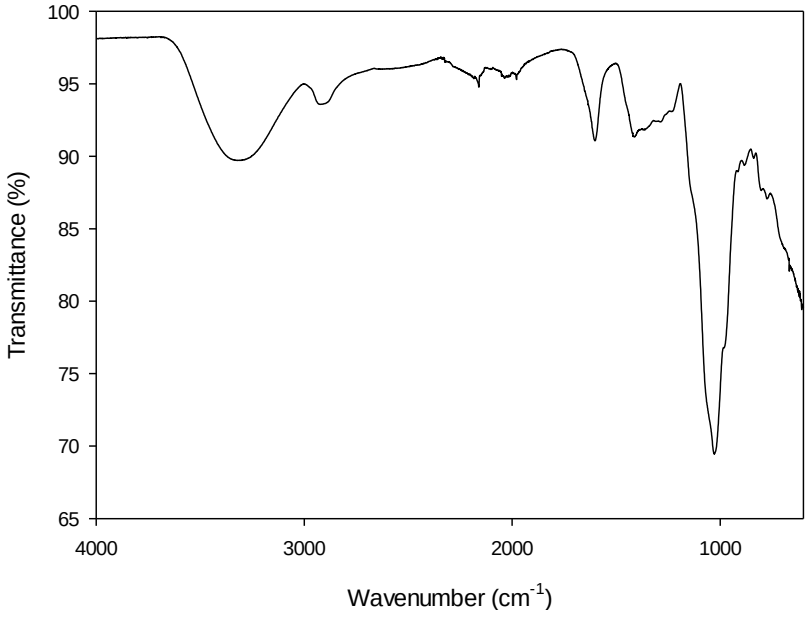

Figure 5.15: FTIR spectra of Gum Arabic.

The FTIR spectrum of Gum Arabic (Figure 5.15) contains a number of characteristic peaks which can be related to its structure. The broad peak at 3400 cm^{-1} can be ascribed to asymmetric stretching of the O-H bond. This is a characteristic peak of polysaccharides and is broad due to the presence of hydrogen bonding. The peak at 2930 cm^{-1} can be ascribed to the stretching vibrations of CH_2 groups in a variety of chemical environments. This peak is also characteristic of polysaccharides.[227, 228] The strong peak at 1612 cm^{-1} is due to the symmetric stretching of the carboxylate anion (COO^-) which is formed from deprotonation of carboxylic acid groups present in a large number of amino acids present in Gum Arabic. The sharp peak at 1415 cm^{-1} and the slight shoulder at 925 cm^{-1} are characteristic of the O-H bending vibration. There are a number of overlapping peaks in the region of 1200 – 1400 cm^{-1}. These can be attributed to CH_2 bending and twisting, C-C stretching, CH_3 bending C-O stretching. The strong peak at 1030 cm^{-1} is due to C-C stretching, and the shoulder at 1075 cm^{-1} can be attributed to asymmetric stretching of COC in an ether ring. The defined shoulder at 975 cm^{-1} is characteristic of the rocking vibration in CH_3 as a methyl substitution of a carboxylate group. Each of the peaks observed is characteristic of the structure of Gum Arabic, and highlights that the majority of the Gum is polysaccharide based, as reported in previous literature.

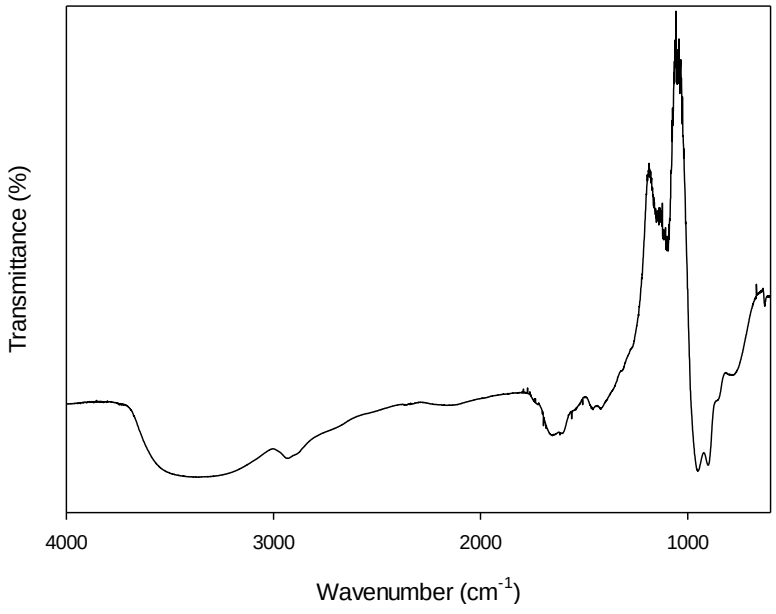

Figure 5.16: FTIR trace of 0.8 µm flat sheet alumina membrane fouled with Gum Arabic.

The fouled membrane shows a large number of peaks characteristic of Gum Arabic. This highlights that adhesion to the membrane surface has occurred. Most of the peaks found in the Gum spectra are also observed in the fouled membrane sample, with the peak at 1412 cm^{-1} showing a shift to

1650 cm^{-1}. This shift suggests that the carboxylate anion has become coordinated with the alumina, due to hydrogen bonding between the alumina and Gum.[229]

5.5.2.3 SEM

SEM was conducted as described in Section 3.6.3. Imaging was carried out on virgin and fouled surfaces to allow a comparison and to determine fouling. Figure 5.17 shows that there is a clear cake layer on the surface of a 0.8 µm flat sheet membrane. The cross sectional image shows that there is a small amount of fouling at the entrances to the pores with no fouling observed in the middle of the cross section. These results are consistent with those detailed in Section 5.5.1.

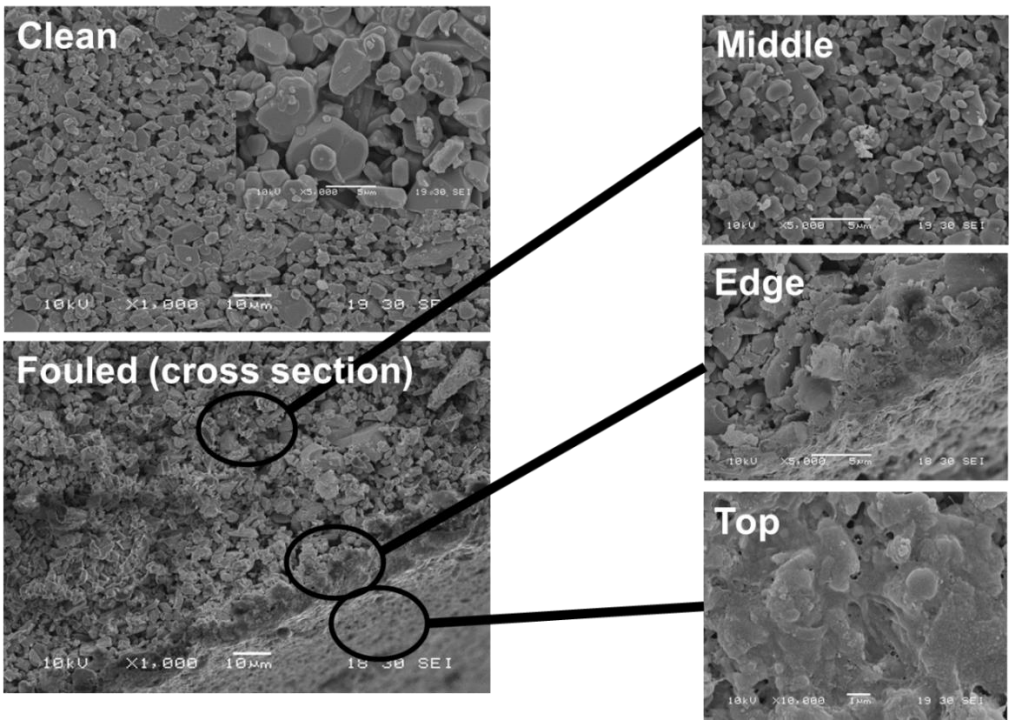

Figure 5.17: Cross-sectional SEM images of virgin and fouled flat sheet 0.8 µm membrane. The cross section has been separated to show the different sections and impact of fouling.

The use of SEM-EDX allowed elemental analysis of the membrane surface. Following fouling, the composition of foulants is shown in Table 5.8. The presence of carbon and elevated levels of oxygen are expected due to the presence of organic foulants. The SEM-EDX results show the presence of calcium following fouling. This suggests that the calcium ions present in the Gum may be playing a role in the adhesion of Gum to the membrane surface due to their positive charge, as alluded to in Section 5.3.3.2. Previous work carried out by Liang *et al.* reported that divalent cations can aggravate fouling through an ion bridging interaction. This may have an impact on the

severity of fouling.[199] The presence of silicon was not expected, and may be a contaminant from the O rings used to seal the membranes in the rig.

Table 5.8: Elemental composition (wt. %) of membrane before and after fouling obtained using SEM EDX. Elements showing '-' were not detected in the sample.

Sample	Al	O	C	Ca	Si
Virgin membrane	50.6 ± 2.2	49.4 ± 4.3	-	-	-
Fouled	42.0 ± 3.8	46.8 ± 7.9	9.6 ± 6.5	0.8 ± 0.4	0.8 ± 0.4

SEM was also carried out on tubular ceramic membranes in order to see if a layer of Gum was also formed on the membrane surface. SEM images for a virgin membrane, and one which had been fouled and cleaned for 10 cycles are shown in Figure 5.18. It can be seen there is the clear formation of a fouling layer on the membrane surface, with little evidence of in-pore fouling. The Gum was not removed effectively during cleaning as discussed further in Chapter 7.

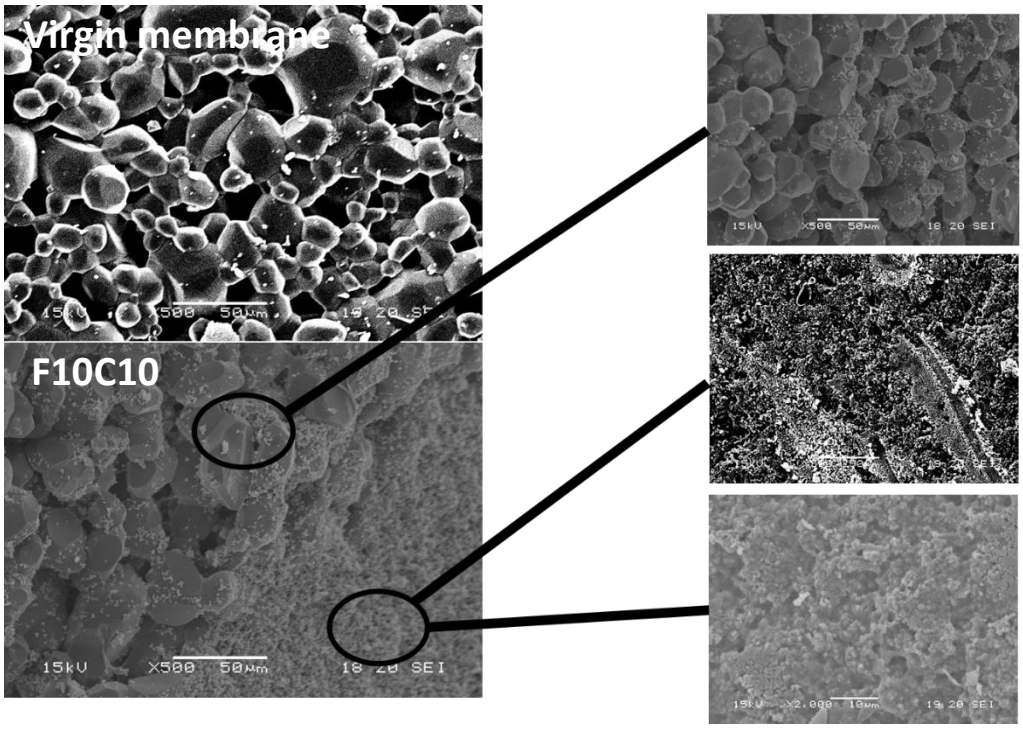

Figure 5.18: SEM images of a 0.8 µm tubular ceramic membrane. F10C10 membrane was fouled and cleaned using sodium hydroxide and citric acid for 10 cycles. Following fouling and cleaning a layer of Gum Arabic is clearly evident on the membrane surface, with little evidence of in-pore fouling. The cross section of F10C10 has been separated to show the different sections and impact of fouling/cleaning.

5.5.2.4 Raman

Raman was investigated to identify any structural changes to the Gum or alumina membrane following fouling. Unfortunately the spectra were found to overlap as shown in Figure 5.19. This prevents the use of Raman spectra for other studies, such as cleaning in Chapter 6.

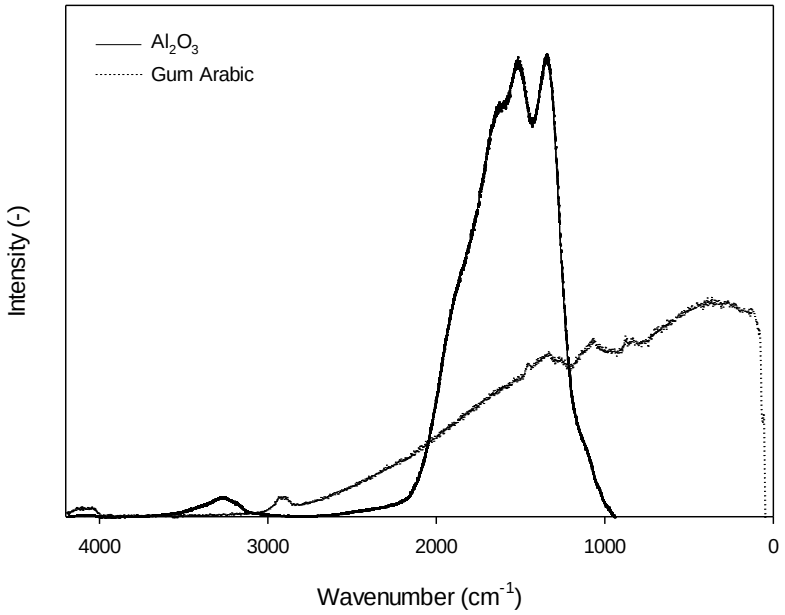

Figure 5.19: Raman spectra of alumina membrane and Gum Arabic. The Gum and alumina peaks overlap preventing full identification.

5.5.2.5 Fouling adhesion

Understanding the electrostatic forces between the Gum and the membrane allows a better insight into the cause of fouling, and potential methods to reduce this. As discussed in Section 5.3.3.2, at ca. pH 5.5 both the membrane and the Gum exhibit negative charges. This means that as the Gum molecules approach the membrane, they experience an opposing electrostatic double layer repulsive force. This opposes the convective motion which is drawing the particles towards the membrane. The use of crossflow velocity and turbulent flow further complicates all of the forces competing on the Gum molecules as they approach the membrane surface. Electrostatic forces between the Gum and membrane are of great importance, as if these are large enough they can lead to reduced fouling. The electrostatic forces between the membrane and Gum have been simulated through the use of a colloidal probe, allowing quantification of the electrostatic interactions as a function of separation distance. Figure 5.20 shows a typical force curve of the

attraction and retraction of the colloid probe to the membrane surface. Adhesion can be influenced by the electrostatic double layer repulsion between negatively charged membrane and silica tip, and also short range repulsive interactions associated with silica.

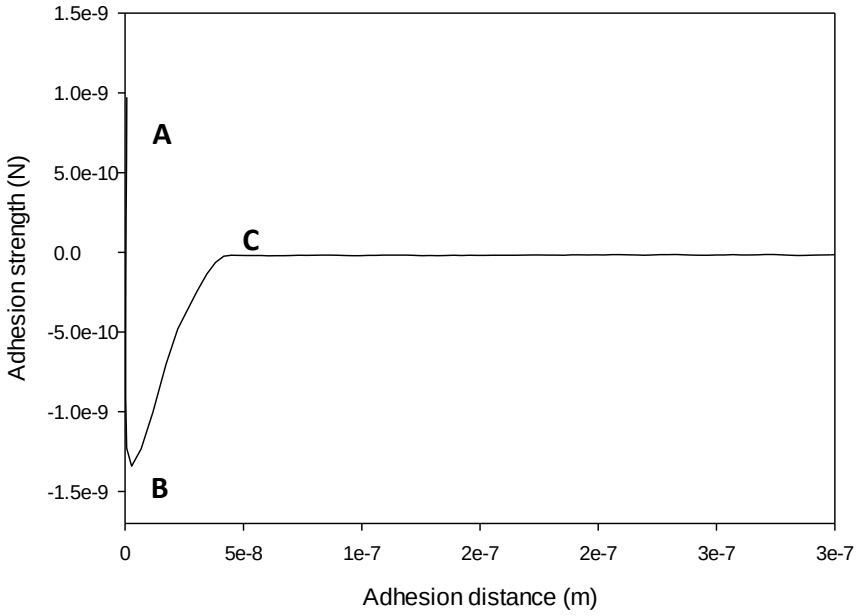

Figure 5.20: Typical force curve obtained for adhesion giving the adhesion strength and distance. At point A the membrane and probe were in contact, and at point C the membrane and probe were separated. Point B allows quantification of the adhesion forces by the difference between B and C, and the distance at point C shows the distance over which the adhesion forces are active.

The average adhesion distance and strength for a virgin membrane and a membrane fouled with Gum Arabic were investigated. The adhesion was measured for 10 different points on the membrane and the average values are reported in Table 5.9. It can be seen that following fouling the adhesion distance remains similar, however the adhesion strength is almost doubled. This suggests that the foulants interact differently with the colloid probe than the membrane surface does.

Table 5.9: Adhesion distance and strength between virgin/fouled membranes and colloidal probe.

Membrane	Adhesion distance (nm)	Adhesion strength (pN)
Virgin	31.8 ± 7.6	690 ± 240
Fouled	36.8 ± 10	1130 ± 330

While the adhesion strength shows that the interactions between the virgin membrane and probe are weaker than the interactions between the probe and the foulant, it does not give much detail about these interactions. Figure 5.21 shows the retraction force curve for both the virgin membrane and fouled membrane. As discussed in Section 4.2.2.6 the virgin membrane shows two distinct types of interaction, whereas the fouled membrane only shows one type of interaction. Based on the results obtained previously in this chapter, such as the zeta potential results in Section 5.3.3.2, it is expected that hydrogen bonding is occurring between the carboxylate groups in the Gum and the silica probe. The reduced adhesion observed for the virgin membrane could be as a result of the larger zeta potential. A more negative zeta potential would be expected to result in a greater repulsive force leading to a reduction in the adhesion through electrostatic double later interactions. Alternatively adhesion may occur between calcium cations present in the foulant layer and the colloid probe.

Interestingly the adhesion distance between the surface and the probe is ca. 37 nm. Mahendran reported that the AGP in Gum forms a compact conformation ca. 36 nm in diameter,[23] and Sanchez reported that Gum Arabic particles have a width of 20 – 30 nm.[40]

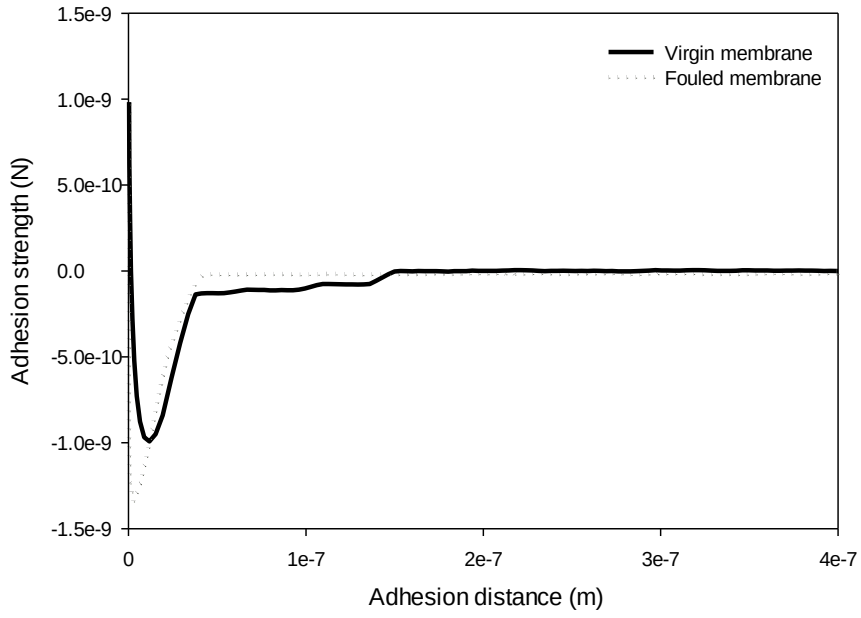

Figure 5.21: Adhesion curve for the retraction of silica probe from membrane before and after fouling with Gum Arabic.

As the probe approaches the surface, an insight into attractive forces can be gained. If attractive forces are present which are stronger than the rate of approach the probe may 'snap in' to contact with the surface. This is represented by a change in the adhesion strength for the approach. As shown in Figure 5.22 this did not occur during the approach of the tip to the virgin membrane, but it was observed with the fouled sample. For the virgin membrane, repulsive forces are seen to occur when the probe is ca. 20 nm from the membrane surface. These repulsive forces are due to the electrostatic double layer of the membrane with slight repulsion at ca. 20 nm and increased repulsion as the tip approaches the surface. For the fouled sample there is an initial slight repulsion at ca. 20 nm from the membrane surface followed by an attractive force of ca. 320 pN ca. 11 nm from the surface, and ca. 260 pN ca. 5 nm from the surface. Repulsive forces then dominate as the probe reaches the surface. The attraction is expected to be caused by calcium cations present in the foulant interacting with the OH groups on the surface of the probe. These results agree with the observed zeta potential results in Section 5.3.3.2 where the ZP showed a large reduction following fouling.

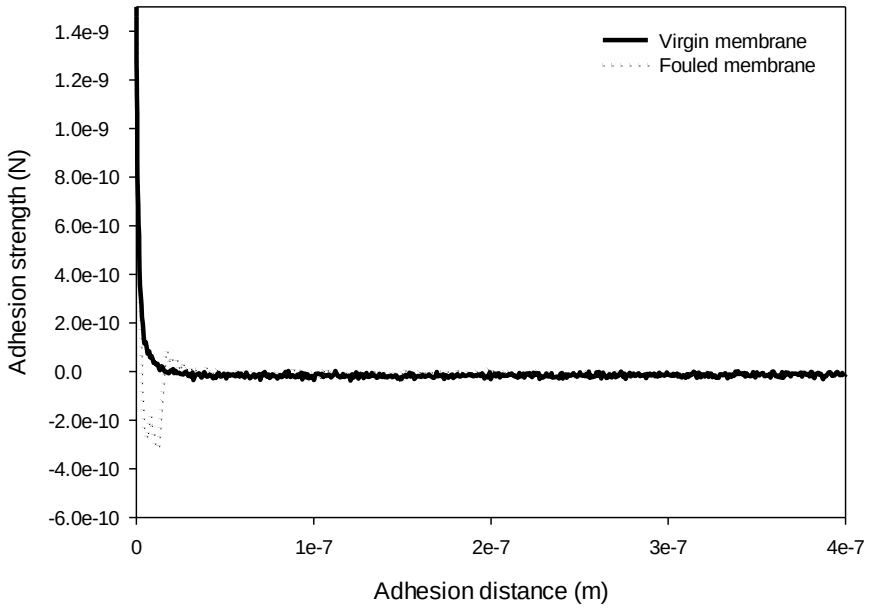

Figure 5.22: Adhesion curve for the approach of silica probe to the membrane before and after fouling.

5.6 Discussion

This section has examined the influence of operating conditions on the permeate flux and separation of Gum Arabic from model waste streams. Gum has been shown to adsorb rapidly onto alumina membranes. In terms of the optimum processing parameters, operating at a high cross-flow velocity and low transmembrane pressure shows advantages in terms of the permeate flux, with a larger throughput being obtained. In addition, operating at a reduced TMP allows greater rejection of Gum as well as a lower energy requirement. Above 3.0 bar the system is no longer pressure controlled, but becomes mass transfer controlled with a limiting flux ca. 142 L m^{-2} h^{-1} for a 0.8 µm tubular ceramic membrane. For this reason studies have been carried out using a CFV of 2.3 m s^{-1} and a TMP of 1.5 bar. This is the greatest crossflow velocity and lowest TMP which can be sustained using the rig set up available.

Investigating the membrane material properties allows an insight into the fouling process with a steady state flux of 2150 ± 150 L m^{-2} h^{-1} for flat sheet ceramic membranes independent of pore size between 0.2 and 2.0 µm. The tubular ceramic membranes showed a steady state flux of 115 ± 1 L m^{-2} h^{-1} for 0.5 and 0.8 µm membranes, whereas a flux ca. 71 L m^{-2} h^{-1} was obtained following filtration through a 0.2 µm membrane. While the flux was higher for flat sheet membranes, the rejection was consistent with pore size for both systems. This suggests that the pore size is not the limiting factor for the flux, but it does affect the rejection coefficient. Using a 0.2 µm membrane resulted in 90 % rejection after 1 cycle (R_a = 0.9), whereas a 2.0 µm membrane only resulted in 30 % rejection (R_a = 0.3).

AFM was used to characterise the flat sheet ceramic membranes and it was shown that the flat sheet membranes have a large roughness, it is expected this is due to the sintering process used to make them. Following fouling there was no significant change to the roughness suggesting that adhesion occurs to form a layer on the surface rather than aggregates being caught in the valleys and resulting in the growth of a foulant layer.

Pre-filtration had a small effect on the initial flux leading to greater pore constriction over the first five minutes. However, after ca. twelve minutes the same steady state flux was obtained regardless of pre-filtration. This suggests there are no advantages of pre-filtering the Gum with fouling being inevitable.

It has been hypothesised that the foulant is present as a cake or gel layer on the membrane surface. This hypothesis was shown to hold true with:

i) Modelling using Hermia and Field laws showing that over the first 5 minutes either pore constriction, cake filtration or a combination of both would occur. Following this cake filtration dominated from 5 – 60 minutes. This trend was shown for each of the processing conditions investigated.

ii) The use of SEM analysis showed the clear formation of a cake layer on the membrane surface, whereas the cross section showed little in pore fouling.

iii) Porisometry data showed no significant change in the porosity of the membranes following fouling. This suggests that there was no significant in-pore fouling.

Based on the characteristics of Gum it is expected that the foulant layer has gel-like properties. The gelling properties of Gum allow it to have a range of uses industrially. Gum has been shown to form a hydro-gel through weak physical interactions such as hydrogen bonds and hydrophobic associations.[230] In addition, the complexation between Ca^{2+} and Gum can lead to a highly cross linked structure resulting in gel-like properties. The layer of foulant on the membrane is too thin to confirm that it is a gel layer rather than cake layer. However, based on the properties of Gum, it is expected that the foulant is a gel or viscous liquid of highly concentrated Gum.

The surface layer was characterised to identify the main foulants and determine a mechanism of attachment of the foulant to the surface. The use of FTIR and SEM-EDX showed that the foulant was mainly organic based, however calcium was also present in the foulant layer. These foulants are expected as Gum is 90 % polysaccharide based (arabinogalactan), with small amounts of glycoprotein and metal salts such as calcium present. The presence of calcium can result in the formation of intermolecular bridging between the calcium and carboxylic groups, leading to a highly compact cross-linked structure.

The use of zeta potential analysis showed that the membrane had a strong negative charge, this is also reported for Gum therefore charge repulsion would be expected. Following fouling the membrane showed very little charge, suggesting the adhesion of positively charged foulants to the membrane surface. Calcium ions are likely to be responsible for some of this reduction in charge as they can reduce the negative charge. The fouled membrane trace is typical of organic foulants so the organic components of the Gum are expected to be playing a role too. The large change in zeta potential following fouling suggests that charge repulsion is not the dominant force at the surface and bonding such as hydrogen bonding may play a strong role.

After formation of a fouling layer, charge repulsions between the adsorbed Gum and the Gum in suspension play a key role in separation properties. The retention is shown to increase following

the formation of a stable layer of Gum adsorbed to the surface this is discussed further in Chapter 7.

Both membrane-foulant and foulant-foulant interactions play a significant role in membrane fouling. In the initial stages of fouling the membrane-foulant interactions are dominant, and result in a rapid flux decline. Following the initial deposition of a foulant layer onto the membrane surface, the foulant-foulant interactions become dominant. This phenomena was also observed by a number of other authors when investigating membrane fouling on ceramic membranes.[203]

Following fouling the membranes become more hydrophobic, suggesting the adhesion of hydrophobic foulants. The protein backbone of Gum and the terminal rhamnose groups have been reported previously to have hydrophobic characteristics. The increase in contact angle suggests these have a role to play in the foulant layer. This fits with the proposal made by Zhang *et al.* who suggested that Gum adsorbs onto alumina through the AGP fraction.[223]

The adhesion is altered following fouling, with a greater adhesion strength between the fouled membrane and colloidal probe than that of the virgin membrane. The colloidal probe has similar OH surface groups to the alumina membrane and this increased adhesion is likely to be representative of the adhesion between the Gum and the membrane. This is suggested by strong interactions between the Gum and membrane over ca. 37 nm.

During the approach of the colloidal probe to the foulant layer attraction was observed at ca. 11 nm and ca. 5 nm from the membrane surface. This suggests that the presence of calcium influences the attraction between Gum and the membrane surface leading to interactions between calcium and the OH groups on the membrane surface.

5.7 Summary

While removal of Gum can be achieved, fouling is a major limitation with deposition of Gum on the membrane surface limiting mass transfer. The membrane pore size can influence the rejection with tighter pore sizes leading to increased separation without compromising the throughput when flat sheet alumina membranes are used.

Significant work was carried out into the fouling to understand the processes which can minimise fouling. Strong chemical interactions are occurring between the hydroxyl groups on the alumina surface and carboxyl and hydroxyl groups on the Gum. Additionally the presence of calcium in the

Gum results in the formation of ion bridges between the Gum and membrane increasing the strength of the deposit. Operation at low TMP and high CFV helps to minimise foulant growth on the membrane surface.

6. Cleaning of membranes fouled with Gum Arabic

In Chapter 5 the influence of a wide range of conditions and their impact on the fouling of Gum Arabic on alumina ceramic membranes was investigated. The level of fouling can be reduced by operating under optimum conditions, however as fouling cannot be mitigated there is therefore the requirement to clean membranes. This chapter investigates a range of cleaning agents and cleaning conditions in order to maximise the foulant removal. One method to remove foulants is through trial and error of different cleaning agents, while this can be successful a more scientific approach is to try to understand how and why different cleaning agents work. A number of cleaning agents were investigated. Detailed studies were carried out with a small number of cleaning agents to identify the interactions and surface chemistry occurring in order to maximise removal of the Gum and understand the surface interactions.

There are a number of different methods available for cleaning, mainly either hydraulic (e.g. scraping the surface) or chemical. The choice of cleaning method used depends on:

1) Module configuration e.g. can the membranes be accessed to undergo mechanical cleaning
2) Chemical and physical resistance of the membrane
3) Nature and degree of fouling

Industrially chemical cleaning is most commonly used. While cleaning in place (CIP) is common, it is not generally selected based on knowledge of the cleaning mechanism and kinetics, but rather involves wastefully excessive procedures which are known to work from previous experience.[125] There has been little published about chemical cleaning due to the lack in fundamental knowledge of the cleaning phenomena (such as mass transfer and reactions).[134]

There are three main ways in which cleaning agents can affect the foulant material:[185]

1) Foulants are removed
2) Morphology of the foulants is changed (through swelling or compaction)
3) Surface chemistry of the deposit is altered (e.g. hydrophobicity or charge modified)

The cleaning of membranes is just as important as the fouling behaviour. The ability to restore the membrane to a consistent condition after filtration means it performs in a predictable manner. It is not always necessary to return the membrane to its virgin condition as the surface is usually

irreversibly modified when using real feeds. The resistance in series approach is often used when looking at fouling and cleaning.

The cleaning efficiency has been calculated using the flux recovery (FR) which is often used as a benchmark in determining the cleaning efficiency. The flux recovery is a ratio of the flux following cleaning (J_C) to the pure water flux measured under the same conditions (J_W). The percentage flux recovery ($\%\ J_r$) has been defined as:[175]

$$\%\ J_r = \left(\frac{J_C}{J_W}\right)\ x\ 100 \qquad \text{Equation 6.1}$$

Where the flux was measured using water at 40 ^{o}C with a TMP of 1.5 bar and CFV 2.3 m s^{-1}.

This chapter aims to show that:

- The choice of cleaning agent can have a significant impact on the flux recovery.
- The mechanism of cleaning, and the foulants removed depends on the cleaning agent used.
- Cleaning agents can affect the properties of foulants which remain on the surface following cleaning.

6.1 Cleaning conditions

While it has been reported that cleaning with a zero TMP is more efficient that cleaning with a positive TMP,[231] no cleaning data throughout the cleaning cycle can be measured. More information can be gained about the cleaning mechanisms by using a positive TMP. In addition, in many applications the whole system is required to be sanitised and cleaned in one stage, meaning that running with a positive TMP allows through membrane and permeate line cleaning to occur *in-situ*.

6.2 Rinsing with water

Initial studies were carried out by rinsing the membrane with water to investigate the removal of foulant from the membrane surface. Cleaning was carried out at high CFV to maximise shear forces on the membrane surface. Bird and Bartlett showed during the filtration of milk protein isolate that the highest flux recovery was observed at high crossflow velocities and low TMP.[175]

Rinsing is used to remove as much foulant as possible before the inclusion of chemical cleaning agents into the system as it reduces the requirement for chemicals. If there is still a high degree of foulants in the system when the cleaning agent is added, it may be consumed in the bulk and will not be available for cleaning.[232] Rinsing was carried out for 15 minutes, this was sufficient for the complete replacement of Gum (or cleaning agents) from the system as the dead volume was filled with water in 20 seconds. The additional time was selected to allow the removal of loosely bound deposits on the membrane surface and subsequent removal from the system, and to comply with industrial standards.[149]

Figure 4.19 showed that following rinsing with water there was ca. 33 % reduction in the resistance due to fouling. This suggests that while some foulant is removed from the membrane leading to a reduction in the total resistance, a considerable amount of fouling remained which could not be removed by rinsing with water alone. This indicates the deposits had a low solubility and could not be removed by shear stress alone. FTIR analysis was carried out to identify if there were particular foulants removed and the spectra can be seen in Figure 6.1. While rinsing allowed a reduction in the total resistance, the FTIR spectra shows the presence of each of the peaks present in Gum on both the fouled and rinsed membranes. There is an increase in the relative intensity of the peak at 975 cm^{-1} attributed to the rocking vibration of CH_3 as a methyl substitution on a carboxylate group. This suggests that some components may be removed more easily than others, however there is not any conclusive evidence of a particular chemical group being completely removed, or removed more easily than other groups. This suggests that there is not one particular component of the Gum removed through rinsing with water, but rather the composition shows little change.

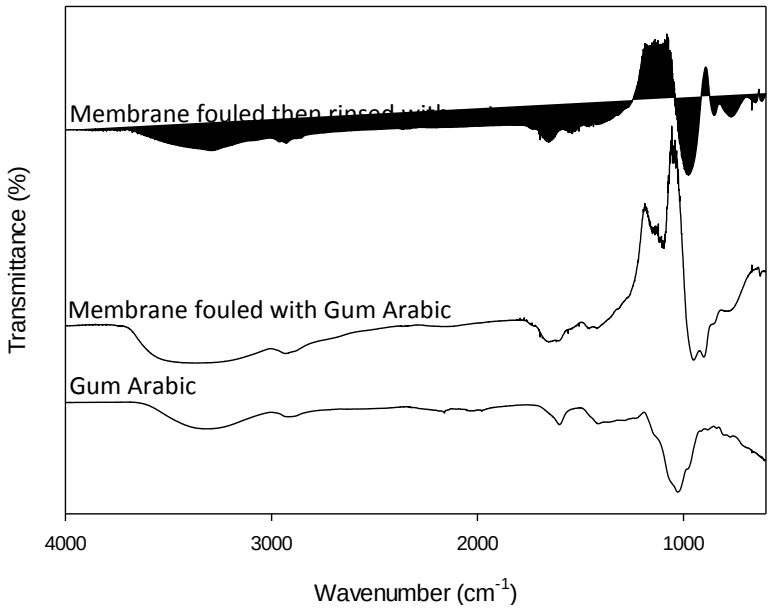

Figure 6.1: FTIR trace of Gum Arabic (bottom), membrane fouled with Gum Arabic (middle) and membrane which had been fouled with Gum Arabic followed by rinsing with water. The virgin membrane has been subtracted from each trace to allow a clear comparison of the foulants.

Foulants which were removed during rinsing were most likely due to reversibly adsorbed foulants, which are released during rinsing or diffusion from the gel/cake fouling layer. Rinsing with water was also shown to be ineffective at restoring the membrane to pristine condition by Blainpain-Avet *et al.* who reported a 48 ± 11 % reduction in the hydraulic resistance following rinsing of a ceramic microfiltration membrane fouled with whey protein.[134]

6.3 Chemical cleaning

Most of the fouling of the membrane was found to be irreversible, meaning it cannot be removed by rinsing with water alone. There are however a number of chemical and hydraulic methods available to remove the irreversible fouling from the membrane. Chemical cleaning was investigated using sodium hydroxide (NaOH), sodium hypochlorite (NaOCl) and citric acid ($C_6H_8O_7$). These chemicals were chosen as they are compatible with the food industry standards and regulations, where Gum is mainly used. In addition Ultrasil 11 was investigated. This is a commercial cleaning agent composed mainly of sodium hydroxide, but with the addition of surfactants and EDTA which acts as a complexing agent.

Generally in chemical cleaning the adhesive bonds between the foulant and membrane are weakened or broken. The scouring action of crossflow can be used to complete the removal.

6.3.1 Sodium hydroxide

Sodium hydroxide (NaOH) is not a surface active cleaning agent, however it has high levels of detergency. Gum Arabic is soluble in low concentrations of sodium hydroxide, however it is insoluble in concentrated solutions.[5] Sodium hydroxide was selected as a cleaning agent due to its ability to hydrolyse proteins and protein complexes (peptidization).[23, 134] While it has been shown that sodium hydroxide leads to hydrolysis of peptides, Mahendran *et al.* showed that the carbohydrate fraction of Gum Arabic is not broken down by sodium hydroxide.[23]

It was hypothesised that using low concentrations of sodium hydroxide may lead to peptide bond hydrolysis, swelling and dissolution leading to increased removal of deposits from the membrane surface and pores.[125, 174] Initial studies showed that sodium hydroxide lead to the removal of some of the Gum with a 0.5 wt. % suspension, leading to a flux recovery of ca. 30 ± 7 % (Figure 6.2). The concentration of 0.5 wt. % was selected to be the same as that defined by Bird and Bartlett.[116] An initial rapid increase in flux (thus reduction in membrane resistance) was observed when sodium hydroxide was added as a cleaning agent (Figure 6.4). Following the initial rapid increase, the flux increase slowed down. This suggests that initial removal or changes in the foulant morphology occur quickly, this has also been observed by a number of authors investigating cleaning in a variety of systems.[125, 134, 174] Repeated cycles were carried out to observe any long term flux decline; this is discussed further in Chapter 7. Further studies were carried out to understand the interactions between the foulant and sodium hydroxide, and are detailed later in this chapter.

Gum Arabic, and in particular the AG fraction, has previously been shown to be very stable across a wide pH range, with enzyme hydrolysis being unable to break it down.[22] This may be why the FR was only 30 ± 7 %, as the Gum is resistant to hydrolysis.

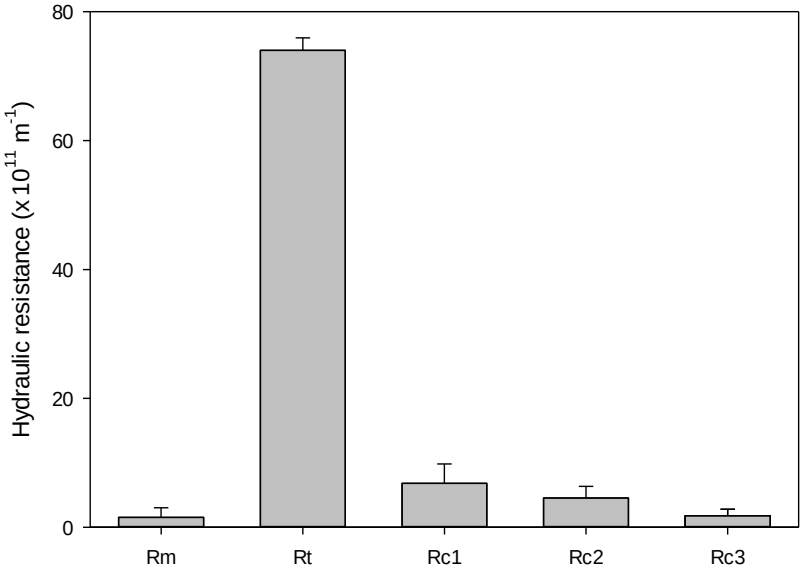

Figure 6.2: Hydraulic resistance of 0.8 µm tubular ceramic membrane cleaned with 0.5 wt. % NaOH only (C1), 0.5 wt. % NaOH + 200 ppm NaOCl (C2) and C2 followed by cleaning with 0.1 wt. % $C_6H_8O_7$ (C3). Resistances are for cleaning of the first cycle for a virgin membrane.

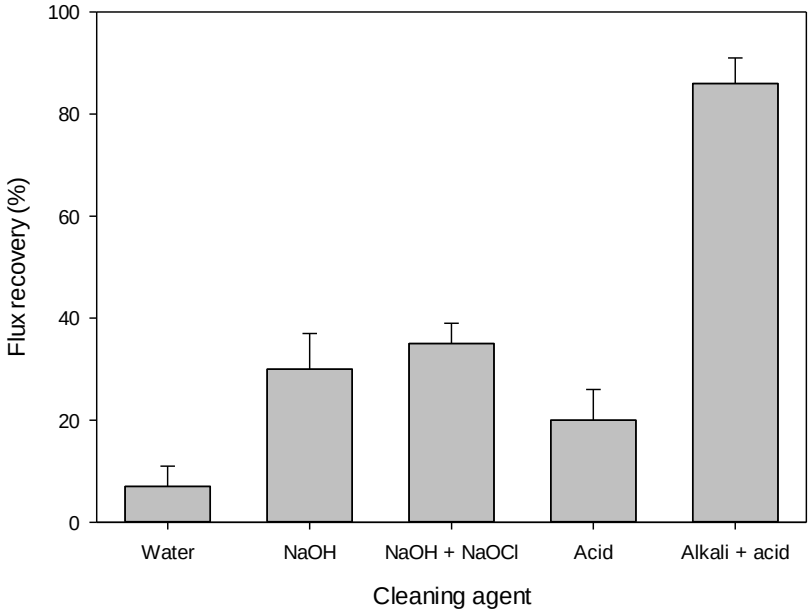

Figure 6.3: Flux recovery of 0.8 µm tubular ceramic membrane fouled with 2.0 wt. % Gum Arabic and cleaned using water, 0.5 wt. % sodium hydroxide, 0.5 wt. % sodium hydroxide + 200 ppm sodium hypochlorite, 0.1 wt. % citric acid, and 0.5 wt. % sodium hydroxide + 200 ppm sodium hypochlorite followed by 0.1 wt. % citric acid. Cleaning was carried out at 60 ^{o}C.

6.3.2 Sodium hypochlorite

Sodium hypochlorite (NaOCl) is an oxidising agent and has previously been shown to be effective for membrane cleaning.[131] The addition of NaOCl to cleaning solutions acts as a sanitizer even at low concentrations.[233] The addition of NaOCl is useful in maintaining good hygiene standards industrially. 200 ppm NaOCl was added to a 0.5 wt. % NaOH cleaning solution following the observations of Gan *et al.* who observed during cleaning following filtration of rough beer, that combining NaOH and NaOCl as cleaning agents was more effective than running in two stages.[234] The use of combined cleaning has the additional benefit of a reduction in the water requirement for dissolution and rinsing the system following cleaning.

Figure 6.2 shows that the membrane resistance is reduced, producing a FR of 35 ± 6 % compared to 30 ± 7 % for cleaning with sodium hydroxide alone. While this increase is small, it was observed consistently and is statistically significant ($P < 0.05$). The oxidising characteristics of NaOCl allow species to be oxidised and removed from the membrane surface.

In addition to the increased FR, observing the resistance during cleaning led to a marked increase in initial cleaning rate for an aged membrane. The flux increased more rapidly with the addition of NaOCl as shown in Figure 6.4. The rapid increase in flux recovery could mean there is the potential for shorter cleaning cycles, which would reduce costs and increase the efficiency industrially.

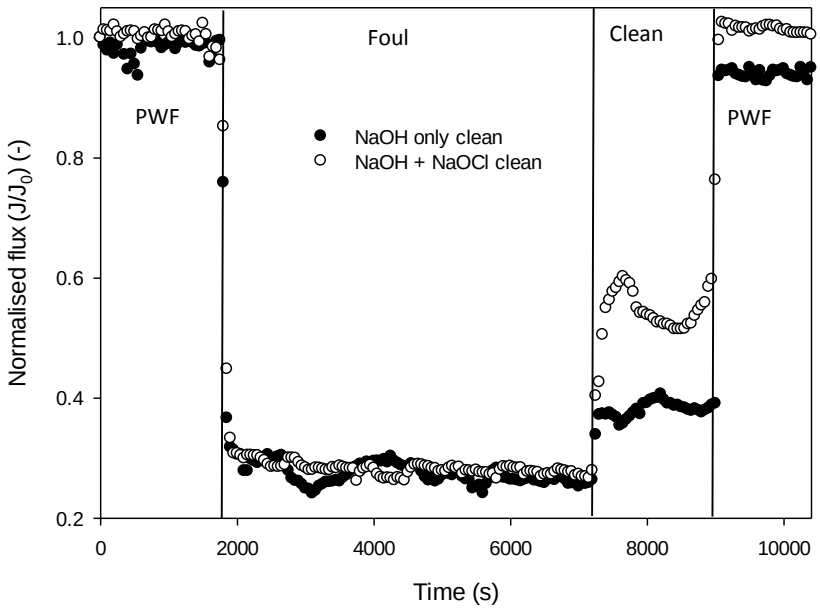

Figure 6.4: Influence of the addition of NaOCl to NaOH on the cleaning of an aged membrane fouled with Gum Arabic. PWF was measured and 2.0 wt. % Gum Arabic used to foul the membrane for 90 minutes prior to cleaning. The 2 cleaning regimes; 0.5 wt. % NaOH only and 0.5 wt. % NaOH + 200 ppm NaOCl, were conducted under standard conditions (60 ^{o}C, TMP 1.5 bar and CFV 2.3 m s^{-1}) and the final PWF measured.

6.3.2.1 Concentration of NaOCl

As NaOCl is an oxidising agent it is used up as it oxidises the foulant. For this reason a study was carried out to determine the concentration of sodium hypochlorite required for the removal of Gum. Four different concentrations were added to 0.5 wt. % NaOH and their cleaning performance investigated. Figure 6.5 shows the optimum concentration was 200 ppm with an increase to 300 ppm showing no further improvement in the membrane performance.

Cheryan suggests 1000 – 2000 ppm NaOCl is effective for cleaning,[60] however these results suggest that for fouling with a low concentration of Gum Arabic, lower concentrations can provide effective results. This has economic benefits and also reduces the risk of corrosion. NaOCl is used up as it is oxidised therefore if fouling is severe it may be used up during the process and a higher concentration will be required.

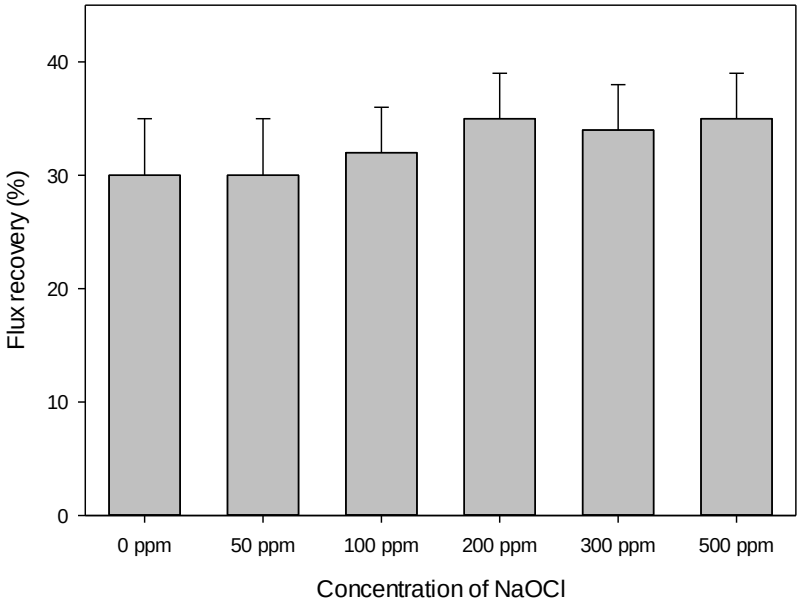

Figure 6.5: Influence of the addition of NaOCl to 0.5 wt. % NaOH on the flux recovery of a 0.8 µm tubular ceramic membrane.

6.3.3 Citric acid

Citric acid ($C_6H_8O_7$) was also investigated as a cleaning agent. Acids are known to dissolve minerals precipitated on the membrane surface. Gum Arabic is known to be a hydrocolloid containing arabinoglactan, protein and minerals. Minerals are adsorbed faster onto the membrane surface than proteins,[131] and the presence of calcium on the membrane surface was shown in Section 5.5.2.3. In other hydrocolloidal systems such as milk, an alkali wash to remove proteins followed by an acid wash to remove any minerals has been shown to be an effective cleaning method.[131, 234] This two stage cleaning method was studied for a membrane fouled with Gum Arabic. Following cleaning with NaOH + NaOCl the membrane was rinsed, and 0.1 wt. % citric acid used for the second stage of cleaning. During the two stage clean the membrane resistance was shown to decrease, leading to a FR of 86 ± 5 %. This can be compared to a 20 ± 6 % FR observed when citric acid was used as a cleaning agent alone.

While a good FR was observed for the two stage cleaning cycle, there remains some irreversible fouling on the membrane surface. It is important to establish what is happening during the cleaning. Cheryan reported that inorganic membranes show a higher water flux when an acid rinse is used after cleaning.[60] This may have a role to play in the increased flux recovery.

Due to the low mineral content of Gum Arabic, it is expected that removal of minerals alone is not fully responsible for the decrease in the membrane resistance following an acid clean. There are a number of other factors which also need to be considered:

i) During the alkali clean, sodium ions may be exchanged from the sodium hydroxide onto the membrane surface, or within the Gum. The ion exchange between hydrogen and sodium would result in the formation of water in solution and sodium enriched Gum. Citric acid is a complexing agent and therefore removes the sodium ions from the Gum leading to the formation of sodium citrate and changes in the chemistry and possibly the conformation of the Gum. This is discussed further in Section 6.6.4.
ii) Panda reported that Gum Arabic is hydrolysed in weak acids.[5] It is therefore possible that the acid may be hydrolysing the Gum in addition to complexing any minerals present.
iii) Acids e.g. citric acid can lead to an increase in the hydrophilicity of the membrane surface causing an increase in the membrane flux. This is investigated further in Chapter 8.
iv) Partially hydrolysed proteinacious deposits produced during the alkali clean may form a shrunken morphology with a smaller voidage.

It is most likely that the increase in flux is caused by a combination of factors i and ii. The rest of this chapter explores these and gives reasoning for this proposition. While the hydrophilicity of the membrane may be increased by the presence of acids, a flux recovery ca. 86 % suggests there is still significant fouling on the membrane surface, or in pores. It is therefore unlikely that a large enough proportion of the membrane surface is available for noticeable changes in the hydrophobicity of the membrane to result in an increased flux. While iv cannot be discounted as it was shown to be important by Blainpain-avet *et al.* for whey proteins,[134] no studies have yet been carried out which show changes to the morphology of Gum at low pHs.

6.3.4 Ultrasil

Ultrasil 11 is a commercial cleaning agent containing sodium hydroxide, surfactants and EDTA. Based on the foulant material containing organic foulants and calcium shown in Chapter 5, the use of Ultrasil 11 was investigated as a one stage cleaner. It was hypothesised that sodium hydroxide may hydrolyse the organic foulant while EDTA leads to the removal of calcium through complexation.

Following cleaning with Ultrasil 11 a flux recovery of 50 ± 6 % was achieved. This recovery is superior to that of cleaning with NaOH/NaOCl alone, however is not as great as that of a membrane cleaned with citric acid following an alkali clean. This suggests factors such as the pH of citric acid are playing a role in the removal of foulants as well as the chelating action.

6.4 Mechanical cleaning

Mechanical cleaning offers an alternative method to chemical cleaning. It can be used in addition to or instead of chemical cleaning. In this study mechanical cleaning was carried out both in water, and in alkaline cleaning solutions to show the effect both of the mechanical clean and a combined clean. For mechanical cleaning the set up and geometry of the membrane and module are important considerations as these determine whether mechanical cleaning is possible. For these reasons flat sheet membranes were used to study the mechanical cleaning as this is much simpler to implement and study than the mechanical cleaning of tubular ceramics.

6.4.1 Backwashing

Backwashing has been shown by a number of authors to increase the cleaning efficiency for membranes fouled by cake filtration. Reversing the flow allows the largest pressure and concentration of cleaning agents to contact the surface between the membrane and foulants. In order to simulate backwashing, a flat sheet membrane was fouled, and then placed upside down in the rig to allow the flow of cleaning agents in the reverse direction.

Figure 6.6 shows that backflushing with water lead to a flux recovery of 6 ± 6 % compared to 5 ± 6 % when rinsed in the forward direction. While a slight increase is seen in the FR for backwashing it is not statistically significant ($P > 0.05$) and lies within the experimental error of the experiment. Comparing backflushing with alkali results in a FR of 12.5 ± 7 % compared with 26 ± 8 % for cleaning in the forward direction. This result is statistically significant ($P < 0.05$) showing that backflushing is less effective than cleaning in the forward direction when combined with chemical cleaning.

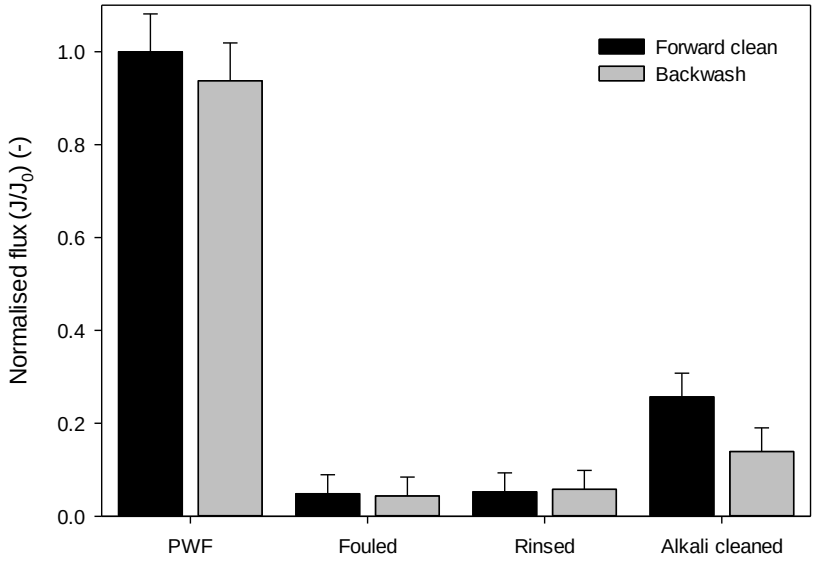

Figure 6.6: Permeate flux for 0.8 µm flat sheet ceramic virgin membrane, fouled membrane, rinsed membrane and alkali cleaned membrane following cleaning in the forward and reverse directions. This highlights that backwashing with alkali leads to a smaller recovery in the flux than cleaning in the forward direction.

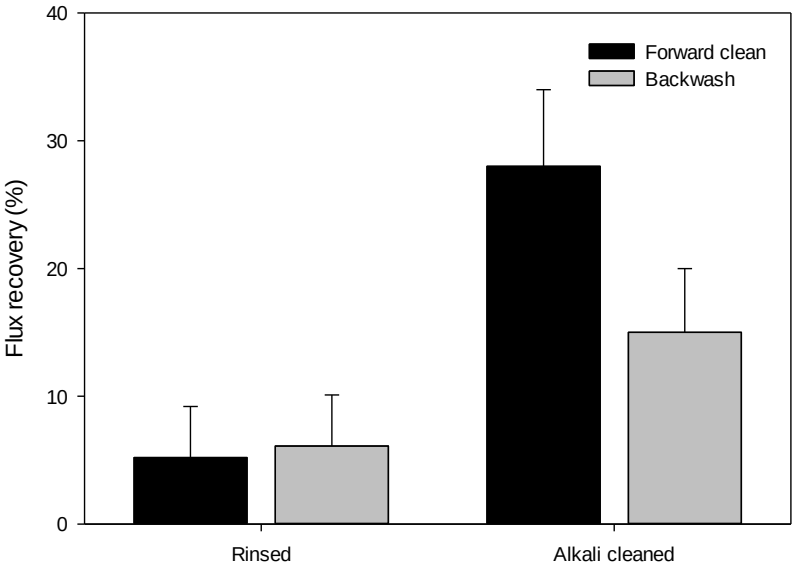

Figure 6.7: Flux recovery following fouling of a 0.8 µm flat sheet membrane with 0.2 wt. % Gum Arabic under standard conditions, followed by cleaning with water, and alkali (0.5 wt. % sodium hydroxide + 200 ppm sodium hypochlorite) at 40 ^{o}C in the forward and reverse directions.

While backwashing would be expected to increase the cleaning efficiency, there are a number of factors which may have resulted in the observed results. Backwashing has previously been shown to be effective in the removal of cake foulants. Its ineffectiveness suggests that as proposed in Chapter 5, the foulant layer may exist as a gel layer. The gel may be deformed rather than removed. Further evidence for the deformability of the layer is shown in Section 8.1.7. Strong hydrogen bonding could be responsible for holding the Gum molecules tightly together in a gel, or to the membrane surface therefore it is possible that these are not weakened during backwashing. Another possibility is that any foulants which are dissolved in the cleaning solution have to pass through this foulant layer making their removal more difficult than just simply dissolving or hydrolysing the foulants which are further from the membrane surface. If the foulants are strongly bound to the membrane surface, the chemical bonds between the surface of the membrane may not be affected by backflushing or the alkaline cleaning agents. Finally if the fouling layer is more compact at the membrane surface than layers above this, the cleaning agent may not be able to pass through as easily. This would result in the layer further from the surface being less accessible to the cleaning agents during backwashing. These foulants are more accessible to the cleaning agents during cleaning in the forward direction.

The reduced effect of backwashing compared with cleaning in the forward direction suggests foulants are strongly bound to the membrane. Foulant-foulant removal may be easier than membrane-foulant removal.

6.4.2 Sonication

Ultrasonic waves lead to the generation of acoustic streaming and cavitation bubbles in a liquid medium. It can lead to microstreaming, microjets and shockwaves leading to the sudden formation, growth and collapse of bubbles.[235] The sudden changes in bubbles can aid cleaning with higher frequencies of ultrasound having increased energy adsorption and leading to improved cleaning. Due to the tenacious deposits left following chemical cleaning or backflushing the use of sonication was investigated as a method achieve an increased flux recovery.

A 0.8 µm flat sheet ceramic membrane was fouled following the standard protocol, and the membrane rinsed before being removed from the filtration rig and placed in an ultrasonic bath containing 0.5 wt. % sodium hydroxide, and 200 ppm sodium hypochlorite at 60 ^{o}C. The ultrasound was switched on and the membrane left soaking in the cleaning solution for 20 minutes. Following cleaning, the membrane was rinsed and the PWF measured. A flux recovery

of 91 ± 5 % was achieved following ultrasonic cleaning. This is a significant improvement compared to the standard cleaning procedure (FR 35 ± 6 %). This is likely to be due to the increased energy input and the formation and collapse of bubbles. Sonication may also have resulted in depolymerisation due to glycosidic fission or disruption of physical aggregates.[236] This result suggests that the use of sonication is effective at removing most of the foulants from the membrane with a slight increase in membrane resistance compared to that of the virgin membrane. It has been reported previously by Lim and Bai that sonication is much more effective at removing cake deposition than pore blocking,[89] this supports this hypothesis that any foulants remaining are in pore.

6.4.3 Shear stress (FDG)

One important factor in the investigation of cleaning methods is determination of the shear stress required to remove the deposit from the surface. Fluid dynamic gauging (FDG) has traditionally been used for measuring the thickness of deposits, however with the foulant layer being measured as ca. 5 µm thick using SEM, this is below the measurable range of the FDG making it unsuitable for this application. Studies were carried out to investigate if significant swelling of the foulant occurred in the presence of sodium hydroxide however no results were obtained for this due to the thickness being below the detection limits of the instrument.

FDG can also be used to apply a known shear stress to a material thus allowing quantification of foulant removal through the application of different stresses followed by imaging the material. Due to the Gum being virtually colourless on the membrane the membrane was stained and imaged following the method described in Section 3.6.7. The colour was measured at 10 different points where stress was applied, and converted into CIE Lab colour space for analysis of lightness, redness and yellowness.[237] Lightness/colour has been plotted against shear stress and compared with that for no stress to show any variability.

Figure 6.8 shows the lightness for a membrane cleaned with water, and a membrane cleaned with alkali both at 60 ^{o}C. It can be observed that there is an increase in the lightness for each of the samples. For the membrane cleaned in water, an initial increase in the lightness is observed when 2 Pa stress is applied to the membrane, however no significant increase in the lightness is observed when stresses over 2 Pa are applied. As the lightness is one measure of foulant on the membrane surface, an increased lightness shows removal of the foulant. This suggests there is initial foulant removal with stresses of 2 Pa, without further improvement when the stress is increased. This

method does not allow the absolute foulant removal to be obtained, however alludes to the stresses required to remove the foulant. Comparing the removal of Gum at different stresses in the presence of NaOH shows a greater removal with the lightness showing an incremental increase from 56.3 ± 0.2 with no stress up to 59.6 ± 0.7 after the application of 50 Pa. Further increasing the stress from 50 to 300 Pa shows no further improvement in the lightness, suggesting no further removal of foulant.

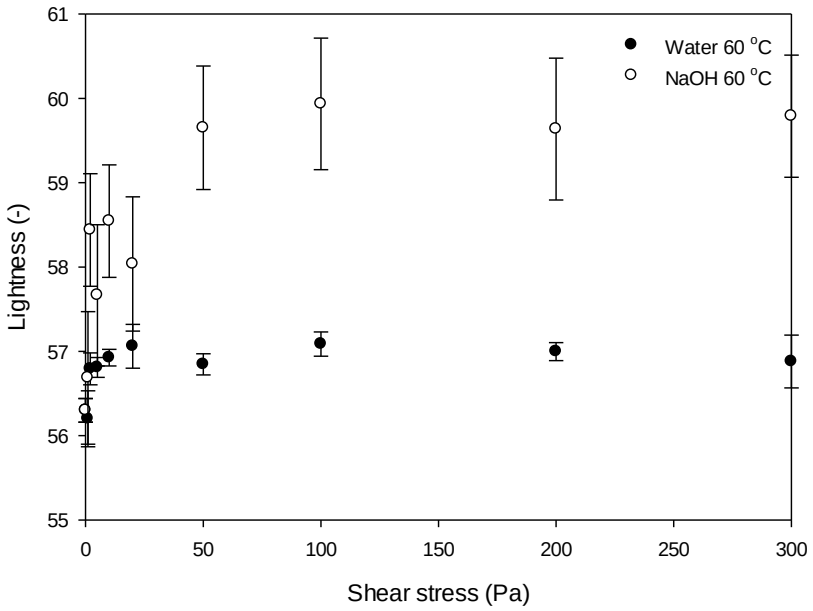

Figure 6.8: Lightness measurements of membrane fouled with Gum Arabic and subject to stresses of 0 – 300 Pa for 60 seconds in water and NaOH at 60 °C.

Lightness is only one parameter measured on the CIE Lab colour scale. The other two parameters are redness (or red-greenness) and yellowness (or yellow-blueness). A similar trend was observed for both of these parameters as shown in Figures 6.9 and 6.10. For the membrane cleaned with water, a shear stress of 200 Pa was required for a statistically significant ($P < 0.05$) change in the redness or yellowness of the membrane. This suggests that a stress of 200 Pa is required for any significant removal of the Gum from the membrane surface when using water as a cleaning agent. Increasing the stress to 300 Pa led to further reduction in the redness and yellowness suggesting increased Gum removal.

Comparing this with the NaOH clean, a shear stress of 1Pa leads to significant removal. A slight decrease in the redness is observed as the shear stress is increased further but little change in the yellowness. The significant reduction in redness and yellowness with a stress of 1 Pa suggests that the sodium hydroxide may remove Gum through a swelling mechanism.

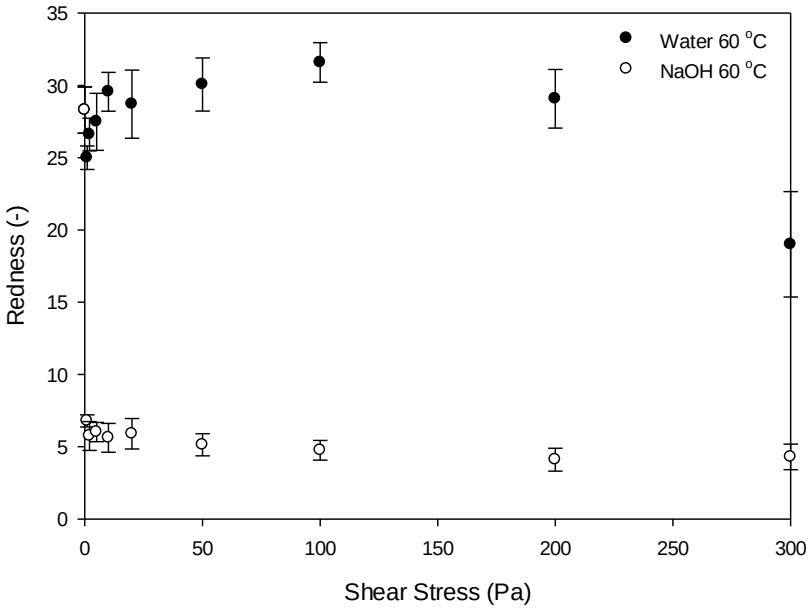

Figure 6.9: Redness measurements of membrane fouled with Gum Arabic and subject to stresses of 0 – 300 Pa for 60 seconds in water and NaOH at 60 °C.

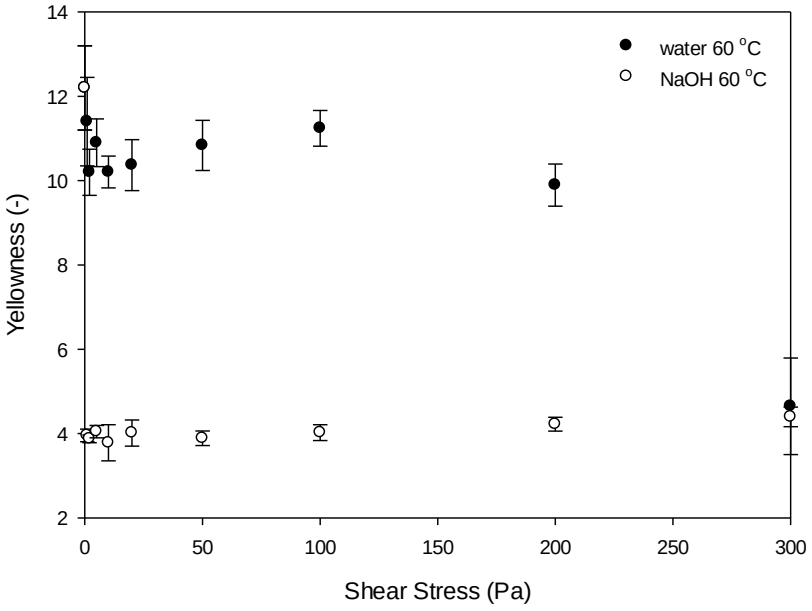

Figure 6.10: Yellowness measurements of membrane fouled with Gum Arabic and subject to stresses of 0 – 300 Pa for 60 seconds in water and NaOH at 60 °C.

In order to test if the Gum swells in 0.5 wt. % sodium hydroxide, a suspension containing ca. 50 wt. % Gum Arabic was produced. This viscous suspension was added to six test tubes, and water added to three of them, and 0.5 wt. % sodium hydroxide added to the other three. The

suspensions were studied over time to give a picture of what occurs and identify any differences between the two protocols. Figure 6.11 shows a series of photographs taken a) when the solutions were initially added, b) after 20 minutes and c) after 24 hours. It can be observed that slow dissolution occurs when water was added to the viscous Gum suspension. The result is somewhat different for the sodium hydroxide solution. It appears that the top layer of the Gum is swelling in the solution. This confirms the hypothesis above that sodium hydroxide leads to swelling of the Gum.

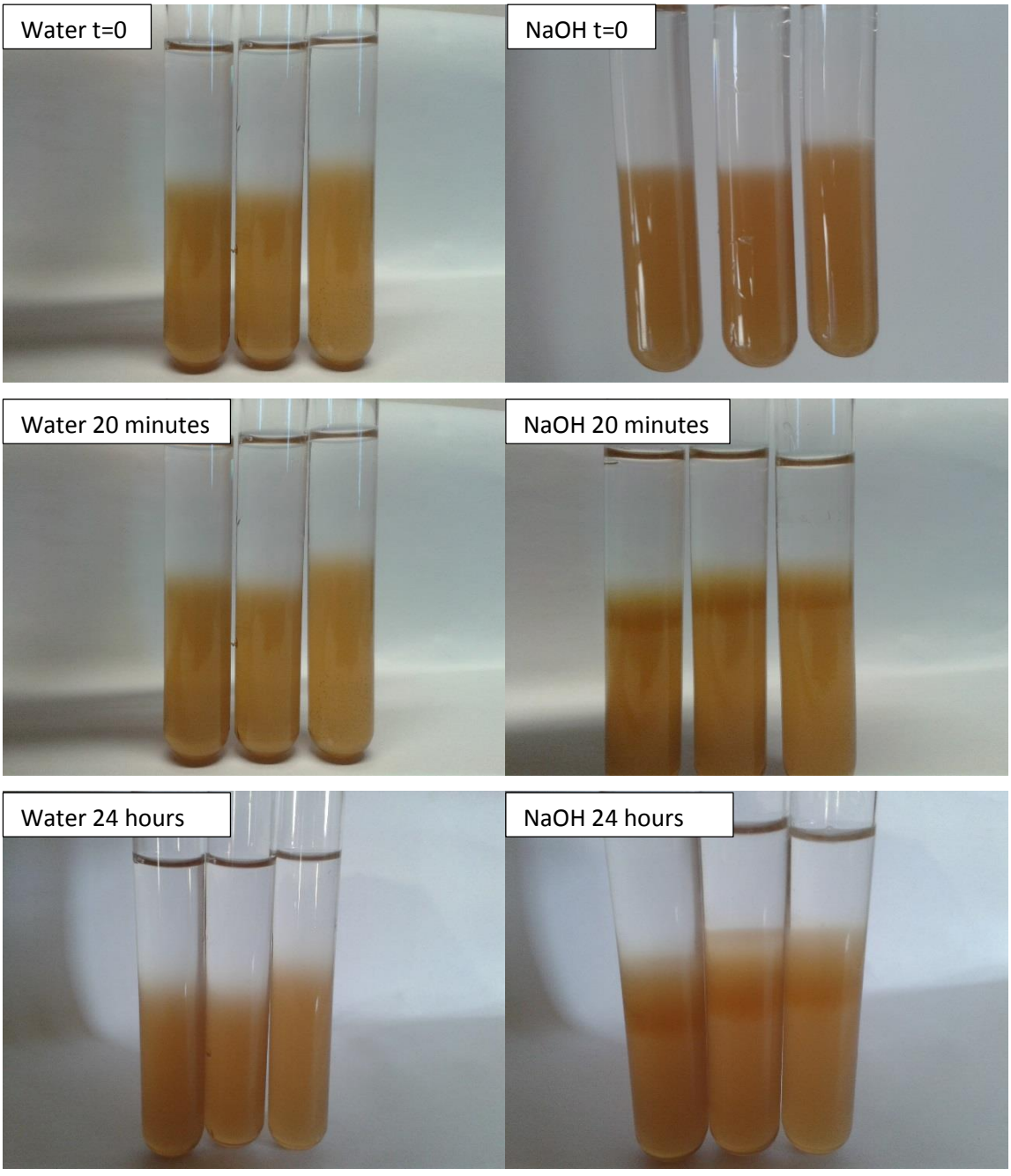

Figure 6.11: Influence of water and sodium hydroxide added to ca. 50 % Gum Arabic suspension. Times represent time after cleaning solutions are added to the viscous Gum suspension.

6.5 Cleaning temperature

The influence of temperature was measured on a two stage cleaning process, where stage one involved cleaning with 0.5 wt. % NaOH with 200 ppm NaOCl and stage two was cleaning with 0.1 wt. % citric acid. CFV and TMP were kept constant at 2.3 m s^{-1} and 1.5 bar respectively. An aged membrane was used to measure the influence of temperature, and to minimise any cycle variations as detailed in Chapter 7. Three cleaning temperatures were chosen: 40, 50 and 60 ^{o}C. These temperatures were chosen as many previous studies have found membrane cleaning to be optimised at 50 ^{o}C,[99, 149, 174] and many commercial cleaning agents (e.g. Ultrasil 11) recommend a maximum cleaning temperature of 60 ^{o}C. 40 ^{o}C was chosen as a lower temperature alternative as it requires less energy to operate at lower temperature. Figure 6.12 shows that the cleaning fluxes are largely influenced by the temperature with 60 ^{o}C allowing almost complete restoration of the membrane flux (FR 98 %), whereas cleaning at 40 and 50 ^{o}C show a reduction in efficiency with a flux recovery of 77% and 85 % respectively. The improvement in cleaning at increased temperature may be as a result of decreased viscosity or increased reaction rate of the cleaning solution. This corresponds with previous literature where decreasing viscosity and increasing reaction rates were found to be responsible for enhanced cleaning rates.[238]

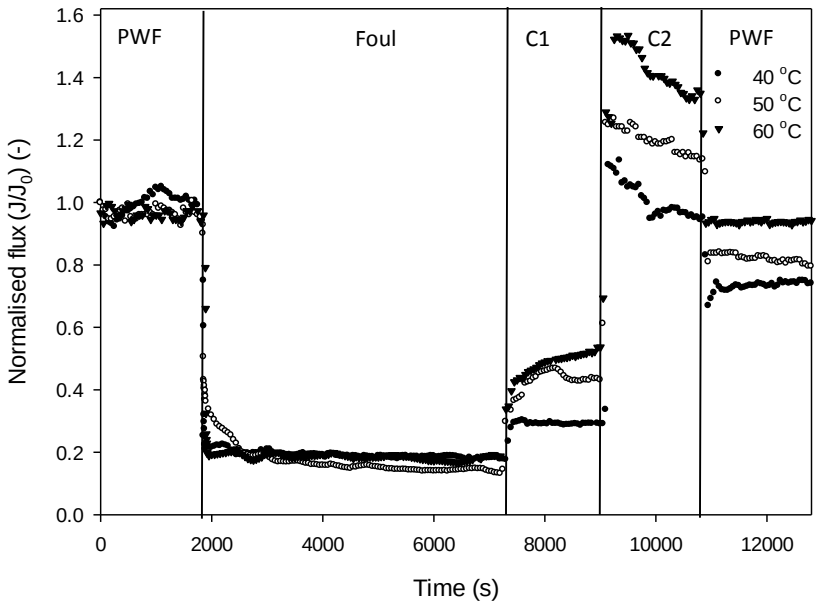

Figure 6.12: Comparison of cleaning temperature for 0.8 µm tubular ceramic membrane fouled with 2.0 wt. % Gum Arabic and cleaned using a two-step procedure of an alkali clean followed by an acid clean. Cleaning was carried out at 40, 50 and 60 °C. PWF and fouling were carried out at 40 ^{o}C. All measurements were carried out at TMP 1.5 bar and CFV 2.3 m s^{-1}.

6.6 Chemical analysis of cleaned membranes

In order to gain a better understanding about how each of the cleaning agents work, flat sheet membranes which have been subjected to fouling, followed by cleaning with the different cleaning agents were analysed. The use of a wide variety of techniques was investigated in order to obtain a picture of how the chemistry of the deposits was influenced by the cleaning agents, and to gain an insight into the possible cleaning mechanisms leading to foulant removal.

6.6.1 Effective contact angle

The contact angle gives an indication about the surface energy and hydrophobicity of the membrane. In Section 5.3.3.1 it was reported that the virgin membrane has an effective contact angle of 37 ± 6 °. Following one fouling cycle the membrane became more hydrophobic with the effective contact angle increasing to 104 ± 7 °. The effective contact angle was measured for membranes following cleaning and the average of 10 points taken. These values are reported in Table 6.1.

Table 6.1: Effective contact angle for 0.8 µm flat sheet membranes under different cleaning conditions. Measurements based on average of 10 points on the membrane.

Membrane	**Effective contact angle (°)**
Virgin	37 ± 6
Fouled	104 ± 7
Alkali cleaned	91 ± 6
Alkali + Acid cleaned	40 ± 9
Ultrasil 11 cleaned	52 ± 10
Alkali cleaned cycle 2 (F2C2)	117 ± 9
Alkali + Acid cleaned cycle 2 (F2C2*)	65 ± 8

Table 6.1 shows that the alkali cleaned membrane gives an effective contact angle between that of the fouled and virgin membrane suggesting that some of the foulants are removed, however a great deal of hydrophobic foulants remain following cleaning. In contrast to this, following alkali and acid cleaning the effective contact angle is very similar to that of the virgin membrane, suggesting that the acid clean can be used to remove the hydrophobic foulants from the membrane surface.

Cleaning with Ultrasil 11 resulted in an effective contact angle between that of the alkali, and alkali + acid cleaning methods. This shows that the addition of surfactants and EDTA helps with the removal of some of the hydrophobic foulants which cannot be removed by sodium hydroxide/ sodium hypochlorite alone. In addition the inclusion of EDTA can act as a complexing agent therefore allowing the removal of metal cations from the foulant.

Interestingly for the second cycle, alkali cleaning has a reduced effect on the foulant with the fouled membrane (F2) showing an effective contact angle of 122 ± 6 ^{o} and the cleaned membrane (F2C2) membrane resulting in an effective contact angle of 117 ± 9 ^{o}. A reduced cleaning effect was also seen following cleaning with citric acid. This suggests that after the first cycle the membrane is irreversibly altered and the foulants dominate the interactions rather than those of the virgin membrane. This is discussed further in Chapter 7.

6.6.2 FTIR

It was shown in Figure 6.1 that rinsing with water had little effect on the chemical composition of the membrane surface through FTIR analysis. Membranes were fouled, and then cleaned using the cleaning protocols mentioned in Sections 6.3 and 6.4. The FTIR spectra for membranes fouled with Gum Arabic and cleaned by chemical cleaning are shown in Figure 6.13. It can be seen that there are few noticeable differences between the spectra. Following cleaning with alkali, the membrane shows little difference with each of the peaks characteristic for Gum Arabic present on the membrane surface. Following cleaning with both alkali and acid it can be seen that a number of the peaks disappear from the spectra, suggesting that these have been removed during the acid clean. The peak at 3400 cm^{-1} due to hydrogen bonded OH groups has disappeared along with the carboxylate (COO^{-}) group at 1612 cm^{-1} and OH bend at 1415 cm^{-1}. The disappearance of these peaks suggests removal of the amino acids which contain carboxylate groups, however the presence of a strong peak at 925 cm^{-1} suggests there is still some OH groups present, however these are unlikely to be hydrogen bonded. The CH_2 stretch at 2930 cm^{-1} has decreased in intensity along with the C-C stretch at 1030 cm^{-1}. While the samples cannot be compared directly the reduction in these peaks suggests some removal of these groups from the surface. In addition while there are still peaks present in the region 1200 – 1400 cm^{-1} these peaks are too small to be correctly identified. The disappearance of these peaks from the spectra suggests that citric acid plays a significant role in the removal of foulants, particularly those which are hydrogen bonded with carboxylate groups. This hypothesis is also supported by the contact angle measurement

where cleaning with citric acid following an alkali clean leads to a contact angle close to that of the virgin membrane.

Following cleaning with Ultrasil 11, the FTIR trace shows very little difference from that of the virgin membrane. This suggests complete removal of the foulants, however the contact angle data and flux recovery data does not support this hypothesis. It is possible that cleaning with Ultrasil 11 removes the surface foulants, however in-pore foulants may remain leading to the differences observed from the effective contact angle and flux data. The difference in spectra between the alkali cleaned and Ultrasil cleaned membrane indicates that the addition of surfactants and EDTA plays a key role, however at present this role has not been identified.

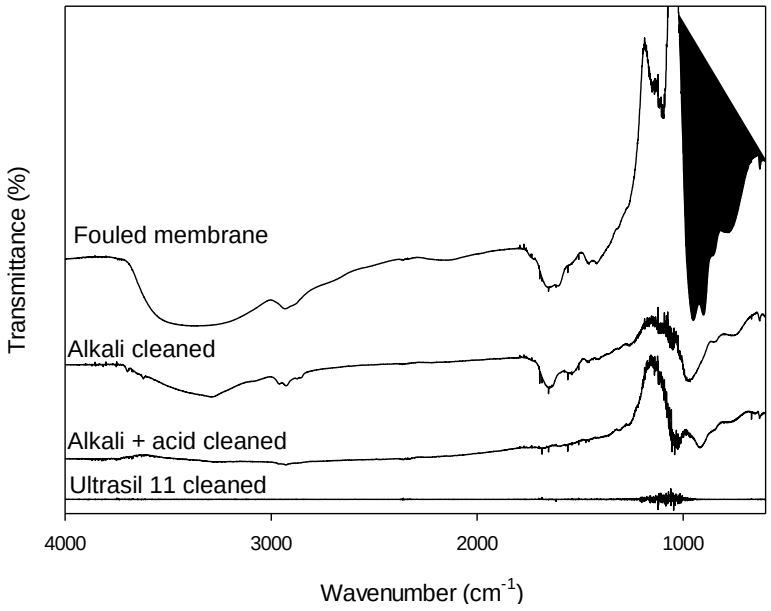

Figure 6.13: FTIR spectra of Fouled membrane (top) and membrane treated with various chemical cleaning agents (alkali, acid and Ultrasil 11 going from top to bottom) showing the changes in measured chemical composition and highlighting removal of Gum Arabic during the cleaning process. The virgin membrane has been subtracted from the spectra.

FTIR analysis was carried out on samples which had been subject to alkali cleaning under different mechanical cleaning conditions. These are shown in Figure 6.14. Following backwashing, as expected the spectra show little difference to those from cleaning with alkali in the forward direction (Figure 6.13). The largest difference between the two samples is the intensity of the peak at 975 cm^{-1} attributed to the rocking vibration of CH_3 as a methyl substitution on a carboxylate group. This suggests that there are differences in the removal mechanism between cleaning in the forward and reverse directions. The presence of each of the peaks characteristic

of Gum in both samples albeit at different intensities suggests that there is no complete removal of one characteristic group but rather the Gum foulant remains on the surface following both cleaning in the forward and reverse direction in the presence of alkali.

Cleaning the membrane in a sonication bath led to very little difference between the cleaned membrane and that of a virgin membrane. This suggests that chemically the surface is restored to that of the virgin membrane. Comparing this with the flux data an FR of 91 ± 5 % was achieved suggesting most of the foulant was removed. Based on this data it can be concluded that sonication is a very effective cleaning method with excellent removal of Gum. Any foulant remaining may be in the pores as this cannot be detected by FTIR which only gives information about the membrane surface. Further characterisation of the membrane surface is detailed in the following sections with SEM-EDX results also showing little evidence of any foulants present on the membrane surface.

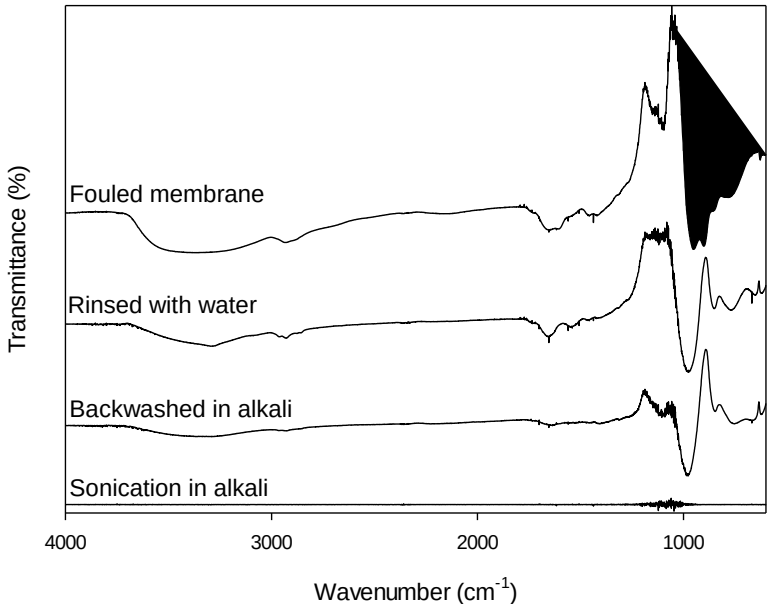

Figure 6.14: FTIR spectra of membrane fouled with Gum Arabic (top), rinsed with water (second from top), backwashed using alkali (second from bottom) and cleaned using ultrasound in alkali cleaning solution (bottom). The virgin membrane has been subtracted from the spectra.

6.6.3 SEM

The use of SEM was shown in Section 5.5.3.3 to give an insight about the fouling of Gum due to the formation of a cake layer on the membrane surface. It could be clearly observed that following

fouling with Gum Arabic, there was the addition of a cake layer to the membrane surface with little change observed through the membrane cross section due to in pore fouling. Membrane samples were analysed following cleaning to provide an indication about the role of cleaning agents on this foulant layer in terms of alterations in the thickness and morphology. Figure 6.15 shows the membrane after cleaning with alkali, and alkali followed by acid.

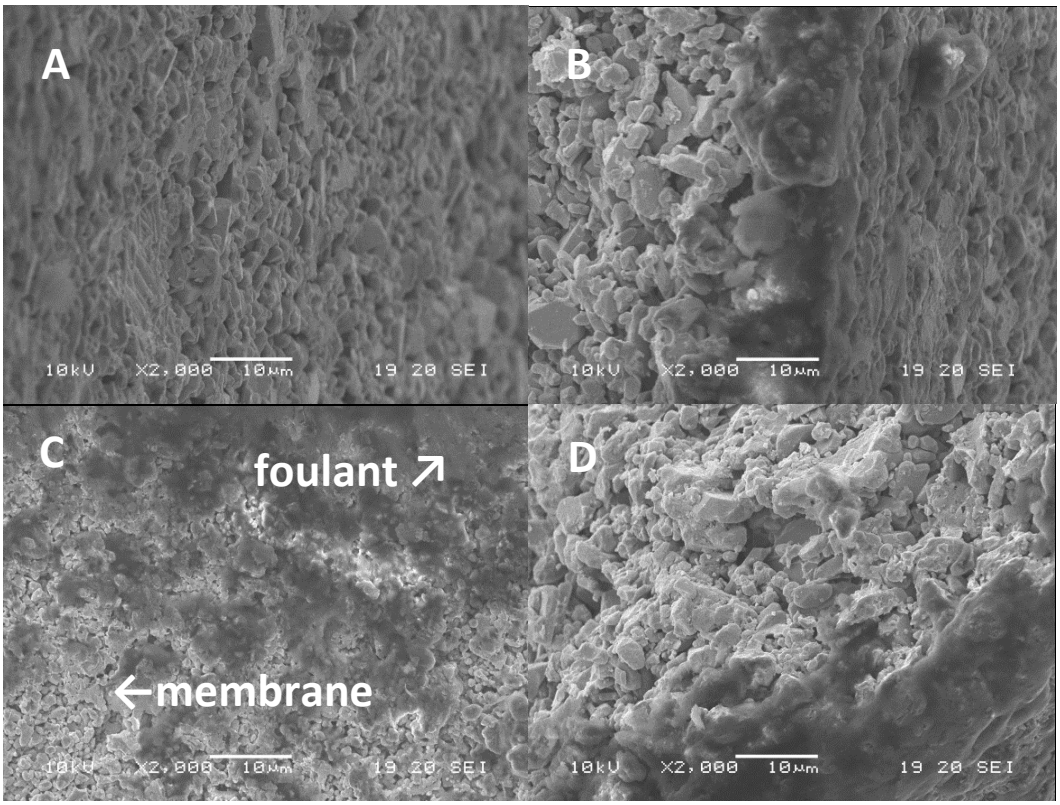

Figure 6.15: SEM images of 0.8 µm flat sheet alumina membrane following cleaning with alkali (a) top and (b) cross section and following cleaning with alkali then acid (c) top and (d) cross section.

The foulant layer remains following both cleaning strategies. Figure 6.15c shows that following acid cleaning the foulant layer is patchier suggesting that the Gum is removed in an uneven manner with increased removal following cleaning with acid. This is supported by the flux data with the acid clean resulting in an increased flux recovery compared to alkali cleaning alone.

6.6.4 SEM-EDX

The use of SEM-EDX was used as a method to determine the elemental composition of the foulant on the membrane surface. The composition was measured for a number of different samples and is shown in Table 6.2. Each measurement was taken for 10 areas on the membrane surface, and

the average and standard deviation are reported. The large errors are expected to be due to an uneven surface coating as shown in Figure 6.15.

Table 6.2: Elemental analysis for membranes fouled and cleaned measured using SEM EDX. Results are in wt. %. Elements showing '-' were not detected in the sample. *also contained 0.2 ± 0.1 wt. % potassium

Sample	Al	O	C	Ca	Si	Na
Virgin membrane	50.6 ± 2.2	49.4 ± 4.3	-	-	-	-
Fouled	42.0 ± 3.8	46.8 ± 7.9	9.6 ± 6.5	0.8 ± 0.4	0.8 ± 0.4	-
Fouled cycle 2	44.3 ± 5.4	46.9 ± 2.8	6.6 ± 2.2	0.6 ± 0.2*	1.6 ± 0.7	-
Alkali cleaned	43.9 ± 3.0	46.9 ± 4.9	7.0 ± 2.4	0.7 ± 0.3	1.4 ± 0.6	0.8 ± 0.2
Alkali cleaned cycle 2	41.9 ± 3.9	46.8 ± 7.3	9.5 ± 2.8	0.5 ± 0.4	1.4 ± 0.7	0.5 ± 0.7
Alkali + acid cleaned	46.5 ± 4.5	46.7 ± 4.6	5.4 ± 0.9	-	1.4 ± 0.5	-
Ultrasil 11 cleaned	44.8 ± 4.3	44.0 ± 5.2	8.7 ± 7.9	-	2.6 ± 1.2	-
Backwashed	44.3 ± 2.8	44.2 ± 5.6	9.0 ± 2.2	0.6 ± 0.1	-	1.1 ± 0.3
Sonication cleaned	51.0 ± 2.8	47.9 ± 3.6	-	-	1.1 ± 1.0	-

The elements present through SEM-EDX analysis help to give an insight as to what is occurring during cleaning. The foulant contains an increased level of oxygen compared to that of the virgin membrane, along with carbon, calcium and silicon. Interestingly no nitrogen was measured, nitrogen would be measured if the foulant was proteinacious, therefore either the foulant is completely arabinogalactan based or there are small amounts of proteinacious deposits which have not been detected using EDX. The presence of silicon is not expected, it may be present in small concentrations in the Gum, however it is more likely that it is a contaminant from the O rings used to seal the membrane holder. Following cleaning the wt. % of carbon and oxygen are shown to decrease. This suggests there has been removal of these to varying degrees depending on the cleaning procedure. The trend observed for the reduction in carbon follows that of the flux recovery, with a two stage alkali-acid clean showing a better flux recovery than an alkali clean, cleaning with Ultrasil or backflushing. The use of sonication appears to remove all of the carbon from the membrane surface, these results agree with those obtained by FTIR for all of the samples except that cleaned with Ultrasil 11.

The use of SEM-EDX showed that calcium was present in the foulant, and there was also the formation of large calcium aggregates as shown in Figure 6.16. The light coloured patches shown in the SEM images were shown to be calcium through SEM-EDX analysis. The presence of calcium may be responsible for some of the reduction in zeta potential shown in Section 5.3.3.2. Calcium

was not removed when cleaning with sodium hydroxide/sodium hypochlorite, however it was removed when citric acid was used as a cleaning agent. This is likely to be due to the chelating effect of citric acid. The removal of calcium was also observed following cleaning with Ultrasil 11 and can be attributed to the chelating effects of EDTA.

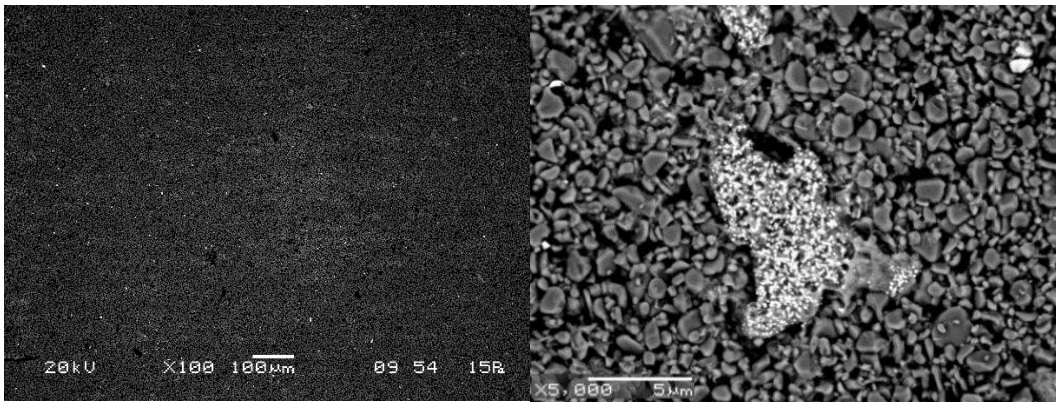

Figure 6.13: Uncoated SEM images of membrane fouled with Gum Arabic showing the presence of calcium aggregates (bright patches). Measured using Topo mode under low vacuum.

As a result of cleaning with sodium hydroxide/ sodium hypochlorite, low concentrations of sodium were observed on the membrane, this suggests that some form of ion exchange is occurring during the cleaning stage. It is possible that sodium is being exchanged for hydrogen in the Gum through an ion exchange mechanism. Either of the following reactions could be taking place:

$$R\text{-}COO^{-}H^{+} + NaOH \rightleftharpoons R\text{-}COO^{-}Na^{+} + H_2O$$

$$R\text{-}O^{-}H^{+} + NaOH \rightleftharpoons R\text{-}O^{-}Na^{+} + H_2O$$

Ion exchange between cleaning agents and a foulant has previously been reported by Weis *et al.* when investigating the removal of spent sulphite liquor from an ultrafiltration membrane.[185] While Ultrasil 11 is sodium hydroxide based it appears ion exchange between the cleaning agent and foulant does not occur, as no sodium can be observed to remain on the membrane following cleaning. It is expected that the presence of EDTA prevents this happening by chelating with any free sodium ions.

6.6.5 Zeta potential

Zeta potential is a useful tool in determining the quality of cleaning. Changes in the zeta potential are not solely based on the removal or attachment of foulants to the membrane surface, but

observed changes in ZP can be due to interactions between the foulant and cleaning agent. The zeta potential was measured for a membrane fouled with Gum and then a) cleaned with sodium hydroxide and sodium hypochlorite, b) firstly alkali cleaned, then cleaned with citric acid, and c) cleaned with Ultrasil 11. The measured zeta potential for each of the cleaning agents is shown in Figure 6.17, along with the virgin and fouled membranes to allow a comparison.

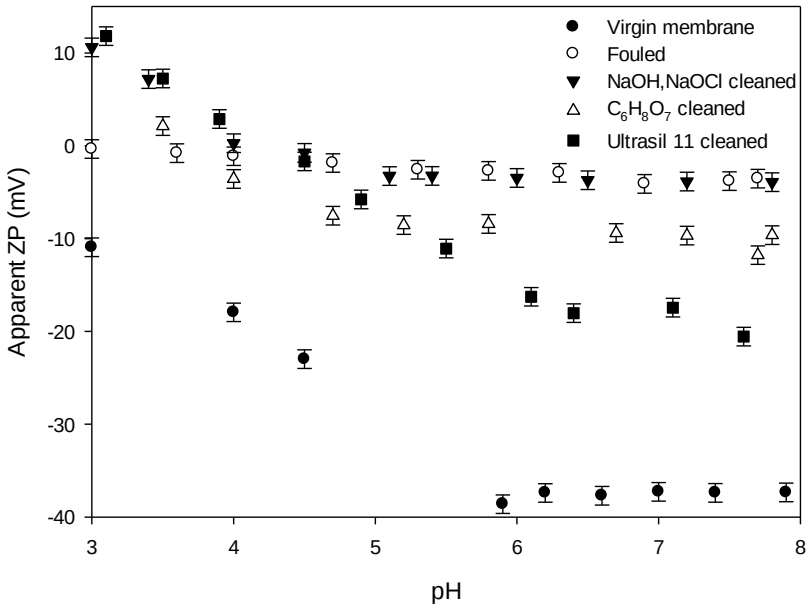

Figure 6.17: Zeta potential measurements over pH range 3.0 – 8.0 for membranes fouled and cleaned under standard conditions.

The zeta potential for a membrane cleaned with alkali shows little difference to those of the fouled membranes at high pH values. Below pH 4.5 the alkali cleaned membrane shows deviation in the measured ZP from that of the fouled membrane. Cleaning the membrane with alkali results in an isoelectric point ca. pH 4.5 with the membrane showing a positive ZP below this. The measured ZP between pH 3.0 and 4.5 is more positive than that measured either the virgin or fouled membrane, suggesting modification to either the membrane or the foulants. Gum Arabic has buffering properties due to the presence of potassium, calcium and magnesium salts of weak acid groups, therefore its buffering is expected to be greater in the neutralisation of acids than alkalis.[5] Based on this it would be expected that greater changes in the zeta potential would be observed at high pHs which contradicts the observed results. It is therefore hypothesised that the metal cations present in the alkali cleaning agent onto the surface and change the properties of the remaining foulants and/or membrane. The positive metal ions in the cleaning agent have the

ability to adhere to the negatively charged fouled surface. This agrees with the results shown by SEM EDX where sodium is present on the alkali cleaned membrane.

Following cleaning with citric acid, the ZP is between that of the virgin membrane and fouled membrane. This suggests that either:

(i) The cleaning protocol does not entirely remove fouling.
(ii) The cleaning agents have changed the properties of the membrane and/or those of the remaining foulants.

Citric acid can act as a chelating agent and therefore the positive charges either from the Na^+ or the positive charges in the zwitterionic amino acids in the Gum may have been neutralised. Looking at the observed zeta potential measurements in light of the flux measurements, and results obtained from FTIR and SEM, it is expected that the citric acid leads to removal of the metal cations resulting in a reduction in the zeta potential. It also removes some of the organic Gum Arabic molecules from the membrane surface which could lead to further reduction in the ZP. Not all of the foulant is removed therefore the zeta potential is of a lower magnitude to that of the virgin membrane.

Cleaning with Ultrasil 11 results in an interesting trend in zeta potential. At high pH values the ZP is ca. -20 mV, this is almost exactly half way between the ZP for the virgin membrane and the foulant. This suggests better removal of the Gum than cleaning with alkali or alkali followed by acid. This agrees with the FTIR results, however it contradicts the hydrophobicity, SEM-EDX and FR measurements. At low pH values however the trend is almost identical to that of the NaOH/NaOCl cleaned membrane showing an isoelectric point ca. 4.5 and displaying a charge of 12 mV at pH 3.1. This indicates that the sodium hydroxide has a significant influence on the foulants which may not only be attributed to the adsorption or ion exchange of sodium. Further work is required to identify what is responsible for this and to gain a full understanding.

For each of the cleaning methods where the ZP was measured, there was a significant difference from the virgin membrane, this shows that the membrane was not restored to its pristine condition. This indicates that the first cycle is decisive in determining the future performance of the membrane with modifications to the membrane/foulant following cleaning. The small changes observed in the ZP following cleaning also suggest that charge effects do not play an important role in the flux recovery over multiple cycles,[185] but rather other effects such as van der Waals, hydrophobic or hydrogen bonding are dominant.

6.6.6 AFM

AFM was used to measure the topography of membranes following different cleaning treatments. The roughness was determined following the method detailed in Section 3.6.8. The S_a (mean roughness) was calculated as an average value from each scan line from a 20 x 20 µm image, and is presented in Table 6.3.

Table 6.3: Mean roughness of membrane surface based on AFM measured across 20 x 20 µm section of a 0.8 µm membrane.

Cleaning	S_a (nm)
None	305 ± 75
Alkali clean	565 ± 149
Alkali + acid clean	359 ± 134
Ultrasil clean	596 ± 162
Sonication	346 ± 140

The roughness of the membranes was shown to increase following cleaning, however this is not necessarily a reflection of the membrane condition as shown in Figure 6.18. The roughness was increased particularly for the samples cleaned with sodium hydroxide or Ultrasil 11, and may be as a result of the foulant swelling in the presence of sodium hydroxide. While the results for the surface roughness for alkali cleaning, and Ultrasil cleaning, are greater than those for the two-stage or sonication clean ($P < 0.05$), the mean roughness calculates the deviation from a central point therefore peaks and valleys can mitigate each other. Comparing the images in Figures 4.13, 5.13 and 6.18, allows a better understanding of the surface roughness. Following fouling the membrane looks like it has a smoother surface, however when considering the scale on the z-axis it can be seen the deviation from 0 increases from 1.6 µm for the virgin membrane to 2.5 µm for the fouled membrane. Following cleaning with the alkali the deviation increases further to 3.0 µm. The presence of aggregates observed on the surface can be held responsible for this increase in roughness, this is also seen in Figure 6.15b using SEM. Following cleaning with acid some of these aggregates are removed leading to a decrease in the mean roughness as shown in Table 6.3.

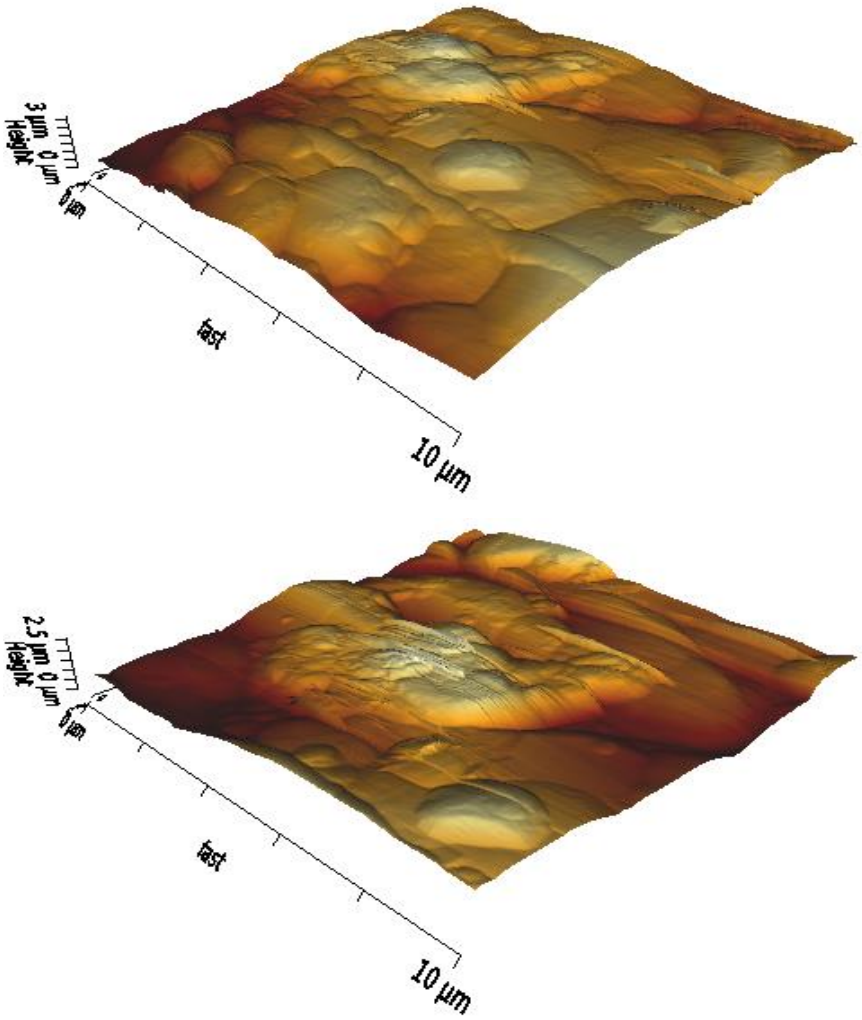

Figure 6.18: AFM images of membrane fouled with Gum Arabic and then a) cleaned with NaOH/NaOCl and b) cleaned with NaOH/NaOCl followed by cleaning with $C_6H_8O_7$.

6.6.7 Adhesion

The use of colloid probe analysis on 0.8 µm flat sheet alumina membranes was carried out in order to determine the adhesion properties of membranes which had been cleaned using the protocols detailed earlier in this chapter. This allows an insight as to the electrostatic forces which are occurring at the interface between the membrane/foulant and solution. Analysis was carried out as described in Section 3.6.8. The average adhesion distance and strength was calculated and is shown in Table 6.4, with typical force curves shown in Figure 6.19.

Table 6.4: Adhesion distance and strength following cleaning. Average and standard deviation of 10 points on the membrane surface are reported. Measurements made on 0.8 µm flat sheet membrane.

Cleaning	Adhesion distance (nm)	Adhesion strength (pN)
None	36.8 ± 11	1130 ± 330
Alkali clean	678 ± 770	9010 ± 3780
Alkali + acid clean	29.1 ± 5.3	535 ± 200
Ultrasil clean	104 ± 81	3940 ± 910
Sonication	90.7 ± 9.7	8690 ± 1420

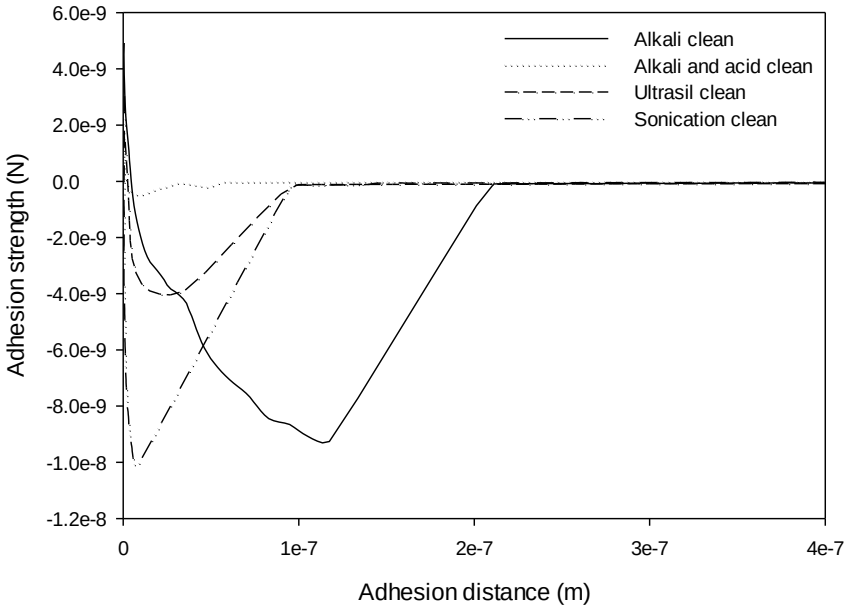

Figure 6.19: Adhesion distance and strength for the retraction of a silica probe from alumina membranes fouled with Gum Arabic and then cleaned using 4 different cleaning protocols.

Comparing the adhesion strength of the cleaned membranes to that of a fouled membrane shows that there are clear changes in the surface chemistry and adhesion properties of the membrane/foulant during cleaning. The alkali clean leads to the formation of a substance with a very high adhesion strength, with the adhesion occurring over an extended distance as shown in Figure 6.19. These results suggest that the Gum Arabic swelling on the membrane surface as it interacts with the sodium hydroxide. Many proteins are known to change conformation with pH and become denatured at high pH, and while the use of SEM-EDX did not show the presence of proteins this may be the case. The curve shows three different peaks suggesting there are three components interacting with the probe each with a different adhesion strength and distance. One of the components has a similar adhesion strength and distance to the peak formed following cleaning with Ultrasil. This suggests the same component is present in both of these samples.

If the Gum is swelling as it interacts with the sodium hydroxide, it would be expected this would lead to a more open structure, leading to a larger surface area of the Gum allowing an increased reaction with the sodium hydroxide or colloidal probe. An increase in the foulant layer thickness may be responsible for the increased adhesion distance if the probe can penetrate through the foulant. With the foulant layer being gel-like it is expected that the probe goes through the Gum layer to the alumina and then has adhesion over a large range as it is retracted through the foulant layer. The use of FDG was carried out to investigate this further, however the thickness of the foulant layer was below the detectable limit of the FDG therefore no conclusive results could be obtained (see Section 6.4.3). Flux measurements have shown the membrane resistance decreases following cleaning with sodium hydroxide. This may be due to some removal of Gum, or entirely due to the remaining foulant having a more open structure due to swelling. The swelling can lead to an increased adhesion with the colloidal probe, and may be why citric acid cleaning was shown to be more effective following an alkali clean, than cleaning with citric acid alone. A more open structure following swelling during the alkali clean will result in a larger surface area for the acid to interact with leading to an increased removal rate.

In addition, when studying the surface of the membrane following cleaning with sodium hydroxide plus sodium hypochlorite, aggregates were observed which had a very large adhesion strength. This is further evidence for the interaction of sodium ions present in the cleaning solution interacting with Gum as suggested in Section 6.6.4.

Cleaning with Ultrasil 11 showed a similar trend to cleaning with sodium hydroxide, however the adhesion strength and distance were somewhat reduced. One of the three peaks present following cleaning with NaOH/NaOCl is present following cleaning with Ultrasil 11. This suggests that cleaning with Ultrasil removed two of the components which are not removed by NaOH/NaOCl alone. At present it cannot be determined what is responsible for the additional peaks in the NaOH/NaOCl cleaned sample to indicate what is removed during the Ultrasil 11 clean, however the presence of metal cations may play a role.

Like sodium hydroxide, Ultrasil 11 also has a high pH, and is mainly composed of sodium hydroxide. It is expected that this also leads to swelling, however the inclusion of EDTA means the presence of metal cations is reduced. This could be responsible for the reduction in adhesion distance. Some of the adhesion in the alkali cleaned sample may be as a result of an interaction between the calcium or sodium cations and the OH groups in the silica surface. EDTA allows these to be chelated, leading to their removal and thus no adhesion due to the presence of electrostatic

interactions between the metal cations and silica surface would be observed. This agrees with the results obtained by SEM-EDX where no metal cations were present following cleaning with Ultrasil.

As was shown for the virgin membrane in Figure 4.15, force mapping was carried out over an area of 10 x 10 μm^2. It can be seen in Figure 6.20 that again the force is not equal across the whole surface. Similar studies were carried out on the fouled and alkali cleaned membranes however these produced system errors due to the sample heights/adhesion strength.

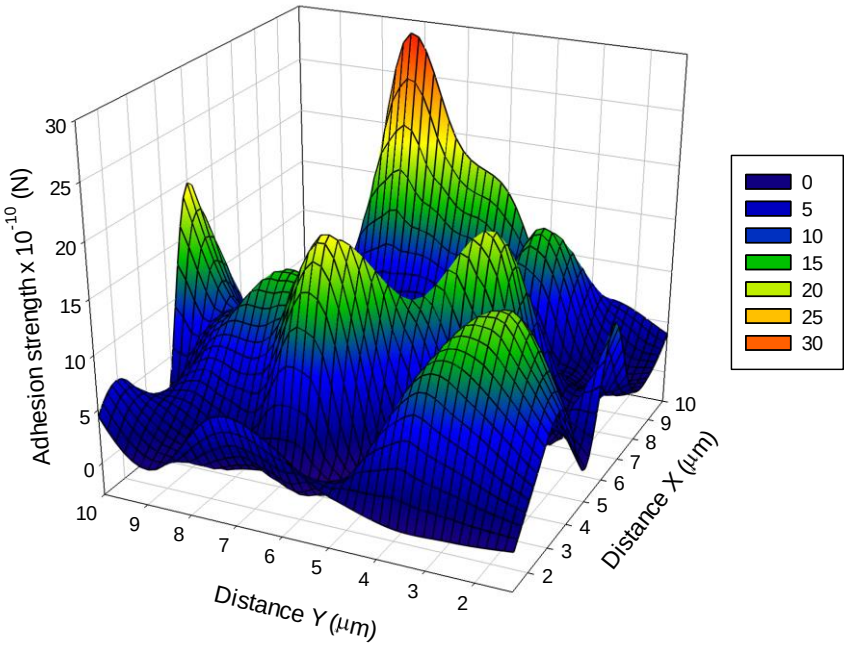

Figure 6.20: Force mapping of adhesion strength measured over 10 x 10 µm area showing that adhesion is not constant across the membrane surface.

Cleaning with citric acid following an alkali clean provided some interesting results. The adhesion strength is largely reduced, to below that of the virgin membrane. There are a number of things which could be responsible for this change:

i) In water the alumina surface is hydrated, providing a large number of OH groups on the surface that interact with the silica probe. Following cleaning with alkali the number of OH groups present on the surface of the alumina may have decreased due to the acidic conditions where the presence of H^+ ions will interact with the OH groups to form water.

ii) Citric acid has a much lower pH, therefore if the Gum is swelling at high pH, it may be compacting at low pH. While this has not been shown previously for Gum Arabic, due

to the complexity in understanding it and identifying the structure, other similar materials have shown this trend e.g. whey protein.[134]

iii) Citric acid can chelate with the Gum, leading to increased removal and changes in the surface chemistry. Any Gum remaining which is present on the surface of the membrane following cleaning would be expected to have been modified by cleaning with acid. The modified product may have a much lower adhesion than that of the membrane or the unmodified Gum.

iv) Gum is removed from the surface and any remaining foulant is present in the pores leading to adhesion characteristics similar to that of the virgin membrane.

The first hypothesis is unlikely to be the case as the sample was well rinsed following cleaning until the rinsing solution had a pH of 7.0. Under these conditions it would be expected that the alumina would be equally hydrated in the presence of water as for the virgin membrane.

While Gum may have been suspended into the cleaning solution and any remaining foulant present in the pores rather than on the surface. This is not in agreement with the SEM data which clearly shows the presence of Gum on the membrane surface. For this reason hypothesis (iv) is unlikely.

In Chapter 8, the modification of a membrane surface using citric acid is investigated. Following modification the adhesion strength is much larger than for the virgin membrane, this again makes the result obtained for the adhesion strength following cleaning surprising. This suggests modification of foulants present on the surface, rather than the membrane itself, is most likely to be responsible for the results obtained.

Attractive interactions were also observed for the different cleaning methods with any attractive forces leading to a “snap in” to contact as a result of interactions attracting the probe quicker than the rate at which it approaches the surface.[160] Figure 6.21 shows attractive forces that were measured on the samples following cleaning with NaOH/NaOCl or Ultrasil 11. The forces were also seen following cleaning with NaOH under sonication. It can be noticed in the zeta potential measurements, for both the NaOH/NaOCl and Ultrasil 11 cleans, that below pH 5.0 they display a positive charge. While adhesion measurements were carried out at neutral pH (pH 7.0), the use of ZP shows that the cleaned membranes have the ability to possess a positive charge. The snap in interaction may be as a result of calcium or sodium cations interacting with the negatively charged hydrated silica tip. The range of these interactions is short. Investigating the distance of these interactions, the sonication cleaned membrane interacts ca. 10 nm from the surface. This

is very similar to that of the fouled membrane and therefore is likely to be due to the presence of calcium cations. For the sample cleaned with Ultrasil the interaction occurred ca. 20 nm from the surface, and the interaction between the tip and NaOH cleaned membrane occurred ca. 65 nm from the surface. The increased distance of interaction may be as a result of swollen foulant on the surface. This particularly looks the case for the NaOH/NaOCl cleaned membrane as the adhesion curve starts to increase showing repulsion, before a sudden decline followed by an increase again. The tip may be pressing against a gel layer, and then cuts through it/forms interactions before reaching the surface. The attractive force may be caused by the presence of sodium or calcium cations, or a combination of the two. This would fit with the results presented earlier in this chapter.

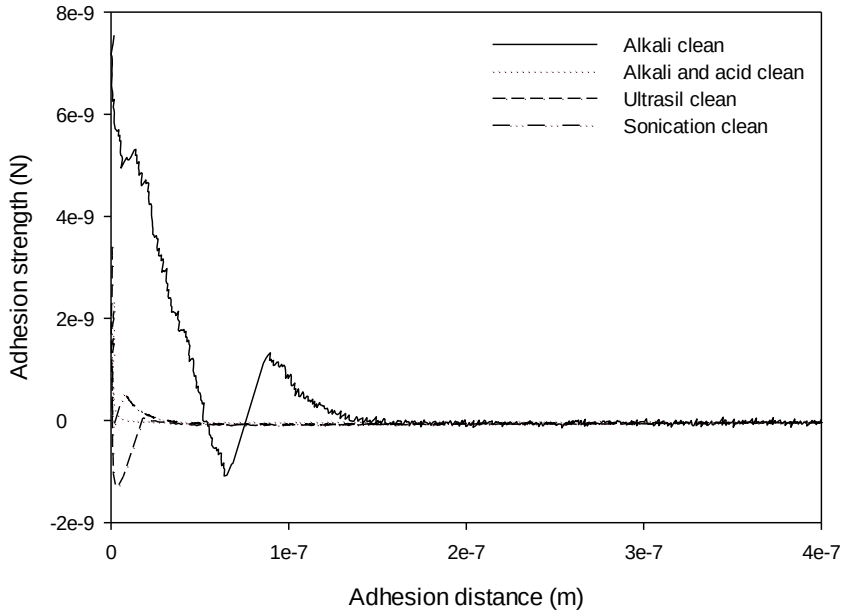

Figure 6.21: Adhesion distance and strength for the approach of a silica probe from alumina membranes fouled with Gum Arabic and then cleaned using four different cleaning protocols.

6.7 Discussion

The results presented in this chapter highlight the complexity of cleaning, and gaining an insight into the surface science occurring during cleaning. A number of cleaning agents were investigated and it can be concluded that each has a very different interaction with the foulant. It was not possible to achieve a chemically clean membrane. A flux recovery below 100 % was achieved for each method investigated. Gum Arabic readily adsorbs onto surfaces of alumina. Multiple layers are likely, therefore some removal of Gum is achieved, however strong bonding (hydrogen bonding) of GA to alumina means achieving a chemically clean membrane is very difficult. The use of harsh cleaning agents was unable to restore the membrane to its pristine condition. Gum is not the only product for which complete removal is very difficult, if not impossible. Gan *et al.* reported that following microfiltration of beer using ceramic membranes complete removal of the foulant was not possible.[234]

Sodium hydroxide leads to an improvement in the flux recovery and a decline in membrane resistance, however following studies it appears that this decline in resistance is likely to be due to swelling of the foulant. The addition of 200 ppm sodium hypochlorite was shown to lead to a 5 % increase in the flux recovery. The foulant layer has been shown by SEM and AFM to be thin, therefore it has not been possible to analyse this layer to confirm if the interaction is definitely a swelling mechanism. The use of FDG suggests that increasing the applied shear stress on a fouled surface to above 50 Pa does lead to further improvements in the lightness compared with that below 50 Pa. Shear stresses of 1 Pa were shown to decrease the redness and yellowness of a stained membrane following stress applied through the use of FDG, with further increases in stress leading to no further removal of the foulant. The use of AFM showed the presence of three types of adhesion interacting over a large distance. Some of the adhesion may be caused through the probe travelling through a swollen layer of Gum. Further evidence for this was seen in the approach curve for the colloidal probe to the membrane surface following cleaning with alkali. A typical approach curve was not observed.

FTIR and zeta potential studies showed little change following cleaning with NaOH/NaOCl from that of the fouled membrane. In addition, SEM pictures show that a layer of Gum remains following cleaning with alkali. Cleaning with NaOH/NaOCl leads to the presence of sodium on the foulant/membrane surface following cleaning suggesting that ion exchange is taking place. The addition of sodium may play a role in forming large aggregates which were observed using AFM.

The action of cleaning with NaOH/NaOCl prior to citric acid cleaning was shown to increase the FR to 86 ± 5 %, compared to a FR of 20 ± 5 % for cleaning with citric acid alone. This result is further evidence for a swelling mechanism as it would allow easier access of the acid to the Gum Arabic foulant, leading to an improved reaction rate and greater flux recovery.

Acid was shown to lead to the removal of a large proportion of the foulants, however some remained on the membrane surface. Zeta potential measurements showed that following cleaning with citric acid the ZP was between that of the fouled membrane and virgin membrane suggesting incomplete removal. This was also shown by FTIR, SEM and SEM-EDX measurements. Cleaning with citric acid allowed the removal of calcium present in the foulant, and sodium remaining from the alkali cleaning stage through a chelating action. The removal of cations may be responsible for some of the reduced adhesion observed following acid cleaning compared to that of the alkali clean alone. Gum is soluble in weak acids therefore cleaning with citric acid may have partly resolubilised the Gum allowing it to be removed from the membrane surface. In addition citric acid can form hydrogen bonds with carboxylic acids, aldehydes and alcohols present in Gum Arabic. This may play a role in its effectiveness in restoring the flux recovery.

In order to understand if the chelating effect of citric acid was responsible for the removal of Gum, or if other properties of the acid had a larger effect, Ultrasil 11 was used as a cleaning agent. Ultrasil is sodium hydroxide based, therefore it would be expected to have a similar mechanism to that of NaOH. However, the role of the addition of surfactants and EDTA were also studied. Ultrasil 11 did not result in ion exchange between the foulant and sodium ions, and led to the removal of calcium. This suggests that the chelating mechanism of EDTA and citric acid are both responsible for the removal of metal cations present in the foulant. The flux recovery following cleaning with Ultrasil was 50 ± 6 %. The cations in the foulant may be holding the structure tightly together, and their removal can lead to the nature of the foulant being changed allowing easier removal. Ultrasil 11 did not perform as well as sodium hypochlorite plus sodium hydroxide followed by acid. This suggests the role of acid is more than just in chelating the metal cations.

As well as chemical cleaning methods, two mechanical cleaning methods were investigated. The use of backflushing was shown to be ineffective. While backwashing is usually effective at removing foulants when cake filtration is the dominant fouling mechanism, this was not the case with Gum. This is further evidence that the foulant may be present on the surface as a gel layer detailed in Chapter 5. Due to water showing little removal of Gum, and it being hypothesised that caustic leads to swelling of the foulant layer, cleaning in the reverse direction would not be

expected to show any advantage over cleaning in the forward direction. This agrees with the results presented.

Cleaning with ultrasound (sonication) was shown to be an effective way to remove the Gum Arabic foulant from the membrane, achieving a flux recovery of 91 ± 5 %. The effectiveness of ultrasound depends on many factors such as orientation and position of ultrasonic field, frequency, power, radiation angle, membrane material, membrane housing, operating pressure and fouling material.[239] The removal may be due to the formation of microbubbles and microjets which help aid in the removal of the foulant layer, or it may lead to glycosidic fission of the Gum Arabic molecules. Based on the resistance of the foulant to chemical cleaning, and the high flux recovery following cleaning with sonication, it is expected that breaking down the carbohydrate is responsible for the removal. The AGP fraction of Gum is responsible for the viscous behaviour of Gum,[39, 240] therefore breaking it down can change the properties of the foulant. Following cleaning in an ultrasonic bath, the FTIR results showed no change from the virgin membrane highlighting surface removal of the Gum. This was confirmed using SEM-EDX which showed that only aluminium, oxygen and a small amount of silicon were present, and suggests a chemically clean membrane. The flux recovery below 100 % suggests that some of the foulant was present in the pores, it is possible that during the sonication, some of the foulant is removed from the membrane surface and trapped in the membrane pores leading to slight pore blockage and a reduction in the flux.

6.8 Summary

In this chapter a number of cleaning methods were investigated for their ability to remove Gum Arabic from a fouled membrane. None of the cleaning agents investigated showed satisfactory flux recovery when investigated alone, however effective cleaning could be achieved through combining cleaning methods. The most successful method of Gum removal was to clean with sodium hydroxide under sonication. While this lead to a FR of 91 ± 5 %, this would be difficult to implement industrially with CIP. Chemical cleaning with 0.5 wt % sodium hydroxide followed by cleaning with 0.1 wt % citric acid lead to a FR of 86 ± 5 %. It has been hypothesised that sodium hydroxide leads to swelling of the foulant layer, and the acid can then chelate sodium and calcium ions as well as break down some of the Gum leading to improved removal.

7. Multiple cycles – the importance of the cleaning protocol

7.1 Introduction

Multiple fouling and cleaning cycles of membranes is a fundamentally important, yet commonly overlooked area of membrane research. Industrially the membrane lifetime is of great importance, with it being impractical and unsustainable to use a new membrane for every cycle. Chemical engineers usually use the performance of the cleaning protocol (defined as the ability to return the membrane to its pristine condition in terms of permeability) as a benchmark when determining the system performance. This is typically noted as the percentage flux recovery.[140, 174] While this can give valuable information, it fails to consider the membrane aging process where the membrane behaviour may be altered as a result of changes in the surface chemistry and surface condition. Modifications to the membrane properties such as hydrophobicity and charge are known to influence the fouling potential both on the membrane surface and inside pores, this cannot be accounted for purely by measuring the flux recovery. This was shown in Chapter 6, and has been investigated further here.

Optimisation of the operating conditions as described in Chapter 5 is one important method to reduce the impact of fouling and associated flux losses. Aside from this, Field *et al.* indicated the three main strategies to reduce fouling:[93]

1. Hydrodynamic changes – this can influence the build-up of foulant by subjecting the membrane to various flow regime changes.
2. Optimisation of cleaning thermo-hydraulics, detergent type and concentration, and cleaning frequency. These factors influence the surface chemistry as well as allowing plant downtime to be minimised and productivity to be maximised.
3. Pre-treatment of the membrane or feed solution in order to influence solute-membrane interactions.

While over the short term, membrane material, porosity and surface roughness are important considerations in determining the cleaning performance, Chapter 6 showed these can be altered following cleaning. Over the long term the surface becomes irreversibly fouled, and the physio-chemical interactions between the cleaning agent and foulant most likely to be dominant, with the membrane material itself becoming less significant.[185]

This chapter focuses on the influence of cleaning agents over multiple cycles to allow a greater understanding of the role sodium hydroxide with sodium hypochlorite, and citric acid have on the

membrane and fouling potential over ten cycles. Ten cycles gives a representative measure of the membrane life.[241]

This chapter aims to show that:

- Membranes are modified substantially by repetitive fouling and cleaning cycles using Gum Arabic as a foulant and sodium hydroxide with sodium hypochlorite and citric acid as cleaning agents.
- There is a synergy between surface chemistry aspects of the membrane and permeate quality when subject to multiple foul-clean cycles.

7.2 Flux recovery

With flux recovery being the benchmark considered by chemical engineers in evaluating the system performance, this was first considered. In order for the membrane to be restored to its virgin PWF the value for flux recovery should be 100 %. Figure 7.1 shows the flux recovery (FR) following two different cleaning strategies over 10 cycles. The cleaning strategies will be referred to as protocol 1 and protocol 2. Protocol 1 involves cleaning the membrane with 0.5 wt. % NaOH with 200 ppm NaOCl at 60 ^{o}C for 20 minutes, and then rinsing the system for 15 minutes to remove any cleaning agents. Protocol 2 begins in an identical manner to protocol 1, but with the inclusion of an acid clean stage following the rinsing step. During the acid clean of protocol 2 the membrane is cleaned with 0.1 wt. % citric acid at 60 ^{o}C for 20 minutes, followed by a further 15 minute rinse to remove the acid cleaning agents from the system.

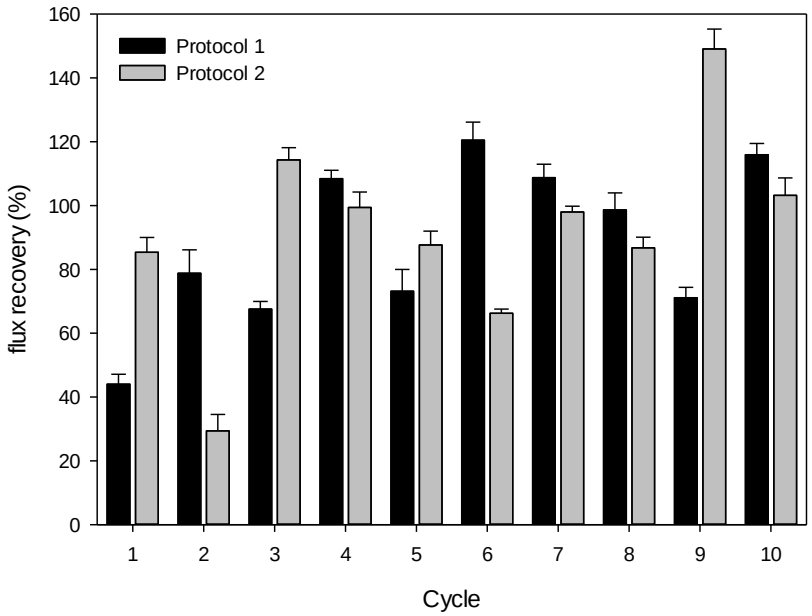

Figure 7.1: Flux recovery following fouling with 2.0 wt. % Gum Arabic for 60 minutes followed by cleaning following two different cleaning strategies, protocol 1 (alkali clean only) and protocol 2 (alkali clean followed by acid clean).

Based on the information obtained in Figure 7.1 it is difficult to identify much difference between the two cleaning cycles, with neither restoring the membrane to its pristine condition following the first cleaning cycle. The flux recovery is higher on the first cycle for protocol 2 suggesting that the acid has a role to play in restoring the membrane flux as shown in Chapter 6. There is a general improvement in the flux recovery for the first four cycles, before plateauing for both cleaning protocols. It is interesting to note that both cleaning regimes produce a FR greater than 100 % for a number of cycles, cycles 4, 6, 8 and 10 for protocol 1, and cycles 3, 9 and 10 for protocol 2. A flux recovery greater than 100 % has previously been reported by a number of authors, and can be attributed to the uneven removal of foulants or swollen agglomerates which are present from the previous cycle.[123, 134] Chapter 6 showed that a FR < 100 % was achieved following cleaning by either protocol, therefore the presence of additional foulants is expected.

In order to try to understand the flux recovery better, the flux recovery compared to the virgin membrane can be seen in Figure 7.2. It can be observed that the flux recovery decreases over the first few cycles for both protocols, and then levels out to be 24 ± 5 % for protocol 2 and 23 ± 6 % for protocol 1. For both protocols the flux recovery is low, showing that aging of the membranes influences the efficiency of filtration. Based purely on the flux recovery data it appears that both cleaning protocols have a negative effect on the membrane performance; however the results in

Chapter 6 suggest cleaning with protocol 2 resulted in an improved cleanliness. While membrane cleanliness can be identified by FR, changes to the membrane surface cannot be identified. This highlights the importance of considering other factors such as the fouling flux, rejection characteristics and the surface interactions which are occurring, to give a better understanding of the membrane performance over multiple cycles.

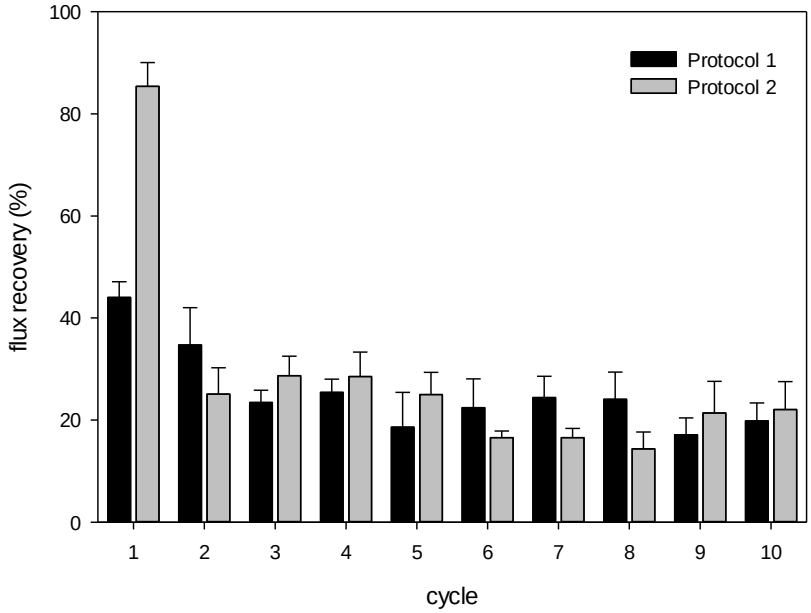

Figure 7.2: Flux recovery compared to virgin membrane following fouling with 2.0 wt. % Gum Arabic for 60 minutes followed by cleaning following two different cleaning strategies, protocol 1 (alkali clean only) and protocol 2 (alkali clean followed by acid clean).

Several authors have previously used the relative flux decline (RFD) as a method to describe the membrane performance during fouling.[134, 149] The RFD is a ratio between the permeate flux at time 0 (J_0) and the final fouling flux (J_f).

$$RFD = \left(1 - \frac{J_f}{J_0}\right) x\ 100\ (\%)$$

While the RFD is one useful parameter in determining the fouling of the membrane, it gives little detail as to the type of fouling, mechanism and chemical interactions which may be occurring.

When looking at the RFD against cycle number Bird *et al.* observed a gradual increase in the RFD over a number of cycles when using polymeric membranes to investigate ultrafiltration with spent sulphite liquor,[185] whereas Blanpain-Avet found no trend in the RFD of whey proteins using tubular ceramic membranes.[134]

Flux decline is a major issue with the relative flux decline after cycle 10 being 96 and 98 % for protocols 1 and 2 respectively. Based on the results shown in Chapter 6, protocol 2 resulted in a greater flux recovery after one cycle, however these results highlight the importance of considering multiple cycles.

7.3 Filtration flux

The influence of the two different cleaning strategies over multiple cycles has been investigated to determine the impact these have on the filtration flux. Figure 7.3 shows the flux during filtration for 0.8 μm tubular ceramic membranes fouled with Gum Arabic and cleaned using the two different cleaning protocols over the first four cycles using a virgin membrane. No pre-treatment was carried out, and therefore the fouling flux during cycle 1 is almost identical for both protocols (minor differences can be accounted for by membrane variation, and slight temperature and pressure variations throughout the experiment). For the first cycle the relative fouling flux for both membranes was 0.087 ± 0.005. For the membrane cleaned using protocol 1, the relative fouling flux showed no significant change after multiple cycles (0.079 ± 0.006 and 0.086 ± 0.006 after cycles 2 and 4 respectively). Following protocol 2 there was a significant increase in the relative fouling flux after cycle 2 to 0.168 ± 0.007 with an insignificant ($P > 0.05$) decrease in the relative fouling flux following further cycles. Following alkali cleaning with citric acid, the fouling flux was almost double that of the membrane which was only subject to alkali cleaning. The increase in flux following cleaning highlights the importance of investigating multiple cycles as well as considering factors other than the flux recovery. The surface chemistry during cleaning can have a large influence on the fouling flux.

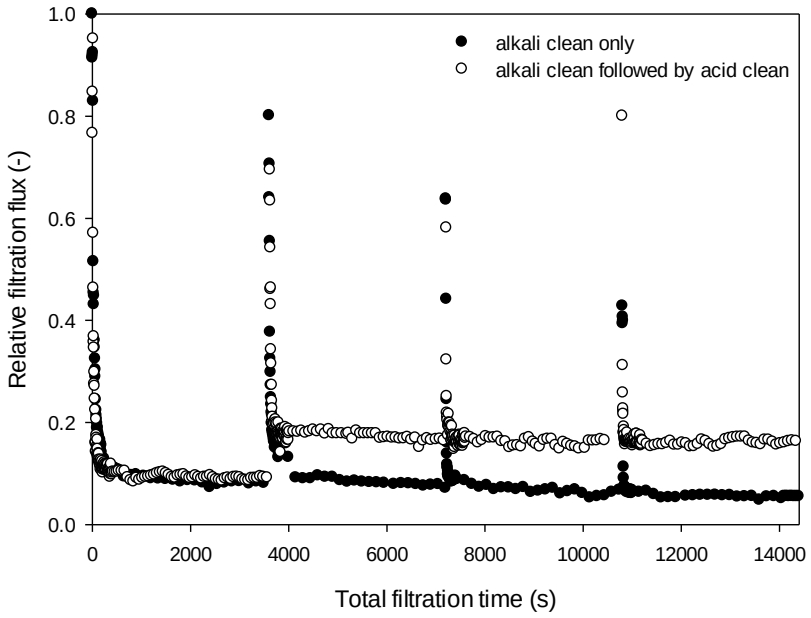

Figure 7.3: Relative filtration fluxes over 4 cycles showing the impact of cleaning with NaOH/NaOCl only, and cleaning with NaOH/NaOCl followed by $C_6H_8O_7$. Flux measured during the filtration of 2.0 wt. % Gum Arabic suspension at 40 ^oC with CFV 2.3 m s^{-1} and TMP 1.5 bar.

Differences observed in charge modification of the foulant are shown by zeta potential measurements in Section 6.6.5, with the membrane showing almost no charge following protocol 1 and a reduced charge compared with the virgin membrane for protocol 2. This demonstrates that the surface was modified following both cleaning cycles. In addition, it was shown in Section 6.6.4 that the foulant contains metal cations, with protocol 1 leading to the addition of sodium cations through ion exchange. These cations were removed when protocol 2 was followed. The change in attraction due to the presence of cations may have an influence on the measured fouling fluxes.

7.4 Resistance-in-series analysis

Figure 7.4 shows the steady state resistances over 10 cycles for a membrane subject only to an alkali clean (protocol 1). The membrane resistance has been divided into the intrinsic membrane resistance (R_m), the irreversible fouling (R_r) (which has been defined as the resistance following rinsing with water), the resistance which can be removed through chemical cleaning (R_c) and the irreversible resistance (R_i), as calculated using Equation 5.2. It can be noted that there is generally an increase in the total resistance for each cycle, with a reduction observed between cycles 6 and

7. The increase can be attributed to additional foulants building up on the membrane surface, and in the membrane pores. The discrepancy between cycles 6 and 7 highlights that the cleaning procedure is not entirely satisfactory with the ability to remove some of the foulants which remained on the membrane following the previous cleaning cycle. This is plausible with the formation of aggregates between the sodium ions from the cleaning agent and the foulant as discussed in Section 6.6.7. The aggregates can build up, and may reach a critical point at which removal becomes easier due to their increased size. Alternatively, additional fouling and cleaning could change the surface chemistry surrounding them, weakening interactions between the foulant and membrane thus allowing easier removal.

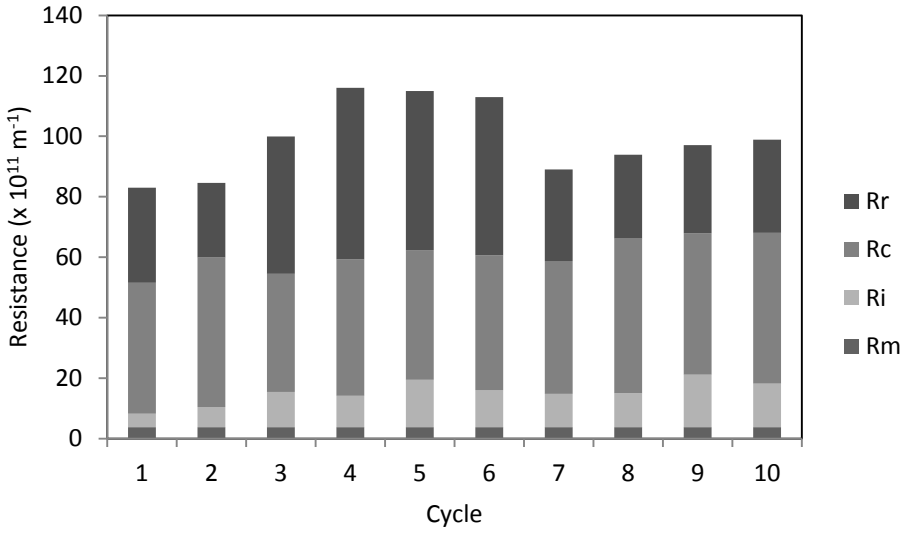

Figure 7.4: Resistance breakdown for 0.8 µm tubular ceramic membrane fouled using 2.0 wt. % Gum Arabic at 40 ^{o}C at TMP 1.5 bar and CFV 2.3 m s^{-1}. Cleaning carried out using protocol 1: 0.5 % NaOH + 200 ppm NaOCl at 60 ^{o}C.

A similar trend was also reported by Blanpain-Avet *et al.* and Gan *et al.* in other microfiltration systems.[134, 234] Gan *et al.* reported that when cleaning beer foulants from ceramic microfiltration membranes, the membrane resistance increased over the first four cycles before reaching a maximum.[234] This agrees with the initial trend shown for cleaning Gum foulants using an alkali clean only, however deviation was shown for cycle 7 where the total resistance decreases.

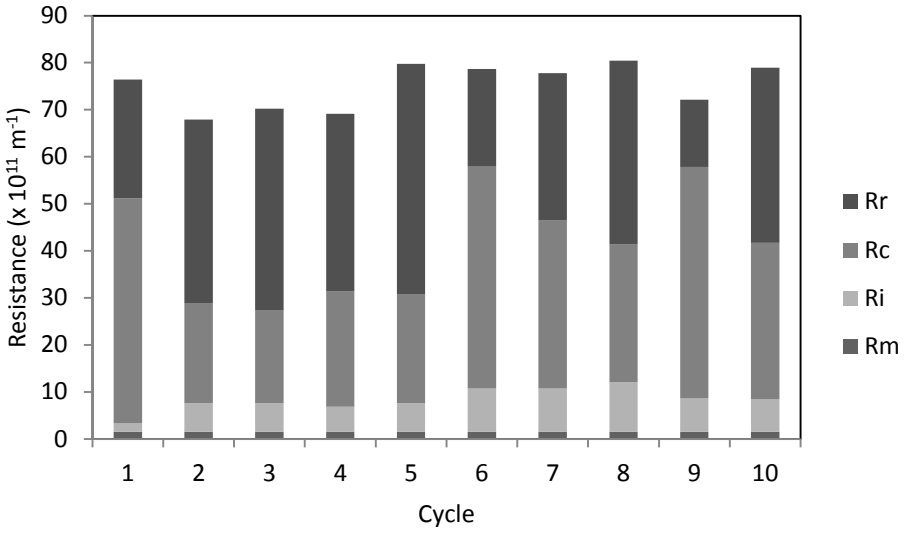

Figure 7.5: Resistance breakdown for 0.8 μm tubular ceramic membrane fouled using 2.0 wt. % Gum Arabic at 40 ^{o}C at TMP 1.5 bar and CFV 2.3 m s^{-1}. Cleaning carried out using protocol 2 - 0.5 % NaOH + 200 ppm NaOCl at 60 ^{o}C, followed by cleaning with 0.1 wt. % $C_6H_8O_7$ at 60 ^{o}C.

The steady state resistances over 10 cycles for a membrane fouled with Gum Arabic, and the cleaned with alkali followed by acid (protocol 2) are shown in Figure 7.5. Comparing Figure 7.5 with Figure 7.4 shows some interesting changes between the membrane resistances for the two cleaning protocols. Whilst there is no clear trend due to aging of the membrane, the membrane cleaned with protocol 2 provides a more consistent membrane resistance, which is generally lower than that for the membrane cleaned with protocol 1. Figure 7.5 shows the total resistance was between 7.0 x 10^{12} m^{-1} and 8.0 x 10^{12} m^{-1} for cleaning protocol 2, compared with a total resistance between 8.0 x 10^{12} m^{-1} and 1.2 x 10^{13} m^{-1} for protocol 1. In addition there is a marked difference between the removal of the foulant from the membrane. Following protocol 2 the amount of foulant which can be removed by rinsing with water is greatly increased compared to protocol 1. Following rinsing with water the resistance is around 6.0 x 10^{12} m^{-1} for the membrane cleaned only with alkali whereas when the membrane has been cleaned with alkali followed by acid the resistance of the membrane following rinsing with water is between 3.0 x 10^{12} m^{-1} and 5.5 x 10^{12} m^{-1}. This again highlights that FR itself is inadequate in providing an understanding of how a membrane performs over a number of cycles.

The differences in membrane resistance, in particular the removal of foulants during the water rinse, shows there are clear differences occurring in the surface chemistry and the adhesion properties of the Gum Arabic to the foulant and the membrane. The results suggest that the foulant is bound to the surface more strongly following the alkali cleaning, this agrees with the

results presented in Chapter 6 where it was hypothesised that cleaning with NaOH/NaOCl leads to swelling of the foulant layer. In addition, these results complement those measured using AFM where an alkali clean was shown to lead to strong adhesion strength with long range interactions, compared to reduced and shorter range interactions observed when protocol 2 is carried out (see Section 6.6.7).

These results are significant as they show that while the flux recovery varies from cycle to cycle for the membranes, the membrane resistance is notably lower and fouling flux greater following cleaning with protocol 2.

7.5 Removal of Gum Arabic

While flux and membrane resistance are very useful measurements in determining the membrane performance, the main role of membranes industrially is for separation. It is therefore important to consider the performance in terms of separation, when determining the system efficiency. Ideally 100 % separation between the desired components will be achieved, however this is not always required, or multiple separations may be required to achieve this. When considering the removal of Gum Arabic from wastewater streams, 71 % removal of the Gum Arabic is required to meet industrial requirements, and to be within the COD limits. Operationally the flux is of great importance, to ensure the system is economically viable. However good separation must also be achieved.

Figure 7.6 shows that retention (represented by rejection coefficient) increases over multiple cycles without a major increase in R_T, which suggests rejection is not due to steric hindrance as the pore size does not change. This agrees with the results shown in Section 5.3.1 where the flux for the first cycle was similar irrespective of the pore size used. The increased rejection may be due to physio-chemical interactions between the modified foulant following cleaning, or due to the build-up of residual fouling. Repulsive charge effects may be occurring between soluble Gum and Gum irreversibly deposited on the membrane surface. Unfortunately it was not possible to analyse membranes which had been fouled for more than two cycles due to fracturing of the flat sheet ceramic membranes. It was shown, however, that following one cycle there were large differences in the zeta potential of cleaned membranes compared to that of the virgin membrane.

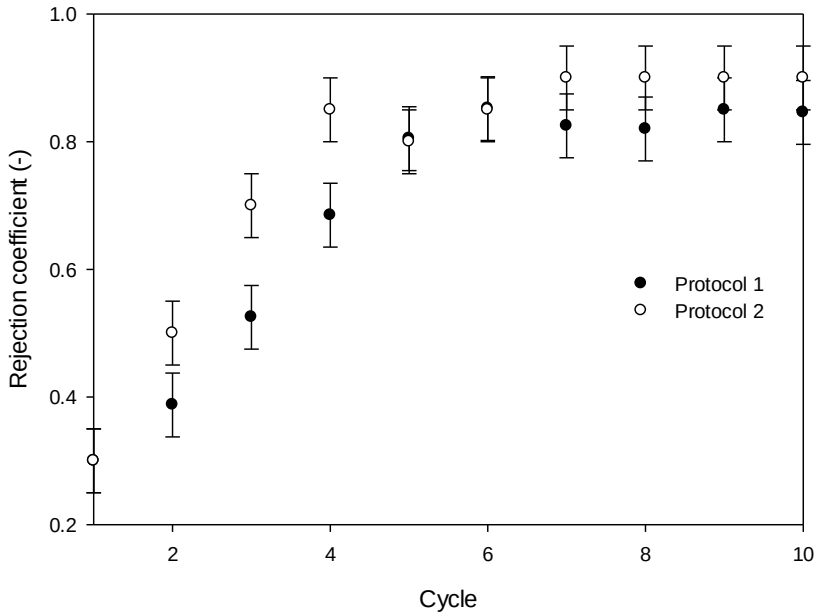

Figure 7.6: Rejection coefficient over 10 cycles using 0.8 µm tubular ceramic membrane and cleaning with alkali (protocol 1) and alkali then acid (protocol 2).

The rejection of Gum is greater following cleaning with protocol 2 (Figure 7.6). It is hypothesised there is the formation of a beneficial fouling layer which leads to increased selectivity, however this is not fully responsible for the increased rejection, otherwise rejection would be expected to be greater for protocol 1. The formation of a beneficial fouling layer seems plausible and agrees with the incomplete flux recovery following cleaning, and the dominance of cake filtration shown in Chapter 6. A similar phenomena was also reported by Bird and co-workers during the ultrafiltration of black tea.[115, 123] Blanpain-Avet *et al.* reported a slight increase in protein retention over several cycles showing a change in membrane selectivity through aging.[134] The additional rejection observed following protocol 2 suggests that charge interactions play an important role in determining the selectivity of the membrane. This is demonstrated further in Chapter 8.

7.6 Summary

These results demonstrate the importance of performing experiments to identify the effects of multiple fouling and cleaning cycles. Based on the results presented in Chapter 6 it would be expected that cleaning with citric acid following cleaning with NaOH/NaOCl (protocol 2) would outperform that of cleaning with NaOH/NaOCl alone (protocol 1). The results presented here show that while cleaning with protocol 2 does outperform cleaning with protocol 1, the difference

is not as large as would be expected. Neither protocol 1 or 2 resulted in restoration of the membrane to its pristine condition, with the presence of foulants remaining on the surface. The presence of these foulants has been shown to influence the surface chemistry which in turn influences the separation and flux in subsequent cycles.

Protocol 2 results in a marked increase in the fouling flux, and improved separation. While the flux recovery is low for both protocols, the increased throughput (flux) and separation achieved following cleaning with both alkali and acid shows that operationally this method should be selected.

8. Influence of pre-treatment on the fouling of Gum Arabic

The objective of this chapter was to determine whether the application of a simple acid or alkali pre-treatment to the membrane could affect both the type of foulant species attaching to the membrane, and improve the membrane separation performance. Nystrom and Zhu, and Zhu and Nystrom reported that cleaning the membrane before filtration can modify the separation process and types of foulant subsequently attaching to the membrane surface.[170, 242] Jezowska *et al.* also reported that a simple pre-treatment with a standard membrane cleaner led to a significant improvement in the permeate flux, however no improvement in the retention was observed.[243]

In some membrane systems, key foulants can be adsorbed onto the membrane as an antifouling pre-treatment and can lead to the formation of a beneficial foulant layer. Such a beneficial fouling layer can lead to improvements in the permeate flux and the selectivity of the system.[115, 123]

It is generally accepted that increasing the hydrophilicity of a membrane can significantly reduce the development of fouling.[199] A large amount of research is currently being undertaken to increase membrane surface hydrophilicity through chemical modification.[244, 245]

Two pre-treatment methods were carried out in this study and were compared to conditioning with water at 40 ^{o}C:

1) Conditioning with water at 40 ^{o}C followed by cleaning with 0.5 wt. % NaOH at 60 ^{o}C
2) Conditioning with water at 40 ^{o}C followed by cleaning with 0.1 wt. % $C_6H_8O_7$ at 60 ^{o}C

Membrane characterisation following pre-treatment was carried out using streaming potential measurements, FTIR, SEM for elemental analysis, AFM, and contact angle measurements.

This chapter aims to show that:

- pre-treatment can have a significant influence on the separation properties of a membrane
- pre-treatment allows a greater understanding of the interactions between the membrane and foulant

8.1 Pre-treatment with citric acid

It has been shown by a number of authors that carboxylic acids can bond easily with the surface atoms in alumina, resulting in a change to the surface properties.[229, 246, 247] The carboxylic acid

selected can influence the properties, with some making the surface more hydrophilic, and others rendering the surface more hydrophobic. The changes are dependent on the chain attached to the carboxylic acid. The alteration of alumina membranes can provide different properties. The carboxylic acid is generally much smaller than the pore size of the membrane when considering MF or UF. This leads to differences in the surface chemistry rather altering than the pore size. Recently Barron *et al.* reported the possibility of creating superhydrophilic membranes by the functionalising alumina at a molecular level, leading to enhanced separation properties without changing the strength of the membrane.[229]

Citric acid is commonly used in the food industry as a cleaning agent as it is compatible with industry standards and has been shown to be effective at removing metallic deposits and ions. For this reason it was investigated as a pre-treatment agent allowing an insight into changes to the fouling propensity and rejection characteristics following fouling. In the presence of water the surface of alumina is terminated with oxygen.[248] Figure 8.1a illustrates how carboxylic acids can be used to functionalise the surface of alumina on a molecular level, and Figure 8.1b shows the attachment of citric acid to the alumina surface.

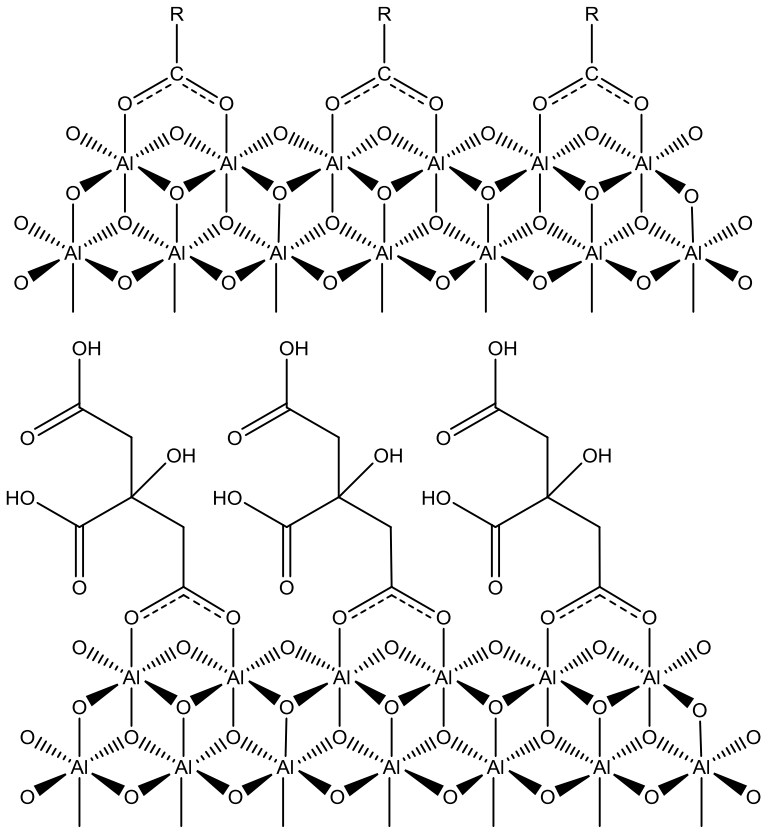

Figure 8.1: A (top) Surface layers of alumina showing coordination of surface oxygen atoms with a carboxylic acid. R depends on the particular acid used. B (bottom) shows the attachment of citric acid groups at a molecular level.

Studies were carried out using 0.5 µm flat sheet ceramic membranes. These were selected as they allow sectioning and surface analysis following pre-treatment, and fouling. It was expected that the carboxylic acids will be protruding into the pore space influencing the membrane properties, however as carboxylic acid is much smaller than the pores in microfiltration, the pore size is therefore not effected.

When the virgin membrane is in a solution of 0.1 wt. % citric acid it is above the pKa_1 value for citric acid (3.13), meaning that one of the carboxylate groups on the acid will be present as the carboxylate anion. This interacts with the alumina surface leading to bond formation and attachment of the acid to the membrane surface. The membrane is negatively charged, however in the presence of citric acid due to the low pH this charge is largely reduced (Figure 4.12).

8.1.1 Rejection of Gum Arabic

Separation is one of the most important characteristics in analysing the performance of a membrane. Ideally 100 % separation would be achieved, however in practice this may be difficult to achieve. There are a large number of factors influencing the separation properties with size exclusion not necessarily being the dominant factor. The use of a 0.5 µm membrane was selected due to the presence of aggregates in the Gum in the size range of 0.1 – 1.0 µm. The concentration of Gum in the permeate was monitored every five minutes throughout a 60 minute fouling cycle of a virgin membrane and membrane pre-treated with 0.1 % citric acid, and the results are shown in Figure 8.2. It can be seen that pre-treating the membrane with citric acid leads to a significant increase in the rejection of Gum. 85 % rejection is achieved after 60 minutes for the membrane pre-treated with acid, compared to 60 % rejection for the untreated membrane. While the citric acid groups may be protruding into the pore space, their size relative to that of the pores is not significant enough to lead to a change in pore size or accessibility. The increase in rejection for the pre-treated membrane signifies that pore size is not the only factor leading to separation, and other factors such electrostatic or chemical interactions may be responsible for this increase in rejection. This was also shown in Section 5.3.1.

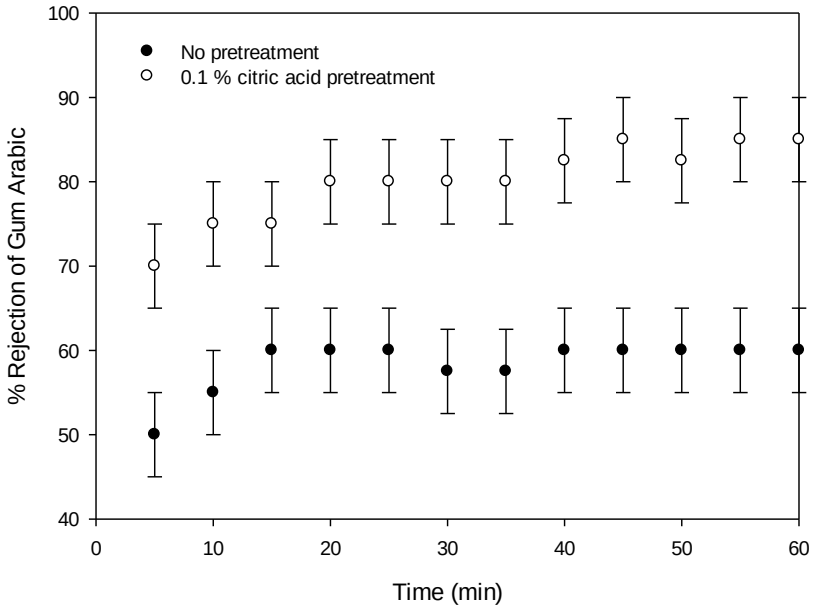

Figure 8.2: Influence of pre-treatment with citric acid on the rejection of Gum Arabic throughout a 60 minute filtration. It was observed that pre-treating the membrane with 0.1 % citric acid led to a significant increase in the rejection of Gum Arabic over a 60 minute cycle compared to an untreated membrane.

8.1.2 Effective contact angle

The effective contact angle allows an indication of the surface energy, and can be used to determine the hydrophobicity of a membrane. Surface modification has been widely used for the improvement of protein adsorption resistance. It is well known that surface hydrophobicity can effectively minimise protein adsorption and thus prevent membrane fouling. Table 8.1 shows the results measured for the effective contact angle of a virgin alumina membrane, and that of a membrane pre-treated with citric acid. Values are also shown for the two membranes following fouling with Gum Arabic. The results show that while citric acid can be used to increase the hydrophilicity of the membrane, subsequent fouling leads to a more hydrophobic surface. These results show that the hydrophilicity of the membrane is increased following pre-treatment, however during filtration fouling occurs, with the pre-treatment being insignificant in preventing hydrophobic foulants attaching to the membrane surface.

Table 8.1: Effective contact angle of water on membrane surface for virgin and acid pre-treated and fouled measured by sessile drop.

Material	Measured effective contact angle (°)	Literature value (°)
Aluminium oxide	37 ± 4	36-42[249-251]
Citric acid treated aluminium oxide	24 ± 5	
Fouled untreated membrane	104 ± 7	
Fouled citric acid treated membrane	112 ± 8	

There are many parameters which affect the interaction between foulants and the membrane surface. Hydrophobicity is only one. This result suggests that while the membrane is more hydrophilic following pre-treatment with citric acid, it does not prevent the attraction of hydrophobic foulants to the membrane surface. It is generally accepted that reducing the contact angle increases the hydrophilicity and reduces the fouling propensity,[143] however Lin *et al.* reported that reducing the contact angle between membrane and colloids may result in a lower negative total interaction energy aggravating membrane fouling.[180] Negative charges on membrane surface may be partly neutralised at acidic pH values, resulting in the decrease in contact angle.

8.1.3 Flux and Membrane resistance

The permeate flux offers a useful means of determining the flow through the membrane and can be used to calculate the membrane resistance, and increase in resistance caused by fouling. The flux has been plotted in Figure 8.3 as normalised flux to remove variation caused by the individual membranes. It can be observed that pre-treating the membranes with citric acid leads to an increase in fouling, with a much sharper initial flux decline. The increased fouling propensity may be due to a number of factors:

i) The increased hydrophobicity means there will be a reduced resistance to flow through the membrane (shown by the reduced membrane resistance in Table 8.2). The increase in flow results in more solutes and foulants being convectively driven towards to membrane surface, allowing an increased number of foulants to be adsorbed onto the membrane surface.

ii) Changes in surface chemistry caused by the adhesion of citric acid to the membrane surface. The presence of citric acid means there are two free carboxylic acid groups attached to the membrane surface allowing more sites for hydrogen bonding. Hydrogen bonding can occur between the carboxylic acid on the citric acid, and the carboxylic acid, aldehyde or alcohol groups present in Gum Arabic. In addition calcium present in the foulant can form ion bridges between carboxylic acid groups leading to stronger bonding. This is likely to be responsible for the increased fouling and has been investigated further using FTIR in Section 8.1.4.

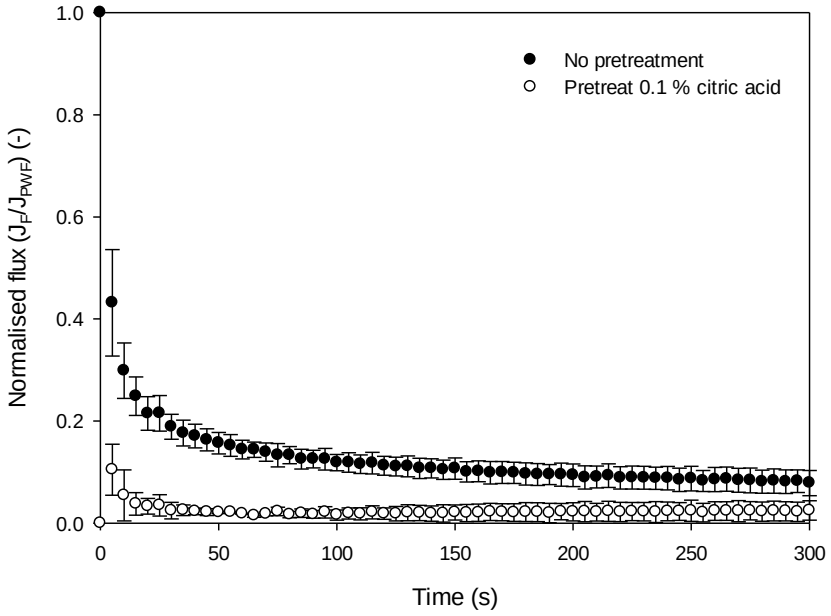

Figure 8.3: Influence of pre-treatment with 0.1 % citric acid on the permeate flux during the first 5 minutes of a fouling cycle. Result based on average of 3 runs with the error bars showing the standard deviation. Standard conditions of 40 ^{o}C, 2.0 wt. % Gum Arabic, TMP 1.5 bar and CFV 2.3 m s^{-1} were used.

The normalised resistance (Table 8.3) shows that for the untreated membrane the total resistance after fouling is 24 times larger than that of the virgin membrane, whereas the pre-treated membrane shows a 30 fold increase in resistance following fouling. The resistance following rinsing gives an indication as to how strongly bound the foulants are, as loose foulants are removed during rinsing. The untreated membrane shows that rinsing is effective at removing a large proportion of fouling, whereas for the pre-treated membrane rinsing only removes a small proportion of the foulants. This further indicates the presence of strong hydrogen bonding or ion bridging between the foulants and the citric acid groups on the alumina surface.

Table 8.2: Membrane resistance for 0.5 µm alumina membranes during fouling following no pre-treatment and pre-treatment with citric acid.

Condition	$\mathbf{R_m}$ (x 10^{10} m^{-1})	$\mathbf{R_T}$ (x 10^{11} m^{-1})	$\mathbf{R_{rinsed}}$ (x 10^{11} m^{-1})
No pre-treatment	1.22 ± 0.8	2.97 ± 0.3	1.2 ± 0.6
0.1 % Citric acid pre-treatment	1.14 ± 0.6	3.53 ± 0.4	2.43 ± 0.7

Table 8.3: Normalised membrane resistance for 0.5 µm alumina membranes during fouling following no pre-treatment and pre-treatment with citric acid where the membrane resistance is set to 1.0.

Condition	$\mathbf{R_m}$	$\mathbf{R_T}$	$\mathbf{R_{rinsed}}$
No pre-treatment	1	24	10
0.1 % Citric acid pre-treatment	1	31	21

The flux curves were fitted to the Hermia-Field model as detailed in Section 3.6.8 to develop an understanding of the fouling mechanism. Table 8.4 displays the r^2 values obtained from fitting the linearised form of the four classic models to the experimental data. The graphs from which the r^2 values have been obtained are in Appendix B. It can be observed that while cake formation dominated over the first five minutes for the membrane which had not been pre-treated, pore constriction was dominant following pre-treatment with citric acid. For 5 – 60 minutes a combination of blocking mechanisms was apparent for both pre-treatment methods. The change in blocking mechanism from cake to pore constriction suggests that the Gum Arabic foulant is interacting with citric acid groups both on the membrane surface and in the pores. This may be responsible for the rapid flux decline which was observed.

Table 8.4: Fouling mechanism based on laws proposed by Hermia[101] and extended for crossflow by Field *et al*[93]. Values are r^2 values are for curve fitting to the linear form of the equation.[91, 102, 103]

Experiment	Time (min)	Pore blocking	Pore constriction	Cake formation	Intermediate pore blocking
0.5 µm no pre-treat	5	0.473	0.948	0.995	0.919
0.5 µm no pre-treat	60	0.499	0.895	0.913	0.933
0.5 µm pre-treated with acid	5	0.636	0.990	0.979	0.966
0.5 µm pre-treated with acid	60	0.516	0.930	0.950	0.939

8.1.4 FTIR and Raman spectroscopy

Spectroscopy is useful in determining changes in the surface and structure of materials. Raman spectroscopy was used to determine if the changes to the alumina following pre-treatment were surface changes or structural changes. Raman spectroscopy shows no change in the core structure of the alumina, with identical spectra being produced before and after functionalisation (Figure 8.4). This confirms, as hypothesised, that changes are due to the adsorption of citric acid on the membrane surface rather than as a result in changes to the core alumina structure.

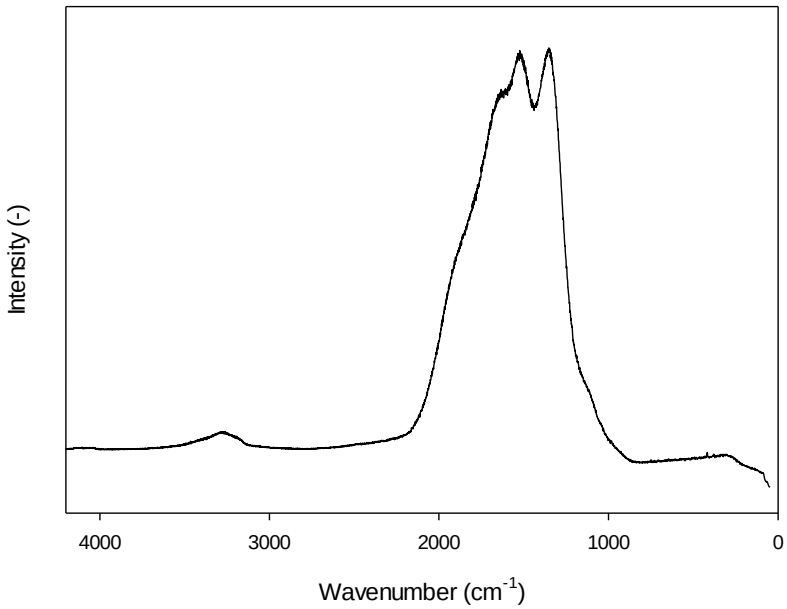

Figure 8.4: Raman spectra of alumina excited at 785 nm. Identical spectra produced before and after pre-treatment with citric acid highlighting that changes are to the surface and not the structure of the alumina.

The use of FTIR shows that the membrane surface is modified in Figure 8.5 (acid spectrum has alumina spectrum removed from it to allow clear identification of differences between the spectra). The functionalised membrane has a broad peak between 3400 and 2800 cm^{-1} due to the presence of carboxylic acid groups. Citric acid contains three carboxylic acid groups, and due to the molecular shape it is likely that only one of these is bonded to the alumina surface leaving the other two in their natural state. The peak around 1000 cm^{-1} can be attributed to the C-O stretch of the carboxylic acid. The sharp peak observed at 1457 cm^{-1} is typical of alkanes due to CH_2 and CH_3. The peak around 1650 cm^{-1} is characteristic of unidentate coordination between a carboxylic acid and alumina[229] showing that only one of the three carboxylic acid groups in citric acid bond with the alumina surface. This not only shows that there is bonding between the citric acid and the alumina, but also shows that the functionalisation of alumina with citric acid will result in an acidic surface due to the presence of two uncoordinated carboxylic acid groups on the citric acid.

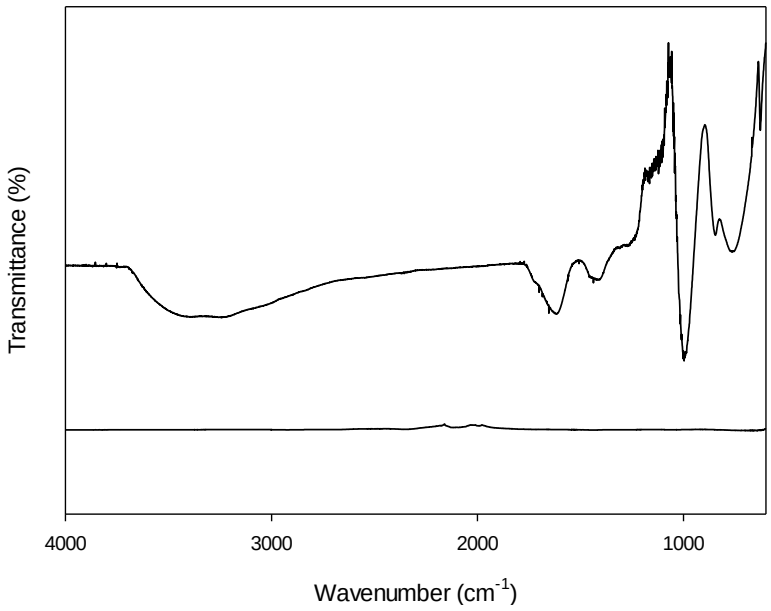

Figure 8.5: FTIR traces of Alumina with no pre-treatment (bottom) and Alumina pre-treated with 0.1 % citric acid (top). Pre-treatment with citric acid leads to the formation of additional peaks due to the presence of bonding between alumina and the carboxylic acid groups on citric acid, along with free carboxylic acid groups, and CH_2 groups.

Following fouling with Gum Arabic, Figure 8.6 shows that Gum Arabic is responsible for fouling. The formation of a layer on the membrane surface can be identified by the use of FTIR. The broad peak at 3400 cm^{-1} can be ascribed to asymmetric stretching of the O-H bond, this is a characteristic peak of polysaccharides and is broad due to the presence of hydrogen bonding. The peak at 2930 cm^{-1} can be ascribed to the stretching vibrations of CH_2 groups in a variety of chemical environments. This peak is also characteristic of polysaccharides.[227, 228] The strong peak at 1612 cm^{-1} in the Gum spectra is due to the symmetric stretching of the carboxylate anion (COO^-) which is formed from deprotonation of carboxylic acid groups present in a large number of amino acids present in Gum. Following adsorption onto the membrane this peak shifts to 1650 cm^{-1} showing the change in coordination from a deprotonated anion to coordination with the alumina surface. The sharp peak at 1415 cm^{-1} and the slight shoulder at 925 cm^{-1} are characteristic of the O-H bending vibration. There are a number of overlapping peaks in the region of 1200 – 1400 cm^{-1}, these can be attributed to CH_2 bending and twisting, C-C stretching, CH_3 bending C-O stretching. The strong peak at 1030 cm^{-1} is due to C-C stretching, and the shoulder at 1075 cm^{-1} can be attributed to asymmetric stretching of COC in an ether ring. The defined shoulder at 975 cm^{-1} is characteristic of the rocking vibration in CH_3 as a methyl substitution of a carboxylate group. The foulant can therefore be characterised as Gum Arabic with little influence between the foulant

formed on the two membrane surfaces, but clear coordination between the Gum and alumina for both samples. These results suggest that strong interactions occur between the alumina surface and Gum Arabic, and also between alumina functionalised with citric acid and Gum Arabic. The broad OH peak suggests that hydrogen bonding may be playing a large role in the fouling network of Gum.

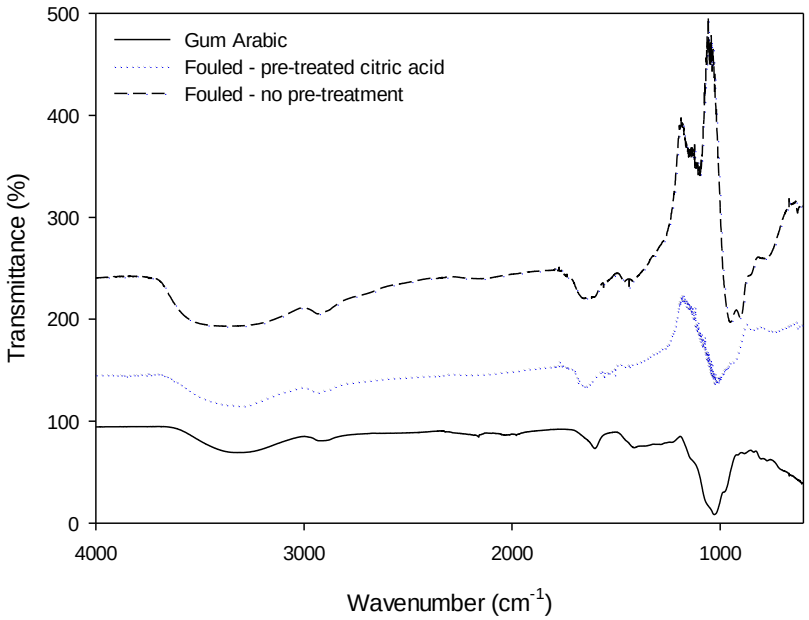

Figure 8.6: FTIR traces of Gum Arabic, alumina fouled with Gum Arabic and citric acid pre-treated alumina fouled with Gum Arabic. It can be clearly seen that Gum is responsible for fouling the membrane with coordination between the carboxylic acid groups on the Gum with the alumina membrane in both fouled cases. Virgin membrane has been subtracted to allow easy identification of the foulants.

8.1.5 Zeta potential measurements

In order to gain a fuller understanding of the effect of pre-treatment and fouling on the membrane charge, surface measurements of the apparent zeta potential through the pores was investigated. Surfaces displaying an increased hydrophilicity (and thus greater surface energy) would be expected to exhibit a stronger absolute charge measured by zeta potential, this is shown in Figure 8.7. The pre-treated surface, which was more hydrophilic, resulted in an increased absolute charge. Figure 8.7 shows that the isoelectric point for the virgin membrane was below 3.0, and displayed a large charge (-10 to -40 mV) with the membrane accepting more negative charge at higher pHs. Following pre-treatment with citric acid, the membrane also displayed a large charge

(+15 to -40 mV) with an increase in the isoelectric point to ca. pH 4. The natural pH of Gum Arabic suspensions is ca. pH 5.5 meaning that both membranes showed a negative charge at this pH, with the acid pre-treated membrane showing a slightly lower charge. Gum shows a slight negative charge at pH 5.5 therefore some charge repulsion between the negatively charged membrane and the negatively charged Gum would be expected.

Following filtration of Gum Arabic, the streaming potential measurements can be seen in Figure 8.8 and show significant differences in both the IEP and the zeta potential for the two samples. The IEP is significantly higher for the membrane pre-treated with citric acid, and lies similar to the natural pH of Gum. The zeta potential shows a significantly larger charge, similar to that of the membrane before fouling. For the untreated membrane the magnitude of the zeta potential is very small for the fouled membrane, suggesting the adhesion of a positively charged foulant to the membrane or pore wall surface. Gum has very good buffering characteristics which suggests there is a large layer of Gum on the membrane surface leading to buffering of the charge. In contrast, the functionalised surface is clearly fouled with Gum, shown through the increased membrane resistance and the FTIR results. However, it does not show these changes in the zeta potential. Clearly there is a large change in the structure or coordination of Gum Arabic on the surface leading to the differences in zeta potential curve when compared to the untreated membrane.

The increase in carboxylate groups on the membrane surface following pre-treatment with citric acid is likely to result in additional sites for hydrogen bonding between the membrane and carboxylate, aldehyde, and alcohol groups found in Gum. COOH groups are polar and are well known to form hydrogen bonds. Additionally the calcium ions in the Gum may be chelated by the citric acid groups on the surface, resulting in neutralisation of their charge and a zeta potential closer to that of the virgin membrane.

Bornaz *et al*. showed that hydrophilic membranes have a strong affinity for fats with the formation of hydrogen bonding between the hydroxyl groups of the membrane surface and triglycerides, this resulted in the membranes behaving like hydrophobic membranes reducing the transfer of water through the membrane.[252, 253] While triglycerides are not present in Gum Arabic, a similar interaction is likely to be occurring leading to the formation of hydrogen bonding between the hydroxyl groups on the membrane surface and the polar OH groups in Gum.

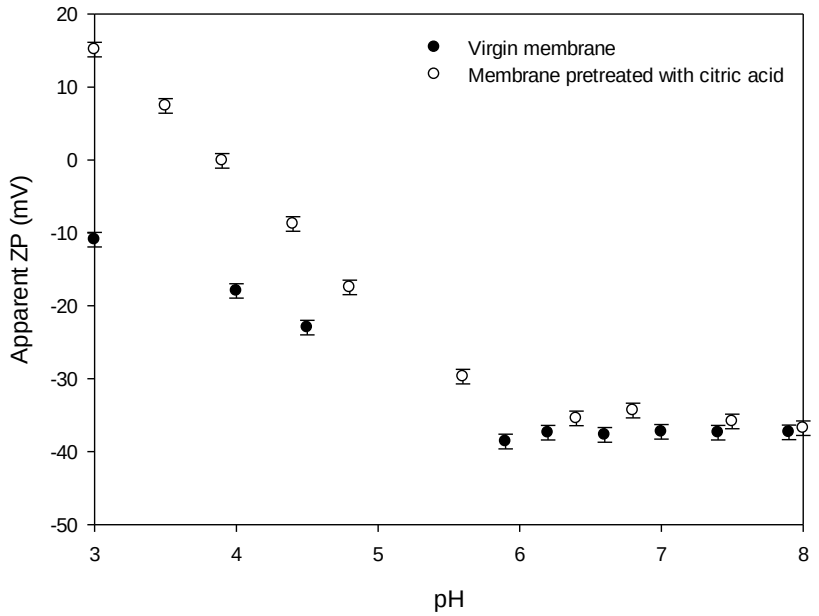

Figure 8.7: Comparison of zeta potential for untreated membrane and membrane treated with 0.1 % citric acid.

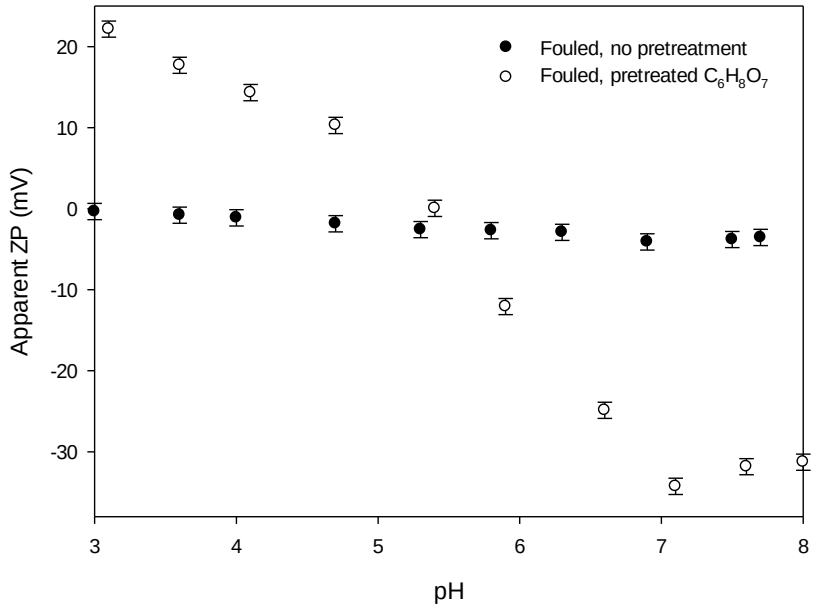

Figure 8.8: Comparison of zeta potential for fouled membranes with and without 0.1 % citric acid pre-treatment.

The separation of polysaccharides and proteins can be controlled by the nature and extent of the charge on the membrane surface.[220] At pH 5.5 the fouled membrane which had been pre-treated

shows a more positive charge than that of the fouled untreated membrane. The charge on a membrane influences separation by repelling ions of like charges and preferentially permeates ions of opposite charges.[222] The further away the pH is from the isoelectric point of the membrane, and particle, the greater the repulsion of particle-particle and particle-membrane if they are oppositely charged. This may have a role in the increased rejection following pre-treatment with citric acid.

8.1.6 SEM-EDX

SEM-EDX provides a useful way to determine the main components present on the membrane surface. Following pre-treatment with citric acid, the concentration of oxygen and carbon was shown to increase relative to that of alumina. This suggests that carboxylic acids are present on the membrane surface, as already shown by FTIR. The pre-treated membrane also contains traces of silicon, and as detailed in Chapter 5, this is attributed to contamination from the O-ring used to hold the membrane in place and form a seal.

Following fouling, the elemental composition of the pre-treated and fouled membrane is similar to that of the membrane which was fouled following conditioning with water (Table 8.5). Any changes in composition observed are within the experimental error. This suggests that there is no significant change to the fouling material. However, changes were observed in the deposition rate, and it is possible the coordination of Gum molecules on the surface is changed.

Table 8.5: SEM-EDX analysis of membrane surface for virgin membrane, pre-treated membrane and fouled membranes. All results are in wt. %. Elements showing '-' were not detected in the sample

Sample	Al	O	C	Ca	Si
Virgin membrane	50.6 ± 2.2	49.4 ± 4.3	-	-	-
Fouled	42.0 ± 3.8	46.8 ± 7.9	9.6 ± 6.5	0.8 ± 0.4	0.8 ± 0.4
Acid pre-treat	43.9 ± 1.7	47.3 ± 3.7	8.2 ± 2.9	-	0.6 ± 0.2
Acid pre-treat – fouled	45.9 ± 6.1	45.8 ± 9.9	6.7 ± 12	0.7 ± 0.5	0.9 ± 0.3

8.1.7 AFM

Different materials have different surface chemistry, and a material can be modified following pre-treatment. The adhesion of particles to a membrane surface can be influenced by the surface

chemistry with electrostatic double layer interactions, van der Waals forces, short-range interactions or particle and membrane deformity. The use of colloidal probe interactions with the membrane surface measured by AFM gives an insight into these interactions. Silica surfaces are known to display very short range repulsive interactions which are due to hydration forces or the presence of a gel like layer of silanol groups which grow on the surface in the presence of water.[160] The electrostatic double layer interactions can be measured as the probe approaches the surface with a more negative ZP expected to lead to greater repulsive forces and opposite charges leading to attraction.

The adhesion strength of the acid pre-treated membrane was compared to that of the virgin membrane by the use of a silica colloidal probe. Averages were taken of 10 points across the membrane surface and are reported in Table 8.6. It can be seen that the adhesion strength is around 10 times greater following pre-treatment with citric acid, this is likely to be responsible for the rapid flux decline shown in Figure 8.3.

Table 8.6: Adhesion distance and strength between pre-treated membranes and colloidal probe.

Preconditioning	Adhesion distance (nm)	Adhesion strength (pN)
Water	31.8 ± 7.6	690 ± 240
Acid ($C_6H_8O_7$)	129 ± 50	6510 ± 3040

Typical force curves for the virgin and pre-treated membranes are shown in Figures 8.9 and 8.10 for the approach and retraction of the colloid probe respectively. The approach curve gives an insight into the electrical double layer of the membrane. Figure 8.9 shows that for the virgin membrane no attraction is observed with repulsion between the membrane and probe from ca. 20 nm from the surface with the repulsion increasing as the probe reaches the surface. The membrane pre-treated with acid shows there are two points where attraction is observed. Forces of ca. 600 pN are observed 30 nm and 20 nm from the surface before repulsion is observed between 20 nm and the surface. This change highlights differences following pre-treatment with the probe being more attracted to the citric acid treated surface. It was shown using FTIR in Section 8.1.4 that carboxylic acid groups are present on the surface. The attraction highlights the importance of hydrogen bonding with bond formations expected between the COOH groups on the membrane surface and OH groups on the silica probe.

For the retraction of the probe the forces between the surface and virgin membrane are small with one peak as discussed previously in Section 4.2.2.6. Following conditioning with citric acid,

the magnitude of this peak increases showing increased adhesion, and there is the formation of a second peak which has a lower adhesion strength but greater adhesion distance. The two different peaks can be attributed to hydrogen bonding between the membrane surface and the OH groups on the silica probe. There are two free binding sites in the citric acid. The presence of terminal or tertiary binding sites may lead to the two peaks formed with the different binding sites possessing different properties. Alternatively, there may be some adhesion between OH groups on the membrane surface and the silica probe.

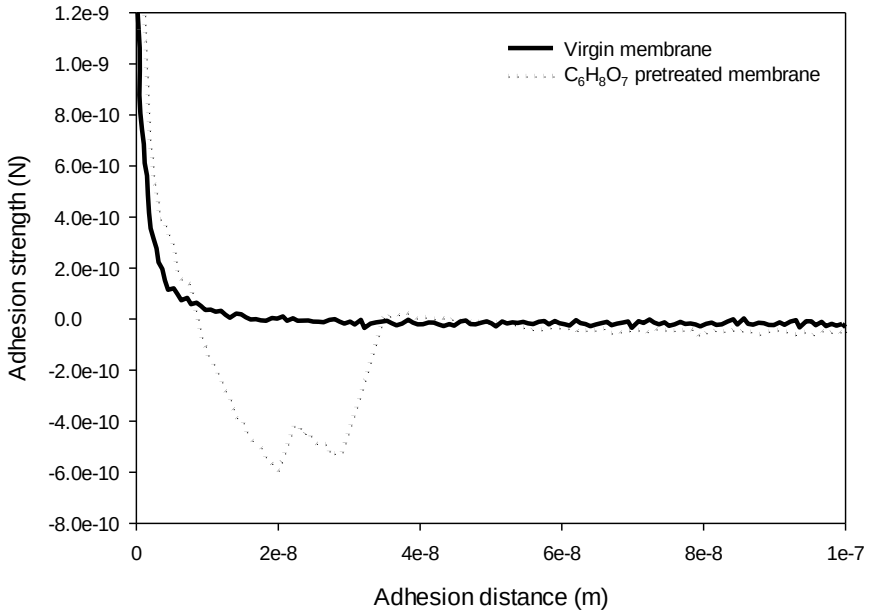

Figure 8.9: Adhesion distance and strength for approach of silica probe to alumina membranes with no pre-treatment (virgin membrane) and pre-treated with citric acid highlighting the differences in surface chemistry and adhesion properties following pre-treatment.

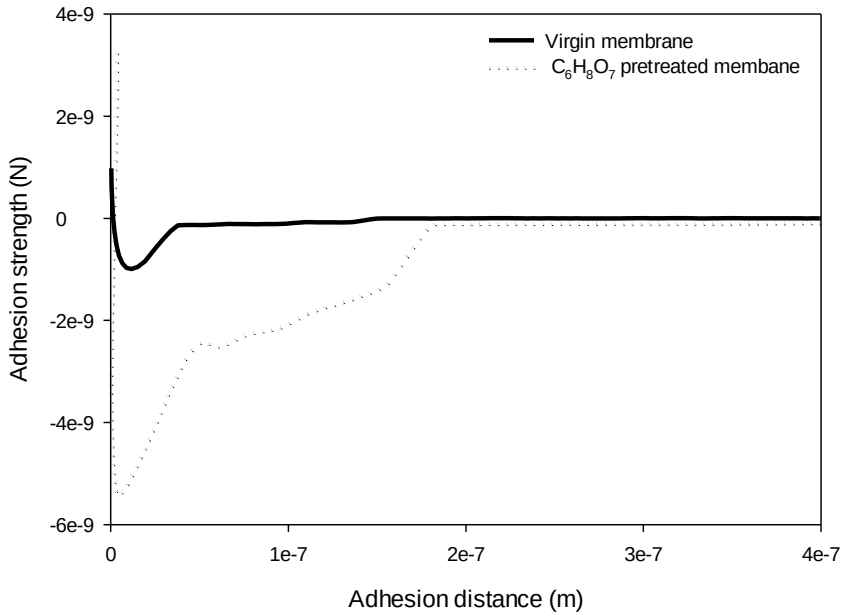

Figure 8.10: Typical adhesion distance and strength for retraction of silica probe from alumina membranes with no pre-treatment (virgin membrane) and pre-treated with citric acid highlighting the differences in surface chemistry and adhesion properties following pre-treatment.

When the membranes were fouled, the average adhesion strength and distance was measured. These are reported in Table 8.7. It can be observed that the adhesion strength is ca. two times larger for the membrane pre-treated with citric acid than for the fouled membrane with no pre-treatment. The adhesion strength is also active over a longer distance showing the surface pre-treated with citric acid leads to an increase in the adhesion distance. Typical forces curves for the approach and retraction of the probe to the membrane are shown in Figures 8.11 and 8.12 respectively.

Table 8.7: Adhesion distance and strength between pre-treated membranes which have been fouled with Gum Arabic and a colloidal probe.

Preconditioning	Adhesion distance (nm)	Adhesion strength (pN)
Water	36.8 ± 10	1130 ± 330
Acid ($C_6H_8O_7$)	591 ± 24	2720 ± 100

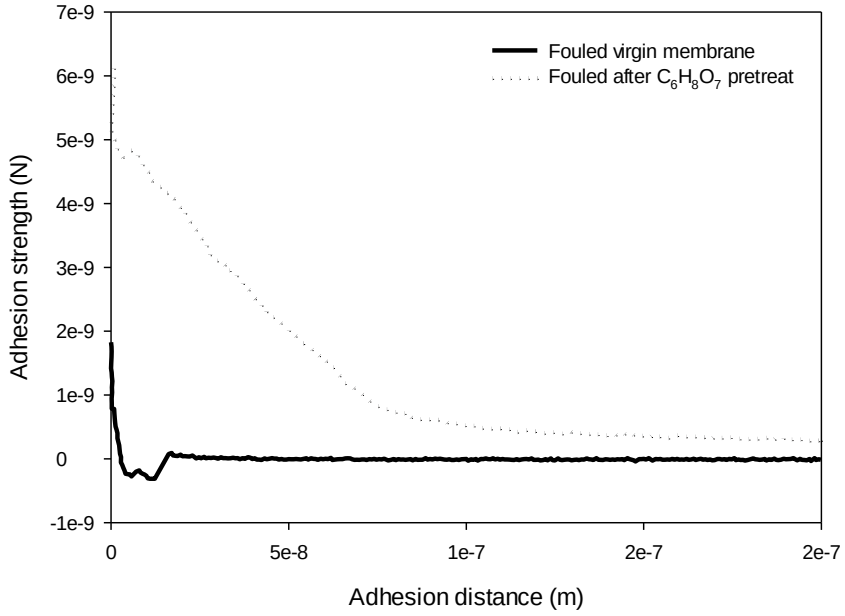

Figure 8.11: Typical adhesion curve as a colloidal probe approaches surface of virgin membrane and citric acid pre-treated membrane following fouling with 2.0 wt. % Gum Arabic.

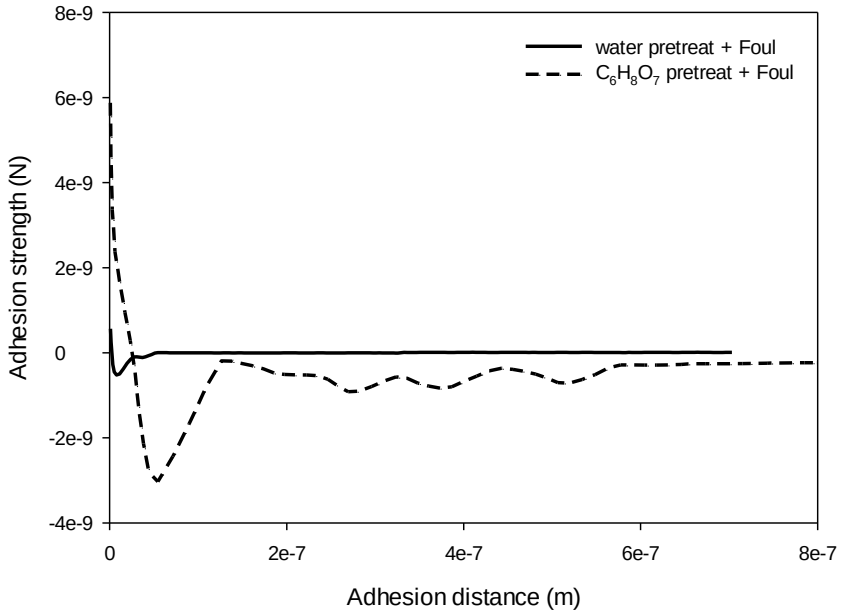

Figure 8.12: Typical adhesion curve as a colloidal probe is retracted from the surface of virgin membrane and citric acid pre-treated membrane following fouling with 2.0 wt. % Gum Arabic.

It is evident that following fouling, the pre-treatment of the membrane has a large influence on the properties of the foulant layer. Gum Arabic is a complex polysaccharide and protein mixture which leads to complications in understanding what is occurring. Studying the approach curve in Figure 8.11 it can be observed that for the pre-treated and fouled membrane there is repulsion ca. 90 nm from the membrane surface whereas for the fouled membrane there is slight repulsion ca. 20 nm from the membrane surface, with attractive forces ca. 320 pN dominating at 11 nm from the surface and ca. 260 pN at 5 nm from the surface. The repulsion in the pre-treated sample suggests the surface is dominated by carboxylic acid groups leading to repulsion between these and the negatively charged probe. However, the virgin membrane which was fouled is likely to have calcium cations leading to the attractive forces between these positive ions and the negatively charged OH groups on the silica probe. This hypothesis agrees with the zeta potential results with larger negative charge being observed for the pre-treated sample shown in Figure 8.8. Additionally, the shape of the approach curve for the fouled membrane following pre-treatment with citric acid suggests the probe may be cutting through a soft layer of foulant.

The membrane treated only with water shows a small adhesion strength over a small distance, when compared with the citric acid pre-treated membrane for retraction of the probe from the membrane. Comparing this with the membranes before fouling, it can be observed that the adhesion strength is increased following fouling. The pre-treated membrane shows a curve which follows the shape of a typical adhesion curve. For both of the fouled samples this peak tails off suggesting a low strength adhesion over a longer distance before the colloid tip and surface are separated. This is particularly evident for the sample pre-treated with citric acid. This curve is typical for samples which are viscous liquids suggesting that the Gum may form a viscous liquid on the membrane surface. With the Gum being highly soluble in water this is plausible, however the gel-like characteristics of Gum may also be responsible for this with the formation of an easily deformed gel layer. The multiple peaks present on retraction from the sample pre-treated with acid and subsequently fouled, suggests there are multiple binding points between the surface and the probe.

The sample pre-treated with acid may have resulted in improved adhesion of the calcium cations, leading to the increase in fouling propensity shown in Figure 8.3. This would lead to alterations in the structure of the foulant layer increasing the negative charge on the membrane surface and leading to improved rejection of Gum through charge interactions.

Studies were carried out on the membrane pre-treated with acid where the same point was tapped repeatedly with the probe to gain an insight into changes over time. It was shown that

there were two surfaces present, with the requirement to break through the first surface before reaching the second surface. The characteristics of the second surface were the same as that of the virgin membrane. This suggests that the citric acid forms a layer in the membrane surface which can be removed through tapping with a silica probe. After 1 minute without tapping the surface is restored.

Following pre-treatment with citric acid and fouling with Gum Arabic, time dependent studies were carried out using the silica probe on one point on the membrane. This time it was necessary to break through two different surfaces to get to the alumina. After one minute characteristics of the alumina surface could still be observed but there was movement of the Gum back to the surface. This is further evidence for the gel-like properties of the foulant layer alluded to in Chapter 5.

8.1.8 Discussion of pre-treatment with citric acid

Pre-treatment with citric acid leads to alterations in the surface chemistry of the alumina surface. This results in enhanced separation properties. The enhanced separation comes with an increase in the fouling propensity and membrane resistance following fouling. Pre-treating the membrane with citric acid results in the addition of carboxylate groups to the membrane confirmed using FTIR and SEM-EDX. The addition of these surface groups not only provides additional sites on the membrane surface for hydrogen bonding to occur, but also increases the attraction of positively charged metal cations such as calcium to the membrane surface. Through the use of zeta potential measurements and AFM studies it is hypothesised that the carboxylate groups on the membrane surface chelate with metal cations such as calcium present in the Gum. It is expected that this results in changes to the structure of the foulant layer. The chelation of cations means that at the surface of the foulant layer in contact with the solution, more negatively charged carboxylate groups from the amino acid of the Gum are present. This increased negative charge may lead to improved rejection characteristics of the Gum.

Pre-treating with acid results in the formation of two free carboxylate groups on the membrane surface for each citric acid molecule. These can form hydrogen bonds with carboxylate, aldehyde and alcohol groups present in Gum Arabic.

8.2 Pre-treatment with sodium hydroxide

Pre-treatment with sodium hydroxide was investigated as it was hypothesised that ion exchange would occur between hydrogen in the hydroxyl groups on the membrane surface and sodium, resulting in the formation of AlONa. Alternatively charge interactions could occur between the negatively charged OH groups on the membrane surface and positive sodium ions resulting in neutralisation of the surface. In a similar manner to pre-treating with citric acid, the pre-treatment with sodium hydroxide allows the possibility of changes in the separation and fouling tendencies of the membrane without compromising its mechanical strength.

8.2.1 Rejection of Gum Arabic

The concentration of Gum Arabic was monitored every five minutes throughout the filtration of 2.0 wt. % Gum Arabic through a 0.5 µm membrane with no pre-treatment, and following pre-treatment with sodium hydroxide. There was no change observed in the rejection of Gum with both samples showing the same rejection as seen for the membrane with no pre-treatment in Figure 8.2.

8.2.2 Effective contact angle

The effective contact angle was measured for membranes pre-treated with NaOH before and after fouling. The average effective contact angles, along with those for the virgin and fouled membranes, are reported in Table 8.8. It can be observed that the effective contact angle following both pre-treatment and fouling following pre-treatment was reduced. This suggests there is a change in the surface energy of the membrane and there is a slight change to the foulants which adhere during the fouling cycle. The attachment of sodium to the membrane is likely to be the influencing factor in this, as the membrane is well rinsed so that the rinsing solution has a pH of 7.0 before the PWF was measured or fouling carried out.

Table 8.8: Effective contact angle of water on membrane surface for virgin and NaOH pre-treated and fouled, measured by sessile drop.

Material	Measured effective contact angle (^{o})
Aluminium oxide	37 ± 4
NaOH treated aluminium oxide	31 ± 10
Fouled untreated membrane	104 ± 7
Fouled NaOH treated membrane	94 ± 10

8.2.3 Flux and membrane resistance

The reduction in contact angle allows an increased throughput of water through the membrane when measuring the PWF. This is due to the increased hydrophilicity and is shown by a reduction in the membrane resistance following pre-treatment. The normalised membrane flux for the first 5 minutes during filtration has been plotted in Figure 8.13. It can be observed that the initial flux decline is slower for the membrane pre-treated with NaOH, however after 60 minutes of fouling the resistance is larger for the pre-treated membrane (Table 8.9). The initial reduction in resistance rate is likely to be caused by the reduced negative charge on the membrane through the addition of sodium cations on the membrane surface. This is shown in Section 8.2.5. Following 60 minutes of filtration, the resistance increased to be 73 times that of the membrane resistance following alkali pre-treatment compared with 24 times that of the virgin membrane for the membrane pre-treated only with water. The increase in resistance may be due to differences in the conformation of the fouling layer leading to a denser fouling layer. Rinsing with water was shown to be ineffective with an increase rather than reduction in membrane resistance observed. This again highlights the possibility that a denser foulant layer is formed. The presence of sodium ions can lead to the formation of ion bridges between the membrane and foulant. This may be responsible for conformational changes in Gum, leading to a denser structure.

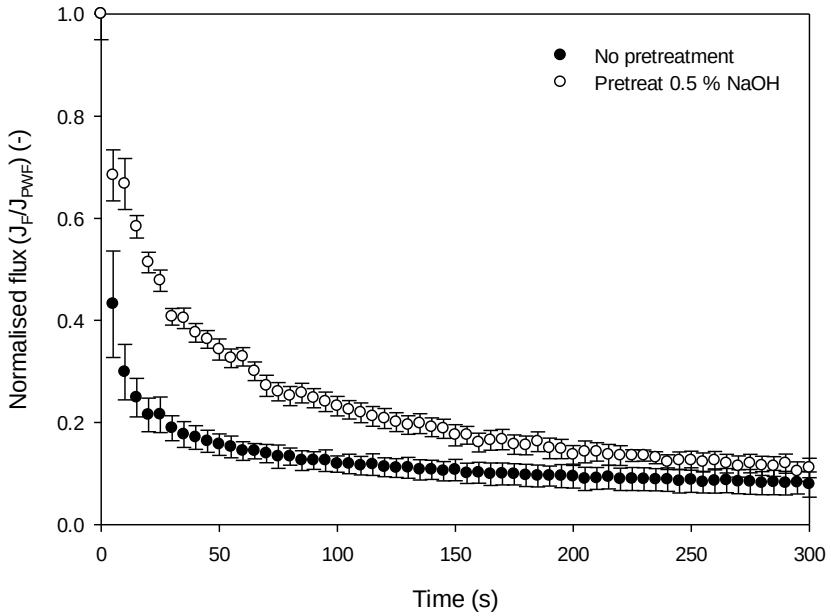

Figure 8.13: Influence of pre-treatment with 0.5 wt. % sodium hydroxide on the permeate flux during the first 5 minutes of a fouling cycle. Results are based on an average of three measurements with the error bars showing the standard deviation.

Table 8.9: Membrane resistance for 0.5 µm alumina membranes during fouling following a) no pre-treatment and b) pre-treatment with 0.5 wt. % sodium hydroxide.

Condition	**R_m** (x10^{10} m^{-1})	**R_T** (x10^{11} m^{-1})	**R_{rinsed}** (x10^{11} m^{-1})
No pre-treatment	1.22 ± 0.8	2.97 ± 0.3	1.2 ± 0.6
0.5 % NaOH pre-treatment	0.75 ± 0.4	5.50 ± 0.9	6.3 ± 0.8

Table 8.10: Normalised membrane resistance for 0.5 µm alumina membranes during and following a) no pre-treatment and b) pre-treatment with 0.5 wt. % sodium hydroxide. The membrane resistance is set to 1.0.

Condition	**R_m**	**R_T**	**R_{rinsed}**
No pre-treatment	1	24	10
0.1 % NaOH pre-treatment	1	74	84

The experimental flux data was fitted to the model detailed in Section 3.6.8 to allow the predominant fouling mechanism to be alluded to. The r^2 values are shown in Table 8.11, with the corresponding graphs shown in Appendix B. While cake formation was the dominant fouling mechanism observed for the first five minutes of filtration for the samples which had not

undergone pre-treatment, the sample which was pre-treated with sodium hydroxide showed pore constriction as the dominant fouling mechanism. This changes however for 5 – 60 minutes with no clear dominant mechanism for the 0.5 µm membranes which had not been pre-treated, whereas cake filtration is clearly dominant following pre-treatment with alkali. These results suggest that different interactions occur between the foulant and membrane, these are discussed in the rest of this chapter.

Table 8.11: Fouling mechanism based on laws proposed by Hermia[101] and extended for crossflow by Field *et al*[93]. Values are r^2 values are for curve fitting to the linear form of the equation.[91, 102, 103]

Experiment	Time	Pore blocking	Pore constriction	Cake formation	Intermediate pore blocking
0.5 µm no pre-treat	5	0.473	0.948	0.995	0.919
0.5 µm no pre-treat	60	0.499	0.895	0.913	0.933
0.5 µm pre-treated with alkali	5	0.891	0.991	0.985	0.942
0.5 µm pre-treated with alkali	60	0.756	0.971	0.995	0.964

8.2.4 FTIR and Raman spectroscopy

In a similar manner to the acid pre-treated membrane, no changes were observed in the Raman spectra following pre-treatment with sodium hydroxide. FTIR also showed little change from the virgin membrane as shown in Figure 8.14. The spectrum of the virgin membrane has been subtracted from that of the citric acid pre-treated and caustic pre-treated membranes, with the caustic spectrum showing almost no difference compared to the marked difference shown for the citric acid pre-treated membrane.

Following fouling of the two membranes the FTIR spectrum was measured and can be observed in Figure 8.15. The spectra are very similar, however the peaks at 3400 cm^{-1} shows an increase in intensity. This suggests for the pre-treated and fouled sample there is an increased presence of the asymmetric stretching of the O-H bond. No conclusions can be drawn on this information alone, however it suggests that either there is additional hydrogen bonding between OH groups, or there are more OH groups on the membrane surface compared with the fouled membrane which did not undergo pre-treatment.

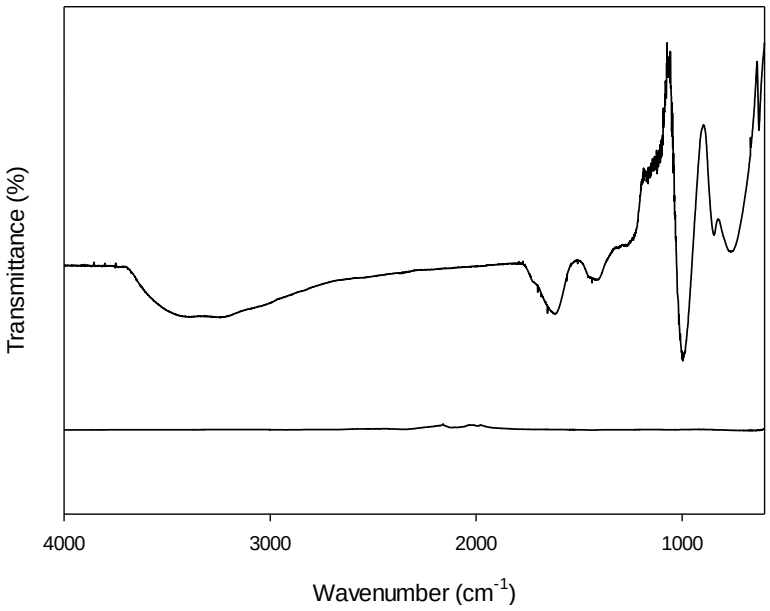

Figure 8.14: FTIR of membrane pre-treated with citric acid (top) and pre-treated with NaOH (bottom). Virgin membrane has been subtracted from spectra.

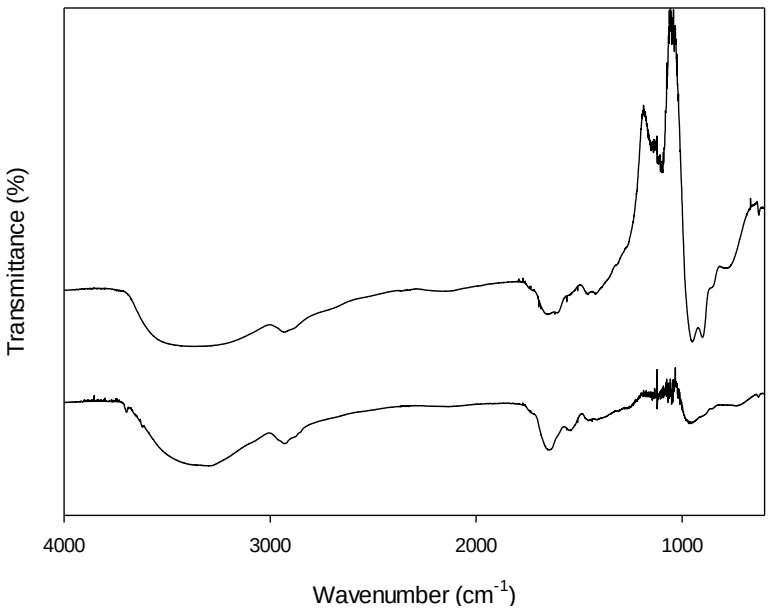

Figure 8.15: Membranes fouled with Gum Arabic following no pre-treatment (top) and alkali pre-treatment (bottom).

8.2.5 Zeta potential measurements

Zeta potential measurements were carried out on a membrane pre-treated with sodium hydroxide before and after fouling to allow a comparison between the membranes and establish changes occurring during the pre-treatment stage. Pre-treatment with NaOH reduces the negative charge of the membrane, shown in Figure 8.16. This reduction in charge is likely to be due to the adhesion of positive cations from the caustic cleaning agent to the negatively charged functional groups (OH^-) on the membrane surface. This has been confirmed using elemental analysis in Section 8.2.6. Following pre-treatment, the IEP is ca. pH 5.4, whereas the IEP of the virgin membrane is below pH 3.0. This shift in the IEP highlights changes to the surface chemistry following pre-treatment, and suggests the adhesion of positive charges to the membrane surface. The negatively charged virgin membrane may attract positive charges of Na^+ present in the NaOH cleaning solution. As a result of the attractive forces, the ions are strongly bound to the membrane surface, or in the membrane pores. It has previously been reported by Zuriaga-Augsti that the effective pore radius may be reduced due to the presence of the cations, which also changes the charge.[203] Based on the small size of sodium cations relative to the pore size in microfiltration, it would be expected this would have little effect. This was confirmed by the reduction in membrane resistance following pre-treatment. The change in charge leads to differences in the electrostatic interactions between the foulant and the membrane.

At the natural pH of Gum, the membrane has a charge of ca. -5 mV compared to ca. -30 mV for the virgin membrane. Based on this it would be expected that the pre-treated membrane would behave differently to the virgin membrane. At high pH values the membranes behave more similarly with the virgin membrane having a charge ca. -40 mV compared to ca. -32 mV for the alkali pre-treated membrane.

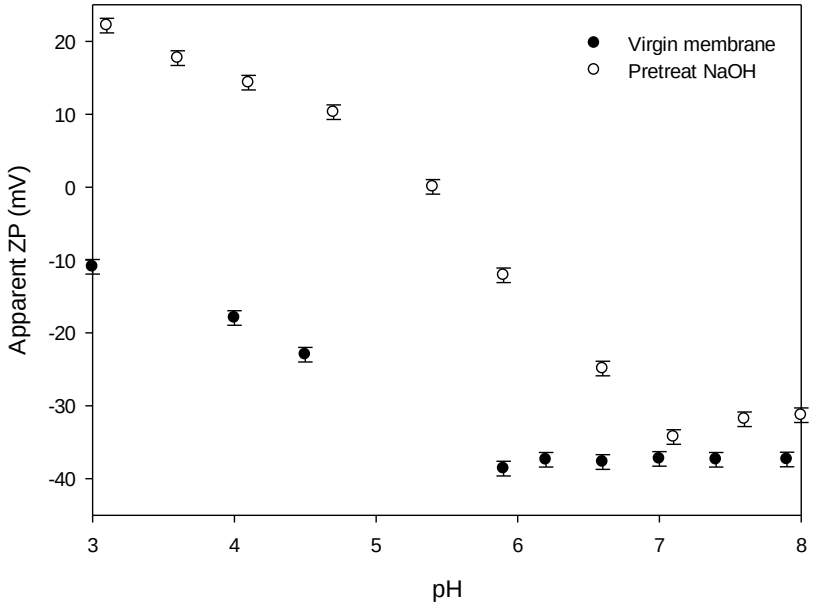

Figure 8.16: Comparison of zeta potential for untreated membrane and membrane pre-treated with 0.5 wt. % sodium hydroxide.

Following fouling, there is again a change in the zeta potential following the two different pre-treatments. For the membrane pre-treated with sodium hydroxide, the IEP following fouling is ca. pH 3.3. The IEP is below pH 3.0 for the fouled membrane which did not undergo pre-treatment. A more negatively charged surface was observed for the fouled membrane which had been pre-treated with sodium hydroxide suggesting that the foulants on the surface are different following the two pre-treatment methods. Comparing this with the FTIR results it is expected there are more OH groups from the aldehyde and alcohol present on the surface of the foulant layer. The reduced charge on the membrane following pre-treatment with sodium hydroxide may lead to a different configuration of Gum on the membrane surface. While the composition is very similar or the same as that of the foulant on the virgin membrane the configuration may be altered depending on the charge on the membrane, leading to attraction of positive, negative or neutral areas of the Gum. With Gum Arabic containing a proteinacious backbone with AG side groups, it is very likely that different functional groups present in the structure interact with different surfaces. This can result in differences in the foulant configuration.

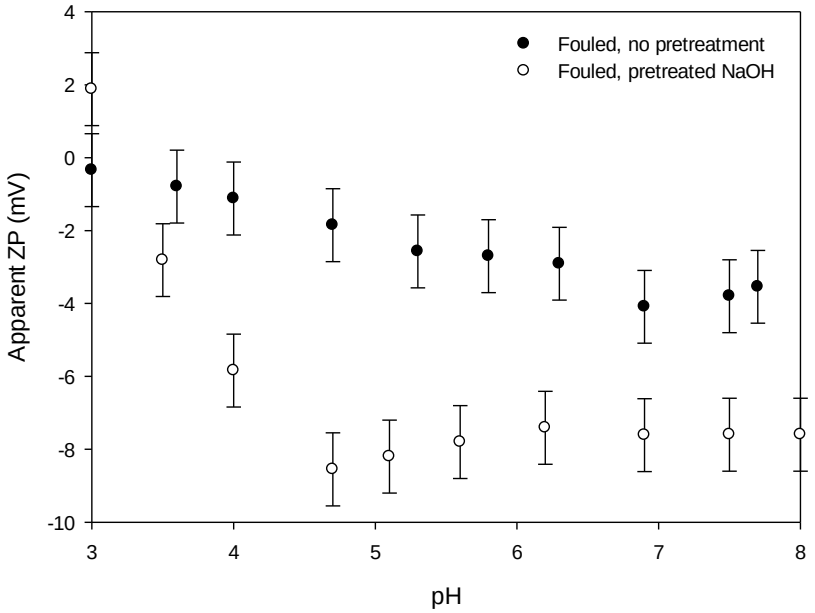

Figure 8.17: Comparison of zeta potential for fouled membranes with and without 0.5 wt. % sodium hydroxide pre-treatment.

8.2.6 SEM-EDX

Elemental analysis was carried out using SEM-EDX on the surface of fouled membranes in order to study the composition of the membranes before and after pre-treatment with sodium hydroxide, and following fouling. It can be seen in Table 8.12 that there is addition of sodium to the membrane highlighting the adsorption of sodium, or formation of ion exchange between sodium and hydrogen previously alluded to in this chapter. Sodium can be held responsible for the changes in zeta potential with positive cations leading to a reduction in the membrane charge.

Following fouling, there was little change to the composition of foulant on the membrane, however the level of calcium was noted to decrease. The presence of sodium on the membrane surface leading to charge neutralisation may result in less adsorption of calcium due to the reduced negative charge on the membrane. This would result in hydrogen bonding being the main fouling mechanism.

Table 8.12: SEM-EDX analysis of membrane surface for virgin membrane, sodium hydroxide pre-treated membrane and fouled membranes. All results are in wt. %. Elements showing '-' were not detected in the sample.

Sample	Al	O	C	Ca	Si	Na
Virgin membrane	50.6 ± 2.2	49.4 ± 4.3	-	-	-	-
Fouled	42.0 ± 3.8	46.8 ± 7.9	9.6 ± 6.5	0.8 ± 0.4	0.8 ± 0.4	-
Alkali pre-treat	44.5 ± 1.3	48.2 ± 3.2	-	-	1 ± 0.3	1.8 ± 0.6
Alkali pre-treat - fouled	42.9 ± 1.7	47.6 ± 3.7	8.2 ± 2.9	0.2 ± 0.2	1.2 ± 0.5	0.5 ± 0.1

8.2.7 AFM

AFM was used to study the different interactions between the membrane and a colloidal probe following pre-treatment with sodium hydroxide. Following pre-treatment, there was a slight increase in the average adhesion strength, with a reduction in the adhesion distance as shown in Table 8.13

Table 8.13: Adhesion distance and strength between virgin and NaOH pre-treated membrane and colloidal probe.

Preconditioning	Adhesion distance (nm)	Adhesion strength (pN)
Water	31.8 ± 7.6	690 ± 240
Alkali (NaOH)	16.5 ± 7.7	950 ± 270

Typical force curves are shown in Figures 8.18 and 8.19 for the approach and retraction of the probe to the membrane surface respectively. It can be seen in Figure 8.18 that during the approach there is very little difference following pre-treatment with both membranes showing repulsion from ca. 15 – 20 nm from the membrane surface. The zeta potential results show that both membranes are negatively charged therefore similar interactions would be expected. The retraction of the probe from the membrane surface shows a subtle difference between the two membranes with the formation of only one peak for the alkali pre-treated membrane compared to the strong adhesion followed by long range weak adhesive interactions observed for the sample which was not pre-treated. This suggests that the addition of sodium cations to the membrane surface counteracts some of these long range adhesive interactions. Based on this reduced membrane fouling would be expected, however this was not shown in Section 8.2.3.

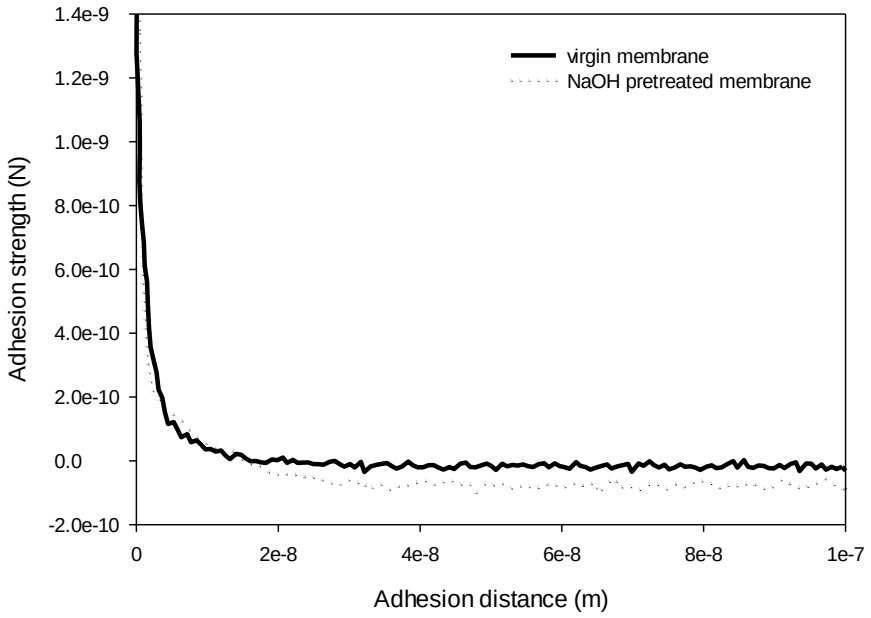

Figure 8.18: Adhesion curve for the approach of silica probe to a) membrane pre-treated with water (virgin membrane) and b) membrane pre-treated with 0.5 wt. % sodium hydroxide.

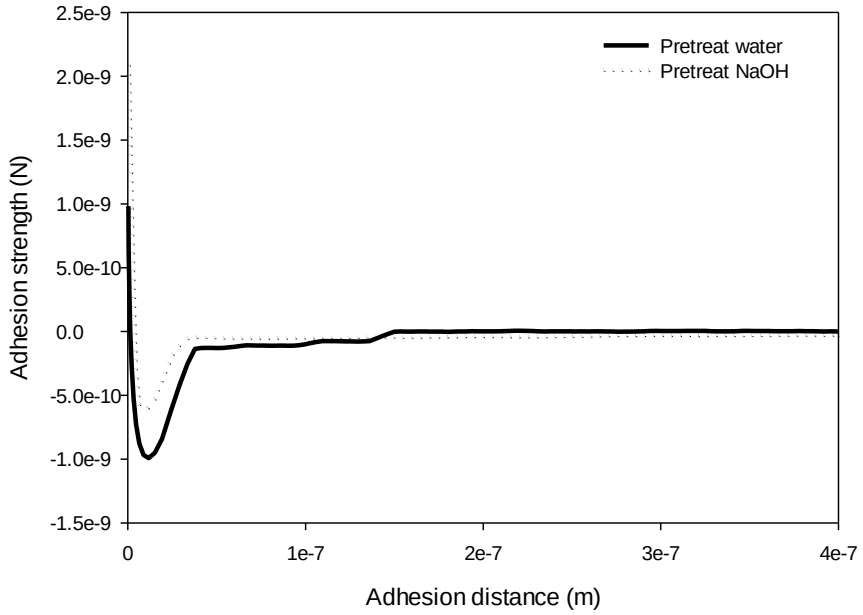

Figure 8.19: Adhesion curve for the retraction of a silica probe to a) membrane pre-treated with water (virgin membrane) and b) membrane pre-treated with 0.5 wt. % sodium hydroxide.

Following fouling, there was a larger difference in the adhesion of the two membranes. Table 8.14 shows the average fouling distance and strength measured across 10 points on the membrane surface for the two fouled membranes. It can be observed that for the membrane pre-treated with alkali and fouled, both the adhesion distance and adhesion strength are increased.

Table 8.14: Adhesion distance and strength between virgin and alkali pre-treated membranes which have been fouled with Gum Arabic and a colloidal probe.

Preconditioning	Adhesion distance (nm)	Adhesion strength (pN)
Water	36.8 ± 10	1130 ± 330
Alkali (NaOH)	881 ± 300	3370 ± 1320

It is evident that following fouling, the pre-treatment of the membrane has a large influence on the properties of the foulant layer. The complexity of Gum leads to difficulties in understanding exactly what is happening, but it is apparent that following pre-treatment with sodium hydroxide that the foulant layer has an increased adhesion strength and distance. During the approach (Figure 8.20) there is less attraction with the pre-treated and fouled sample showing a small adhesion peak ca. 5 nm from the surface, compared the two larger peaks 20 nm and 11 nm from the surface on the fouled sample which was pre-treated with water alone.

For the retraction curve, Figure 8.21 shows that the adhesion strength is greater following fouling than before fouling. This is due to the wide range of groups in the Gum which can interact with the silica probe. Both curves show a neat curve similar in shape to a typical adhesion curve with a tail caused by long range interactions. The tail due to long range interactions is still present for the sample fouled following NaOH pre-treatment, however this is less pronounced than for the other fouled sample. This shows there is a period of long range weak interactions before the tip and sample are separated. These are typical of gel and viscous liquid samples highlighting that the foulant layer is likely to be a gel layer as alluded to in Chapter 5, for both samples.

The results in Section 8.2.4 and 8.2.5 suggested that following pre-treatment with sodium hydroxide and subsequent fouling, there were more OH or COOH groups on the surface compared with the fouled membrane which had not undergone any pre-treatment. While it is unknown what is responsible for the change in conformation in Gum under these conditions the adhesion strength following fouling, corroborates this suggestion. If there are additional OH and COOH groups on the membrane surface these can form hydrogen bonds with OH groups on the silica tip leading to an increase in the adhesion.

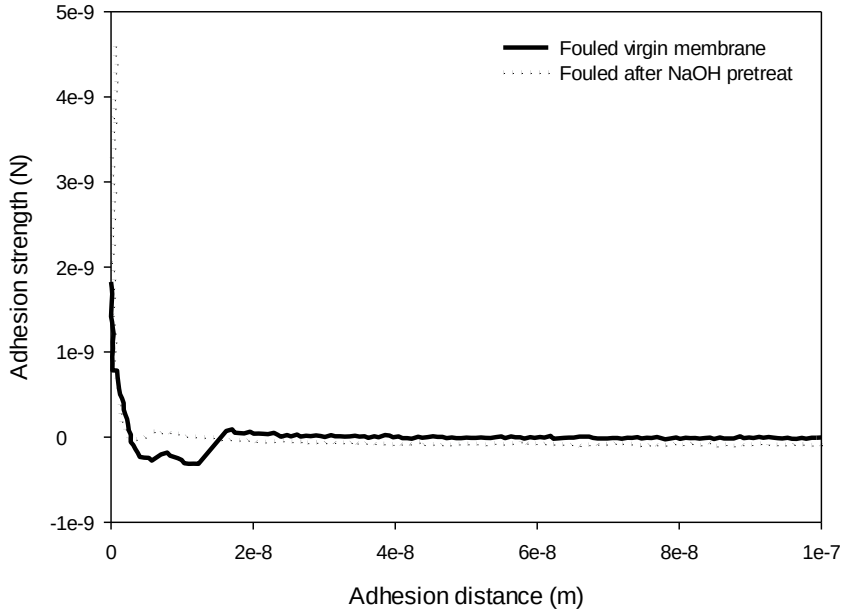

Figure 8.20: Adhesion strength on the approach of silica probe to membranes fouled with Gum Arabic following pre-treatment with a) water and b) sodium hydroxide.

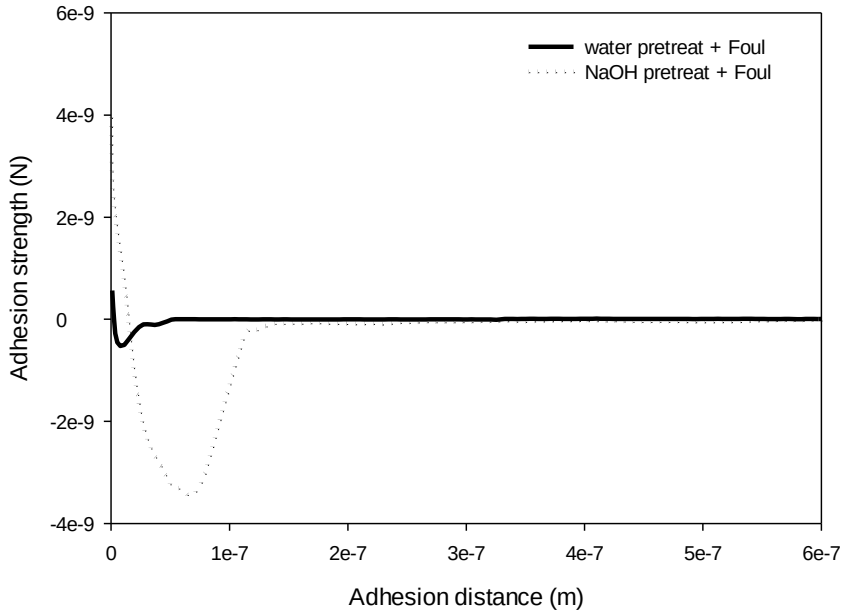

Figure 8.21: Adhesion strength on the retraction of silica probe to membranes fouled with Gum Arabic following pre-treatment with a) water and b) sodium hydroxide.

8.2.8 Discussion of NaOH pretreatment

A simple pre-treatment using sodium hydroxide, which is a commonly used cleaning agent, leads to alterations in the foulant layer formed during the microfiltration of 2.0 wt. % Gum Arabic. The initial flux decline is reduced following pre-treatment, however it is hypothesised that a denser foulant layer is formed leading to an increase in the membrane resistance following 60 minutes of filtration. Studies carried out showed that there is adhesion of sodium to the membrane during pre-treatment. This results in a reduction in the membrane charge at the natural pH of Gum Arabic. The fouled samples show variation which is likely to be due to a conformational change in the foulant layer. Following pre-treatment with sodium hydroxide, the results obtained suggest that the foulant layer contained more OH or COOH groups on the membrane surface. This leads to an increased potential for hydrogen bonding and may be responsible for the increased fouling severity. It is possible that the reduced charge on the membrane surface prevents the adhesion of calcium cations to the membrane surface resulting in hydrogen bonding being the most prevalent mechanism by which the foulant layer forms. The formation of hydrogen bonding is generally slower than charge interactions and could be responsible for the reduction in fouling rate. Strong hydrogen bonding within Gum is known to lead to the gel like properties, therefore increases in this may be responsible for producing a denser foulant layer. Further work is required to investigate the density of the foulant layer, however as the layer is so thin (reported in Chapter 5) this is challenging to investigate with current technologies available.

8.3 Summary

In terms of separation, pre-treatment with citric acid outperforms the membranes with no pre-treatment (only water) and following pre-treatment with sodium hydroxide. The enhanced separation comes with a penalty of increased fouling compared to the virgin membrane. It is expected that the increase in separation is due to electrostatic and charge interactions shown by the large difference in ZP for fouling following pre-treatment with citric acid compared to fouling of a virgin membrane.

Pre-treatment with citric acid leads to the formation of strong bonding between the citric acid and the membrane surface. This leads to the formation of two free carboxylic acid groups on the surface and leads to an increase in the IEP of the membrane. Citric acid acts as a chelating group with metal cations. It is therefore proposed that the increase in fouling rate following pre-

treatment with citric acid leads to attraction between the positively charged metal cations in the Gum (calcium ions) and the negatively charged carboxylic acid groups on the membrane surface.

Pre-treatment with sodium hydroxide results in the presence of sodium cations on the membrane surface, this reduces the zeta potential on the membrane resulting in a small negative charge at the natural pH of Gum. This leads to little charge interaction suggesting that hydrogen bonding is the dominant mechanism of fouling for this sample.

The adhesion of the membranes has been measured using AFM with a colloidal probe, giving an insight as to what is occurring. Pre-treatment with citric acid leads to a layer with strong adhesion forces. The strong forces observed are likely to be hydrogen bonds forming between the carboxylic acid groups on the membrane and OH groups on the silica surface. Following fouling the adhesion strength was greatest for the membrane pre-treated with sodium hydroxide. It is hypothesised that the pre-treatment influences the conformation of Gum in the fouling layer with an increased number of OH or COOH groups found on the surface of the foulant following alkali pre-treatment. The increase of these groups allows an increase in hydrogen bonding between the surface and probe resulting in greater adhesion strength and distance. The adhesion following fouling is smaller for the acid pre-treated membrane, which again highlights the importance of hydrogen bonding between the probe and silica tip.

It was hoped that pre-treatment would allow a reduction in the fouling propensity of the membrane and the development of antifouling membranes. This was not achieved, however an increase in separation could be achieved. While antifouling membranes could not be formed following these pre-treatment methods they allowed a greater insight into the cause of membrane fouling and the interaction between the surface of the membrane and foulant.

9. Conclusions, recommendations and future work

9.1 Conclusions

This thesis aims to show the potential for membrane technology to be used in the industrial application of removing Gum Arabic from the waste streams produced through spray drying during the industrial processing of Gum. Detailed conclusions are given in the discussion and summary at the end of each chapter, so this chapter aims to bring together the overall findings of the thesis and provide recommendations and further studies which can be carried out.

The aim of this thesis as eluded to in the title is to reduce both water and energy consumption during the filtration of Gum Arabic. The focus has been on the wastewater produced. This waste from the spray driers is one of the areas of biggest environmental and financial concern during the process. The water produced contains ca. 2.0 wt. % Gum Arabic, which has a high COD. Not only does this lead to the disposal of very large quantities of water, but it is an expensive and energy intensive process with the water needing tankered away and injected into land. While membranes require energy in the form of pumps to allow separation, this is seen as a much more energy friendly method compared with alternatives such as land injection and distillation.

The rejection of ca. 90 % of Gum from the model waste solution not only allows water to be disposed using a cheaper alternative to land injection, it also means there can be a huge saving in water costs. This saving can be obtained by recycling water as illustrated in Figure 1.1.

Studies carried out show the use of membrane technology to be effective in the removal of Gum Arabic from a model process wastewater stream. The use of a 0.8 µm alumina ceramic membrane allowed ca. 90 % rejection of Gum in the permeate after seven cycles. However fouling, which is inevitable in complex food products, was found to be a problem.

The permeate flux decreased quickly when the feed suspension contained Gum Arabic under both static and dynamic conditions. A number of factors were investigated and it was shown that fouling can be minimised by applying a high crossflow velocity and a low transmembrane pressure during filtration. High temperatures also led to a reduction in viscosity, and this also aids the filtration process, however an increase in temperature led to a reduction in rinsable fouling (that which could be removed through rinsing with water).

The membrane pore size had little effect on the permeate flux following 60 minutes of filtration, however increased separation was achieved using 0.2 µm membranes compared to larger pore

sizes. Pre-filtration showed little influence on the permeate flux with an increase in pore constriction observed over the first five minutes for pre-filtered Gum compared with cake filtration for the unfiltered Gum.

The foulant layer is hypothesised to be a gel layer which fits well with the results shown by SEM, porosometry, AFM and the known properties of Gum Arabic. Complexation between calcium ions and carboxylic acid groups can lead to a highly cross-linked gel-like structure. The presence of calcium was shown using SEM-EDX.

Following the initial deposition of a foulant layer on the membrane surface, leading to rapid flux decline, foulant-foulant interactions become dominant. The foulant layer has a large number of carboxylic acid, aldehyde and alcohol groups on the surface which can form hydrogen bonds. This leads to increased adhesion between a colloidal probe and the fouled surface.

Most of the fouling observed was irreversible, and could not be removed through rinsing with water; therefore, a chemical cleaning protocol was developed. The use of a two stage clean of a combined cleaning solution containing 0.5 wt. % sodium hydroxide and 200 ppm sodium hypochlorite followed by 0.1 wt. % citric acid led to a flux recovery of 86 ± 5 %. The use of citric acid as a single component cleaning agent shows some promise, however it was not found to be as effective as when followed by alkali cleaning. It is hypothesised that the sodium hydroxide leads to swelling of the Gum, and citric acid dissolves the foulant and chelates the sodium and calcium cations leading to weakening and dissolution of the foulant layer. The chelation of the metal cations can remove strong ion bridges, leading to weakening of the structure of the foulant layer.

Two mechanical cleaning methods were investigated. Backwashing was ineffective and this is expected to be as a result of the easy deformability of the gel-like foulant layer. Cleaning under sonication resulted in a flux recovery of 91 ± 5 % and is expected to be as a result of breaking down the carbohydrate and protein into sugar and amino acid moieties.

While cleaning over one cycle gives a good indication as to the removal mechanisms, it does not give any information about the long term aging of the membrane. Ten cycles were studied with two cleaning protocols. Cleaning with alkali followed by acid resulted in a greater flux recovery than cleaning with alkali alone over the first cycle. This significant increase was not observed over multiple cycles. After 10 cycles the difference in FR was small with a FR of 24 ± 5 % for the two stage clean compared with 23 ± 6 % for the alkali clean alone. In addition to the flux recovery it is important to consider the fouling flux and separation properties. A higher filtration flux was

observed following the two stage clean, along with increased separation. This suggests that while the FR is similar for both cleaning protocols, the two stage clean leads to an improvement in separation efficiency.

Pre-treating the membranes was conducted using an alkali cleaning agent (sodium hydroxide) and an acidic cleaning agent (citric acid). Neither pre-treatment method reduced the membrane fouling, however increased separation was observed following pre-treatment with citric acid. The increased separation can be attributed to rapid adsorption of positively charged calcium cations to the negatively charged carboxylic acid groups on the membrane surface leading to a foulant layer on the surface. Repulsion then occurs between the foulant layer and Gum in suspension increasing the rejection.

9.2 Recommendations

Microfiltration can be applied to allow separation of Gum Arabic and water allowing reuse of both the Gum and water. Fouling is a large issue. It is hypothesised there is the formation of a highly cross-linked gel like layer on the membrane surface therefore regular cleaning will be required. In order to minimise fouling and optimise separation a 0.2 µm membrane should be operated at low transmembrane pressure and high crossflow velocity. Operation ca. 30 ^{o}C allows a reduction in viscosity increasing the flux, but allows greater removal of Gum through rinsing with water.

In order to clean the membrane effectively cleaning should be carried out in the presence of ultrasound. A two stage chemical clean was also shown to be effective using 0.5 wt. % sodium hydroxide + 200 ppm sodium hypochlorite followed by citric acid. Citric acid not only allows greater removal of the Gum but also allows improved separation properties for the subsequent cycles.

9.3 Future work

This study has gained an insight about the fouling mechanism and characteristics of the microfiltration of Gum Arabic, however there is further work which can be carried out to build on the understanding gained here.

9.3.1 Hybrid system

The use of a hybrid system could be investigated to 'polish' the permeate leading to increased Gum removal. Microfiltration was investigated here in order to maintain a high throughput, however it was established that the pore size was not the limiting factor for permeate flux. The use of ultrafiltration systems could be investigated both for the filtration of 2.0 wt. % model wastewater or to polish the permeate resulting in a two stage system with the potential for improved separation properties.

9.3.2 Gum pre-treatment

The model waste stream created comprised only of spray dried Gum which had been processed. At *Kerry Ingredients* (Cam, UK) ca. 90 % of the waste comes from the spray driers, however ca. 10 % is raw Gum obtained earlier in the process.[7] A comparison study should be carried out between the raw and spray dried Gum to determine if they have the same separation properties and fouling mechanisms. The presence of bark and sand may lead to further complications in membrane fouling.

It has previously been reported that harsh conditions such as spray drying lead to alterations in the Gum structure. This can lead to an increase in the aggregates formed. Raw Gum may not contain aggregates and therefore its behaviour during microfiltration should be studied.

While the work carried out in this study has focused on spray dried Gum Arabic, which has undergone thermal pasteurisation due to the industrial relevance for *Kerry Ingredients* (Cam, UK), there are a number of other methods used for the decontamination of Gum Arabic during processing. Until this year chemical treatment with ethylene bromine has been common, however this has now been banned due to the harm it causes to the ozone layer.[254, 255] This has led to the investigation of alternative decontamination methods. Thermal pasteurisation is commonly used, however there are alternative methods of decontamination such as gamma/electron radiation.[256] It is known that heat treatment can influence the structure and properties of Gum Arabic, and heating too much can result in denaturation of the protein. Zaied *et al.* reported that following irradiation there is no adverse effect on the physical properties of the final Gum product.[256] However investigations as to the influence of pasteurisation on the Gum structure and thus the impact on fouling of ceramic membranes would be interesting to see if there are any differences based on the decontamination method particularly when free radicals can be detected in Gum Arabic 60 days after irradiation.[255]

Pre-treatment of the Gum in terms of pH, ionic strength and peroxidation could be considered. These were not investigated during this study as they can prevent the reuse of Gum. They may greatly reduce the fouling and lead to increased separation allowing reuse of water with a reduction in the requirement to clean the system. This may lead to improved environmental benefits reducing the impact of the process.

9.3.3 Alternative membrane systems

Only one material was investigated in this study – α-alumina. It was discovered that interactions occurred between the hydroxyl groups on the membrane surface and Gum. The use of a membrane material with no charge which cannot form hydrogen bonds may lead to a reduction in the fouling propensity. Gum contains many negatively charged alcohol and carboxylic acid groups, however it also contains metal cations. Due to this it can form charge interactions with positively or negatively charged membranes. In addition carboxylic acid groups can form strong hydrogen bonds. A membrane material which prevents this may reduce fouling. Separation may be affected and this also needs to be considered. Bernat *et al.* reported that ceramics often lead to improved separation characteristics due to the adsorption phenomena.[192]

Recently the development of membranes operated with electric fields or ultrasonic fields superimposed has showed great promise for complex or charged solutions as the separation is not only carried out by size exclusion, but also by charge separation. This can allow a reduction in the fouling as well as increases in rejection of charged components. A number of authors have shown this to work with proteinacious solutions.[58, 257-259] The electric field acts as an additional driving force along with the TMP. This may not have an influence as it has been shown to prevent fouling mainly where there is a large concentration polarisation, however due to the charges associated with Gum Arabic this process has good potential for increased separation. The use of electrically enhanced membrane filtration (EMF) has been shown to reduce the formation of a surface layer of foulant on the membrane surface. EMF offers the potential for extremely low fouling due to electrostatic repulsion between the membrane surface and foulant. pH and ionic strength allow control on the charge on the protein. Since proteins carry a net electric charge an electrical field can be used to reduce the influence of a polarized layer.[58] Sung *et al.* observed that as voltage increased, the cake layer decreased, and at critical voltage no particle deposition was observed.[260]

9.3.4 Cleaning agents

This study only investigated a small number of cleaning agents in order to determine their properties and to understand the processes resulting in the foulant removal. Investigation should be carried out using surfactants to gain an understanding about how these influence the foulant layer and subsequent removal.

Hydrogen peroxide (H_2O_2) should be investigated as an oxidising agent rather than NaOCl. H_2O_2 has the advantage that it does not contain chlorine therefore is often considered environmentally friendly and only produces water as a by-product. A case study for this is required with the whole process considered as the production of hydrogen peroxide can be energy intensive, therefore at the low concentrations, the required concentration of NaOCl may be more environmentally friendly.

10. Bibliography

1. Sparreboom, E., Cam accounting mass balance 2012. *Kerry Ingredients*, 2013.
2. Ali, B. H.; Ziada, A.; Blunden, G., Biological effects of gum arabic: A review of some recent research. *Food Chem. Toxicol.* **2009,** *47*, 1-8.
3. Islam, A. M.; Phillips, G. O.; Sljivo, A.; Snowden, M. J.; Williams, P. A., A review of recent developments on the regulatory, structural and functional aspects of gum arabic. *Food Hydrocolloids* **1997,** *11*, 493-505.
4. Verbeken, D.; Dierckx, S.; Dewettinck, K., Exudate gums: occurrence, production, and applications. *Appl. Microbiol. Biotechnol.* **2003,** *63*, 10-21.
5. Panda, H., *The Complete Technology Book On Natural Products (Forest Based)*. National Institute of Industrial Research **2002**.
6. Chandrasekhar, K. Global Gum Arabic market is estimated to be worth $800.3 million by 2019, at a CAGR of 6.7 % from 2014 to 2019. www.prnewswire.com/news-releases/global-gum-arabic-market-is-estimated-to-be-worth-8003-million-by-2019-at-a-carg-of-67-from-2014-to-2019-507365731.html (accessed 31-8-15),
7. Carr, D., Information about Gum processing at Kerry. Cam, UK, **2012**.
8. Idris, O. H. M.; Williams, P. A.; Phillips, G. O., Characterisation of gum from Acacia senegal trees of different age and location using multidetection gel permeation chromatography. *Food Hydrocolloids* **1998,** *12*, 379-388.
9. Al-Assaf, S.; Sakata, M.; McKenna, C.; Aoki, H.; Phillips, G. O., Molecular associations in acacia gums. *Struct. Chem.* **2009,** *20*, 325-336.
10. Nussinovitch, A., *Hydrocolloid Applications: Gum technology in the food and other industries*. Springer US.**2012**; p 354.
11. Yanniotis, S.; Taoukis, P.; Stodforos, N.; Karathanos, V. T., *Advances in Food Process Engineering Research and Applications*. Springer: USA, **2013**.
12. Furlong, A.; Collis, A. *Chemical Engineering Matters - A review of IChemE's technical strategy*; Institute of Chemical Engineers. Feburary 2013, **2013**.
13. Water scarcity. www.un.org/waterforlifedecade/scarcity.shtml (accessed 31-08-2015),
14. Schuchmann, H. P.; Kohler, K.; Emin, M. A.; Schubert, H., *Food Process Engineering Research and Innovation in a Fast Changing World: Paradigms/Case Studies*. Springer: USA, **2013**.
15. Pouliot, Y., Membrane processes in dairy technology - From a simple idea to worldwide panacea. *International Dairy Journal* **2008,** *18*, 735-740.
16. Henning, D. R.; Baer, R. J.; Hassan, A. N.; Dave, R., Major advances in concentrated and dry milk products, cheese, and milk fat-based spreads. *J. Dairy Sci.* **2006,** *89*, 1179-1188.
17. Eckner, K. F.; Zottola, E. A., Potential for the low-temperature pasturisation of Dairy fluids using membrane processing. *J. Food Prot.* **1991,** *54*, 793-797.
18. Head, L. E.; Bird, M. R., The removal of psychrotropicspores from milk protein isolate feeds using tubular ceramic microfilters. *J. Food Process Eng.* **2013,** *36*, 113-124.
19. Walkling-Ribeiro, M.; Rodriguez-Gonzalez, O.; Jayaram, S.; Griffiths, M. W., Microbial inactivation and shelf life comparison of 'cold' hurdle processing with pulsed electric fields

and microfiltration, and conventional thermal pasteurisation in skim milk. *International Journal of Food Microbiology* **2011,** *144*, 379-386.

20. Decloux, M.; Dornier, M.; Gratius, I., Crossflow microfiltration of gum arabic solutions: Comparison of the classical system with the co-current permeate flow system. *International Journal of Food Science and Technology* **1996,** *31*, 153-166.
21. Bechervaise, P. The microfiltration of high solids content gum arabic streams for the purpose f removing thermo-resistant spores. University of Bath, Bath, **2013**.
22. Renard, D.; Lavenant-Gourgeon, L.; Lapp, A.; Nigen, M.; Sanchez, C., Enzymatic hydrolysis studies of arabinogalactan-protein structure from Acacia gum: The self-similarity hypothesis of assembly from a common building block. *Carbohydr. Polym.* **2014,** *112*, 648-661.
23. Mahendran, T.; Williams, P. A.; Phillips, G. O.; Al-Assaf, S.; Baldwin, T. C., New insights into the structural characteristics of the arabinogalactan - Protein (AGP) fraction of gum Arabic. *J. Agric. Food. Chem.* **2008,** *56*, 9269-9276.
24. Jayme, M. L.; Dunstan, D. E.; Gee, M. L., Zeta potentials of gum arabic stabilised oil in water emulsions. *Food Hydrocolloids* **1999,** *13*, 459-465.
25. Dror, Y.; Cohen, Y.; Yerushalmi-Rozen, R., Structure of gum arabic in aqueous solution. *Journal of Polymer Science Part B-Polymer Physics* **2006,** *44*, 3265-3271.
26. Ma, F.; Bell, A. E.; Davis, F. J.; Chai, Y., Effects of high hydrostatic pressure and chemical reduction on the emulsification properties of gum arabic. *Food Chem.* **2015,** *173*, 569-576.
27. Motlagh, S.; Ravines, P.; Karamallah, K. A.; Ma, Q., The analysis of Acacia gums using electrophoresis. *Food Hydrocolloids* **2006,** *20*, 848-854.
28. Whistler R; Danie, R., Function of polysaccharide. In *Food Additives* Whistler, R. L., Ed. Dekker: New York, **1990**.
29. Qi, W.; Fong, C.; Lamport, D. T. A., Gum-Araboc glycoprotein is a twisted hairy rope - a new model based on O-glactosylhydroxyproline as the polysaccharide attachment site. *Plant Physiology* **1991,** *96*, 848-855.
30. Mao, P.; Zhao, M.; Zhang, F.; Fang, Y.; Phillips, G. O.; Nishinari, K.; Jiang, F., Phase separation induced molecular fractionation of gum arabic-Sugar beet pectin systems. *Carbohydr. Polym.* **2013,** *98*, 699-705.
31. Picton, L.; Bataille, I.; Muller, G., Analysis of a complex polysaccharide (gum arabic) by multi-angle laser light scattering coupled on-line to size exclusion chromatography and flow field flow fractionation. *Carbohydr. Polym.* **2000,** *42*, 23-31.
32. Nie, S.-P.; Wang, C.; Cui, S. W.; Wang, Q.; Xie, M.-Y.; Phillips, G. O., A further amendment to the classical core structure of gum arabic (Acacia senegal). *Food Hydrocolloids* **2013,** *31*, 42-48.
33. Churms, S. C.; Merrifield, E. H.; Stephen, A. M., Some new aspects of the Molecular structure of Accacia-Senegal gum (Gum Arabic). *Carbohydr. Res.* **1983,** *123*, 267-279.
34. Anderson, D. M. W.; Stoddart, J. F., Studies on uronic acid materials: XV. The use of molecular-sieve chromatography in studies on Acacia Senegal gum (gum arabic). *Carbohyd Res* **1966,** *2*, 104-114.
35. Cui, S. W.; Phillips, G. O.; Blackwell, B.; Nikiforuk, J., Characterisation and properties of Acacia senegal (L.) Willd. var. senegal with enhanced properties (Acacia (sen) SUPERGUM (TM)): Part 4. Spectroscopic characterisation of Acacia senegal var. senegal and Acacia (sen) SUPERGUM (TM) arabic. *Food Hydrocolloids* **2007,** *21*, 347-352.

36. Defaye, J.; Wong, E., Structural sudies of Gum Arabic, the exutate polysaccharide from Accacia-Senegal. *Carbohydr. Res.* **1986,** *150*, 221-231.

37. Street, C. A.; Anderson, D. M. W., Refinement of structures previously proposed for Gum Arabic and other Accacia exudates. *Talanta* **1983,** *30*, 887-893.

38. Wang, Q.; Burchard, W.; Cui, S. W.; Huang, X.; Phillips, G. O., Solution properties of conventional gum arabic and a matured gum arabic (Acacia (sen) SUPER GUM). *Biomacromolecules* **2008,** *9*, 1163-1169.

39. Randall, R. C.; Phillips, G. O.; Williams, P. A., Fractionation and characterization of gum from Acacia senegal. *Food Hydrocolloids* **1989,** *3*, 65-75.

40. Sanchez, C.; Schmitt, C.; Kolodziejczyk, E.; Lapp, A.; Gaillard, C.; Renard, D., The acacia gum arabinogalactan fraction is a thin oblate ellipsoid: A new model based on small-angle neutron scattering and ab initio calculation. *Biophys. J.* **2008,** *94*, 629-639.

41. Nie, S.-P.; Wang, C.; Cui, S. W.; Wang, Q.; Xie, M.-Y.; Phillips, G. O., The core carbohydrate structure of Acacia seyal var. seyal (Gum arabic). *Food Hydrocolloids* **2013,** *32*, 221-227.

42. Dickinson, E., Hydrocolloids at interfaces and the influence on the properties of dispersed systems. *Food Hydrocolloids* **2003,** *17*, 25-39.

43. Elmanan, M.; Al-Assaf, S.; Phillips, G. O.; Williams, P. A., Studies on Acacia exudate gums: Part VI. Interfacial rheology of Acacia senegal and Acacia seyal. *Food Hydrocolloids* **2008,** *22*, 682-689.

44. Al-Majed, A. A.; Abd-Allah, A. R. A.; Al-Rikabi, A. C.; Al-Shabanah, O. A.; Mostafa, A. M., Effect of oral administration of arabic gum on cisplatin-induced nephrotoxicity in rats. *Journal of Biochemical and Molecular Toxicology* **2003,** *17*, 146-153.

45. Al-Majed, A. A.; Mostafa, A. M.; Al-Rikabi, A. C.; Al-Shabanah, O. A., Protective effects of oral Arabic gum administration on gentamicin-induced nephrotoxicity in rats. *Pharmacol. Res.* **2002,** *46*, 445-451.

46. Ali, B. H., Does gum arabic have an antioxidant action in rat kidney? *Renal Failure* **2004,** *26*, 1-3.

47. Codipilly, C. N.; Wapnir, R. A., Proabsorptive action of gum arabic in isotonic solutions orally administered to rats. II. Effects on solutes under normal and secretory conditions. *Digestive Diseases and Sciences* **2004,** *49*, 1473-1478.

48. Wapnir, R. A.; Wingertzahn, M. A.; Mayse, J.; Teichberg, S., Gum arabic promotes rat jejunal sodium and water absorption from oral rehydration solutions in two models of diarrhea. *Gastroenterology* **1997,** *112*, 1979-1985.

49. Teichberg, S.; Wingertzahn, M. A.; Moyse, J.; Wapnir, R. A., Effect of gum arabic in an oral rehydration solution on recovery from diarrhea in rats. *Journal of Pediatric Gastroenterology and Nutrition* **1999,** *29*, 411-417.

50. Li, X.; Fang, Y.; Al-Assaf, S.; Phillips, G. O.; Nishinari, K.; Zhang, H., Rheological study of gum arabic solutions: Interpretation based on molecular self-association. *Food Hydrocolloids* **2009,** *23*, 2394-2402.

51. Mothe, C. G.; Rao, M. A., Rheological behavior of aqueous dispersions of cashew gum and gum arabic: effect of concentration and blending. *Food Hydrocolloids* **1999,** *13*, 501-506.

52. Sanchez, C.; Renard, D.; Robert, P.; Schmitt, C.; Lefebvre, J., Structure and rheological properties of acacia gum dispersions. *Food Hydrocolloids* **2002,** *16*, 257-267.

53. Weinbreck, F.; Wientjes, R. H. W., Rheological properties of whey protein/gum arabic coacervates. *J. Rheol.* **2004,** *48*, 1215-1228.

54. Li, X. B.; Fang, Y. P.; Zhang, H. B.; Nishinari, K.; Al-Assaf, S.; Phillips, G. O., Rheological properties of gum arabic solution: From Newtonianism to thixotropy. *Food Hydrocolloids* **2011,** *25*, 293-298.

55. Garti, N., Hydrocolloids as emulsifying agents for oil-in-water emulsions. *J. Dispersion Sci. Technol.* **1999,** *20*, 327-355.

56. Renard, D.; Garnier, C.; Lapp, A.; Schmitt, C.; Sanchez, C., Structure of arabinogalactan-protein from Acacia gum: From porous ellipsoids to supramolecular architectures. *Carbohydr. Polym.* **2012,** *90*, 322-332.

57. Lopez-Torrez, L.; Nigen, M.; Williams, P.; Doco, T.; Sanchez, C., Acacia senegal vs. Acacia seyal gums - Part 1: Composition and structure of hyperbranched plant exudates. *Food Hydrocolloids* **2015,** *51*, 41-53.

58. Saxena, A.; Tripathi, B. P.; Kumar, M.; Shahi, V. K., Membrane-based techniques for the separation and purification of proteins: An overview. *Adv. Colloid Interface Sci.* **2009,** *145*, 1-22.

59. Decloux, M.; Lameloise, M.-L.; Brocard, A.; Bisson, E.; Parmentier, M.; Spiraers, A., Treatment of acidic wastewater arising from the refining of vegetable oil by crossflow microfiltration at very low transmembrane pressure. *Process Biochemistry* **2007,** *42*, 693-699.

60. Cheryan, M., *Ultrafiltration and Microfiltration Handbook*. 2nd ed.; CRC press. **1998**.

61. Sutherland, K., Microfiltration: a job for a membrane. In *tcetoday.* **2012**; pp 38 - 40.

62. Gutman, R. G., *Membrane filtration. The technology of pressure driven crossflow processes*. 1987 ed.; 10P Publishing Ltd. **1987**.

63. Bellona, C.; Drewes, J. E.; Xu, P.; Amy, G., Factors affecting the rejection of organic solutes during NF/RO treatment - a literature review. *Water Res.* **2004,** *38*, 2795-2809.

64. Argyle, I., Synthetic membrane performance modification by selective species adsorption for the separation and purification of nutraceuticals. *Transfer report, University of Bath* **2011**.

65. Mulder, M., *Basic Principles of Membrane Technology*. 2 ed.; Kluwer Academic Publishers. **2000**.

66. Parameshwaran, K.; Fane, A. G.; Cho, B. D.; Kim, K. J., Analysis of microfiltration performance with constant flux processing of secondary effluent. *Water Res.* **2001,** *35*, 4349-4358.

67. Huisman, I. H.; Tragardh, G.; Tragardh, C.; Pihlajamaki, A., Determining the zeta-potential of ceramic microfiltration membranes using the electroviscous effect. *Journal of Membrane Science* **1998,** *147*, 187-194.

68. Baker, R. W., Overview of Membrane Science and Technology. In *Membrane Technology and Applications*, John Wiley & Sons, Ltd. **2004**; pp 1-14.

69. Belfort, G.; Davis, R. H.; Zydney, A. L., The behaviour of suspensions and macromolecular solutions in cross-flow microfiltration. *Journal of Membrane Science* **1994,** *96*, 1-58.

70. Hamachi, M.; Gupta, B. B.; Ben Aim, R., Ultrafiltration: a means for decolorization of cane sugar solution. *Sep. Purif. Technol.* **2003,** *30*, 229-239.

71. Shirazi, S.; Lin, C.-J.; Chen, D., Inorganic fouling of pressure-driven membrane processes - A critical review. *Desalination* **2010,** *250*, 236-248.

72. Lee, S.-J.; Dilaver, M.; Park, P.-K.; Kim, J.-H., Comparative analysis of fouling characteristics of ceramic and polymeric microfiltration membranes using filtration models. *Journal of Membrane Science* **2013,** *432*, 97-105.

73. Wagner, J., Membrane Filtration Handbook: Practical tips and Hints. 2 ed. Osmotics Inc: Minnetonka, **2001**.

74. Hofs, B.; Ogier, J.; Vries, D.; Beerendonk, E. F.; Cornelissen, E. R., Comparison of ceramic and polymeric membrane permeability and fouling using surface water. *Separation and Purification Technology* **2011,** *79*, 365-374.

75. Lee, S.; Cho, J., Comparison of ceramic and polymeric membranes for natural organic matter (NOM) removal. *Desalination* **2004,** *160*, 223-232.

76. Lee, S.-J.; Kim, J.-H., Differential natural organic matter fouling of ceramic versus polymeric ultrafiltration membranes. *Water Research* **2014,** *48*, 43-51.

77. Majewska-Nowak, K. M., Application of ceramic membranes for the separation of dye particles. *Desalination* **2010,** *254*, 185-191.

78. Saboya, L. V.; Maubois, J. L., Current developments of microfiltration technology in the dairy industry. *Lait* **2000,** *80*, 541-553.

79. Alpatova, A.; Kim, E.-S.; Dong, S.; Sun, N.; Chelme-Ayala, P.; El-Din, M. G., Treatment of oil sands process-affected water with ceramic ultrafiltration membrane: Effects of operating conditions on membrane performance. *Separation and Purification Technology* **2014,** *122*, 170-182.

80. Makardij, A.; Chen, X. D.; Farid, M. M., Microfiltration and ultrafiltration of milk: Some aspects of fouling and cleaning. *Food and Bioproducts Processing* **1999,** *77*, 107-113.

81. Weis, A.; Bird, M. R., The influence of multiple fouling and cleaning cycles upon the membrane processing of lignosulphonates. *Food Bioprod. Process.* **2001,** *79*, 184-187.

82. Jaffrin, M. Y.; Ding, L. H.; Akoum, O.; Brou, A., A hydrodynamic comparison between rotating disk and vibratory dynamic filtration systems. *Journal of Membrane Science* **2004,** *242*, 155-167.

83. Lee, S. S.; Burt, A.; Russotti, G.; Buckland, B., Microfiltration of recombinant yeast-cells using a rotating-disk dynamic filtration system. *Biotechnol. Bioeng.* **1995,** *48*, 386-400.

84. Vogel, J. H.; Kroner, K. H., Controlled shear filtration: A novel technique for animal cell separation. *Biotechnol. Bioeng.* **1999,** *63*, 663-674.

85. Parnham, C. S.; Davis, R. H., Protein recovery from cell debris using rotary and tangential cross-flow microfiltration. *Biotechnol. Bioeng.* **1995,** *47*, 155-164.

86. Luque, S.; Mallubhotla, H.; Gehlert, G.; Kuriyel, R.; Dzengeleski, S.; Pearl, S.; Belfort, G., A new coiled hollow-fiber module design for enhanced microfiltration performance in biotechnology. *Biotechnol. Bioeng.* **1999,** *65*, 247-257.

87. Schutyser, M.; Rupp, R.; Wideman, J.; Belfort, G., Dean vortex membrane microfiltration and diafiltration of rBDNF E-coli inclusion bodies. *Biotechnol. Progr.* **2002,** *18*, 322-329.

88. Fane, A. G.; Fell, C. J. D., A review of fouling and fouling control in ultrafiltration. *Desalination* **1987,** *62*, 117-136.

89. Lim, A. L.; Bai, R., Membrane fouling and cleaning in microfiltration of activated sludge wastewater. *Journal of Membrane Science* **2003,** *216*, 279-290.

90. Iritani, E.; Katagiri, N.; Sengoku, T.; Yoo, K. M.; Kawasaki, K.; Matsuda, A., Flux decline behaviors in dead-end microfiltration of activated sludge and its supernatant. *Journal of Membrane Science* **2007,** *300*, 36-44.

91. Madaeni, S. S.; Samieirad, S., Chemical cleaning of reverse osmosis membrane fouled by wastewater. *Desalination* **2010,** *257*, 80-86.

92. Simon, A.; Price, W. E.; Nghiem, L. D., Effects of chemical cleaning on the nanofiltration of pharmaceutically active compounds (PhACs). *Sep. Purif. Technol.* **2012,** *88*, 208-215.

93. Field, R. W.; Wu, D.; Howell, J. A.; Gupta, B. B., Critical flux concept for microfiltration fouling. *Journal of Membrane Science* **1995,** *100*, 259-272.

94. Suki, A.; Fane, A. G.; Fell, C. J. D., Flux decline in protein ultrafiltration. *Journal of Membrane Science* **1984,** *21*, 269-283.

95. Khatib, K.; Rose, J.; Barres, O.; Stone, W.; Bottero, J. Y.; Anselme, C., Physico-chemical study of fouling mechanisms of ultrafiltration membrane on Biwa lake (Japan). *Journal of Membrane Science* **1997,** *130*, 53-62.

96. Ma, H. M.; Hakim, L. F.; Bowman, C. N.; Davis, R. H., Factors affecting membrane fouling reduction by surface modification and backpulsing. *Journal of Membrane Science* **2001,** *189*, 255-270.

97. Al-Amoudi, A.; Lovitt, R. W., Fouling strategies and the cleaning system of NF membranes and factors affecting cleaning efficiency. *Journal of Membrane Science* **2007,** *303*, 6-28.

98. Song, L. F., A new model for the calculation of the limiting flux in ultrafiltration. *Journal of Membrane Science* **1998,** *144*, 173-185.

99. Evans, P. J.; Bird, M. R.; Pihlajamaki, A.; Nystrom, M., The influence of hydrophobicity, roughness and charge upon ultrafiltration membranes for black tea liquor clarification. *Journal of Membrane Science* **2008,** *313*, 250-262.

100. Bowen, W. R.; Calvo, J. I.; Hernandez, A., Steps of membrane blocking in flux decline during protein microfiltration. *Journal of Membrane Science* **1995,** *101*, 153-165.

101. Hermia, J., Constant pressure blocking filtration laws - application to power-law non newtonian fluids. *Transactions of the Institution of Chemical Engineers* **1982,** *60*, 183-187.

102. Nataraj, S.; Schomaecker, R.; Kraume, M.; Mishra, I. M.; Drews, A., Analyses of polysaccharide fouling mechanisms during crossflow membrane filtration. *Journal of Membrane Science* **2008,** *308*, 152-161.

103. Tracey, E. M.; Davis, R. H., Protein Fouling of Track-Etched Polycarbonate Microfiltration Membranes. *J. Colloid Interface Sci.* **1994,** *167*, 104-116.

104. Li, Q. L.; Elimelech, M., Organic fouling and chemical cleaning of nanofiltration membranes: Measurements and mechanisms. *Environmental Science & Technology* **2004,** *38*, 4683-4693.

105. Mahlangu, T. O.; Thwala, J. M.; Mamba, B. B.; D'Haese, A.; Verliefde, A. R. D., Factors governing combined fouling by organic and colloidal foulants in cross-flow nanofiltration. *Journal of Membrane Science* **2015,** *491*, 53-62.

106. Ye, Y.; Le Clech, P.; Chen, V.; Fane, A. G., Evolution of fouling during crossflow filtration of model EPS solutions. *Journal of Membrane Science* **2005,** *264*, 190-199.

107. Susanto, H.; Arafat, H.; Janssen, E. M. L.; Ulbricht, M., Ultrafiltration of polysaccharide-protein mixtures: Elucidation of fouling mechanisms and fouling control by membrane surface modification. *Sep. Purif. Technol.* **2008,** *63*, 558-565.

108. Simoes, M.; Simoes, L. C.; Vieira, M. J., A review of current and emergent biofilm control strategies. *Lwt-Food Science and Technology* **2010,** *43*, 573-583.

109. Goosen, M. F. A.; Sablani, S. S.; Ai-Hinai, H.; Ai-Obeidani, S.; Al-Belushi, R.; Jackson, D., Fouling of reverse osmosis and ultrafiltration membranes: A critical review. *Sep. Sci. Technol.* **2004,** *39*, 2261-2297.

110. Ma, H. M.; Bowman, C. N.; Davis, R. H., Membrane fouling reduction by backpulsing and surface modification. *Journal of Membrane Science* **2000,** *173*, 191-200.

111. Jones, S. The Application of Enhanced Fluid Dynamic Guaging as a Fouling Sensor for Pressure Driven Membrane Separations in the Food Industry. University of Bath, Bath, UK, **2012**.

112. Gilron, J.; Hasson, D., Calcium-sulfate fouling of reverse-osmosis membranes - flux decline mechanism. *Chem. Eng. Sci.* **1987,** *42*, 2351-2360.

113. Pervov, A. G., Scale formation prognosis and cleaning procedure schedules in reverse-osmosis systems operation. *Desalination* **1991,** *83*, 77-118.

114. Marshall, A. D.; Munro, P. A.; Tragardh, G., The effect of protein fouling in microfiltration and ultrafiltration on pemeate flux, protein retention and selectivity - a literature-review. *Desalination* **1993,** *91*, 65-108.

115. Wu, D.; Bird, M. R., The fouling and cleaning of ultrafiltration membranes during the filtration of model tea component solutions. *Journal of Food Process Engineering* **2007,** *30*, 293-323.

116. Bartlett, M. Chemical Cleaning of Fouled Membrane Systems. PhD, University of Bath, Bath, UK, **1998**.

117. Bian, R.; Yamamoto, K.; Watanabe, Y., The effect of shear rate on controlling the concentration polarization and membrane fouling. *Desalination* **2000,** *131*, 225-236.

118. Jonsson, G., Boundary-layer phenomena during ultrafiltration of dextran and whey-protein solutions. *Desalination* **1984,** *51*, 61-77.

119. Metsamuuronen, S.; Howell, J.; Nystrom, M., Critical flux in ultrafiltration of myoglobin and baker's yeast. *Journal of Membrane Science* **2002,** *196*, 13-25.

120. Kuo, K. P.; Cheryan, M., Ultrafiltration of acid whey in a spiral-wound unit - effect of operating parameters on membrane fouling. *J. Food Sci.* **1983,** *48*, 1113-1118.

121. Head, L. E.; Bird, M. R., Backwashing of Tubular ceramic microfilters fouled with milk protein isolate feeds. *J. Food Process Eng.* **2013,** *36*, 228-240.

122. de Barros, S. T. D.; Andrade, C. M. G.; Mendes, E. S.; Peres, L., Study of fouling mechanism in pineapple juice clarification by ultrafiltration. *Journal of Membrane Science* **2003,** *215*, 213-224.

123. Evans, P. J.; Bird, M. R., The role of black tea feed conditions upon ultrafiltration performance during membrane fouling and cleaning. *J. Food Process Eng.* **2010,** *33*, 309-332.

124. Kosutic, K.; Kunst, B., RO and NF membrane fouling and cleaning and pore size distribution variations. *Desalination* **2002,** *150*, 113-120.

125. Shorrock, C. J.; Bird, M. R., Membrane cleaning: Chemically enhanced removal of deposits formed during yeast cell harvesting. *Food and Bioproducts Processing* **1998,** *76*, 30-38.

126. Song, J.; Cheng, Q.; Kopta, S.; Stevens, R. C., Modulating artificial membrane morphology: pH-induced chromatic transition and nanostructural transformation of a bolaamphiphilic conjugated polymer from blue helical ribbons to red nanofibers. *J. Am. Chem. Soc.* **2001,** *123*, 3205-3213.

127. Filipcsei, G.; Csetneki, I.; Szilagyi, A.; Zrinyi, M.; Springer-Verlag, B., Magnetic field-responsive smart polymer composites. In *Oligomers Polymer Composties Molecular Imprinting*, **2007**; Vol. 206, pp 137-189.

128. Meng, H.; Li, G., A review of stimuli-responsive shape memory polymer composites. *Polymer* **2013,** *54*, 2199-2221.

129. Romney, A. J. D., *CIP: Cleaning in Place*. 2 ed.; The Society of Dairy Technology: Cambridge, **1990**; p 224.

130. Lin, J. C.-T.; Lee, D.-J.; Huang, C., Membrane Fouling Mitigation: Membrane Cleaning. *Sep. Sci. Technol.* **2010,** *45*, 858-872.

131. Mohammadi, T.; Madaeni, S. S.; Moghadam, M. K., Investigation of membrane fouling. *Desalination* **2003,** *153*, 155-160.

132. Simon, A.; Price, W. E.; Nghiem, L. D., Influence of formulated chemical cleaning reagents on the surface properties and separation efficiency of nanofiltration membranes. *Journal of Membrane Science* **2013,** *432*, 73-82.

133. Chen, J. P.; Kim, S. L.; Ting, Y., Optimization of membrane physical and chemical cleaning by a statistically designed approach. *Journal of Membrane Science* **2003,** *219*, 27-45.

134. Blanpain-Avet, P.; Migdal, J. F.; Benezech, T., The effect of multiple fouling and cleaning cycles on a tubular ceramic microfiltration membrane fouled with a whey protein concentrate - Membrane performance and cleaning efficiency. *Food and Bioproducts Processing* **2004,** *82*, 231-243.

135. Wallberg, O.; Jonsson, A. S.; Wickstrom, P., Membrane cleaning - a case study in a sulphite pulp mill bleach plant. *Desalination* **2001,** *141*, 259-268.

136. Jonsson, C.; Jonsson, A. S., Influence of the membrane material on the adsorptive fouling of ultrafiltration membranes. *Journal of Membrane Science* **1995,** *108*, 79-87.

137. Capannelli, G.; Bottino, A.; Gekas, V.; Tragardh, G., Protein fouling behavious of ultrafiltration membranes prefared with varying degrees of hydrophilicity. *Process Biochem.* **1990,** *25*, 221-224.

138. Lockley, A. K.; White, W. J. P.; Hall, G. M., A method of assessing protein adsorption onto ultrafiltration membranes. *International Journal of Food Science and Technology* **1988,** *23*, 11-15.

139. Silverstein, T. P., The real reason why oil and water don't mix. *J. Chem. Educ.* **1998,** *75*, 116-118.

140. Vaisanen, P.; Bird, M. R.; Nystrom, M., Treatment of UF membranes with simple and formulated cleaning agents. *Food and Bioproducts Processing* **2002,** *80*, 98-108.

141. Hunter, R. J., *Zeta Potential in Colloid Science: Principles and Applications*. Academic Press: London, **1981**.

142. Heimenz, P. C., *Principles of Colloid and Surface Chemistry*. 3rd ed.; Dekker: New York, **1997**.

143. Nystrom, M.; Pihlajamaki, A.; Ehsani, N., Characterisation of Ultrafiltration Membranes by Similtaneous Streaming Potential and Flux Measurements. *Journal of Membrane Science* **1994,** *87*, 245-256.

144. Chan, R.; Chen, V., Characterization of protein fouling on membranes: opportunities and challenges. *Journal of Membrane Science* **2004,** *242*, 169-188.

145. Nabe, A.; Staude, E.; Belfort, G., Surface modification of polysulfone ultrafiltration membranes and fouling by BSA solutions. *Journal of Membrane Science* **1997,** *133*, 57-72.

146. Weis, A.; Bird, M. R.; Nystrom, M.; Wright, C., The influence of morphology, hydrophobicity and charge upon the long-term performance of ultrafiltration membranes fouled with spent sulphite liquor. *Desalination* **2005,** *175*, 73-85.

147. Klein, M.; Aserin, A.; Ben Ishai, P.; Garti, N., Interactions between whey protein isolate and gum Arabic. *Colloids and Surfaces B-Biointerfaces* **2010,** *79*, 377-383.

148. Nakao, S., Determination of pore-size and pore-size distribution. *Journal of Membrane Science* **1994,** *96*, 131-165.

149. Weis, A. Fouling and cleaning synergy in ultrafiltration membrane systems : chemical cleaning after filtration of spent sulphite liquor PhD, University of Bath, Bath, **2004**.

150. Hoek, E. M. V.; Bhattacharjee, S.; Elimelech, M., Effect of membrane surface roughness on colloid-membrane DLVO interactions. *Langmuir* **2003,** *19*, 4836-4847.

151. Riedl, K.; Girard, B.; Lencki, R. W., Interactions responsible for fouling layer formation during apple juice microfiltration. *J. Agric. Food. Chem.* **1998,** *46*, 2458-2464.

152. Marti, O.; Drake, B.; Hansma, P. K., Atomic force microscopy of liqud-covered surfaces - atomic resolution images. *Appl. Phys. Lett.* **1987,** *51*, 484-486.

153. Binnig, G.; Quate, C. F.; Gerber, C., Atomic force microscope. *Phys. Rev. Lett.* **1986,** *56*, 930-933.

154. Garcia, R.; Perez, R., Dynamic atomic force microscopy methods. *Surf. Sci. Rep.* **2002,** *47*, 197-301.

155. Butt, H. J., Measuring electrostatic, vanderwaals, and hydration forces in electrolyte-solutions with an atomic force microscope. *Biophys. J.* **1991,** *60*, 1438-1444.

156. Singh, S.; Khulbe, K. C.; Matsuura, T.; Ramamurthy, P., Membrane characterization by solute transport and atomic force microscopy. *Journal of Membrane Science* **1998,** *142*, 111-127.

157. Bottino, A.; Capannelli, G.; Grosso, A.; Monticelli, O.; Cavalleri, O.; Rolandi, R.; Soria, R., SURFACE CHARACTERIZATION OF CERAMIC MEMBRANES BY ATOMIC-FORCE MICROSCOPY. *Journal of Membrane Science* **1994,** *95*, 289-296.

158. Bowen, W. R.; Doneva, T. A.; Yin, H. B., Atomic force microscopy studies of membrane-solute interactions (fouling). *Desalination* **2002,** *146*, 97-102.

159. Bowen, W. R.; Doneva, T. A., Atomic force microscopy studies of membranes: Effect of surface roughness on double-layer interactions and particle adhesion. *Journal of Colloid and Interface Science* **2000,** *229*, 544-549.

160. Bowen, W. R.; Doneva, T. A., Atomic force microscopy studies of nanofiltration membranes: surface morphology, pore size distribution and adhesion. *Desalination* **2000,** *129*, 163-172.

161. Ducker, W. A.; Xu, Z.; Clarke, D. R.; Israelachvili, J. N., Forces between alumina surfaces in salt-solutions - non-DLVO forces and the implications for colloidal processing. *J. Am. Ceram. Soc.* **1994,** *77*, 437-443.

162. Bowen, W. R.; Hilal, N.; Lovitt, R. W.; Wright, C. J., Direct measurement of interactions between adsorbed protein layers using an atomic force microscope. *J. Colloid Interface Sci.* **1998,** *197*, 348-352.

163. Tuladhar, T. R.; Paterson, W. R.; Macleod, N.; Wilson, D. I., Development of a novel non-contact proximity gauge for thickness measurement of soft deposits and its application in fouling studies. *Can. J. Chem. Eng.* **2000,** *78*, 935-947.

164. Gale, G. E., A thickness measuring device using pneumatic gauging to detect the sample. *Measurement Science & Technology* **1995,** *6*, 1566-1571.

165. Chew, J. Y. M.; Paterson, W. R.; Wilson, D. I., Fluid dynamic gauging for measuring the strength of soft deposits. *J. Food Eng.* **2004,** *65*, 175-187.

166. Jones, S. A.; Chew, Y. M. J.; Bird, M. R.; Wilson, D. I., The application of fluid dynamic gauging in the investigation of synthetic membrane fouling phenomena. *Food and Bioproducts Processing* **2010,** *88*, 409-418.

167. Jones, S. A.; Chew, Y. M. J.; Wilson, D. I.; Bird, M. R., Fluid dynamic gauging of microfiltration membranes fouled with sugar beet molasses. *J. Food Eng.* **2012,** *108*, 22-29.

168. Lewis, W. J. T.; Chew, Y. M. J.; Bird, M. R., The application of fluid dynamic gauging in characterising cake deposition during the cross-flow microfiltration of a yeast suspension. *Journal of Membrane Science* **2012,** *405*, 113-122.

169. Lister, V. Y.; Lucas, C.; Gordon, P. W.; Chew, Y. M. J.; Wilson, D. I., Pressure mode fluid dynamic gauging for studying cake build-up in cross-flow microfiltration. *Journal of Membrane Science* **2011,** *366*, 304-313.

170. Zhu, H. H.; Nystrom, M., Cleaning results characterized by flux, streaming potential and FTIR measurements. *Colloids and Surfaces a-Physicochemical and Engineering Aspects* **1998,** *138*, 309-321.

171. Madaeni, S. S.; Zarbakhsh, M., A comparison between various hybrid systems of microfiltration membrane and bacteria for removal or organic compounds. *Chem. Eng. Commun.* **2010,** *197*, 1057-1067.

172. Kotsanopoulos, K. V.; Arvanitoyannis, I. S., Membrane Processing Technology in the Food Industry: Food Processing, Wastewater Treatment, and Effects on Physical, Microbiological, Organoleptic, and Nutritional Properties of Foods. *Critical Reviews in Food Science and Nutrition* **2015,** *55*, 1147-1175.

173. Nanostone Ceramic membranes. http://www.nanostone.com/ceramic-membranes/ (accessed 14-9-15),

174. Bird, M. R.; Bartlett, M., CIP optimisation for the food industry - relationships between detergent concentration, temperature and cleaning time. *Food and Bioproducts Processing* **1995,** *73*, 63-70.

175. Bird, M. R.; Bartlett, M., Measuring and modelling flux recovery during the chemical cleaning of MF membranes for the processing of whey protein concentrate. *J. Food Eng.* **2002,** *53*, 143-152.

176. Matzinos, P.; Alvarez, R., Effect of ionic strength on rinsing and alkaline cleaning of ultrafiltration inorganic membranes fouled with whey proteins. *Journal of Membrane Science* **2002,** *208*, 23-30.

177. Clesceri, L. S.; Greenberg, A. E.; Eaton, A. D., *Standard Methods for examinations of water and wastewater*. 20 ed.; American Public Health Association: Washington DC, **1998**.

178. Glicksman, M.; Sand, R. E., *Gum Arabic*. Academic Press Inc.**1973**.

179. Gashua, I. B.; Williams, P. A.; Yadav, M. P.; Baldwin, T. C., Characterisation and molecular association of Nigerian and Sudanese Acacia gum exudates. *Food Hydrocolloids* **2015,** *51*, 405-413.

180. Lin, T.; Lu, Z.; Chen, W., Interaction mechanisms and predictions on membrane fouling in an ultrafiltration system, using the XDLVO approach. *Journal of Membrane Science* **2014,** *461*, 49-58.

181. Rees, T., Severn Trent water analysis report. Environmental, Ed.**2013**.

182. Argyle, I. S.; Pihlajamaki, A.; Bird, M. R., Black tea liquor ultrafiltration: Effect of ethanol pre-treatment upon fouling and cleaning characteristics. *Food and Bioproducts Processing* **2015,** *93*, 289-297.

183. Wachs, I. E., Raman and IR studies of surface metal oxide species on oxide supports: Supported metal oxide catalysts. *Catal. Today* **1996,** *27*, 437-455.

184. Yaney, P. P.; Becker, R. J., The Application of Raman-Spectroscopy to the Study of Adsorbed Molecules on Alumina Surfaces. *Appl. Surf. Sci.* **1980,** *4*, 356-373.

185. Weis, A.; Bird, M. R.; Nystrom, M., The chemical cleaning of polymeric UF membranes fouled with spent sulphite liquor over multiple operational cycles. *Journal of Membrane Science* **2003,** *216*, 67-79.

186. Ariza, M. J.; Benavente, J., Streaming potential along the surface of polysulfone membranes: a comparative study between two different experimental systems and determination of electrokinetic and adsorption parameters. *Journal of Membrane Science* **2001,** *190*, 119-132.

187. Smit, W.; Stein, H. N., Electroosmotic zeta-potential measurements on single crystals. *J. Colloid Interface Sci.* **1977,** *60*, 299-307.

188. Yang, D.; Krasowska, M.; Sedev, R.; Ralston, J., The unusual surface chemistry of alpha-Al2O3 (0001). *Phys. Chem. Chem. Phys* **2010,** *12*, 13724-13729.

189. Moritz, T.; Benfer, S.; Arki, P.; Tomandl, G., Influence of the surface charge on the permeate flux in the dead-end filtration with ceramic membranes. *Separation and Purification Technology* **2001,** *25*, 501-508.

190. Grun, M.; Kurganov, A. A.; Schacht, S.; Schuth, F.; Unger, K. K., Comparison of an ordered mesoporous aluminosilicate, silica, alumina, titania and zirconia in normal-phase high-performance liquid chromatography. *Journal of Chromatography A* **1996,** *740*, 1-9.

191. Franks, G. V.; Meagher, L., The isoelectric points of sapphire crystals and alpha-alumina powder. *Colloids and Surfaces a-Physicochemical and Engineering Aspects* **2003,** *214*, 99-110.

192. Bernat, X.; Pihlajamaeki, A.; Fortuny, A.; Bengoa, C.; Stueber, F.; Fabregat, A.; Nystroem, M.; Font, J., Non-enhanced ultrafiltration of iron(III) with commercial ceramic membranes. *Journal of Membrane Science* **2009,** *334*, 129-137.

193. Vrijenhoek, E. M.; Hong, S.; Elimelech, M., Influence of membrane surface properties on initial rate of colloidal fouling of reverse osmosis and nanofiltration membranes. *Journal of Membrane Science* **2001,** *188*, 115-128.

194. Yelken, G. O.; Polat, M., Determination of electrostatic potential distribution by atomic force microscopy (AFM) on model silica and alumina surfaces in aqueous electrolyte solutions. *Appl. Surf. Sci.* **2014,** *301*, 149-155.

195. Guell, C.; Davis, R. H., Membrane fouling during microfiltration of protein mixtures. *Journal of Membrane Science* **1996,** *119*, 269-284.

196. Choo, K. H.; Lee, C. H., Membrane fouling mechanisms in the membrane-coupled anaerobic bioreactor. *Water Research* **1996,** *30*, 1771-1780.

197. Ousman, M.; Bennasar, M., Determination of Various Hydraulic Resistances during Cross-flow Filtration of a Starch Grain Suspension Through Inorganic Membranes. *Journal of Membrane Science* **1995,** *105*, 1-21.

198. Jiraratananon, R.; Chanachai, A., A study of fouling in the ultrafiltration of passion fruit juice. *Journal of Membrane Science* **1996,** *111*, 39-48.

199. Liang, S.; Qi, G.; Xiao, K.; Sun, J.; Giannelis, E. P.; Huang, X.; Elimelech, M., Organic fouling behavior of superhydrophilic polyvinylidene fluoride (PVDF) ultrafiltration membranes functionalized with surface-tailored nanoparticles: Implications for organic fouling in membrane bioreactors. *Journal of Membrane Science* **2014,** *463*, 94-101.

200. Kanani, D. A.; Sun, X.; Ghosh, R., Reversible and irreversible membrane fouling during in-line microfiltration of concentrated protein solutions. *Journal of Membrane Science* **2008,** *315*, 1-10.

201. Harker, J. H.; Coulson, J. M.; Backhurst, J. R.; Richardson, J. F., *Chemical Engineering: Particle Technology and Seperation Processes*. 5th ed.; Butterworth-Heomeman Ltd**2002**; Vol. 2, p 1232.

202. Loh, S.; Beuscher, U.; Poddar, T. K.; Porter, A. G.; Wingard, J. M.; Husson, S. M.; Wickramasinghe, S. R., Interplay among membrane properties, protein properties and operating conditions on protein fouling during normal-flow microfiltration. *Journal of Membrane Science* **2009,** *332*, 93-103.

203. Zuriaga-Agusti, E.; Alventosa-deLara, E.; Barredo-Damas, S.; Alcaina-Miranda, M. I.; Iborra-Clar, M. I.; Mendoza-Roca, J. A., Performance of ceramic ultrafiltration membranes and fouling behavior of a dye-polysaccharide binary system. *Water Research* **2014,** *54*, 199-210.

204. Alpatova, A.; Kim, E. S.; Dong, S.; Sun, N.; Chelme-Ayala, P.; Gamal El-Din, M., Treatment of oil sands process-affected water with ceramic ultrafiltration membrane: Effects of operating conditions on membrane performance. *Sep. Purif. Technol.* **2014,** *122*, 170-182.

205. Kelly, S. T.; Zydney, A. L., Mechanisms for BSA fouling during microfiltration. *Journal of Membrane Science* **1995,** *107*, 115-127.

206. Hua, F. L.; Tsang, Y. F.; Wang, Y. J.; Chan, S. Y.; Chua, H.; Sin, S. N., Performance study of ceramic microfiltration membrane for oily wastewater treatment. *Chemical Engineering Journal* **2007,** *128*, 169-175.

207. Alventosa-deLara, E.; Barredo-Damas, S.; Alcaina-Miranda, M. I.; Iborra-Clar, M. I., Ultrafiltration technology with a ceramic membrane for reactive dye removal: Optimization of membrane performance. *Journal of Hazardous Materials* **2012,** *209*, 492-500.

208. Kalhoinen, M.; Pekkarinen, M.; Manttari, M.; Nuortila-Jokinen, J.; Nystrom, M., Comparison of the performance of two different regenerated cellulose ultrafiltration membranes at high filtration pressure. *Journal of Membrane Science* **2007,** *294*, 93-102.

209. Meien, O. F.; Nobrega, R., Ultrafiltration model for partial solute rejection in the limiting flux region. *Journal of Membrane Science* **1994,** *95*, 277-287.

210. Bhattacharya, P. K.; Todi, R. K.; Tiwari, A.; Bhattacharjee, C.; Bhattacharjee, S.; Datta, S., Studies on ultrafiltration of spent sulfite liquor using various membranes for the recovery of lignosulphonates. *Desalination* **2005,** *174*, 287-297.

211. Pradanos, P.; Arribas, J. I.; Hernandez, A., Mass transfer coefficient and retention of PEGs in low pressure crossflow ultrafiltration through asymmetric membranes. *Journal of Membrane Science* **1995,** *99*, 1-20.

212. Kelly, S. T.; Zydney, A. L., Protein fouling during microfiltration: Comparative behavior of different model proteins. *Biotechnol. Bioeng.* **1997,** *55*, 91-100.

213. Xujiang, Y. Z.; Dodds, J.; Leclerc, D., Cake characteristics in cross-flow and dead-end microfiltration. *Filtration & Separation* **1995,** *32*, 795-798.

214. Guell, C.; Czekaj, P.; Davis, R. H., Microfiltration of protein mixtures and the effects of yeast on membrane fouling. *Journal of Membrane Science* **1999,** *155*, 113-122.

215. Chhaya; Sharma, C.; Mondal, S.; Majumdar, G. C.; De, S., Clarification of Stevia extract by ultrafiltration: Selection criteria of the membrane and effects of operating conditions. *Food and Bioproducts Processing* **2012,** *90*, 525-532.

216. Mondal, S.; Rai, C.; De, S., Identification of Fouling Mechanism During Ultrafiltration of Stevia Extract. *Food and Bioprocess Technology* **2013,** *6*, 931-940.

217. Brans, G.; Schroen, C.; van der Sman, R. G. M.; Boom, R. M., Membrane fractionation of milk: state of the art and challenges. *Journal of Membrane Science* **2004,** *243*, 263-272.

218. Pihlajamaki, A. Electrochemical Characterisation of Filter Media Properties and their Exploitation in Enhanced Filtration. Doctoral Dissertation, Lappeenranta University of Technology. **1998**.

219. Anderson, D. M. W., Chemotaxomomic aspects of the chemistry of Acacia gum exudates. *Kew Bulletin* **1978,** *3*, 529 - 536.

220. Saxena, A.; Shahi, V. K., pH controlled selective transport of proteins through charged ultrafilter membranes under coupled driving forces: An efficient process for protein separation. *Journal of Membrane Science* **2007,** *299*, 211-221.

221. Hodgins, G. R.; Cyan, E. D.; Timmerman, R. Removal of metal ions from gum arabic solutions for lithographic plates. US2950195, **1960**.

222. Rice, G. S.; Kentish, S. E.; O'Connor, A. J.; Barber, A. R.; Pihlajamaki, A.; Nystrom, M.; Stevens, G. W., Analysis of separation and fouling behaviour during nanofiltration of dairy ultrafiltration permeates. *Desalination* **2009,** *236*, 23-29.

223. Zhang, H.; Shan, G.; Liu, H.; Xing, J., Surface modification of gamma-Al2O3 nano-particles with gum arabic and its applications in adsorption and biodesulfurization. *Surface & Coatings Technology* **2007,** *201*, 6917-6921.

224. El Rayess, Y.; Albasi, C.; Bacchin, P.; Taillandier, P.; Raynal, J.; Mietton-Peuchot, M.; Devatine, A., Cross-flow microfiltration applied to oenology: A review. *Journal of Membrane Science* **2011,** *382*, 1-19.

225. Saha, N. K.; Balakrishnan, M.; Ulbricht, M., Sugarcane juice ultrafiltration: FTIR and SEM analysis of polysaccharide fouling. *Journal of Membrane Science* **2007,** *306*, 287-297.

226. Wang, H.; Williams, P. A.; Senan, C., Synthesis, characterization and emulsification properties of dodecenyl succinic anhydride derivatives of gum Arabic. *Food Hydrocolloids* **2014,** *37*, 143-148.

227. Brambilla, L.; Riedo, C.; Baraldi, C.; Nevin, A.; Gamberini, M. C.; D'Andrea, C.; Chiantore, O.; Goidanich, S.; Toniolo, L., Characterization of fresh and aged natural ingredients used in historical ointments by molecular spectroscopic techniques: IR, Raman and fluorescence. *Analytical and Bioanalytical Chemistry* **2011,** *401*, 1827-1837.

228. Tiwari, A., Gum arabic-graft-polyaniline: An electrically active redox biomaterial for sensor applications. *Journal of Macromolecular Science Part a-Pure and Applied Chemistry* **2007,** *44*, 735-745.

229. Barron, A. R., The interaction of carboxylic acids with aluminium oxides: journeying from a basic understanding of alumina nanoparticles to water treatment for industrial and humanitarian applications. *Dalton Trans.* **2014,** *43*, 8127-8143.

230. Gulrez, S. K. H.; Al-Assaf, S.; Phillips, G. O., Hydrogels: Methods of Preparation, Characterisation and Applications. In *Progress in Molecular and Environmental Bioengineering - From Analysis and Modeling to Technology Applications*, Carpi, P. A., Ed. InTech. **2011**; pp 117 - 150.

231. SiHassen, D.; OuldDris, A.; Jaffrin, M. Y.; Benkahla, Y. K., Optimisation of an intermittent cross-flow filtration process of mineral suspensions. *Journal of Membrane Science* **1996,** *118*, 185-198.

232. Tragardh, G., Membrane cleaning. *Desalination* **1989,** *71*, 325-335.

233. Young, S. B.; Setlow, P., Mechanisms of killing of Bacillus subtilis spores by hypochlorite and chlorine dioxide. *Journal of Applied Microbiology* **2003,** *95*, 54-67.

234. Gan, Q.; Howell, J. A.; Field, R. W.; England, R.; Bird, M. R.; McKechinie, M. T., Synergetic cleaning procedure for a ceramic membrane fouled by beer microfiltration. *Journal of Membrane Science* **1999,** *155*, 277-289.

235. Li, J. X.; Sanderson, R. D.; Jacobs, E. P., Ultrasonic cleaning of nylon microfiltration membranes fouled by Kraft paper mill effluent. *Journal of Membrane Science* **2002,** *205*, 247-257.

236. Stephen, A. M.; Phillips, G. O., *Food Polysaccharides and Their Applications*. Taylor & Francis. **2006**.

237. Colorbasics. CIE 1931 Color Space. http://www.colorbasics.com/CIESystem/ (accessed 10-08-20115),

238. Bird, M. R.; Fryer, P. J.; Inst Chem, E., *An analytical model for the cleaning of food process plant*. **1992**; Vol. 126, p 325-330.

239. Teng, M.-Y.; Lin, S.-H.; Juang, R.-S., Effect of ultrasound on the separation of binary protein mixtures by cross-flow ultrafiltration. *Desalination* **2006,** *200*, 280-282.

240. Fauconnier, M. L.; Blecker, C.; Groyne, J.; Razafindralambo, H.; Vanzeveren, E.; Marlier, M.; Paquot, M., Characterization of two Acacia gums and their fractions using a Langmuir film balance. *J. Agric. Food. Chem.* **2000,** *48*, 2709-2712.

241. Tran-Ha, M. H.; Wiley, D. E.; Lawrence, N. D.; Iyer, M., Development of a standard cleaning protocol to evaluate the effect of cleaning on membrane performance. *Australian Journal of Dairy Technology* **2002,** *57*, 20-29.

242. Nystrom, M.; Zhu, H. H., Characterization of cleaning results using combined flux and streaming potential methods. *Journal of Membrane Science* **1997,** *131*, 195-205.

243. Jeżowska, A.; Schipolowski, T.; Wozny, G., Influence of simple pre-treatment methods on properties of membrane material. *Desalination* **2006,** *189*, 43-52.

244. Jagdheesh, R., Fabrication of a Superhydrophobic Al2O3 Surface Using Picosecond Laser Pulses. *Langmuir* **2014,** *30*, 12067-12073.

245. Tasaltin, N.; Sanli, D.; Jonas, A.; Kiraz, A.; Erkey, C., Preparation and characterization of superhydrophobic surfaces based on hexamethyldisilazane-modified nanoporous alumina. *Nanoscale Research Letters* **2011,** *6*.

246. Allara, D. L.; Nuzzo, R. G., Spontaneously organized molecular assemblies. 1. Formation, dynamics, and physical properties of n-alkanoic acids adsorbed from solution on an oxidized aluminum surface. *Langmuir* **1985,** *1*, 45-52.

247. Ulrich, H. J.; Stumm, W.; Cosovic, B., Adsorption of aliphatic fatty acids on aquatic interfaces. Comparison between two model surfaces: the mercury electrode and δ-Al2O3 colloids. *Environ. Sci. Technol.* **1988,** *22*, 37-41.

248. Argyris, D.; Ho, T. A.; Cole, D. R.; Striolo, A., Molecular Dynamics Studies of Interfacial Water at the Alumina Surface. *J. Phys. Chem. C* **2011,** *115*, 2038-2046.

249. Vogelson, C. T.; Keys, A.; Edwards, C. L.; Barron, A. R., Molecular coupling layers formed by reactions of epoxy resins with self-assembled carboxylate monolayers grown on the native oxide of aluminium. *J. Mater. Chem.* **2003,** *13*, 291-296.

250. Maguire-Boyle, S. J.; Barron, A. R., A new functionalization strategy for oil/water separation membranes. *Journal of Membrane Science* **2011,** *382*, 107-115.

251. DeFriend, K. A.; Barron, A. R., A simple approach to hierarchical ceramic ultrafiltration membranes. *Journal of Membrane Science* **2003,** *212*, 29-38.

252. Bornaz, S.; Fanni, J.; Parmentier, M., Filtration in Hydrophobic Media 1: Evidence for Molecular-selection by Cross-flow Filtration of Butter Oil. *Journal of the American Oil Chemists Society* **1995,** *72*, 1139-1142.

253. Bornaz, S.; Fanni, J.; Parmentier, M., Filtration in Hydrophobic Media 2: A Triglyceride Partition Phenomenon as Observed by Tangertian Filtration of Butter Oil. *Journal of the American Oil Chemists Society* **1995,** *72*, 1143-1148.

254. Anderson, D. M. W.; Bridgeman, M. M. E.; Farquhar, J. G. K.; McNab, C. G. A., The chemical characterisation of the test article used in toxilogical studies of Gum Arabic Accacia-senegal. *International Tree Crops Journal* **1983,** *2*, 245-254.

255. Leonor, S. J.; Gomez, J. A.; Kinoshita, A.; Calandreli, I.; Tfouni, E.; Baffa, O., ESR spectroscopic properties of irradiated gum Arabic. *Food Chem.* **2013,** *141*, 1860-1864.

256. Zaied, S. F.; Youssef, B. M.; Desouky, O.; El Dien, M. S., Decontamination of gum arabic with gamma-rays or electron beams and effects of these treatments on the material. *Appl. Radiat. Isot.* **2007,** *65*, 26-31.

257. Bargeman, G.; Dohmen-Speelmans, M.; Recio, I.; Timmer, M.; van der Horst, C., Selective isolation of cationic amino acids and peptides by electro-membrane filtration. *Lait* **2000,** *80*, 175-185.

258. Bargeman, G.; Koops, G. H.; Houwing, J.; Breebaart, I.; van der Horst, H. C.; Wessling, M., The development of electro-membrane filtration for the isolation of bioactive peptides: the effect of membrane selection and operating parameters on the transport rate. *Desalination* **2002,** *149*, 369-374.

259. Lapointe, J. F.; Gauthier, S. F.; Pouliot, Y.; Bouchard, C., Selective separation of cationic peptides from a tryptic hydrolysate of beta-lactoglobulin by electrofiltration. *Biotechnol. Bioeng.* **2006,** *94*, 223-233.

260. Sung, M.; Huang, C. P.; Weng, Y.-H.; Lin, Y.-T.; Li, K.-C., Enhancing the separation of nano-sized particles in low-salt suspensions by electrically assisted cross-flow filtration. *Sep. Purif. Technol.* **2007,** *54*, 170-177.

Appendix A

Pressure transducer calibration

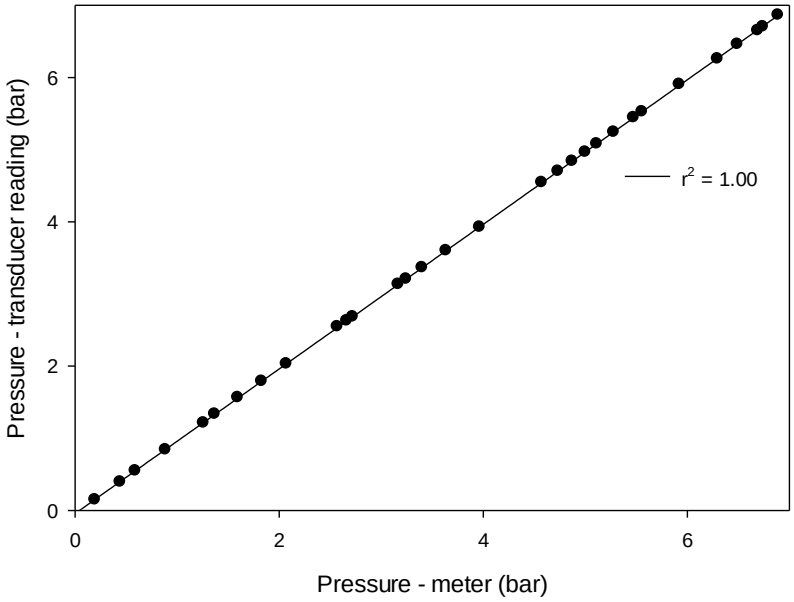

Figure A1: P1 pressure transducer calibration.

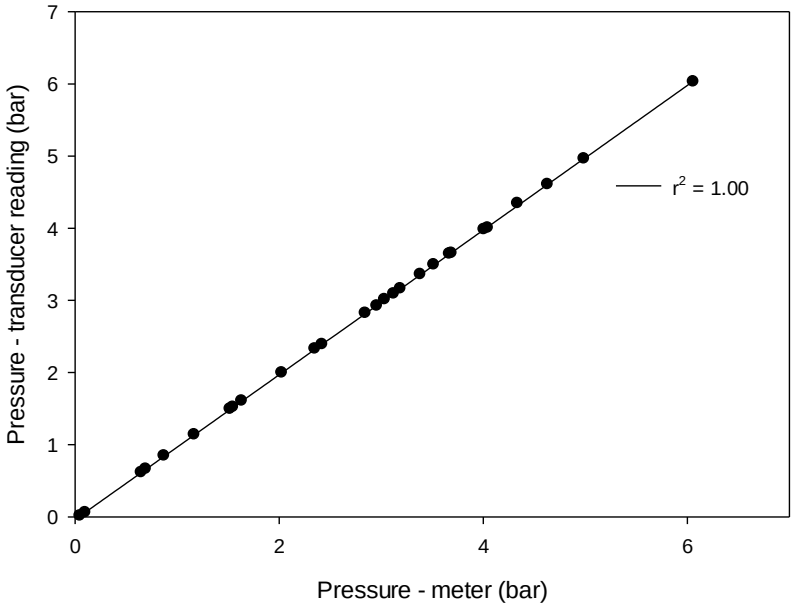

Figure A2: P3 pressure transducer calibration.

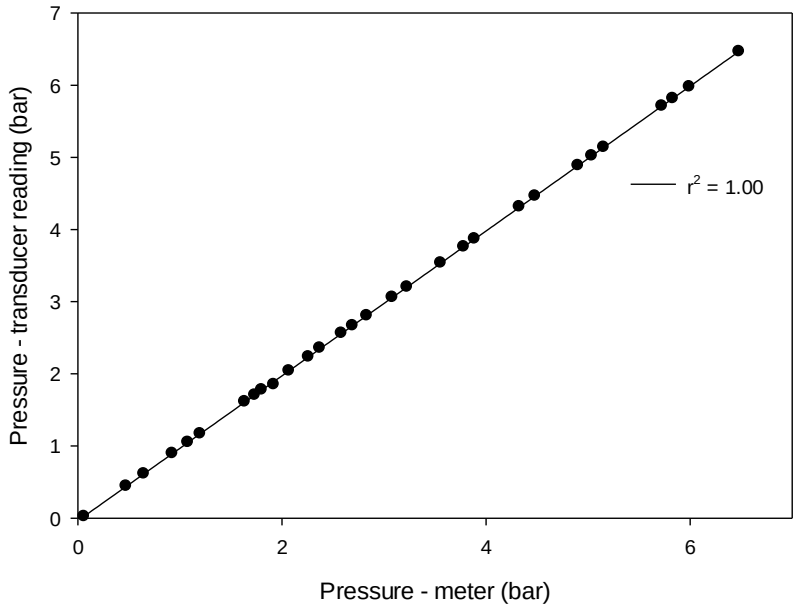

Figure A3: P4 pressure transducer calibration.

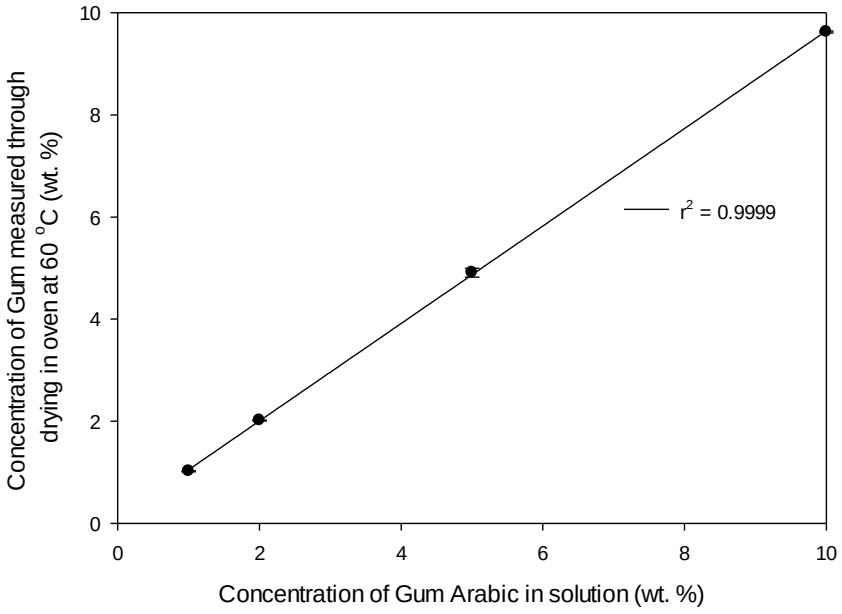

Figure A4: Dry weight calibration.

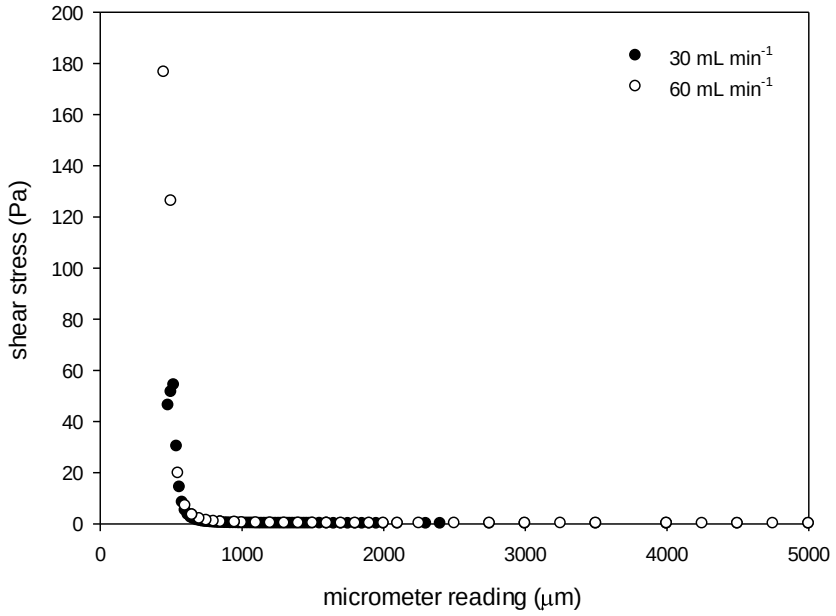

Figure A5: FDG calibration at 40 ^{o}C and flow rate 30 and 60 mL min^{-1} measurements average of three repeats. Error bars are too small to be observed.

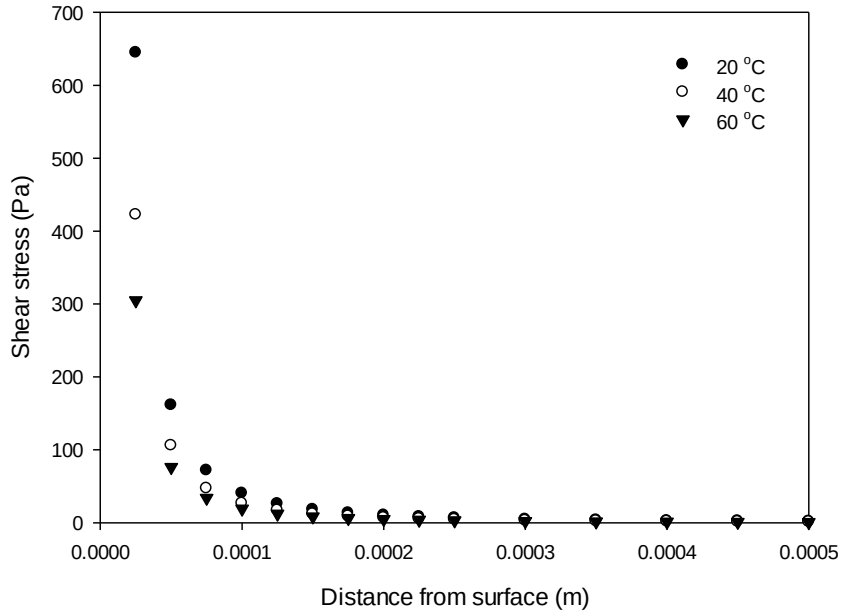

Figure A6: Calibration of shear stress measured at 20, 40 and 60 ^{o}C as gauge approaches membrane surface. Measured at flow rate of 60 mLmin^{-1}. Used to calculate distance the tip needed to be from the surface to apply stress of 1 – 300 Pa on membrane fouled with Gum Arabic in Section 6.4.3.

Appendix B

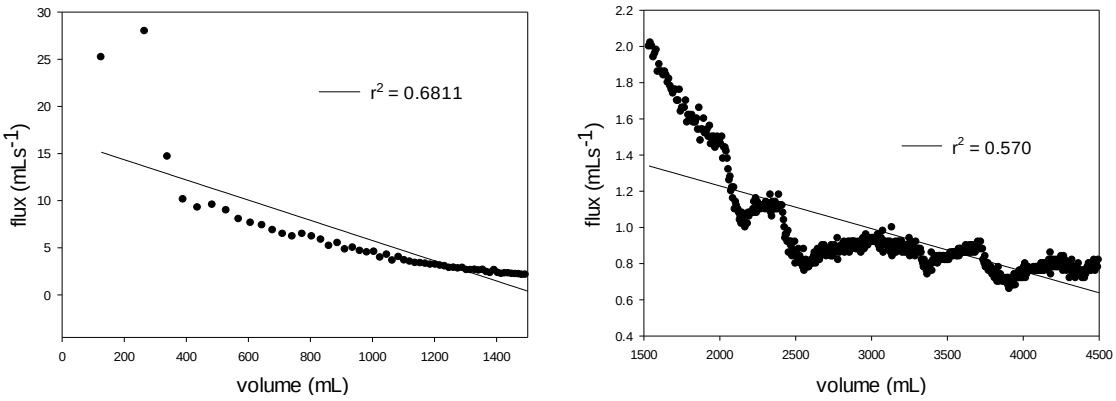

Figure B1: Pore blocking model fitted to 2.0 µm flat sheet data for first 5 minutes (left) and 5-60 minutes (right).

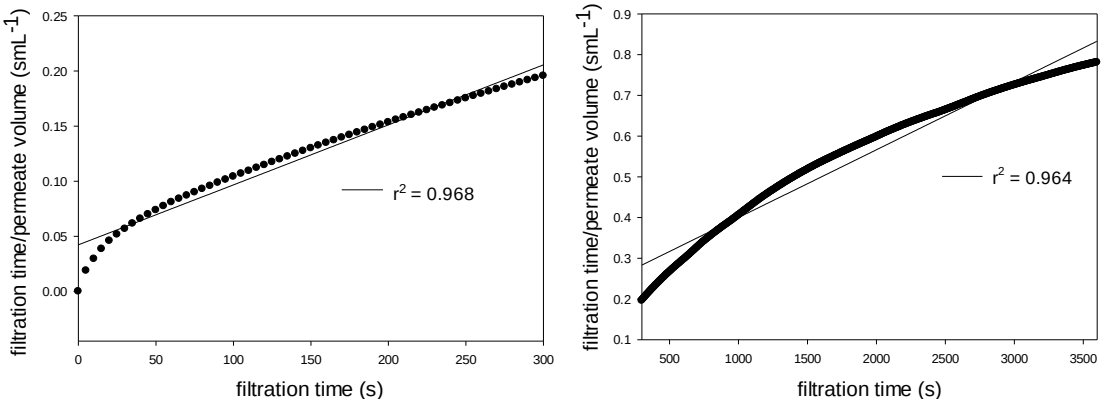

Figure B2: Pore constriction model fitted to 2.0 µm flat sheet data for first 5 minutes (left) and 5-60 minutes (right).

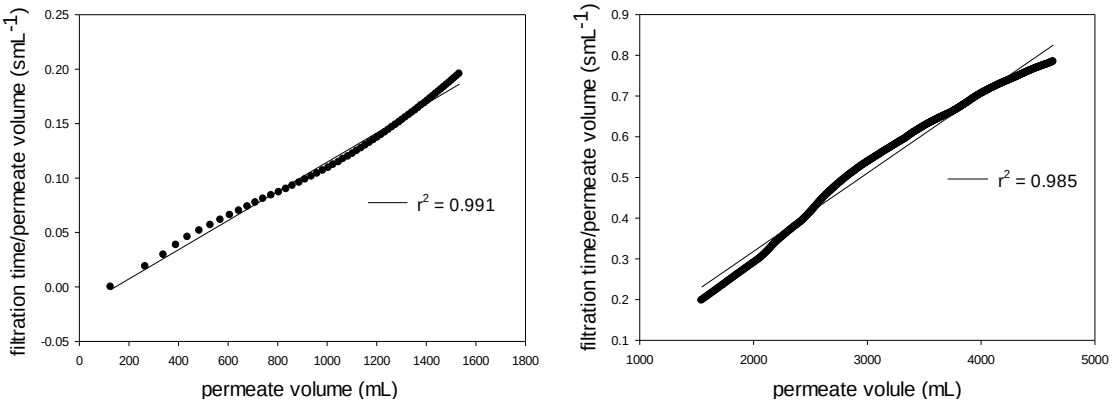

Figure B3: Cake filtration model fitted to 2.0 µm flat sheet data for first 5 minutes (left) and 5-60 minutes (right).

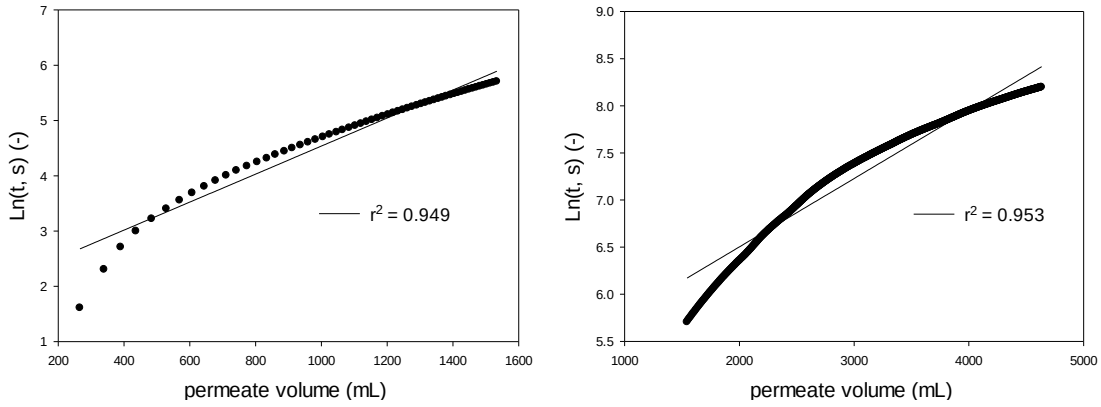

Figure B4: Intermediate blocking model fitted to 2.0 µm flat sheet data for first 5 minutes (left) and 5 – 60 minutes (right).

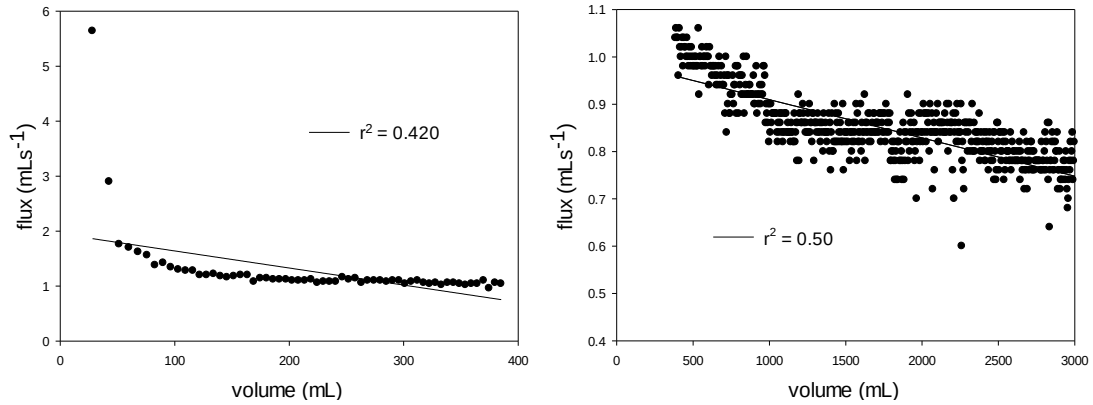

Figure B5: Pore blocking model fitted to 0.8 µm flat sheet data for first 5 minutes (left) and 5-60 minutes (right).

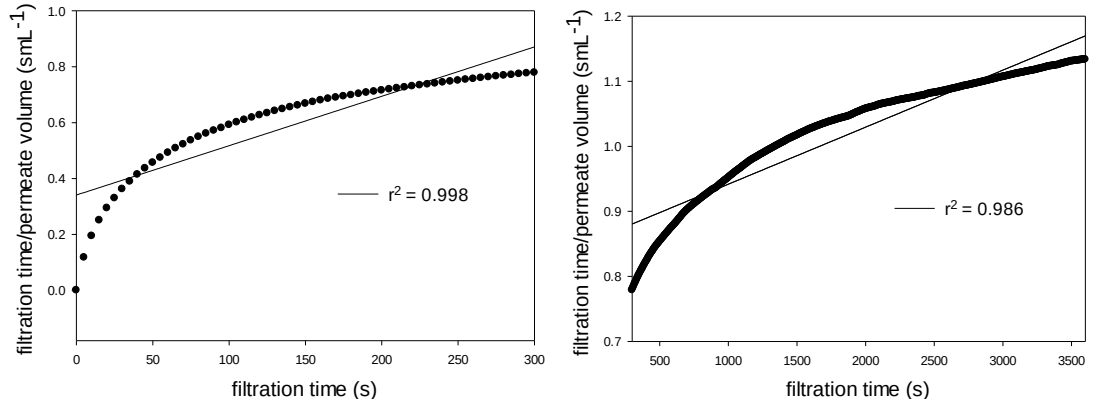

Figure B6: Pore constriction model fitted to 0.8 µm flat sheet data for first 5 minutes (left) and 5 – 60 minutes (right).

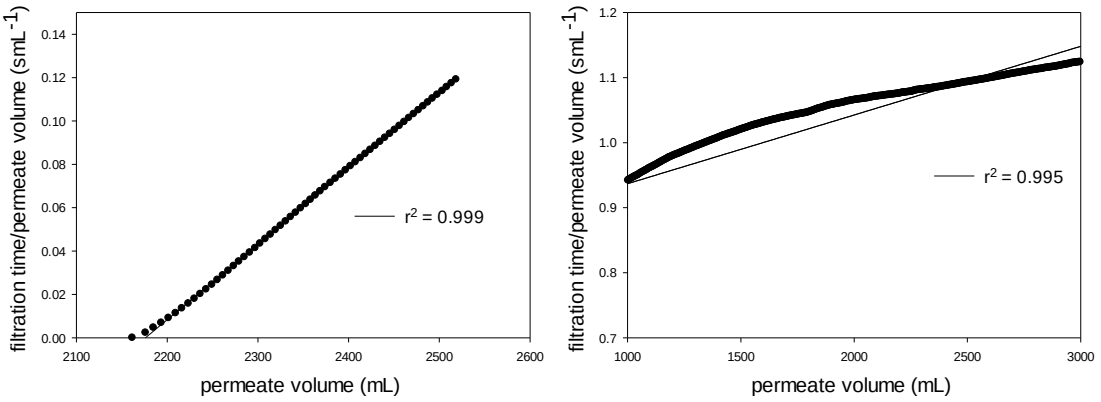

Figure B7: Cake filtration model fitted to 0.8 µm flat sheet data for first 5 minutes (left) and 5 – 60 minutes (right).

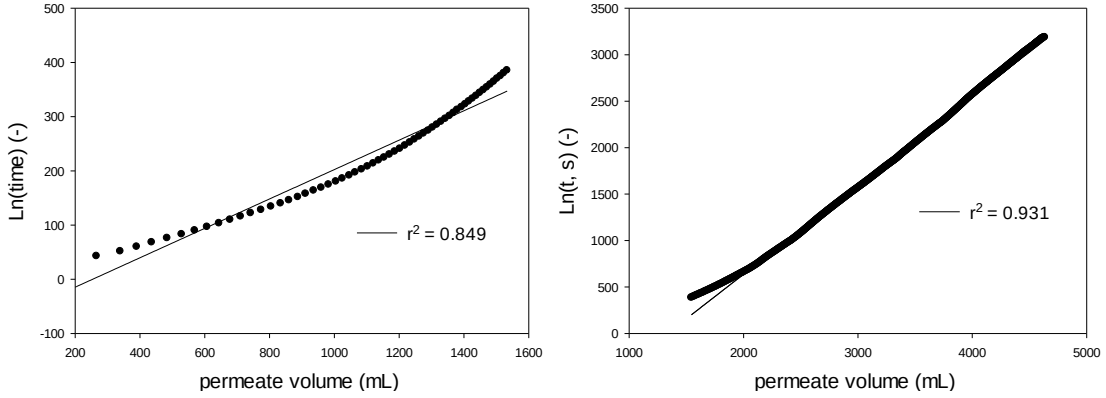

Figure B8: Intermediate blocking model fitted to 0.8 µm flat sheet data for first 5 minutes (left) and 5 – 60 minutes (right).

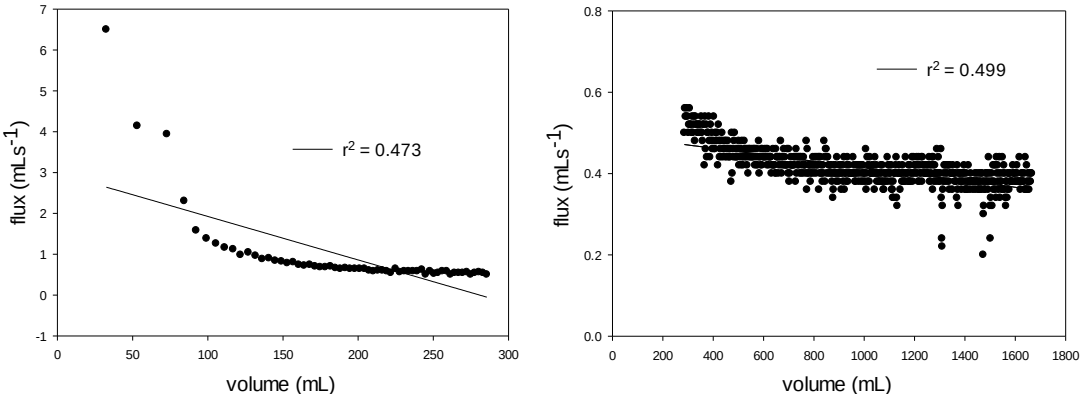

Figure B9: Pore blocking model fitted to 0.5 µm flat sheet data for first 5 minutes (left) and 5 – 60 minutes (right).

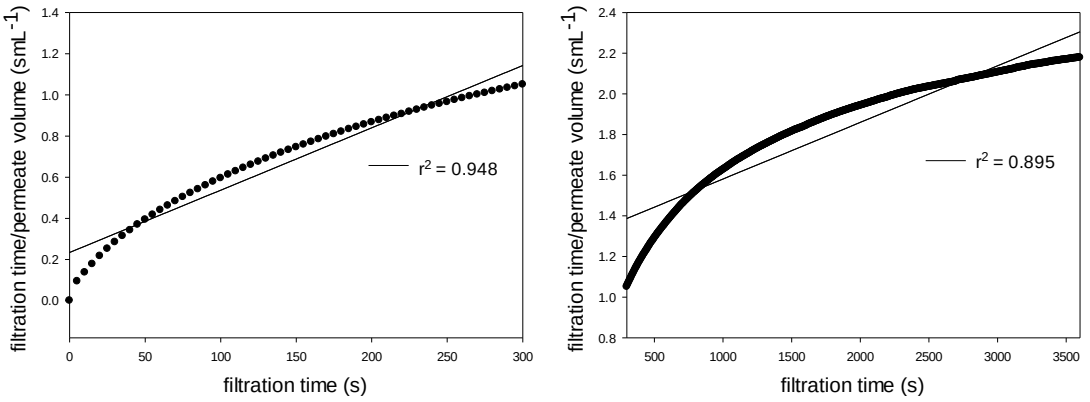

Figure B10: Pore constriction model fitted to 0.5 µm flat sheet data for first 5 minutes (left) and 5 – 60 minutes (right).

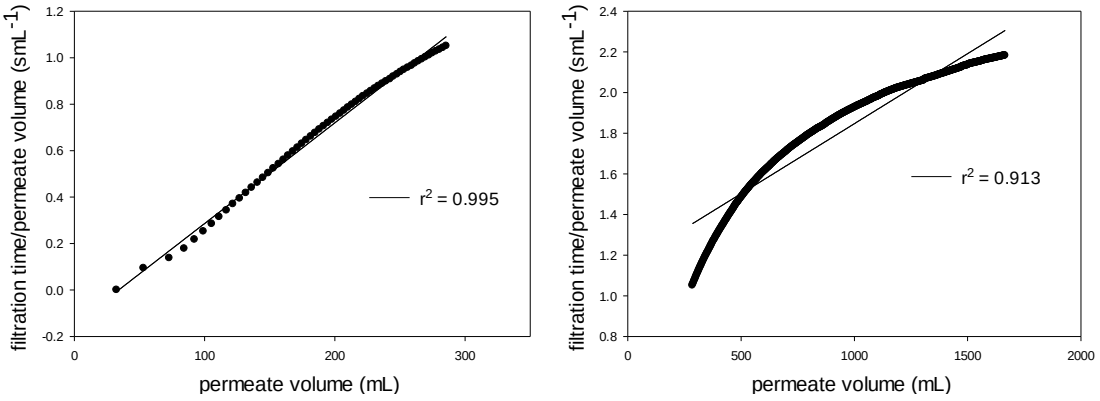

Figure B11: Cake filtration model fitted to 0.5 µm flat sheet data for first 5 minutes (left) and 5 – 60 minutes (right).

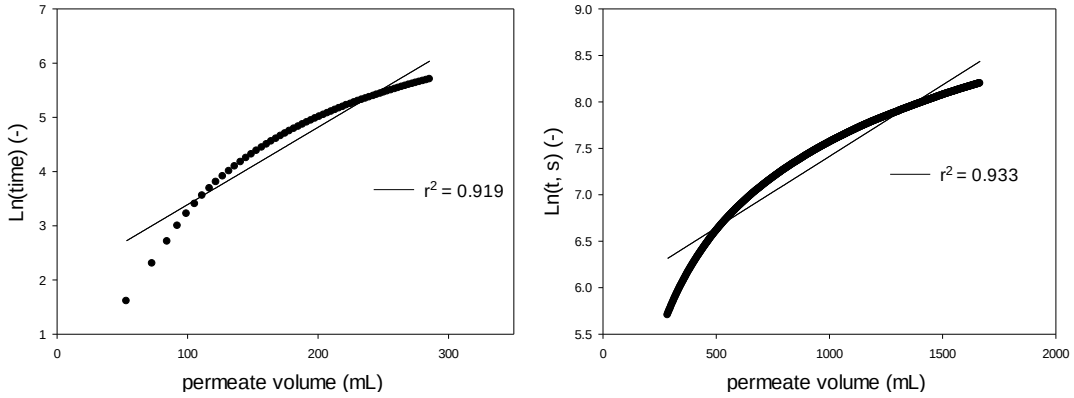

Figure B12: Intermediate blocking model fitted to 0.5 µm flat sheet data for first 5 minutes (left) and 5 – 60 minutes (right).

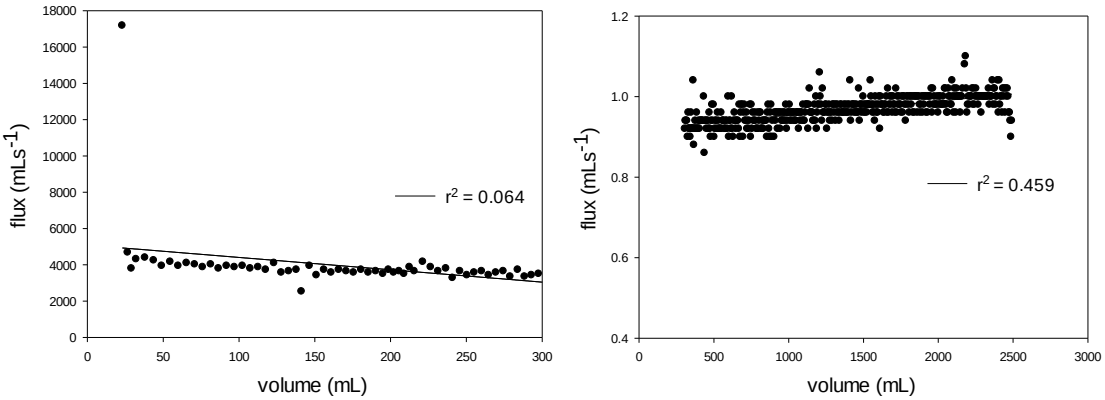

Figure B13: Pore blocking model fitted to 0.2 µm flat sheet data for first 5 minutes (left) and 5 – 60 minutes (right).

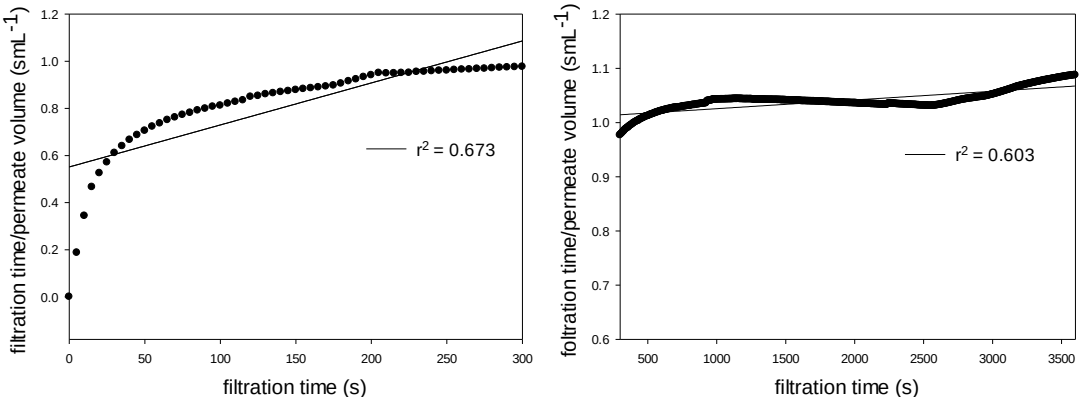

Figure B14: Pore constriction model fitted to 0.2 µm flat sheet data for first 5 minutes (left) and 5 – 60 minutes (right).

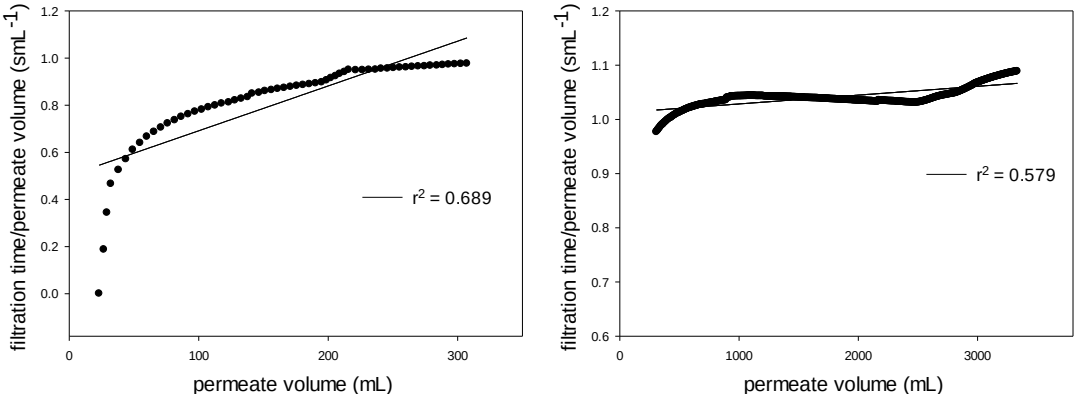

Figure B15: Cake filtration model fitted to 0.2 µm flat sheet data for first 5 minutes (left) and 5 – 60 minutes (right).

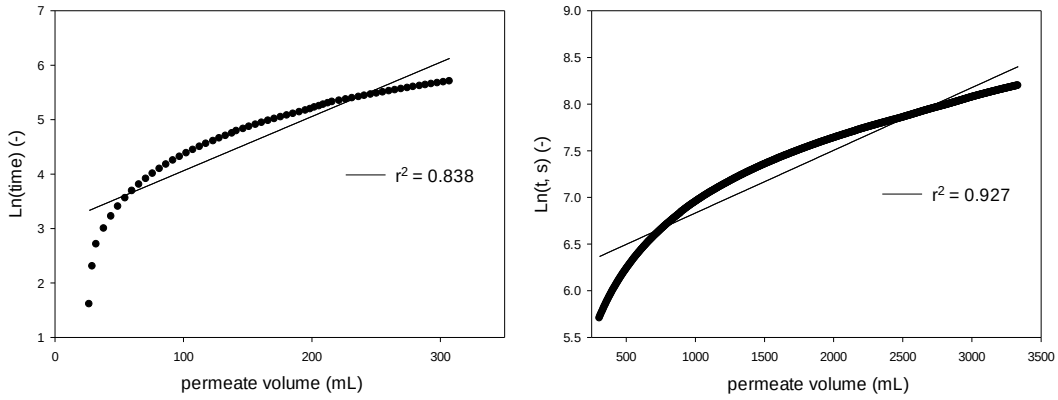

Figure B16: Intermediate blocking model fitted to 0.2 µm flat sheet data for first 5 minutes (left) and 5 – 60 minutes (right).

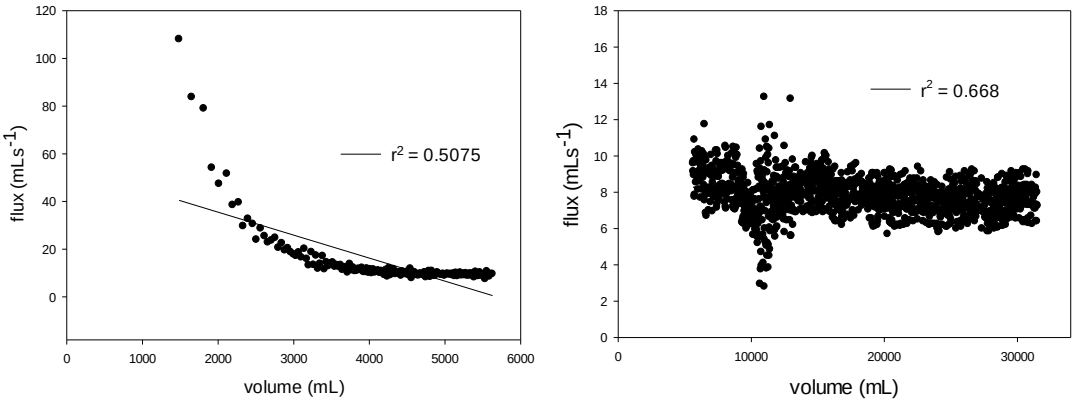

Figure B17: Pore blocking model fitted to 0.8 µm tubular ceramic cycle 1 data for first 5 minutes (left) and 5 – 60 minutes (right).

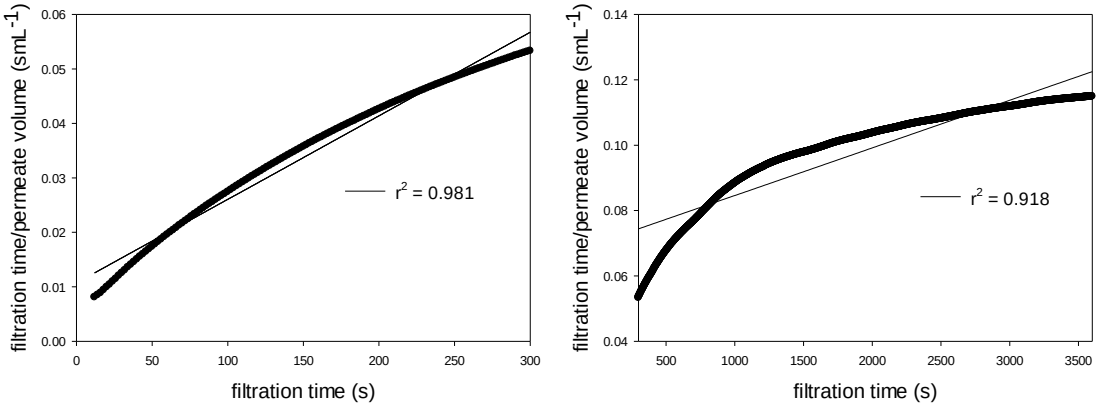

Figure B18: Pore constriction model fitted to 0.8 µm tubular ceramic cycle 1 data for first 5 minutes (left) and 5 – 60 minutes (right).

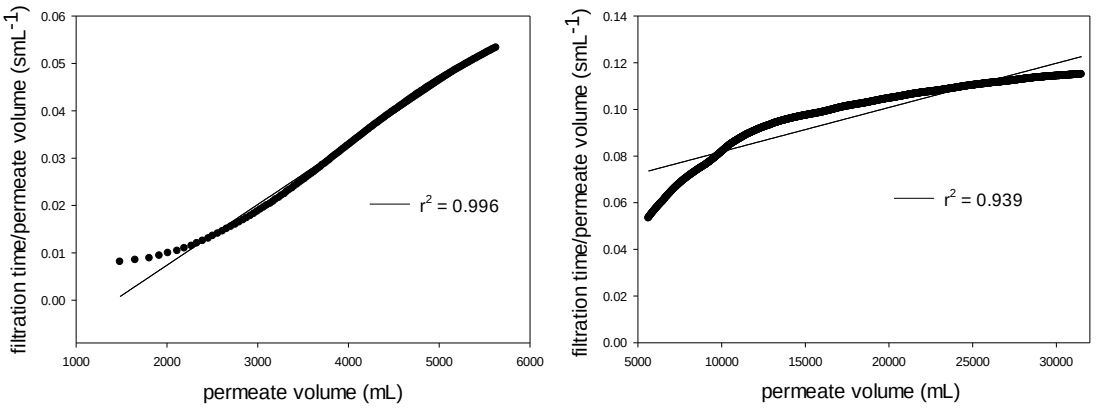

Figure B19: Cake filtration model fitted to 0.8 µm tubular ceramic cycle 1 data for first 5 minutes (left) and 5 – 60 minutes (right).

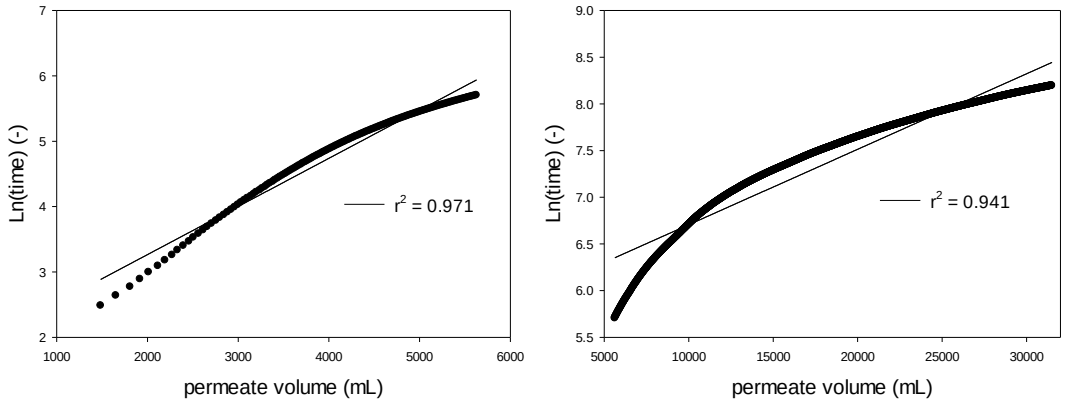

Figure B20: Intermediate blocking model fitted to 0.8 µm tubular ceramic cycle 1 data for first 5 minutes (left) and 5 – 60 minutes (right).

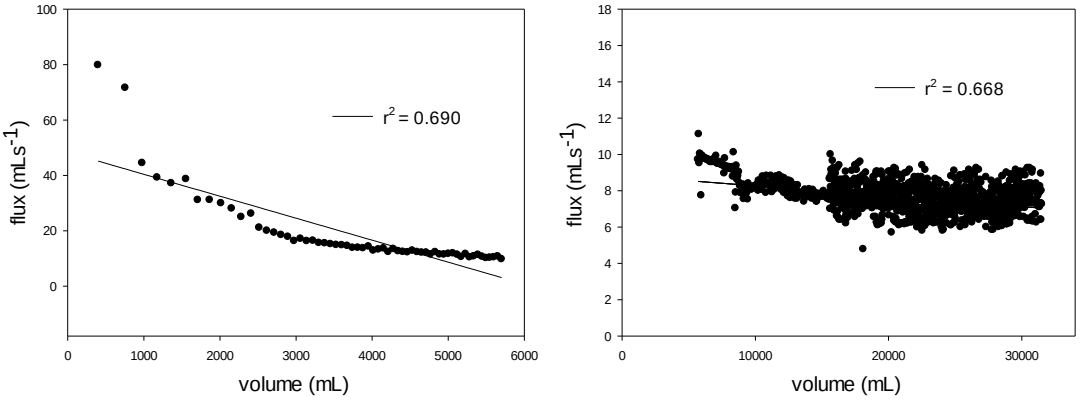

Figure B17: Pore blocking model fitted to 0.8 µm tubular ceramic cycle 10 data for first 5 minutes (left) and 5 – 60 minutes (right).

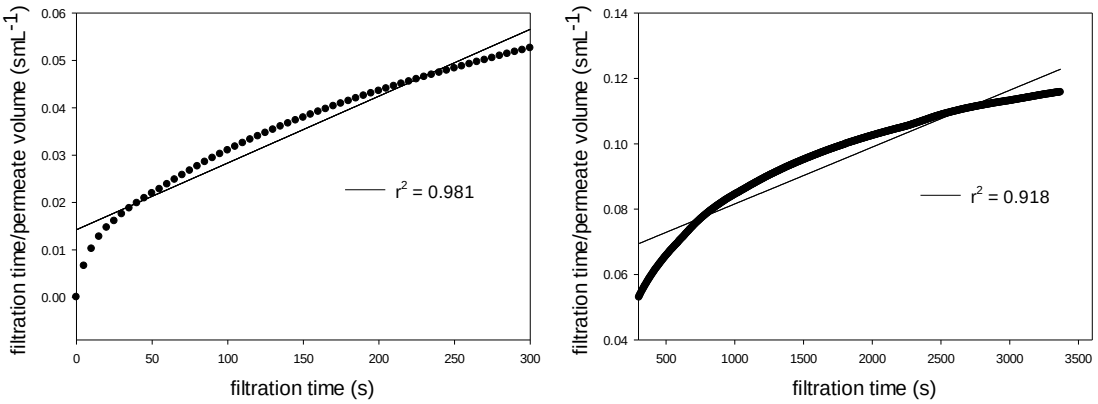

Figure B18: Pore constriction model fitted to 0.8 µm tubular ceramic cycle 10 data for first 5 minutes (left) and 5 – 60 minutes (right).

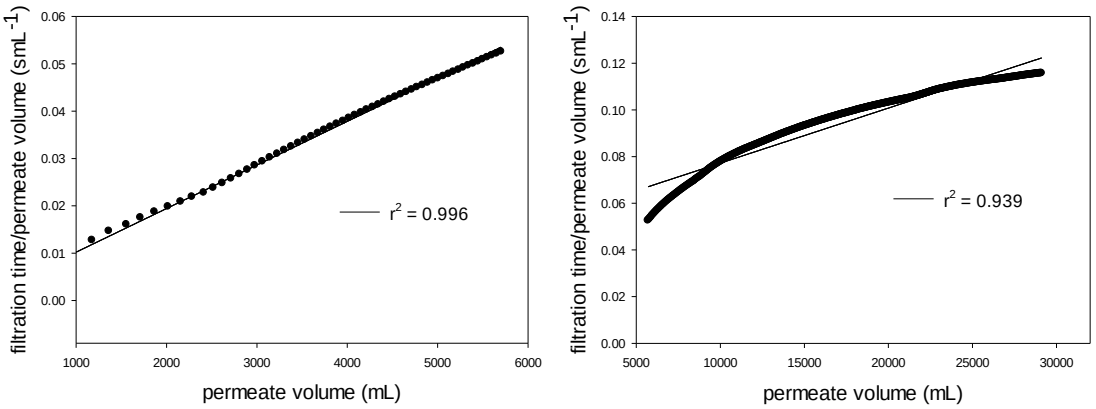

Figure B19: Cake filtration model fitted to 0.8 µm tubular ceramic cycle 10 data for first 5 minutes (left) and 5 – 60 minutes (right).

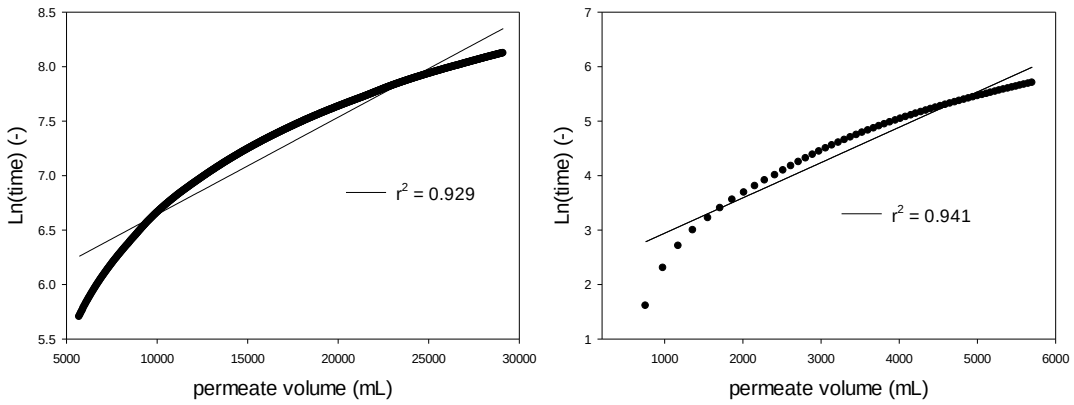

Figure B20: Intermediate blocking model fitted to 0.8 µm tubular ceramic cycle 10 data for first 5 minutes (left) and 5 – 60 minutes (right).

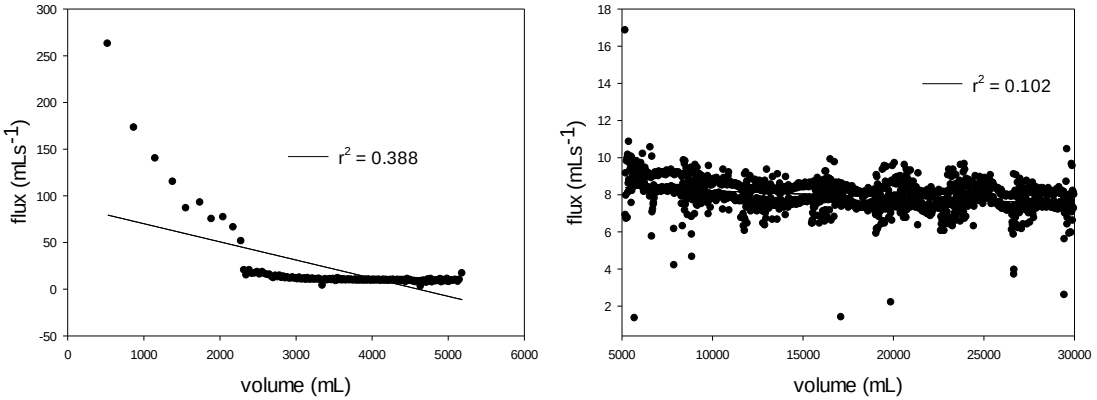

Figure B21: Pore blocking model fitted to 0.5 µm tubular ceramic cycle 1 data for first 5 minutes (left) and 5 – 60 minutes (right).

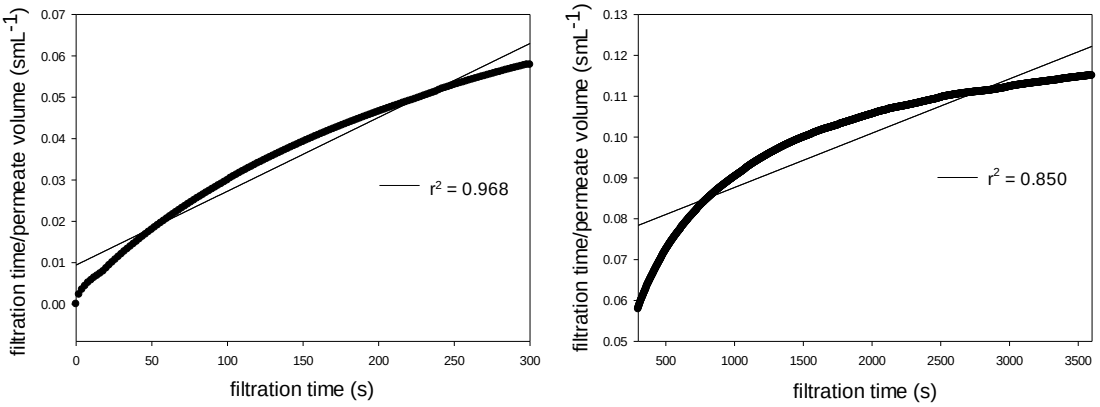

Figure B22: Pore constriction model fitted to 0.5 µm tubular ceramic cycle 1 data for first 5 minutes (left) and 5 – 60 minutes (right).

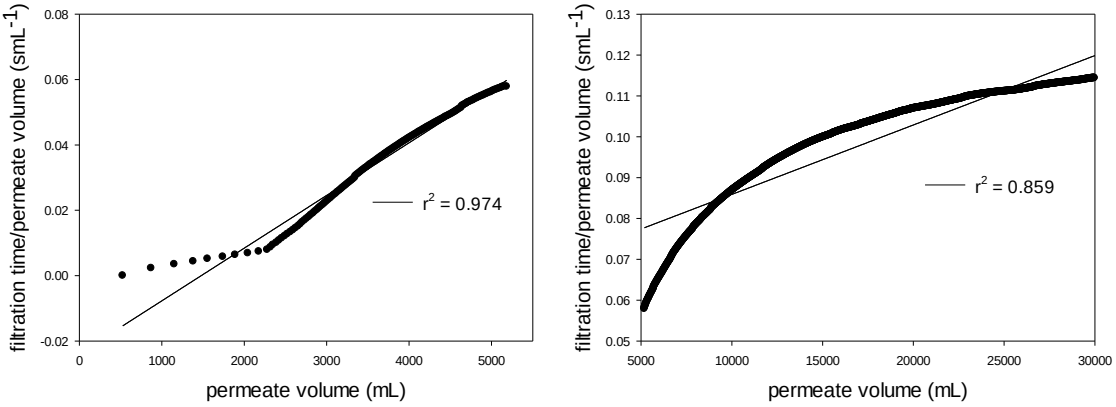

Figure B23: Cake filtration model fitted to 0.5 µm tubular ceramic cycle 1 data for first 5 minutes (left) and 5 – 60 minutes (right).

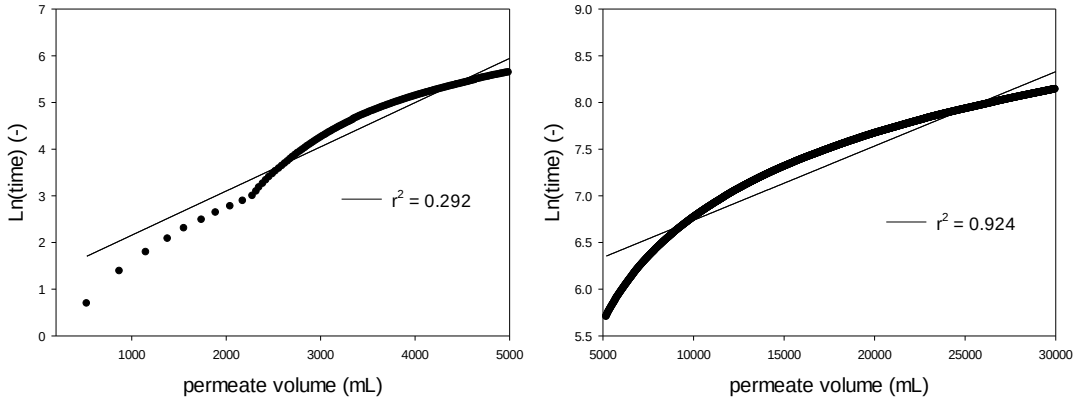

Figure B24: Intermediate blocking model fitted to 0.5 µm tubular ceramic cycle 1 data for first 5 minutes (left) and 5 – 60 minutes (right).

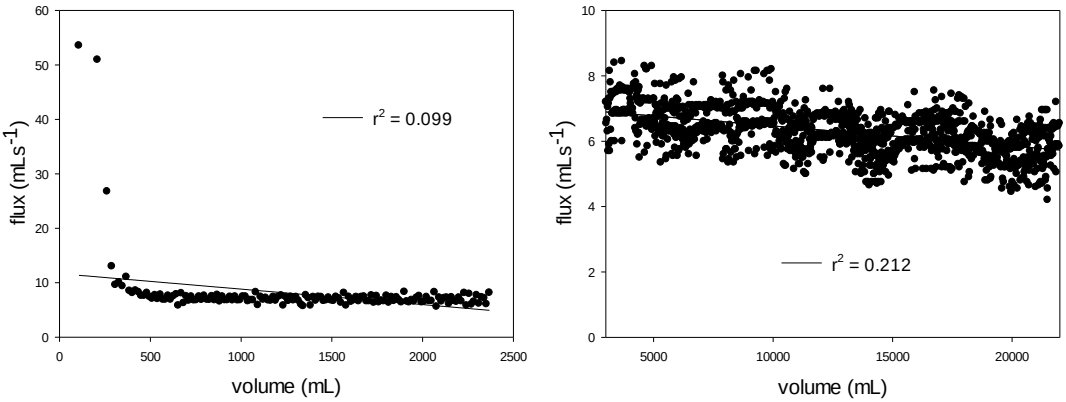

Figure B25: Pore blocking model fitted to 0.5 µm tubular ceramic cycle 10 data for first 5 minutes (left) and 5 – 60 minutes (right).

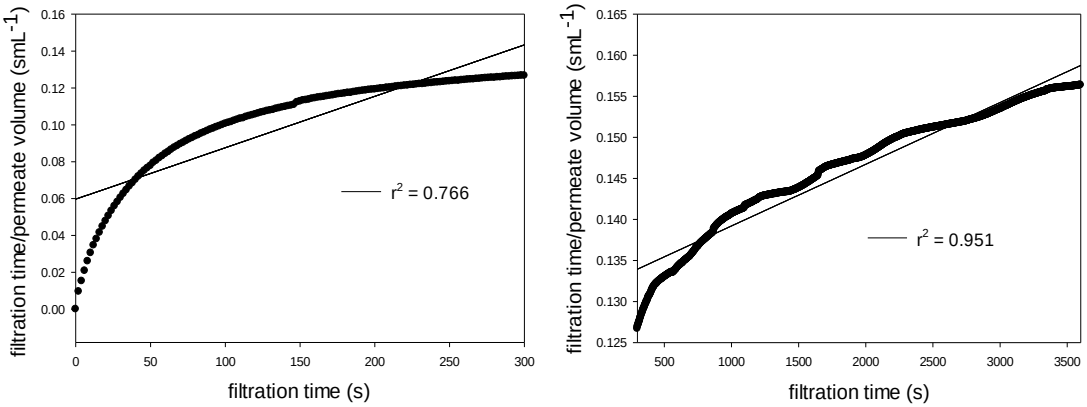

Figure B26: Pore constriction model fitted to 0.5 µm tubular ceramic cycle 10 data for first 5 minutes (left) and 5 – 60 minutes (right).

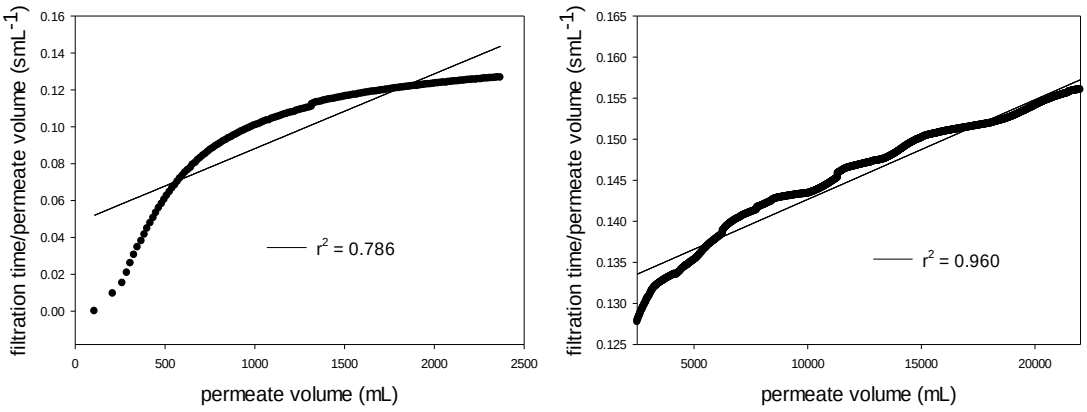

Figure B27: Cake filtration model fitted to 0.5 µm tubular ceramic cycle 10 data for first 5 minutes (left) and 5 – 60 minutes (right).

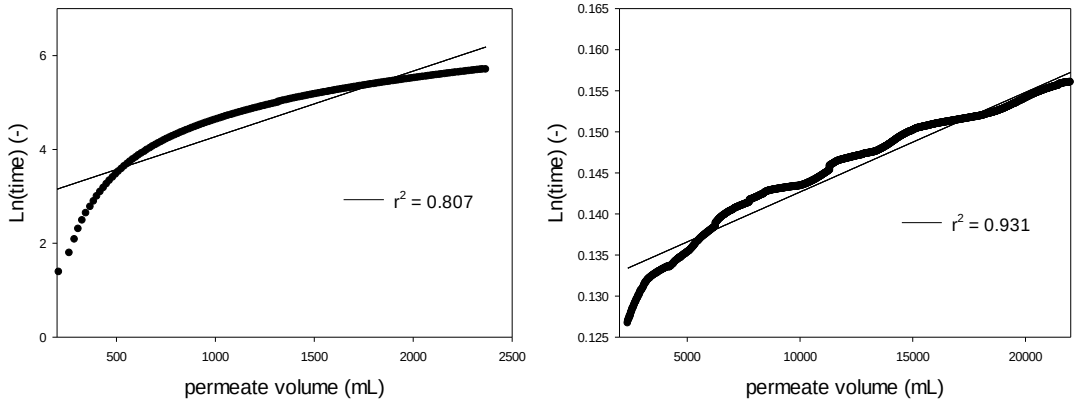

Figure B28: Intermediate blocking model fitted to 0.5 µm tubular ceramic cycle 10 data for first 5 minutes (left) and 5 – 60 minutes (right).

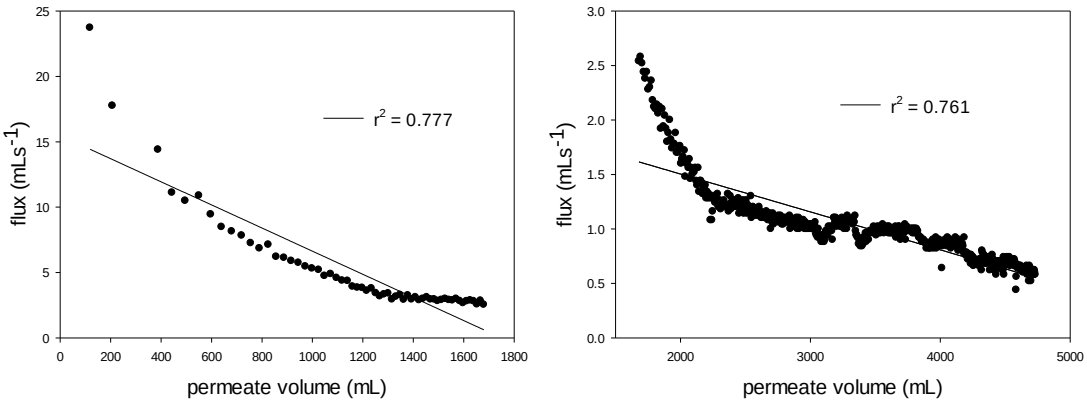

Figure B29: Pore blocking model fitted to pre-filtered Gum through a 0.8 µm flat sheet data for first 5 minutes (left) and 5 – 60 minutes (right).

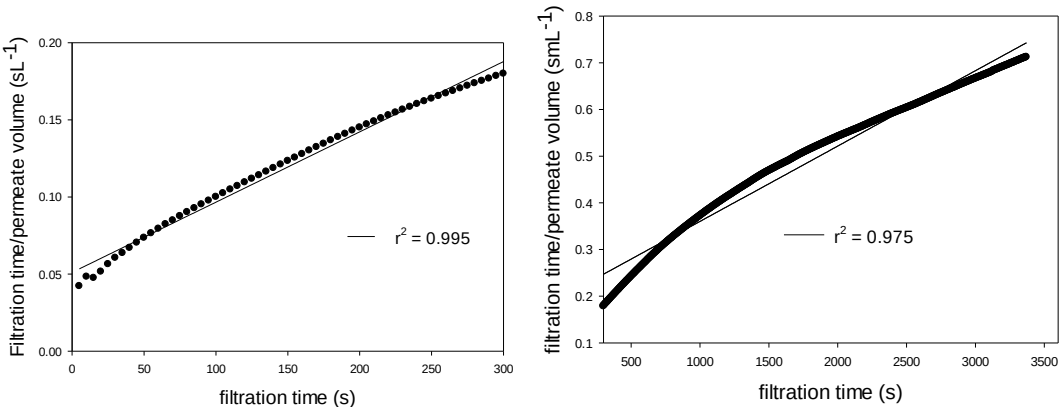

Figure B30: Pore constriction model fitted to pre-filtered Gum through a 0.8 µm flat sheet data for first 5 minutes (left) and 5 – 60 minutes (right).

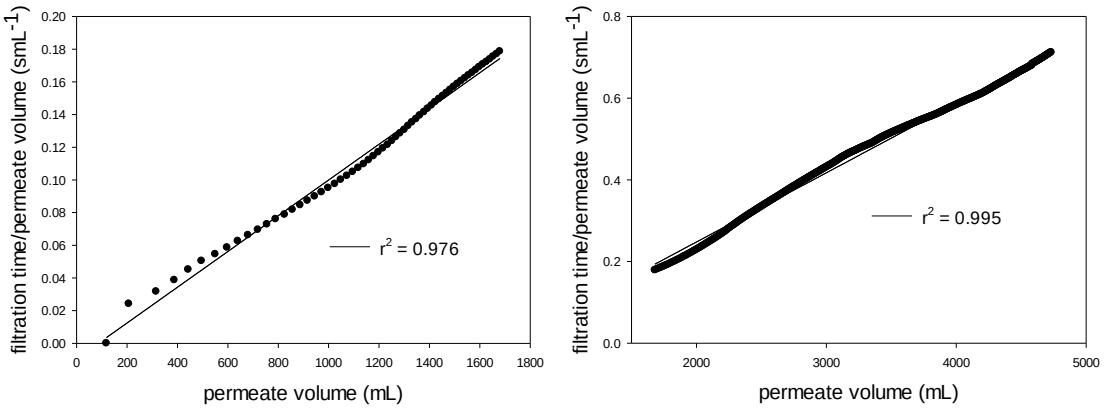

Figure B31: Cake filtration model fitted to pre-filtered Gum through a 0.8 µm flat sheet data for first 5 minutes (left) and 5 – 60 minutes (right).

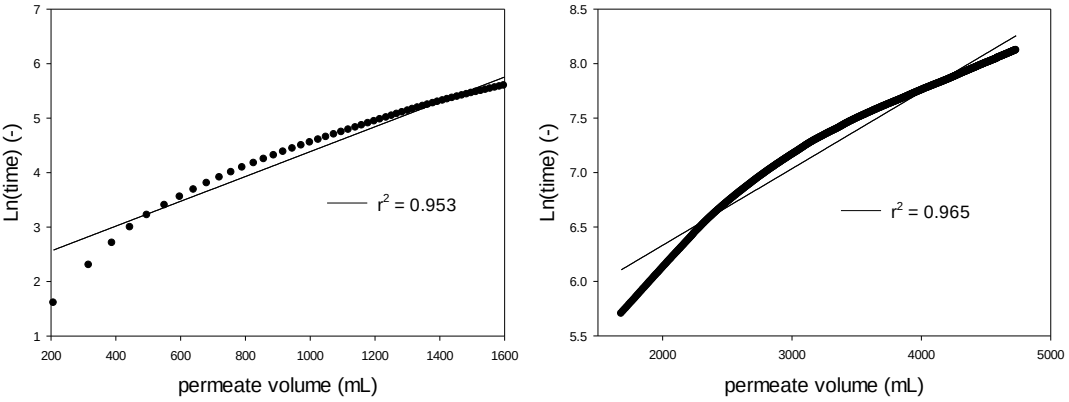

Figure B32: Intermediate blocking model fitted to pre-filtered Gum through a 0.8 µm flat sheet data for first 5 minutes (left) and 5 – 60 minutes (right).

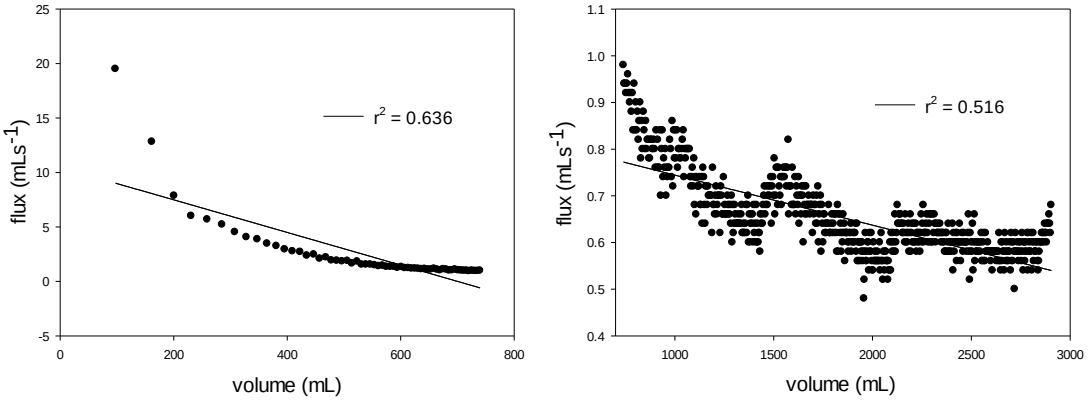

Figure B33: Pore blocking model fitted to Gum through a 0.5 µm flat sheet pre-treated with citric acid data for first 5 minutes (left) and 5 – 60 minutes (right).

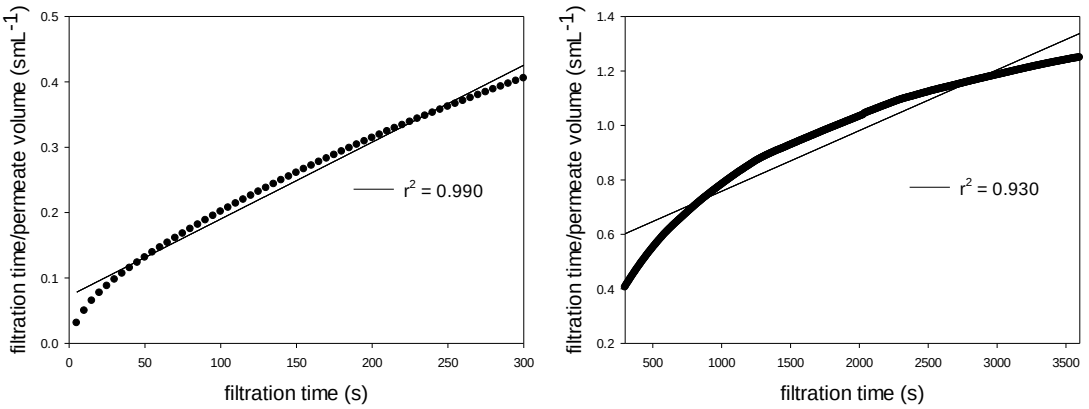

Figure B34: Pore constriction model fitted to Gum through a 0.5 µm flat sheet pre-treated with citric acid data for first 5 minutes (left) and 5 – 60 minutes (right).

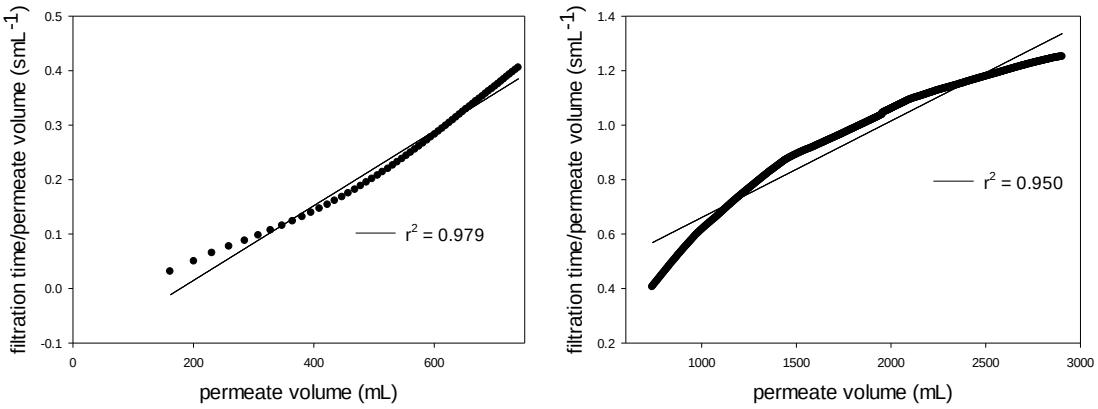

Figure B35: Cake filtration model fitted to Gum through a 0.5 µm flat sheet pre-treated with citric acid data for first 5 minutes (left) and 5 – 60 minutes (right).

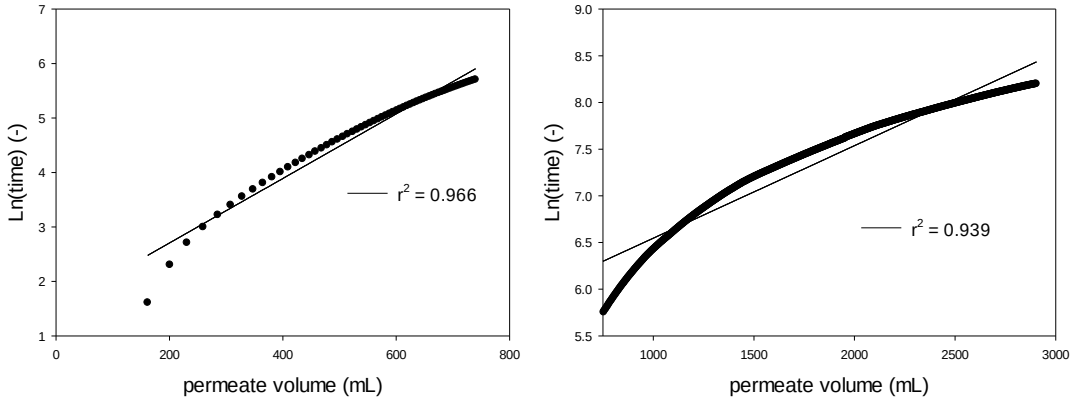

Figure B36: Intermediate blocking model fitted to Gum through a 0.5 µm flat sheet pre-treated with citric acid data for first 5 minutes (left) and 5 – 60 minutes (right).

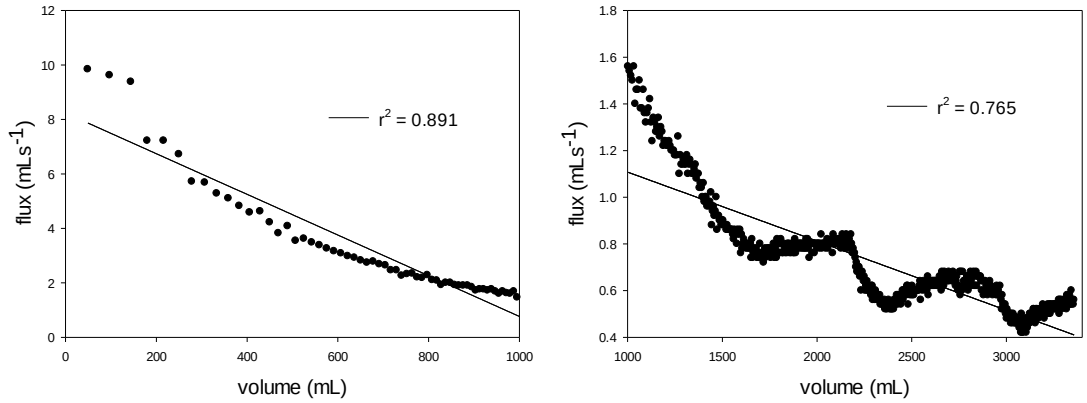

Figure B37: Pore blocking model fitted to Gum through a 0.5 µm flat sheet pre-treated with sodium hydroxide/sodium hypochlorite data for first 5 minutes (left) and 5 – 60 minutes (right).

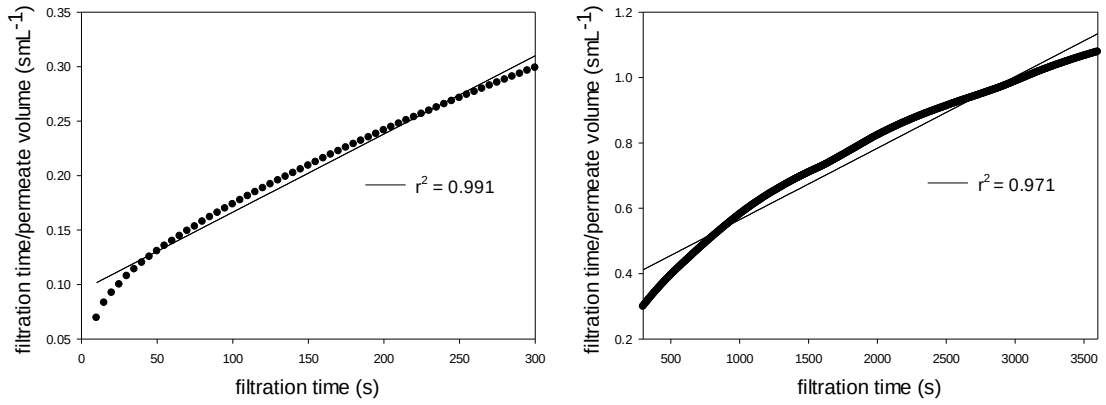

Figure B38: Pore constriction model fitted to Gum through a 0.5 µm flat sheet pre-treated with sodium hydroxide/sodium hypochlorite data for first 5 minutes (left) and 5 – 60 minutes (right).

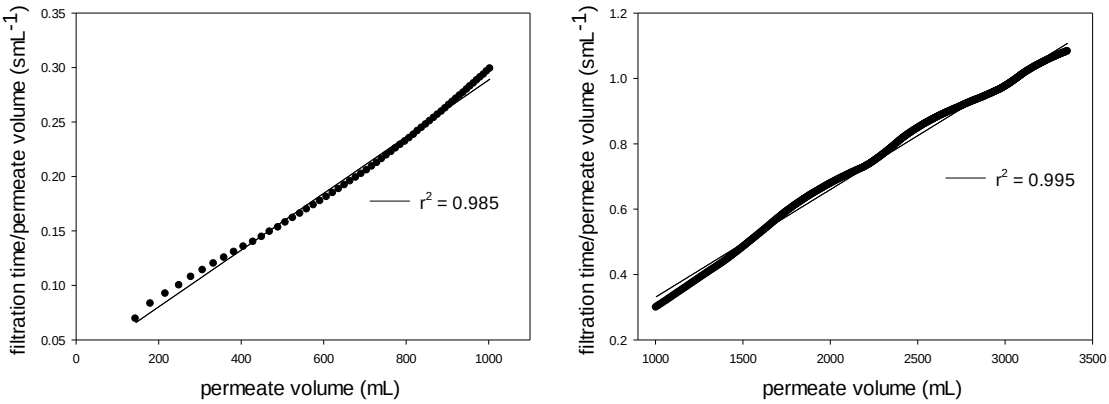

Figure B39: Cake filtration model fitted to Gum through a 0.5 µm flat sheet pre-treated with sodium hydroxide/sodium hypochlorite data for first 5 minutes (left) and 5 – 60 minutes (right).

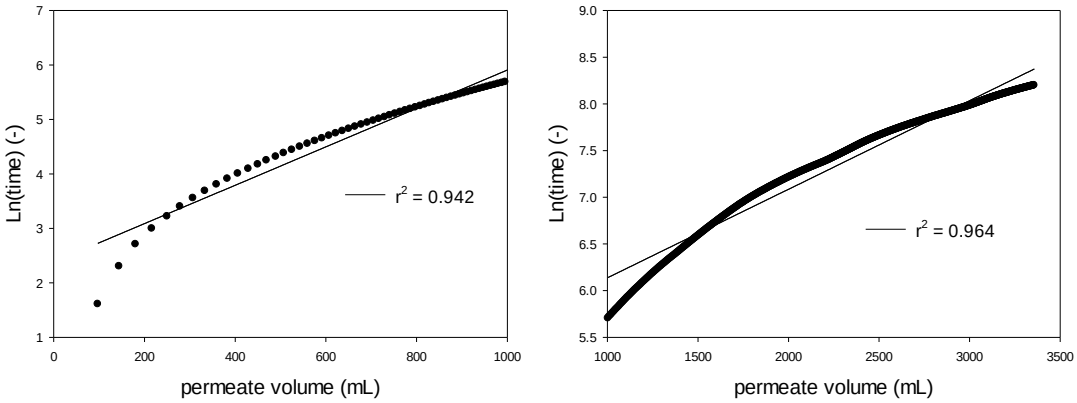

Figure B40: Intermediate blocking model fitted to Gum through a 0.5 µm flat sheet pre-treated with sodium hydroxide/sodium hypochlorite data for first 5 minutes (left) and 5 – 60 minutes (right).

Appendix C

Example calculations

C1: Example flux calculation

Flux was calculated using Equation 2.3 as follows:

$$J = \frac{\Delta V}{A_m \Delta t} = \frac{(37.7)}{(0.244)(0.00139)} = 111000\ gm^{-2}h^{-1}$$

This could be converted into L m^{-2} h^{-1} by dividing by the density of solution e.g. 992.2 kg m^{-3} for water at 40 °C

$$\frac{(111000)}{(992.2)} = 112\ Lm^{-2}h^{-1}$$

Reported fluxes (unless otherwise specified) are produced from triplicate experiments with the average and standard deviation used as the measure and error.

C2: Example resistance calculation

The membrane resistance was calculated using Equation 4.2 as follows:

1.5 bar = 1.5 x 10^5 N m^{-2}

112 L m^2 h^{-1} = 3.11 x 10^{-5} m s^{-1}

$$R_T = \frac{\Delta P}{J\mu} = \frac{(1.5\ x\ 10^5)}{(3.11\ x\ 10^{-5})(0.653\ x\ 10^{-3})} = 7.38\ x\ 10^{12}\ m^{-1}$$

C3: Example calculation for Reynolds number

The Reynolds number has been calculated using Equation 4.1 as follows:

$$Re = \frac{uL}{\mu}$$

L is the effective channel hydraulic diameter where a is the channel height and b is the channel width:

$$L = \frac{2ab}{a+b} = \frac{(2)(4\ x\ 10^{-3})(4\ x\ 10^{-3})}{(4\ x\ 10^{-3})\ +\ (4\ x\ 10^{-3})} = 4\ x\ 10^{-3}$$

$$Re = \frac{uL}{\mu} = \frac{(2.3)(4\ x\ 10^{-3})}{6.58\ x\ 10^{-5}} = 13900$$

C4: Example calculation for flux recovery

The flux recovery was calculated using Equation 6.1 as follows:

$$\%\, J_r = \left(\frac{J_C}{J_W}\right) x\ 100 = \left(\frac{4657}{5418}\right) x\ 100 = 86\ \%$$

C5: Example calculation for zeta potential

Streaming potential measurements were carried out through the pores. The streaming current was measured at 5 different TMP through the pores. The streaming current through the pores formed a linear correlation to pressure allowing the finite differential in the Helmholtz-Smoluchowski equation to be obtained. From this the apparent zeta potential through the membrane pores can be calculated.

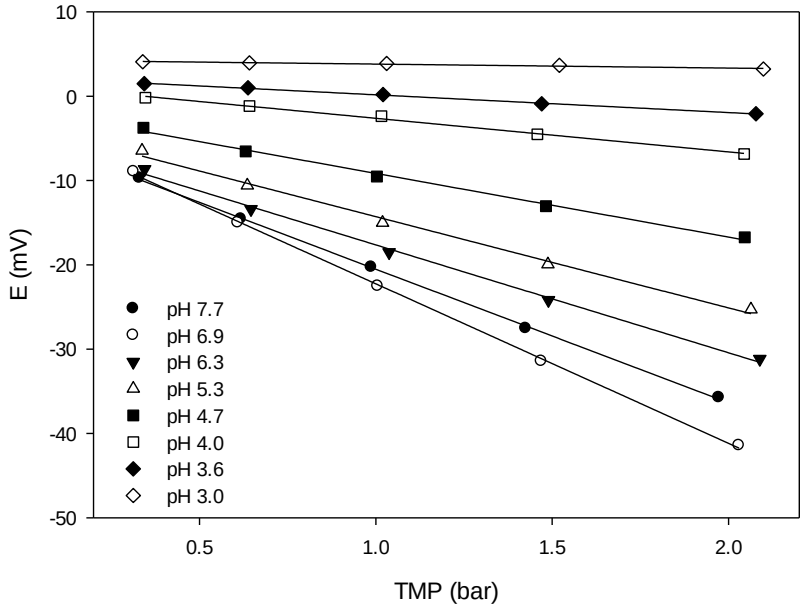

Figure C1: Raw streaming current data plotted against TMP (data for 0.8 µm fouled membrane).

Table C1: Calculated apparent zeta potential from the streaming current/pressure gradient data in Fig. C1

pH (-)	Slope (mVbar^{-1})	ζ- potential (mV)
7.7	-15.86	-3.54
6.9	-18.93	-4.09
6.3	-12.81	-2.91
5.3	-10.84	-2.57
4.7	-7.55	-1.85
4.0	-3.99	-1.12
3.6	-2.1	-0.79
3.0	-0.47	-0.34

$$\zeta = \frac{\Delta E}{\Delta P}\frac{\mu k}{\varepsilon_0 \varepsilon_r} = (-15.86)x\ \frac{(0.8904)(173.75)}{(78.4)(8.854)} = -3.54$$

Where $\Delta E/\Delta P$ is the slope, μ is the solution viscosity, k is the conductivity. ε_0 is the permittivity of a vacuum and ε_r is the dielectric constant of water.